QUANTUM MECHANICAL STUDIES OF THE MECHANISMS OF SOME TRANSITION METAL ORGANOMETALLIC REACTIONS

A thesis submitted to the Department of Chemistry, College of Science, Kwame Nkrumah University of Science and Technology, Kumasi

in partial fulfillment of the requirements for the degree of

DOCTOR OF PHILOSOPHY

in Chemistry

By:

Richard Tia, BSc. (Hons.)

December, 2009

DECLARATION

I hereby declare that this thesis is my own work towards the Ph.D. and that, to the best of my knowledge and belief, it contains no material that has been accepted for the award of any other degree in any educational institution nor material previously published or written by another person, except where due reference is made in the text of the thesis.

Richard Tia ...…….. ….……

(Candidate) Signature Date

Certified by:

Evans Adei, BSc, M.Phil., Ph.D. …… ……..
(Supervisor) Signature Date

and

J. A. M. Awudza, BSc, M.Phil., Ph.D. ..…….. …….

(Head of Department) Signature Date

TABLE OF CONTENTS

Title Page

Declaration……..…ii

Table of Contents……iii

List of Figures…….vi

List of Schemes……..xii

List of Tables……xiii

List of Abbreviations ……...xiv

Acknowledgement……xv

Dedication……xvii

Publications Arising From the Work Reported in the Thesis……...xix

Abstract…….xx

CHAPTER ONE

Introduction……..1

References……..11

CHAPTER TWO

Density Functional Theory Studies of the Mechanisms of Oxidation of Ethylene by Chromyl Chloride

2.1 Introduction……..16

2.2 Details of Calculation……..... 24

2.3 Results and Discussions……...25

2.3.1 Formation of epoxide……25

2.3.2 Formation of Acetaldehyde and Vinyl Alcohol……33

2.3.3 Formation of 1,2-Chlorohydrin and 1,2-Dichloroethane……..34

2.4 Conclusion……...39

References……..41

CHAPTER THREE

Density Functional Theory Studies of the Mechanistic Aspects of Olefin Metathesis Reactions

3.1 Introduction……..45

3.2 Details of Calculations.……...51

3.3 Results and Discussions.……..…52

3.3.1 Reactions of Cl_4MCH_2 (M=Cr, Mo, W, Ru, Re) with Ethylene……...52

3.3.2 Reactions of $Cl_2(O)M=CH_2$ (Cr, Mo, W, Ru, Re) with Ethylene……74

3.4 Conclusion……...88

References……..90

CHAPTER FOUR

Density Functional Theory Studies of the Mechanistic Aspects of Transition-Metal-Assisted Formation of 1,2- Dinitrosoalkanes

4.1 Introduction……..94

4.2 Details of Calculations..……...97

4.3 Results and Discussions..……98

4.3.1 Reactions of $CpM(NO)_2$(M=Co, Rh, Ir) with Ethylene……98

4.3.2 Reactions of $CpM(NO)_2$(M=Co, Rh, Ir) with 2-Norbonene……...108

4.3.3 Reactions of $CpM(NO)_2$(M=Co, Rh, Ir) with Trans-1-phenylpropene…..117

4.3.4 Reactions of $CpM(NO)_2$(M=Co, Rh, Ir) with Cyclopentene……..124

4.3.5 Reactions of $CpM(NO)_2$(M=Co, Rh, Ir) with Cyclohexene……...129

4.3.6 Reactions of $CpM(NO)_2$(M=Co, Rh, Ir) with 2,3-Dimethyl-2-butene…...135

4.4 Conclusion…….140

References……143

CHAPTER FIVE

Concluding Remarks……146

References……151

APPENDIX

Optimized Geometries and Absolute Energies of Computed Structures…….154

LIST OF FIGURES

Figure 2.1 Optimized geometries of the main stationary points involved in the [2+2] and [3+2] addition reactions between CrO_2Cl_2 and ethylene for the formation of the epoxide precursor….27

Figure 2.2 Optimized geometrical parameters (in Å) of the stationary points on epoxide ring-opening……...28

Figure 2.3 Reaction profiles of the three suggested mechanisms for the formation of the epoxide precursor from the addition of CrO_2Cl_2 to ethylene on the singlet PES……29

Figure 2.4 Optimized geometries of the main stationary points involved in the [2+2] and [3+2] addition reactions between CrO_2Cl_2 and ethylene for the formation of chlorohydrin and dichloride precursors..……...35

Figure 2.5 Energy profile of the three suggested mechanisms for the formation of the 1,2-chlorohydrin precursor from the addition of CrO_2Cl_2 and ethylene on the singlet PES……..36

Figure 2.6 Energy profiles of the two suggested mechanisms for the formation of the dichloride precursor from addition of CrO_2Cl_2 and ethylene……..38

Figure 3.1 Optimized geometries of the main stationary points involved in the reaction of Cl_4CrCH_2 with ethylene…….53

Figure 3.2 Energetics of the reactions of Cl_4CrCH_2 with ethylene……...55

Figure 3.3 Optimized geometries of the main stationary points involved in the reaction of Cl_4MoCH_2 with ethylene……58

Figure 3.4 Energetics of the reactions of Cl_4MoCH_2 with ethylene……..……59

Figure 3.5 Optimized geometries of the main stationary points involved in the reaction of Cl_4WCH_2 with ethylene…….62

Figure 3.6 Energetics of the reactions of Cl_4WCH_2 with ethylene……..…….63

Figure 3.7 Optimized geometries of the main stationary points involved in the reactions of Cl_4RuCH_2 with ethylene…….66

Figure 3.8 Energetics of the reactions of Cl_4RuCH_2 with ethylene……..……67

Figure 3.9 Optimized geometries of the main stationary points involved in the reaction of Cl_4ReCH_2 with ethylene…….69

Figure 3.10 Energetics of the reactions of Cl_4ReCH_2 with ethylene…….70

Figure 3.11 Summary of the Possible Reaction Paths for the Reaction of Cl_4MCH_2 (M=Cr, Mo, W, Ru, Re) with Ethylene……..71

Figure 3.12 Optimized geometries of the main stationary points involved in the reactions of $Cl_2(O)CrCH_2$ with ethylene……75

Figure 3.13 Energetics of the reactions of $Cl_2(O)CrCH_2$ with ethylene……..……76

Figure 3.14 Optimized geometries of the main stationary points involved in the reactions of $Cl_2(O)MoCH_2$ with ethylene……..78

Figure 3.15 Energetics of the reactions of $Cl_2(O)MoCH_2$ with ethylene……..……79

Figure 3.16 Optimized geometries of the main stationary points involved in the reaction of $Cl_2(O)WCH_2$ with ethylene……80

Figure 3.17 Energetics of the reactions of $Cl_2(O)WCH_2$ with ethylene……..……..81

Figure 3.18 Optimized geometries of the main stationary points involved in the reaction of $Cl_2(O)RuCH_2$ with ethylene……...83

Figure 3.19 Energetics of the reactions of $Cl_2(O)RuCH_2$ with ethylene……..….84

Figure 3.20 Optimized geometries of the main stationary points involved in the reaction of $Cl_2(O)ReCH_2$ with ethylene……...85

Figure 3.21 Energetics of the reactions of $Cl_2(O)ReCH_2$ with ethylene……..…….86

Figure 4.1a Optimized geometries of the $CpM(NO)_2$ (M = Co, Rh, Ir) reactant minima……99

Figure 4.1b Optimized geometries of the π-complexes formed from the interaction of $CpM(NO)_2$ (M = Co, Rh, Ir) with ethylene ..…….101

Figure 4.1c Optimized geometries of the transition states and products formed from [3+2] addition of $CpM(NO)_2$ (M = Co, Rh, Ir) with ethylene……103

Figure 4.1d Energy profiles of the [3+2] and [2+2] addition reaction of $CpM(NO)_2$ (M = Co, Rh, Ir) with ethylene……...105

Figure 4.1e Optimized geometries of the stationary points involved in the [2+2] addition of ethylene to $CpM(NO)_2$ (M = Co, Rh, Ir)……106

Figure 4.2a Optimized geometries of the π-complexes formed from the interaction of $CpM(NO)_2$ (M = Co, Rh, Ir) with 2-norbonene……...108

Figure 4.2b Optimized geometries of the stationary points involved in the [3+2] reaction of $CpM(NO)_2$ (M = Co, Rh, Ir) with 2-norbonene……...110

Figure 4.2c Energy profiles of the [3+2] and [2+2] addition reaction of $CpM(NO)_2$ (M = Co, Rh, Ir) with 2-norbonene……112

Figure 4.2d Optimized geometries of the stationary points involved in the [2+2] addition reaction between $CpCo(NO)_2$ and 2-norbonene……..114

Figure 4.2e Optimized geometries of the stationary points involved in the [2+2] addition reaction between $CpRh(NO)_2$ and 2-norbonene……..115

Figure 4.2f Optimized geometries of the stationary points involved in the [2+2] addition reaction between $CpIr(NO)_2$ and 2-norbonene……116

Figure 4.3a Optimized geometries of the π-complexes formed from the interaction of $CpM(NO)_2$ (M = Co, Rh, Ir) with trans-1-phenylpropene……...118

Figure 4.3b Optimized geometries of the stationary points involved in the [3+2] addition reaction of $CpM(NO)_2$ (M = Co, Rh, Ir) with trans-1-phenylpropene……120

Figure 4.3c Optimized geometries of the stationary points involved in the [2+2] addition reaction of $CpM(NO)_2$ (M = Co, Rh, Ir) with trans-1-phenylpropene……122

Figure 4.3d Energy profile of the [3+2] and [2+2] addition reaction of $CpM(NO)_2$ (M = Co, Rh, Ir) with trans-1-phenylpropene……123

Figure 4.4a Optimized geometries of the π-complexes formed from the interaction of $CpM(NO)_2$ (M = Co, Rh, Ir) with cyclopentene……..124

Figure 4.4b Optimized geometries of the stationary points involved in the [3+2] addition reaction of $CpM(NO)_2$ (M = Co, Rh, Ir)with cyclopentene……126

Figure 4.4c Optimized geometries of the stationary points involved in the [2+2] addition reaction of $CpM(NO)_2$ (M = Co, Rh, Ir)$_2$ with cyclopentene……...127

Figure 4.4d Energy profiles of the [3+2] and [2+2] addition reactions of $CpM(NO)_2$ (M = Co, Rh, Ir) with cyclopentene……...128

Figure 4.5a Optimized geometries of the π-complexes formed from the interaction of $CpM(NO)_2$ (M = Co, Rh, Ir) with cycloxene……...129

Figure 4.5b Optimized geometries of the stationary points involved in the [3+2] addition reaction of $CpM(NO)_2$ (M = Co, Rh, Ir) with cyclohexene…….131

Figure 4.5c Optimized geometries of the stationary points involved in the [2+2] addition reaction of $CpM(NO)_2$ (M = Co, Rh, Ir) with cyclohexene…….132

Figure 4.5d Energy profiles of the [3+2] and [2+2] addition reaction of $CpM(NO)_2$ (M = Co, Rh, Ir) with cyclohexene……134

Figure 4.6a Optimized geometries of the π-complexes formed from the interaction of $CpM(NO)_2$ (M = Co, Rh, Ir) with 2,3-dimethyl-2-butene……...135

Fig. 4.6b Optimized geometries of the stationary points involved in the [3+2] addition reaction of $CpM(NO)_2$ (M = Co, Rh, Ir) with 2,3-dimethyl-2-butene……...137

Fig. 4.6c Optimized geometries of the stationary points involved in the [2+2] addition reaction of $CpM(NO)_2$ (M = Co, Rh, Ir) with 2,3-dimethyl-2-butene……...138

Figure 4.6d Energy profile of the [3+2] and [2+2] addition reaction between $CpM(NO)_2$ (M = Co, Rh, Ir) and 2,3-dimethyl-2-butene…….139

LIST OF SCHEMES

Scheme 2.1 Possible Pathways for the Reaction of $LnMO_2$ with Alkene…….17

Scheme 2.2 Proposed Mechanism for Reaction of Cl_2CrO_2 with ethylene Involving Organometallic Intermediates ……...19

Scheme 2.3 Mechanism Involving Direct Attack on Heteroatom Ligands …….……20

Scheme 2.4 Mechanisms of the CrO_2Cl_2-mediated formation of epoxide, acetaldehyde and vinyl alcohol……22

Scheme 2.5 Mechanisms of the CrO_2Cl_2-Mediated Formation of Chlorohydrins and Dichlorides…….23

Scheme 3.1: The Herrison-Chauvin Non-pairwise Mechanism of Olefin Metathesis……..47

Scheme 4.1: Bergman's Proposed Mechanism for the Formation of 1,2-Dinitrosoalkanes…….96

Scheme 4.2: Rappé's Proposed Mechanism of 1,2-Dinitrosoalkane Formation……...97

LIST OF TABLES

Table 1.1 Performance and Costs of Theoretical Models……8

Table 2.1. Imaginary Frequencies (in cm^{-1}) of All First-Order Saddle Points Involved in the Suggested Mechanisms for the Formation of Epoxide, Acetaldehyde, Dichloride and Chlorohydrin precursors……28

Table 3.1. Calculated Relative Energies (in $kcalmol^{-1}$) of the Main Stationary Points for the [2+2] and [3+2] Addition of Cl_4MCH_2(M=Cr, Mo, W, Ru, Re) Complexes to Ethylene…….57

Table 3.2 Activation Barriers (in $kcalmol^{-1}$) of the Various Pathways in the Reaction of $Cl_2(O)MCH_2$ (M=Cr, Mo, W, Ru, Re) with Ethylene……...77

Table 4.1: Relative energies (in $kcalmol^{-1}$) of the Transition States Formed from [3+2] and [2+2] Addition of Olefins to $CpM(NO)_2$ (M=Co, Rh, Ir)……107

LIST OF ABBREVIATIONS

B3LYP – Becke three parameter Lee-Yang-Parr functional

B97 – Becke 97 functional

BP86 – Becke-Perdew 86 functional

CFT – Crystal Field Theory

CNDO – Complete Neglect of Differential Overlap

DFT – Density Functional Theory

DNA – Deoxyribonucleic acid

HCTH – Hamprecht- Cohen-Tozer- Handy functional

HF – Hartree-Fock

MCSCF– Multi-Configurational Self-Consistent Field

MNDO – Modified Neglect of Differential Overlap

PM3(tm) – Parameterized Model 3 for transition metals

PMO – Perturbational Molecular Orbital

PPP – Pariser-Parr-Pople

QM/MM – Quantum Mechanics/Molecular Mechanics (Combined methods)

ACKNOWLEDGEMENT

My journey through the doctoral program will not have been successful without the love, support and co-operation of all those who care for me. Now that I stand at the end of that long

but exciting journey, it is my greatest pleasure to acknowledge all those individuals who contributed to the final product: they who provided at one time or another, either the critical push that helped me to make the effort, or the critical support at a time when I needed it most.

I am extremely grateful to my supervisor, Dr. Evans Adei, who gave unstintingly of his time and experience, for initiating me into the 'cult' of theoretical chemists. In the course of the last three years Dr. Adei has taught me the inherent mysteries and cohesiveness of molecular quantum mechanics, leading me through the maze of equations to reveal the underlying beauty of nature. In the process, he taught me more than chemistry – he taught me life – and for this I am eternally grateful. My time as Dr. Adei's doctoral student may well prove to be the most important in my ultimate development as a scientist and human being.

My sincere thanks are due to Professor James H. Ephraim, formerly of the Department of Chemistry, for his pieces of advice and encouragement, especially at the beginning. The great man must have seen beyond the difficult beginnings and took it upon himself to spur us on through the very tough times, even when conventional wisdom dictated otherwise. Professor Anthony A. Adimado has always been a source of inspiration, and we revere him for that. I am also thankful to Dr. Johannes A. M. Awudza, Dr. Sylvester K. Twumasi, Dr. S. Osafo Acquaah and Mr. N. K. Asare-Donkor for their support and encouragement over the years.

Our group received a substantial financial support from the National Council for Tertiary Education (NCTE) through the Teaching and Learning Innovation Fund (TALIF) to set up a Molecular Modeling and Informatics facility where this work was done. This generous support is gratefully acknowledged. I am also grateful for a KNUST scholarship that made available some funds for my studies.

My parents have been a constant source of encouragement and wisdom over the years, and I am grateful for their prodigious efforts in ensuring, when times were sometimes very hard, that I received the best education Ghana had to offer. It is amazing that they were prepared to forgo so much so I could come this far.

I am very grateful to my wonderful siblings and cousins - Esther, Moses, Rob, David, Peter, Charles and Sophie - who in the course of the last three years must have felt they have lost their once attentive brother and cousin to the study desk and computer screen in a far-away university campus. I am particularly grateful for their love and prayers and the sacrifices they have had to make for my sake.

Finally, I express my greatest gratitude to the Lord God Almighty for giving me life and for blessing me in all I do to make this day come true. This is certainly the doing of the Lord and it is marvelous in our eyes.

To each of the persons mentioned above and many others, I have just one more thing to say: "*ego gratias ago vos summopere quod ego sum valde memor*".

DEDICATION

To my kid sister Sophie

"There can be no question that in the Schrödinger equation we very nearly have the mathematical foundation for the solution of the whole problem of atomic and molecular structure."

G. N. Lewis, 1933

Publications Arising From the Work Reported in the Thesis

1. Tia, R. and Adei, E. (2009**)** Density Functional Theory Studies of the Mechanisms of Oxidation of Ethylene by Chromyl Chloride, *Inorg. Chem*. **48**, 11434.

2. Tia, R. and Adei, E. (2010) Density Functional Theory Studies of the Mechanistic Aspects of Olefin Metathesis Reactions. *Dalton Trans.*, **39**, 7575.
3. Tia, R. and Adei, E. Density Functional Theory Studies of the Mechanistic Aspects of Olefin Metathesis Reactions Involving Metal Oxo-alkylidene Complexes. *Dalton Trans*. (revised manuscript submitted).
4. Tia, R. and Adei, E.; Density Functional Theory Studies of the Mechanistic Aspects of Transition-Metal-Assisted Formation of 1,2-Dinitroso Complexes of Cobalt (in preparation).
5. Tia, R. and Adei, E.; Density Functional Theory Studies of the Mechanistic Aspects of Transition-Metal-Assisted Formation of 1,2-Dinitroso Complexes of Rhodium (in preparation).
6. Tia, R. and Adei, E.; Density Functional Theory Studies of the Mechanistic Aspects of Transition-Metal-Assisted Formation of 1,2-Dinitroso Complexes of Iridium (in preparation).

ABSTRACT

The mechanistic pathways of three organometallic reactions, namely the oxidation of ethylene by chromyl chloride leading to the formation of epoxide, 1,2-dichloroethane, 1,2-chlorohydrin, acetaldehyde, and vinyl alcohol precursors; the olefin metathesis reaction involving ethylene and

metal methylidene Cl_4MCH_2(M=Cr, Mo, W, Ru, Re) and metal oxo-methylidene $Cl_2(O)MCH_2$(M=Cr, Mo, W, Ru, Re) complexes; and the transition-metal-assisted formation of 1,2-dinitroso complexes of cobalt and its congeners have been studied using hybrid density functional theory at the B3LYP/LACVP* level of theory. The formation of the epoxide precursor ($Cl_2(O)Cr\text{-}OC_2H_4$) was found to take place via initial [2+2] addition of ethylene across the Cr=O bond of CrO_2Cl_2 to form a chromaoxetane intermediate, as opposed to [3+2] addition across the two Cr=O bonds of CrO_2Cl_2 as suggested in earlier studies. The hitherto unexplored pathway involving initial [3+2] addition of ethylene across the Cr=O and Cr-Cl bonds of CrO_2Cl_2 was found to be more favorable than the [3+2] addition across the two Cr-O bonds of CrO_2Cl_2. The formation of the 1,2-dichloroethane precursor was found to take place via [3+2] addition of ethylene across the two Cr-Cl bonds of CrO_2Cl_2. The 1,2-chlorohydrin precursor was also found to originate from [3+2] addition of ethylene across the Cr-O and Cr-Cl bonds of CrO_2Cl_2 as opposed to [2+2] addition of ethylene across the Cr-Cl bond. Also the vinyl alcohol and acetaldehyde precursors were found to arise from a direct attack of one of the carbon atoms of ethylene on an oxygen atom of CrO_2Cl_2 through a triplet intermediate. In the reactions of Cl_4MCH_2(M=Cr, Mo, W, Ru, Re) with ethylene it was found that the formation of the metallacyclobutane through formal [2+2] cycloaddition, a key step in the olefin metathesis reaction according to the Herrison-Chauvin mechanism, is a low-barrier process in each of the complexes studied. It was also found that the active species for the formation of the metallacyclobutane is a carbene complex and not a carbenoid complex. One key factor was found to be responsible for the difference in metathesis activity in these complexes: the stability of the carbenoid complexes relative to the carbenes. In Cr and Ru, the carbenoid complexes are more stable than the carbenes and thus Cl_4CrCH_2 and Cl_4RuCH_2 are likely to exist in the lower-

energy carbenoid Cl_3MCH_2Cl form as opposed to the carbene $Cl_4M{=}CH_2$ form. This is likely to deplete the reaction surface of the active species of the process, making Cl_4MCH_2(M=Cr, Ru) not suitable for olefin metathesis. This suggests that whereas Cl_4MCH_2 (M = Mo, W, Re) may catalyze olefin metathesis, Cl_4MCH_2 (M = Cr, Ru) may not. The W and Re complexes have been found to have greater metathesis activity than the Mo complex. In the $Cl_2(O)MCH_2$ (M=Mo, W, Re) complexes the metathesis reaction has favorable energetics and is found to be more feasible than the side-reactions studied while in the $Cl_2(O)MCH_2$(M=Cr, Ru) complexes, the olefin metathesis is found to be less favorable than the side reactions. In the transition-metal-assisted formation of 1,2-dinitrosoalkanes, it was found that the activation barriers for the one-step [3+2] addition pathway for the formation 1,2-dinitrosoalkanes are generally very low while the activation barriers for the [2+2] addition of the C=C bond of the olefins across the M-N bonds of $CpM(NO)_2$ (M=Co, Rh, Ir) to form an intermediate are generally very high. A transition state for the re-arrangement of the products of [2+2] addition to the products of [3+2] addition could not be located, indicating that the re-arrangement of the products of [2+2] addition by reductive elimination involving the second metal-nitrogen π-bond to form the observed 1,2-dintrosoalkanes as suggested in the work of Rappé and Upton may not be possible. Therefore it is concluded that the direct one-step [3+2] addition pathway proposed by Bergman and Becker for the formation of 1,2-dinitrosoalkanes is a more plausible pathway.

CHAPTER ONE

1.1 INTRODUCTION

Theoretical Chemistry is the subfield of chemistry where mathematical methods are combined with fundamental laws of physics to study processes of chemical relevance. The term *computational chemistry* is used when the mathematical method is sufficiently developed that it can be automated for implementation on a computer (Jensen, 2007; Helgaker, *et. al.*, 2000; Cramer, 2004; Leach, 2001).

Computational chemistry (also called molecular modeling) is critical in basic and applied molecular science research in areas which are relevant to the chemical, pharmaceutical, polymer and petroleum industries, and in nanotechnology and the environment. Molecular modeling methods are now routinely used to investigate the structure, dynamics and thermodynamics of inorganic, biological, and polymeric systems, encompassing such areas as protein folding, enzyme catalysis, protein stability, conformational changes associated with biomolecular function, molecular recognition of proteins, DNA, membrane complexes, materials science and catalysis, and rational drug design. Not only are these areas important to the needs of developed countries but they should also be of interest to emerging economies such as Ghana.

The key to theoretical chemistry is molecular quantum mechanics. Soon after its formulation (Schrödinger, 1926), it became clear that solution of the time-independent Schrödinger equation

$$H(\mathbf{r}; \mathbf{R})\, \Psi(\mathbf{r}; \mathbf{R}) = E(\mathbf{R})\, \Psi(\mathbf{r}; \mathbf{R})$$

could, in principle, lead to direct quantitative prediction of most, if not all, chemical phenomena (Dirac, 1929; Lewis, 1933). In the above equation $\Psi(\mathbf{r}; \mathbf{R})$ is the molecular wave function, which

depends explicitly on the 3*n* coordinates of all *n* electrons, and implicitly on the nuclear coordinates. (The implicit rather than explicit nuclear coordinate dependence is because the Born-Oppenheimer separation (Born and Oppenheimer, 1927) of (slow) nuclear motion from (fast) electronic motion has been made.) E(**R**) is the molecular energy, which depends parametrically on the nuclear positions. Hence, E(**R**) defines the potential energy surface (PES) obtained from solution of the Schrödinger equation subject to the Born-Oppenheimer approximation. **H**(**r**; **R**) is the molecular electronic Hamiltonian operator, subject to frozen nuclei, consisting of kinetic energy, electron-nuclear attraction, electron-electron repulsion and nuclear-nuclear repulsion terms. In atomic units, H has the explicit form

$$\boldsymbol{H(r;R)} = -\ \frac{1}{2}\sum_i^n\left(\frac{\partial^2}{\partial xi^2} + \frac{\partial^2}{\partial yi^2} + \frac{\partial^2}{\partial zi^2}\right) - \sum_i^n\sum_\alpha^A\frac{Z\alpha}{|ri - R\alpha|} + \frac{1}{2}\sum_i^n\sum_j^n\frac{1}{|ri - rj|} + \frac{1}{2}\sum_\alpha^A\sum_\beta^A\frac{Z\alpha Z\beta}{|R\alpha - R\beta|}$$

Quantum mechanics has had a remarkable success as a predictive tool in structure and reactivity studies of organic and organometallic systems. Quantum mechanical calculations can provide useful information concerning the shapes (geometries), the relative energies, and the frequencies of stationary points (usually minima and transition states) on the potential energy surface as well as the electron distribution in molecular species. The shape of a molecular species is one of its fundamental characteristics. It can, for example, provide clues to the existence of theoretical principles (why is it that benzene has six equal-length C-C bonds, but cyclobutadiene has two “short” and two “long” bonds (Carpenter, 1988)) or act as a guide to designing useful molecules (docking a candidate drug into the active site of an enzyme requires knowledge of the shapes of the drug and the active site (Vinter and Gardner, 1994)). The relative energies of molecular species is fundamental to a knowledge of their kinetic and thermodynamic behavior,

and this can be important in attempts to synthesize them. The vibrational frequencies of a molecule provide information about the electronic nature of its bonds, and prediction of the spectra represented by these frequencies may be useful to experimentalists. Calculation of the electron density distribution enables the prediction of the dipole moment, the charge distribution, the bond orders, and the shapes of various molecular orbitals. Thus, quantum mechanical calculations can furnish information about the mechanisms and product distributions of chemical reactions, either directly by examining the structures and relative energies of reaction transition states, or indirectly by modeling the steric and electronic demands of the reactants.

A theoretical approach is specifically well suited for studying trends, since calculations are not restricted by the normal limitations in the laboratory such as tedious preparations or faltering stabilities. Once the appropriate structures on the potential energy surface have been optimized, a reaction mechanism can always be mapped out by finding the lowest energy reaction path that connects the reactants to the products via suitable transition states and intermediates. Quantitative quantum chemical calculations leading directly to information about transition states and reaction mechanisms are now common, while qualitative (reactant-based) models will always be needed for systems which are too large to be subjected to the more rigorous treatments.

By their very nature, (transition-metal) organometallic reactions involve highly reactive species often not amenable to direct observation (Torrent *et. al*., 2000). The first use of Quantum Mechanics in studies of inorganic elementary reaction steps made use of several simplifying assumptions and only provided rather approximate solutions to the fundamental underlying equations. Best known is perhaps the use of crystal field theory (CFT) to rationalize observed trends in the rate of ligand substitution reactions involving transition metal complexes (Jordan,

1991; Atwood, 1997). Other approaches include the perturbational molecular orbital (PMO) theory (Dewar, 1965; Woodward and Hoffmann, 1970; Pearson, 1976; Albright *et. al*., 1985; Fukui, 1971) in which trends in rates are rationalized in terms of symmetry arguments (*ibid*.) and hardness and softness (Pearson, 1976) of the reactive centers on the reactants. Progress in both theory (software) and computer technology (hardware) has changed this state of affairs drastically in recent years. The last two decades have witnessed the establishment of quantum chemical methods as a standard tool for quantitative calculations of metal compounds, after numerous theoretical studies had proved that the calculated values are very accurate.

Two different quantum chemical methods have been proven to give geometries, bond energies, activation barriers, vibrational frequencies, and other chemically important properties of transition-metal organometallic compounds with an accuracy that is generally sufficient for synthetic chemistry. These are high-level *ab initio* methods and density functional theory (DFT) methods.

Most *ab initio* methods use Hartree-Fock (HF) theory as the starting point of the theoretical procedure (Helgaker, 2000; Szabo and Ostlund, 1989). However, the HF approximation can only be used if the electronically excited states are clearly higher in energy than the ground state. This is not always the case for transition-metal compounds, because the energy levels of the occupied and empty valence s and d orbitals are much closer to each other than the s and p valence orbitals of the main group elements (Davidson, 1989, 1991; Salahub and Zerner, 1989). Compounds of first row transition metals which have a partly filled d-shell require a multi-configuration self-consistent field (MCSCF) wave function instead of a Hartree-Fock wave function. MCSCF calculations are, however, much more expensive than HF calculations.

The calculation of relativistic effects is necessary to achieve accurate results for compounds of the second and particularly the third row transition metals, where relativistic corrections may become more important than correlation energy (Pyykkö, 1988). Relativistic effects are less important for the first row metals, except for Cu where the neglect of relativity may lead to significant errors (Pyykkö, 1988; Antes and Frenking, 1995). The accurate calculation of relativistic effects is achieved through approximate solutions of the Dirac equation, which for one-electron systems has the general form

$$H_D \mathbf{\Psi}(\mathbf{r}) = E\, \mathbf{\Psi}(\mathbf{r})$$

where $H_D = c\boldsymbol{\alpha}.\{\mathbf{p} + e\mathbf{A}(\mathbf{r})\} - e\emptyset(\mathbf{r}) + \boldsymbol{\beta}mc^2$

is the one-electron Dirac Hamiltonian. Here, $\boldsymbol{\alpha}$ and $\boldsymbol{\beta}$ are 4 x 4 matrices and the wave function $\mathbf{\Psi}$ is a four-component column matrix. The Dirac Hamiltonian to order υ^2/c^2 can be written (upon decoupling the particle and anti-particle solutions) as

$$H = H_s + \Delta H_{rel} + \Delta H_{so} + \Delta H_d$$

where H_s is the original Schrödinger Hamiltonian, ΔH_{rel} is the relativistic correction to the kinetic energy (the mass-velocity term), ΔH_{so} is the spin-orbit term and ΔH_d is the Darwin term. The mass-velocity term leads to a contraction of the s and p and decontraction of the d and f functions. Full four-component calculations are, however, too time-consuming to become practical for transition metal compounds that are important for synthetic purposes. The easiest and most common way of treating relativistic effects is the use of quasi-relativistic effective core potentials (ECPs) that are parametrized with respect to relativistic all-electron calculations of the atoms.

The last decades have seen tremendous development of density functional theory (DFT) methods. These methods combine the simplicity and general applicability of the Hartree-Fock method with the accuracy of correlated models that include the effects of connected doubles and triples. DFT includes electron correlation in its theoretical basis, in contrast to wave function methods, which must take correlation into account by add- ons to *ab initio* HF theory , or by parameterization in semi- empirical methods. DFT methods have become particularly popular for the calculation of transition metal compounds because the gradient-corrected (non-local) exchange and correlation functionals give results which have a comparable and frequently even higher accuracy than *ab initio* calculations, at a fraction of the computational expense (Torrent *et. al*., 2000). The most important parameter for a DFT calculation is the choice of the exchange and correlation functionals. The most common functionals which give good results for transition metals (Torrent *et. al*., 2000) are BP86 (Becke, 1988; Perdew, 1986), B3LYP (Becke, 1993; Lee, 1988; Stevens, 1994), B97 (Becke, 1997), B97-1, and HCTH (Hamprecht *et. al*, 1998). Relativistic effects can be considered in DFT calculations in the same way as in *ab initio* calculations by using relativistic ECPs. Approximate treatments of relativistic corrections have been developed (van Lanthe *et. al*, 1993, van Lanthe *et. al*, 1996). Among the DFT levels of theory considered appropriate for the treatment of relativistic effects in organometallic reactions is the B3LYP/LACVP* level of theory. The LACVP* basis set is a relativistic effective core-potential that describes the atoms H – Ar with the 6-31G* basis while heavier atoms are modeled with the LANL2DZ basis set which uses the all-electron valence double zeta basis set (D95V), developed by Dunning, for first row elements (Dunning and Hay, 1976) and the Los Alamos ECP plus double zeta basis set developed by Wadt and Hay for the atoms Na – La, Hf – Bi (Hay and Wadt, 1985a; 1985b; Wadt and Hay, 1985). An inherent drawback of DFT methods is the

fact that they contain empirical elements and cannot be systematically refined towards the exact solution like *ab initio* methods, making it difficult to establish, for a given chemical problem, the trustworthiness of the calculations or even to detect its failure.

Suitably parameterized semi-empirical molecular orbital schemes such as PM3(tm) (Wavefunction, 1993) have also been employed for the study of transition metal organometallic systems (Adei, 1996), but with the development of improved algorithms and far faster computers in recent times, the relative advantage of these over *ab initio* and DFT schemes has diminished considerably. Another important group of computational methods for calculating large transition metal complexes with bulky ligands consists of a combination of quantum chemical techniques with molecular mechanics methods (Woo *et. al*., 1998). Though these QM/MM methods appear promising, they cannot be considered as standard levels of theory yet.

Theoretical studies of organic reactions have, compared to organometallic systems, been much easier (Davidson, 1991). The application of quantum mechanics to organic chemistry dates back to Hückel's π- electron model of the 1930s (Hückel, 1931; 1932; 1937). Approximate quantum mechanical treatment for organic molecules continued throughout the 1950s and 1960s with, for example, Pariser-Parr-Pople (PPP) (Pople, 1953; Pariser and Parr, 1953), Complete Neglect of Differential Overlap (CNDO) (Pople *et.al*., 1965), Modified Neglect of Diatomic Overlap (MNDO) (Dewar and Thiel, 1977), and related models. Application of *ab initio* approaches, such as Hartree-Fock theory, began in the 1970s, flourished in the 1980s, with the development of computer codes that allowed for automated optimization of ground and transition states and incorporation of electron correlation using configuration interaction or perturbation techniques.

Table 1.1 gives a summary of the performance and cost of theoretical models employed in the treatment of organic and organometallic systems.

Table 1.1 Performance and Cost of Theoretical Models (Hehre, 2003)

			Density Functional		*Ab initio*		
Task	Molecular mechanics	Semi-empirical	EDF1	B3LYP	Hartree-Fock	LMP2	MP2
Geometry (organic)	Fair to good	Good	Good	Good	Good	N/A	Good
Geometry (transition metals)	Poor	Good	Good	Good	Poor	N/A	Fair
Transition-state geometry	N/A	Fair to good	Good	Good	Good	N/A	Good
Thermochemistry (non-isodesmic)	N/A	Poor	Good	Good	Fair to good	Good	Good
Thermochemistry (isodesmic)	N/A	Poor	Good	Good	Good	Good	Good
Cost	Very low	Low	Moderate	Moderate	Moderate	High	High

The remarkable evolution of organometallic chemistry, notably of the transition metals, over the last few decades, has enriched and transformed chemical science and technology to a degree and in ways that have been rarely matched throughout the history of chemistry. These include the discovery of radically new types of chemical compounds (Halpern, 1981), novel structures and binding modes, unprecedented reactivity patterns, unsuspected roles of organometallic chemistry in biology (Lenhart and Hodgin, 1961; Hodgin, 1965; Thauer, 1998, Ragsdale and Kumar, 1996), powerful new synthetic methodologies, new materials, and whole new classes of catalysts and catalytic processes of extraordinary versatility and selectivity.

Today, the field plays a pivotal role in the development of new technologies including the synthesis of pharmaceuticals, fuels, sensors, exhaust gas converters and industrial feedstock, the development of sustainable energy solutions and in the development of new materials ranging from novel polymers to nanomaterials. The olefin metathesis reaction for instance has opened new industrial routes to important petrochemicals, oleochemicals, polymers and specialty chemicals (Mol, 2004) and has gained widespread use in research and industry for making products ranging from medicines and polymers to enhanced fuels (Ivin and Mol, 1997).

Much of the conceptual framework of the field of organometallics has been laid in the course of the last few decades including the discovery of most of the basic metal-ligand combinations and elementary reaction steps that constitute the 'building blocks' of organometallic chemistry, recognition of the role of organometallics in biology, discovery of many important organometallic-based catalytic processes such as Ziegler-Natta catalysis, olefin metathesis, amination of alkenes through 1,2-dinitrosoalkane formation (Becker *et. al.*, 1980, Le Gall *et. al*., 1998), oxidation of alkenes by Cr(VI) oxo complexes (Goldberg and Ault, 2006), Wacker oxidation of ethylene, and rhodium-catalyzed carbonylation of methanol (Collman, 1987).

Notwithstanding the basic understanding of the mechanistic framework of organometallic reactions such as catalysis, the elucidation of the mechanisms of organometallic reactions continues to be an active field of research with many challenges to be surmounted. Increasingly detailed knowledge and understanding of such reaction pathways continue to be achieved through enhanced appreciation of the basic underlying chemistry, as well as increasingly powerful tools for elucidating elusive mechanistic details. Among the tools that are providing such important insights are *in situ* spectroscopic methods, notably infrared and NMR, for

identifying and structurally characterizing species present in solution, fast reaction methods such as flash photolysis that permit the detection of short-lived transient species and determination of the rates of their reactions in real time (Boese, 1997), application of the chemically induced dynamic nuclear polarization (CIDNP) technique that permits identification of intermediates that do not accumulate in sufficiently high concentrations to be detected directly (Sweany and Halpern, 1977) and, as has been noted above, quantum mechanical calculations which provide information about the geometries, relative energies, electron distribution and vibrational frequencies of stable and transient molecular species involved in reactions. An understanding of the detailed mechanistic pathways of organometallic reactions will drastically increase the ability to design and "fine tune" catalytic activities and selectivities, find new ways to extend and exploit these groundbreaking discoveries and, thereby, sustain the importance, distinctiveness and vitality of the field.

REFERENCES

Adei, E. (1996) Semi-empirical PM3(tm) Exploration of Some Elementary Transition Metal Organometallic Reactions; *Ph.D. Dissertation*, UC, Irvine, CA.

Albright, T. A.; Burdett, J. K.; Whangbo, M.-H. (1985) Orbital Interactions in Chemistry; John Wiley and Sons, New York.

Antes, I.; Frenking, G. (1995) Theoretical studies of organometallic compounds. XIV. Structure and bonding of the transition metal methyl and phenyl compounds MCH_3 and MC_6H_5(M = Cu, Ag, Au) and $M(CH_3)_2$ and $M(C_6H_5)_2$ (M = Zn, Cd, Hg). *Organometallics* 14: 4263 – 4268.

Atwood, J. D. (1997) Inorganic and Organometallic Reaction Mechanisms; VCH, New York.

Becke, A. D. (1988) Density-functional exchange-energy approximation with correct asymptotic behavior *Phys*. *Rev*. *A*. 38, 3098.

Becke, A. D. (1993) Density-functional thermochemistry. III. The role of exact exchange. *J*. *Chem*. *Phys*. 98: 5648.

Becke, A. D. (1997) Density-functional thermochemistry. V. Systematic optimization of exchange-correlation functionals. *J*. *Chem*. *Phys*. 107: 8554.

Becker, P. N.; White, M. A.; Bergman, R. G. (1980) A new method for 1,2-diamination of alkenes using cyclopentadienylnitrosylcobalt dimer/NO/$LiAlH_4$. *J. Am. Chem. Soc.* 102: 5676 – 5677.

Boese, W.; Farlane, K. M.; Rabor, J.; Ford, P. C. (1997) Photochemistry as a tool for elucidating organometallic reaction mechanisms. *Coord. Chem. Rev*. 159: 135 – 151.

Born, M.; Oppenheimer, J. R. (1927) Zur Quantentheorie der Moleküle. *Ann. Phys.* 84: 457 – 484.

Carpenter, B. K. (1988) In: Advances in Molecular Modeling; D. Liotte (Ed.) JAI Press Inc., Greenwich, Connecticut.

Collman, J. P.; Hegedus, L.S.; Finke, R.G. (1987) Principles and Applications of Organo-transition Metal Chemistry; University Science Books, Mill Valley, CA.

Cramer, C. J. (2004) Essentials of Computational Chemistry. Theories and Models, 2nd ed.; John Willey and Sons, Ltd., Chichester.

Davidson, E. R. (1989) The Challenge of d and f electrons; Salahub, D. R. and Zerner, M. C. (eds.) ACS Symposium, Washington, D.C., 157.

Davidson, E. R. (1991) Quantum Theory of Matter: Introduction. *Chem. Rev*. 91: 649.

Dewar, M. J. S. (1965) Molecular Orbital Theory for Organic Chemists. *Adv. Chem. Phys*. 8: 65.

Dewar, M. J. S.; Thiel, W. (1977) Ground states of molecules. 38. The MNDO method. Approximations and parameters. *J. Am. Chem. Soc*. 99: 4899 – 4904.

Dirac, P. A. M. (1929) Quantum Mechanics of Many-Electron Systems. *Proc. Roy. Soc. (London)* 123: 714-733.

Dunning, T. H., Jr.; Hay, P. J. (1976) In: Modern Theoretical Chemistry, H. F. Schaefer, III,; Plenum, New York, Vol. 3.

Fukui, K. (1971) Recognition of stereochemical paths by orbital interaction. *Acc. Chem. Res*. 4: 57 – 64.

Goldberg, N.; Ault, B. S. (2006) A matrix isolation study of the reactions of $OVCl_3$ with a series of silanes. *J. Mol. Struct.* 787: 203 – 208.

Halpern, J. (1981) Mechanistic aspects of homogeneous catalytic hydrogenation and related processes. *Inorg. Chim. Acta* 50: 11 – 19.

Hamprecht, F. A.; Cohen, A. J.; Tozer, D. J.; Handy, N. C. (1998) Development and assessment of new exchange-correlation functionals. *J. Chem. Phys*. 109: 6264.

Hay, P. J.; Wadt, W, R. (1985) *Ab initio* effective core potentials for molecular calculations. Potentials for the transition metal atoms Sc to Hg. *J. Chem. Phys*. 82: 270.

Hay, P. J.; Wadt, W, R. (1985) *Ab initio* effective core potentials for molecular calculations. Potentials for K to Au including the outermost core orbitals. *J. Chem. Phys*. 82: 299.

Hehre, W. J. (2003) A Guide to Molecular Mechanics and Quantum Chemical Calculations; Wavefunction, Inc., Irvine, CA.

Helgaker, T.; Jørgensen, P.; Olsen, J. (2000) Molecular Electronic-Structure Theory; John Willey and Sons, Ltd; Chichester.

Hodgkin, D. C. (1965) The Structure of the Corrin Nucleus from X-ray Analysis. *Proc. Roy. Soc.* (*London*) A288: 294 – 305.

Hückel, E. *Z.* (1931) Quantentheoretische beitrage zum benzolproblem. I. Die elektronen- konfiguration des benzols und verwandter beziehungen. *Physik* 70: 204 – 2864.

Hückel, E. *Z.* (1932) Quantentheoretische beiträge zum problem der aromatischen und ungesättigten erbindungen. III. *Z. Phys.* 76: 628 – 48.

Hückel, E. *Z.* (1937) The theory of unsaturated and aromatic compounds. *Elektrochem. Angew. Physik Chem*. 42: 752 and 827.

Ivin, K. J.; Mol, J. C. (1997) Olefin Metathesis and Metathesis Polymerization; Academic Press, San Diego, CA.

Jensen, F. (2007) Introduction to Computational Chemistry, 2nd ed.; John Willey and Sons, Ltd., Chichester.

Jordan, R. (1991) Reactions of Inorganic and Organometallic Systems; Oxford University Press, Oxford.

Le Gall, T.; Mioskowski, C.; Lucet, D. (1998) The Chemistry of Vicinal Diamines. *Angew. Chem., Int. Ed.* 37: 2580 – 2627.

Leach, A. R. (2001) Molecular Modelling. Principles and Applications, 2nd ed.; Prentice Hall, Harlow, England.

Lee, C.; Yang, W.; Parr, R. G. (1988) Development of the Colle-Salvetti correlation-energy formula into a functional of the electron density. *Phys. Rev. B.* 37: 785.

Lenhart, P. G.; Hodgkin, D. C. (1961) Structure of the 5,6-Dimethylbenzimidazolyl cobamide Coenzyme. *Nature* 192: 937 – 938.

Lewis, G. N. (1933) The Chemical Bond. *J. Chem. Phys.*1: 17.

Mol, J. C. (2004) Industrial applications of olefin metathesis. *J. Mol. Catal. A: Chemical* 213: 39 – 45.

Pariser, R.; Parr, R. G. (1953) A semi-empirical theory of the electronic spectra and electronic structure of complex unsaturated molecules. I. *J. Chem. Phys.* 21: 466.

Pearson, R. G. (1976) Symmetry Rules for Chemical Reactions; John Wiley and Sons, New York.

Perdew, J. P. (1986) Density-functional approximation for the correlation energy of the inhomogeneous electron gas. *Phys. Rev. B.* 33: 8822.

Pople, J. A. (1953) Electron interaction in unsaturated hydrocarbons. *Trans. Faraday Soc.* 49: 1375.

Pople, J. A.; Santry, D. P.; Segal, G. A. (1965) Approximate self-consistent molecular orbital theory. I. Invariant procedures. *J. Chem. Phys.* 43: S129.

Pyykkö, P. (1988) Relativistic effects in structural chemistry. *Chem. Rev.* 88: 563 – 594.

Ragsdale, S. W.; Kumar, M. (1996) Nickel-containing carbon monoxide dehydrogenase/ acetyl-CoA synthase. *Chem. Rev.* 96: 2515 – 2540.

Salahub, D. R.; Zerner, M. C. (1989) The Challenge of d and f electrons; Salahub, D. R. and Zerner, M. C. (eds.) ACS Symposium, Washington, D.C.

Schrödinger, E. (1926) Quantisierung als Eigenwertproblem (Erste Mitteilung). *Ann. Phys.* 79: 361 – 376.

Spartan, Wavefunction, Inc.; 18401 Von Karman Ave., # 370, Irvine, CA, 92715, USA.

Stevens, P. J.; Delvin, F. J.; Chablowski, C. F.; Frisch, M. J. (1994) *Ab initio* calculation of vibrational absorption and circular dichroism spectra using density functional force fields
J. Phys. Chem. 98: 11623 – 11627.

Sweany, R. L.; Halpern, J. (1977) Hydrogenation of α-methylstyrene by hydridopentacarbonylmanganese (I). Evidence for a free-radical mechanism. *J. Am. Chem. Soc.* 99: 8335 – 8337.

Szabo, A.; Ostlund, N. S. (1989) Modern Quantum Chemistry. Introduction to

Advanced Electronic Structure Theory; McGraw-Hill, New York.

Thauer, R. K. (1998) Biochemistry of methanogenesis: A tribute to Marjory Stephenson: 1998
Marjory Stephenson Prize Lecture. *Microbiology*; 144, 2377 – 2406.

Torrent, M.; Solá, M.; Frenking, G. (2000) Theoretical Studies of Some Transition-Metal-Mediated Reactions of Industrial and Synthetic Importance. *Chem. Rev*. 100: 439 – 494.

Van Lenthe, E.; Baerends, E. J.; Snijders, J. G. (1993) Relativistic regular two-component Hamiltonians. *J. Chem. Phys*. 99: 4597.

Van Lenthe, E.; Snijders, J. G.; Baerends, E. J. (1996) The zero-order regular approximation for relativistic effects: The effect of spin–orbit coupling in closed shell molecules. *J. Chem. Phys*. 105: 6505.

Vinter, J. L.; Gardner, M. (1994) Molecular Modelling and Drug Design; Macmillan, London.

Wadt, W. R.; Hay, P. J. Hay (1985) *Ab initio* effective core potentials for molecular calculations. Potentials for main group elements Na to Bi. *J. Chem. Phys*. 82: 284.

Woo, T.; Cavallo, L.; Ziegler, T. (1998) Implementation of the IMOMM Methodology for Performing Combined QM/MM Molecular Dynamics Simulations and Frequency Calculations. *Theor. Chim. Acta* 100: 307 – 313.

Woodward, R. B.; Hoffmann, R. (1970) The Conservation of Orbital Symmetry; Verlag Chemie, Berlin.

CHAPTER TWO

DENSITY FUNCTIONAL THEORY STUDIES OF THE MECHANISMS OF OXIDATION OF ETHYLENE BY CHROMYL CHLORIDE

2.1 INTRODUCTION

The oxidation of alkenes by transition metal oxo species such as OsO_4, RuO_4, MnO_4^- and Cr(VI) oxo complexes is of central importance in preparative organic chemistry. Oxidations carried out in this way are often relatively gentle and remarkably specific compared to the direct

application of elemental oxygen (Goldberg and Ault, 2006).

A number of mechanistic questions surrounding the reaction of transition metal oxo complexes with alkenes remain unresolved, despite having been the subject of extensive experimental and theoretical studies (Sharpless *et. al*., 1977; Freeman, 1975; Samsel *et. al*., 1985; Rappé and Goddard, 1980a; 1980b; 1982a; 1982b; Upton and Rappé, 1985). Mechanistic proposals put forward in the past to explain the interaction of transition metal oxo units with C-C π bonds have often been untested by experiment and based on limited precedent. An understanding of the mechanism of oxidation of alkenes by Cr(VI) oxo species has been hindered by the fact that diverse solvents and ligands have been utilized in the various experimental studies reported, and these factors can have dramatic effects on the course of the reaction (Walba *et. al*., 1984).

A well-known example of the mechanistic dilemma of olefin oxidation is the bishydroxylation of alkenes by OsO_4, $KMnO_4$ and related species. Criegee *et. al*. (1936; 1942) proposed a concerted [3+2] cycloaddition pathway (path A in Scheme 2.1). This proposal won wide acceptance among organic chemists (Corey *et. al*., 1989; 1993; Schröder, 1980), in part due to the ease with which analogy can be drawn with other dipolar cycloadditions. Theoretical work also suggested that such a hypothesis is consistent with calculations on species presumably lying on the reaction coordinate (Jorgensen and Hoffmann, 1986; Wu, 1992). The formal product of the [3+2] addition, a five membered metallacycle (osma-2,5-dioxolane), was experimentally characterized, which upon hydrolysis gives diols (Schröder, 1980).

Scheme 2.1 Possible pathways for the Reaction of $LnMO_2$ with Alkene (Gable and Phan, 1994).

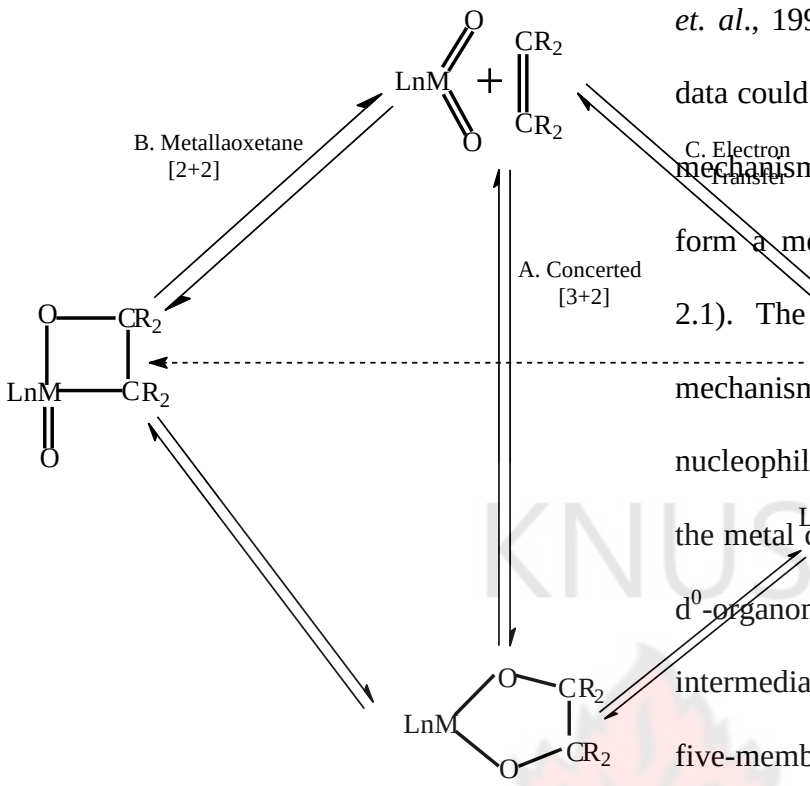

Unlike OsO_4 and $KMnO_4$ which react with olefins to form predominantly diols without significant epoxide formation, chromyl chloride reacts with alkenes to form predominantly epoxides, without diol formation (Schröder, 1980) as might be expected from path A of Scheme 2.1. The concerted [3+2] pathway was thus challenged by Sharpless and co-workers (Sharpless *et. al*., 1977; Hentges and Sharpless, 1980; Nortey *et. al*. 1994; Nortey *et. al*., 1996), who asserted that all known data could easily be explained by a stepwise mechanism involving [2+2] cyclization to form a metallaoxetane (path B of Scheme 2.1). The underlying assumption of this mechanism is that the olefin, albeit a weak nucleophile, always interacts initially with the metal center, followed by formation of a d^0-organometallic intermediate. The intermediate subsequently rearranges to the five-membered metallacycle.

Wallis and Kochi (1988a, 1988b) have also proposed a third mechanism (path C in Scheme 2.1) to explain the oxidation of olefins by oxo transition metal complexes. It involves an initial electron transfer, and addition of the odd electron intermediate to give a metallaoxetane and/or metalladiolate.

In Scheme 2.2, the two reaction pathways (A and B), which were suggested to arise from the π- complex **2**, lead to the formation of the Cr(IV) organometallic intermediates. In path A, there is alkene insertion into the Cr-Cl bond (cis-

chlorometalation) to give the alkylchromium intermediate **3**. The dichloride **5** and the chromium derivative of the dichlorohydrin **6** are subsequently generated from **3** by reductive elimination (path a) and by migration of the alkyl group from the chromium to the oxygen (path a'), respectively. The four-membered ring intermediate **4**, formed via [2+2] cycloaddition from the π-complex **2** in path B, leads to the formation of either the chlorohydrin precursor **6** (path b) or the epoxide precursor **7** (path b'). Sharpless *et. al.* (1977) reasoned that the formation of the organometallic intermediate in Scheme 2.2 could rationalize the primary products of epoxides, chlorohydrins and dichlorides formed from cis-addition of ethylene to chromyl chloride (Scheme 2.3).

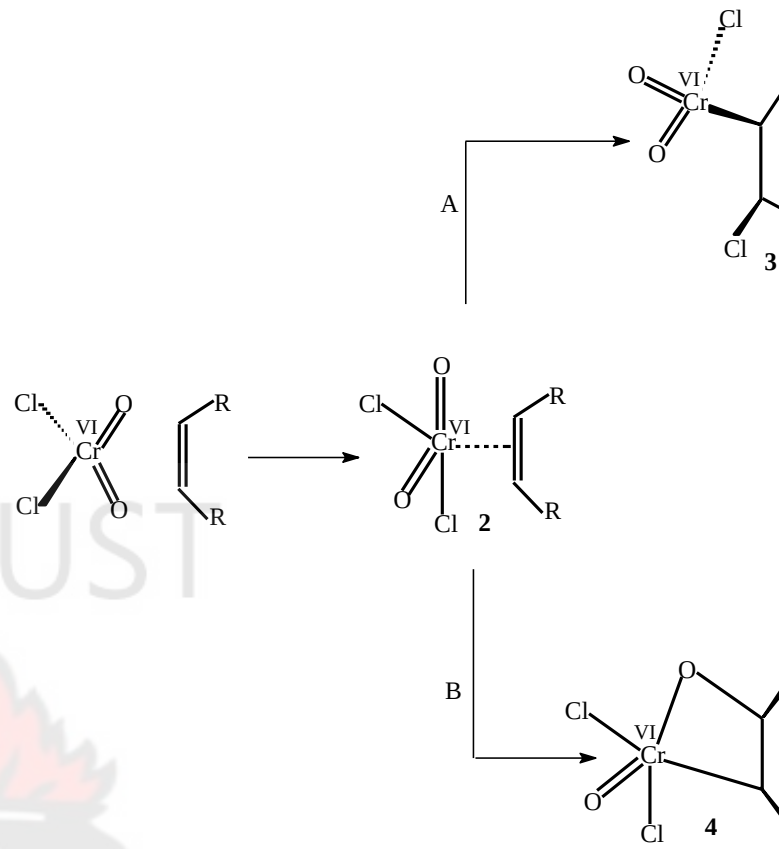

Scheme 2.2 Proposed Mechanism for Reaction of Cl_2CrO_2 with Olefins Involving Organometallic Intermediates (Sharpless *et. al.*, 1977).

Evidence for the stepwise mechanism was provided by nonlinear Eyring plots of enantioselectivity as a function of the reciprocal of temperature for asymmetric dihydroxylations (Göbel and Sharpless, 1993). Support for the [2+2] addition in the oxidation of olefins by chromyl chloride was provided by Rappé and Goddard (1980, 1982a, 1982b) in a theoretical work on olefin oxidations.

Scheme 2.3 Mechanism Involving Direct Attack on the Heteroatom Ligands (Sharpless *et. al.*, 1977).

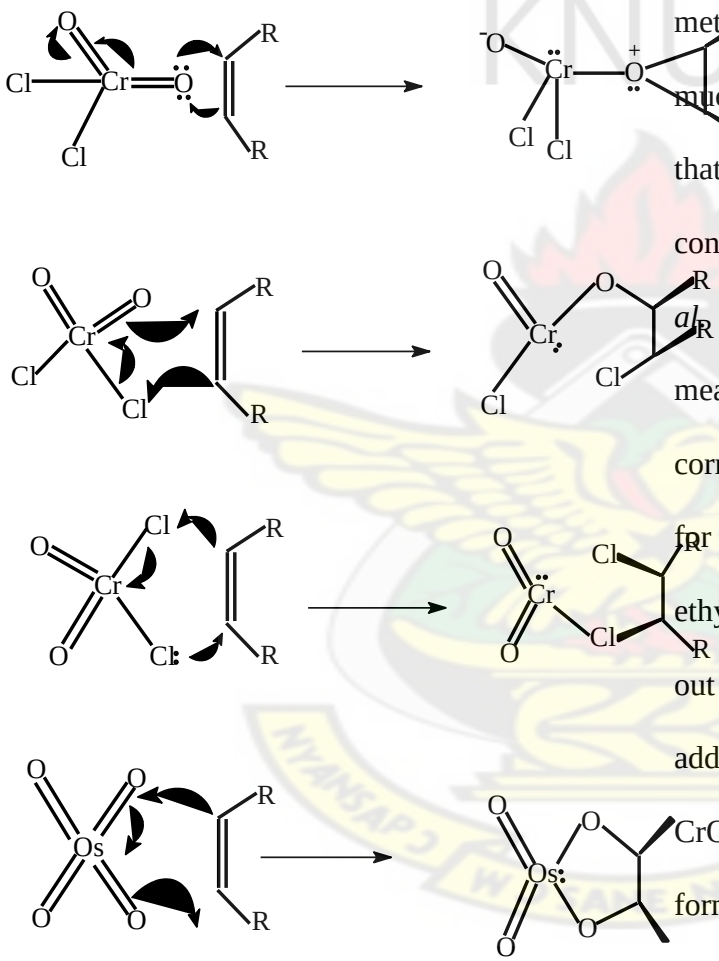

Pidun *et. al*. (1996), Dapprich *et. al*. (1996) and Torrent *et. al.* (1997) computed the [2+2] and [3+2] activation barriers for the reaction of OsO_4 with ethylene and found that the activation energy of the [2+2] addition to form the four-membered cyclic metallaoxetane was very high (> 39 kcal mol^{-1}) whereas the activation energy for the [3+2] addition to form the five-membered metallacycle (osma-2,5-dioxolane) was much smaller (<10 kcal mol^{-1}), indicating that the addition reaction follows the concerted [3+2] mechanism. Del Monte *et. al.* (1997) also compared computed and measured kinetic isotope effects and corroborated the concerted reaction pathway for the addition reaction of OsO_4 with ethylene. Torrent *et. al*. (1998) also carried out DFT calculations on the [2+2] and [3+2] addition of ethylene to Cr=O bonds in CrO_2Cl_2 and found the [3+2] addition to form the five-membered metallacycle to be more favorable than the [2+2] addition to form the four-membered cyclic chromaoxetane. In another study, Torrent *et. al.* (1999) found that contrary to earlier assumptions (Sharpless *et. al.*, 1977), the

formation of the epoxide precursor from the reaction between CrO_2Cl_2 and ethylene does not involve a chromaoxetane intermediate derived from [2+2] cycloaddition to the Cr=O linkage but rather an ester intermediate derived from [3+2] addition of ethylene to the chromium-oxygen bonds in CrO_2Cl_2. Torrent *et. al.* (1999) also concluded that the chlorohydrins should arise from a [3+2] cycloaddition. In matrix isolation experiments, Limberg *et. al.* (1998, 1999) have produced IR-spectroscopic proof for O=$CrCl_2$-epoxide and O=CrCl-acetaldehyde complexes as primary products in olefin oxidation with chromyl chloride (CrO_2Cl_2).

In this work, the reaction between CrO_2Cl_2 and ethylene leading ultimately to the formation of ethylene oxide (epoxide), 1,2-chlorohydrin, 1,2-dichloroethane, vinyl alcohol and acetaldehyde (Schemes 2.4 and 2.5) is studied theoretically using hybrid density functional theory. The geometries and relative energies of the reactants, transition states, relevant intermediates and products are computed to help provide insight into the mechanistic channel of these reactions.

Scheme 2.4 Mechanisms of the CrO_2Cl_2-mediated formation of epoxide, acetaldehyde and vinyl alcohol

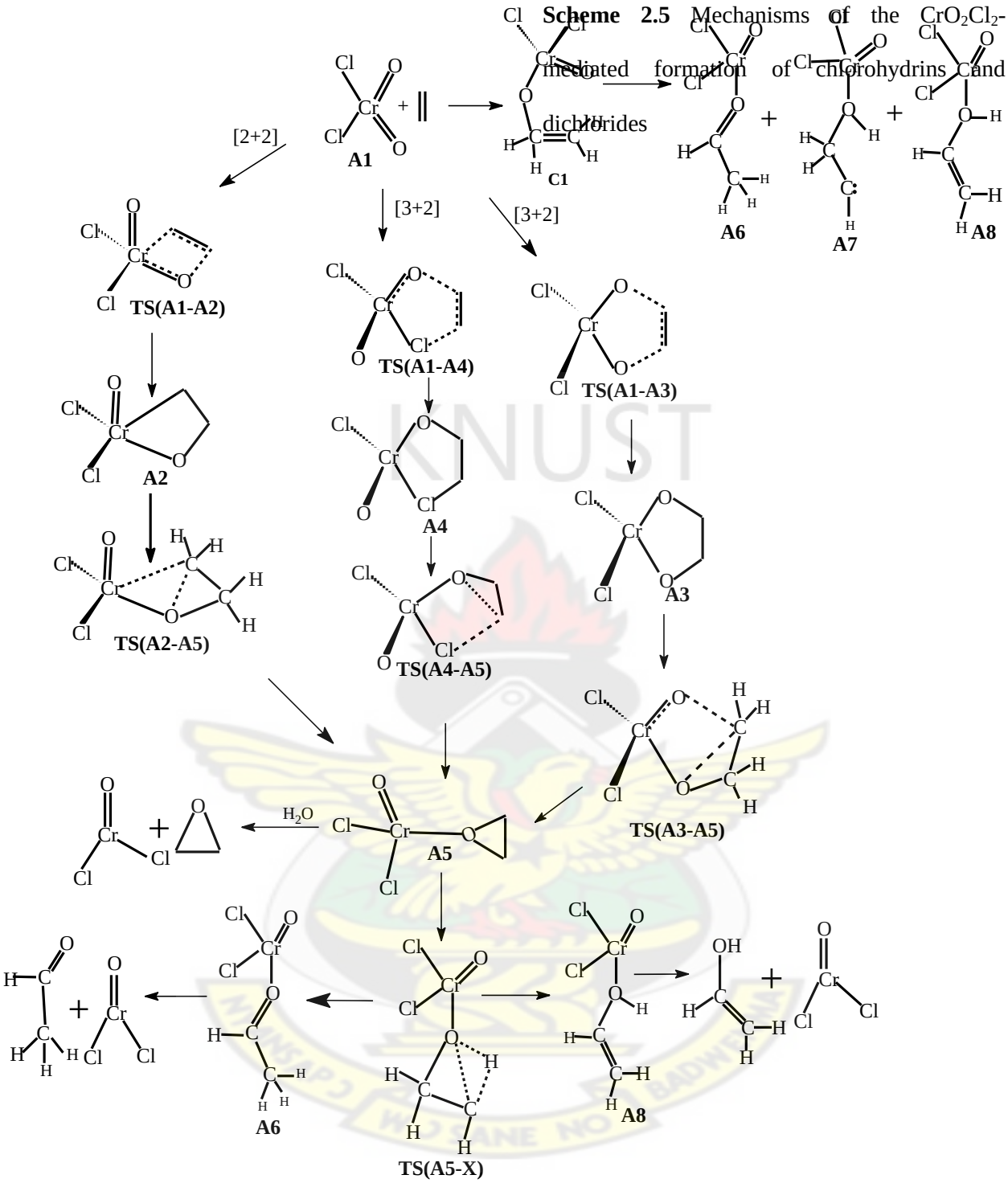

Scheme 2.5 Mechanisms of the CrO_2Cl_2-mediated formation of chlorohydrins and dichlorides

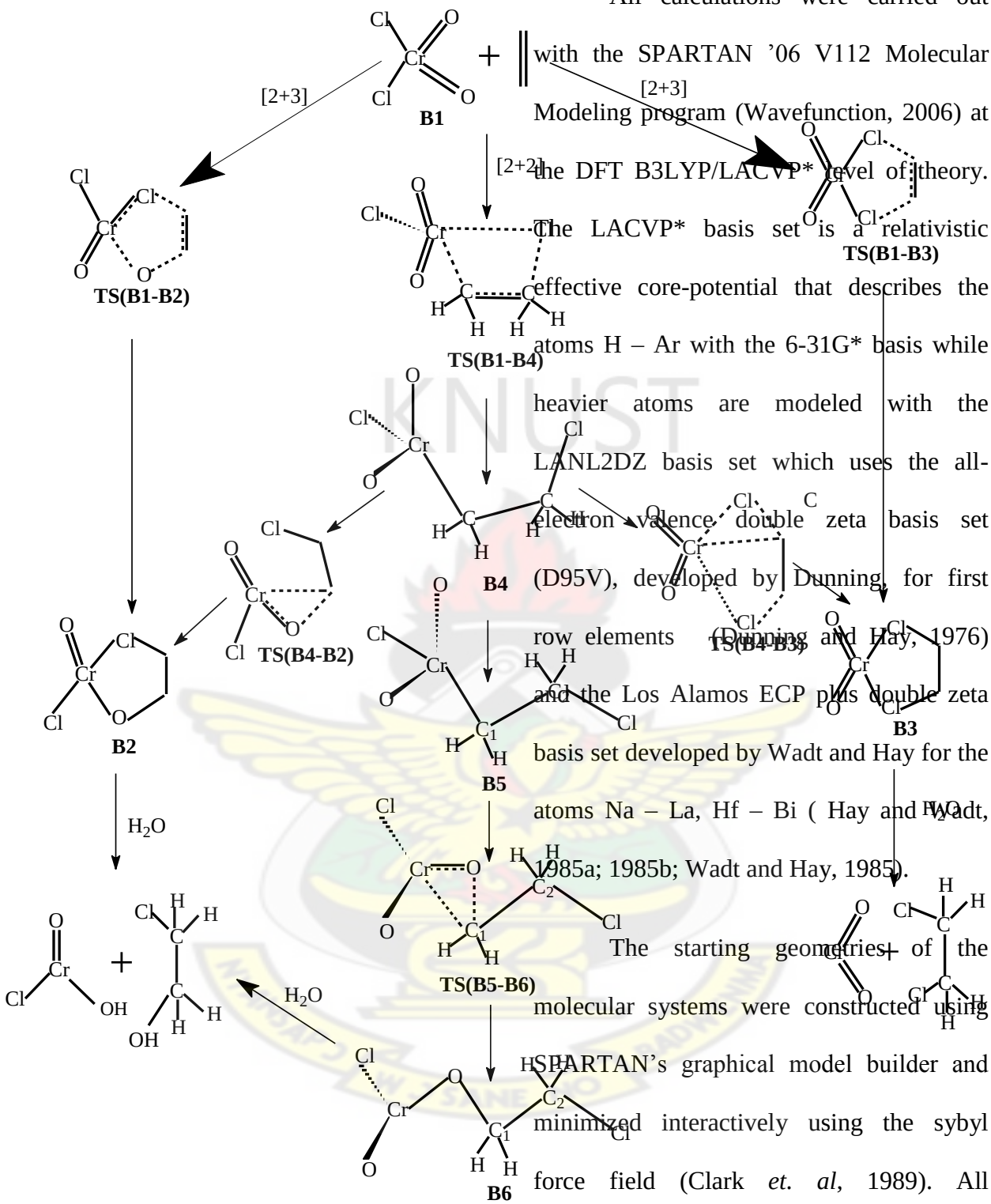

All calculations were carried out with the SPARTAN ’06 V112 Molecular Modeling program (Wavefunction, 2006) at the DFT B3LYP/LACVP* level of theory. The LACVP* basis set is a relativistic effective core-potential that describes the atoms H – Ar with the 6-31G* basis while heavier atoms are modeled with the LANL2DZ basis set which uses the all-electron valence double zeta basis set (D95V), developed by Dunning, for first row elements (Dunning and Hay, 1976) and the Los Alamos ECP plus double zeta basis set developed by Wadt and Hay for the atoms Na – La, Hf – Bi (Hay and Wadt, 1985a; 1985b; Wadt and Hay, 1985).

The starting geometries of the molecular systems were constructed using SPARTAN’s graphical model builder and minimized interactively using the sybyl force field (Clark *et. al*, 1989). All geometries were fully optimized without any symmetry constraints. The optimized geometries were subjected to full frequency

2.2 DETAILS OF CALCULATIONS

calculations to verify the nature of the stationary points. Equilibrium geometries were characterized by the absence of imaginary frequencies. The transition state structures were located by a series of constrained geometry optimizations in which the forming- and breaking-bonds were fixed at various lengths while the remaining internal coordinates were optimized. The approximate stationary points located from such a procedure were then fully optimized using the standard transition state optimization procedure in SPARTAN. All first-order saddle-points were shown to have a Hessian matrix with a single negative eigenvalue, characterized by an imaginary vibrational frequency along the reaction coordinate. All the computations were performed on Dell Precision T3400 Workstation computers.

2.3 RESULTS AND DISCUSSION

The DFT geometry optimization of the Cl_2CrO_2 reactant on the singlet PES gave a structure **A1** (Scheme 2.4 and Figure 2.1) with C_{2v} symmetry, in agreement with experiment (Marsden and Hedberg, 1982). The two Cr=O double bonds are each 1.555 Å long and 108.55^o apart. These values are in good agreement with the experimentally estimated values of 1.581 Å and 108.5^o (Marsden and Hedberg, 1982) and the calculated values of 1.571 Å and 108.7^o respectively (Torrent, 1999). The two Cr-Cl bonds are each 2.114 Å long and 111.27^o apart. These values are also in good agreement with the experimentally determined values of 2.126 Å and 113.3^o respectively (Marsden and Hedberg, 1982) and the calculated values of 2.104 Å and 112.0^o respectively (Torrent, 1999). A triplet **A1** (**A1/t**) has been computed to be 38.03 kcal mol^{-1} less stable than the singlet **A1**.

The interaction of the Cl_2CrO_2 and ethylene apparently does not lead to a π-bonded complex. An extensive search of the

singlet and triplet PES in an attempt to locate a π-bonded complex proved unsuccessful. This notwithstanding, its existence cannot be definitely ruled out, keeping in mind the well-known difficulties for DFT methods to describe weak interactions (Kristán and Pulay, 1994; Wright, 1996; Peréz-Jordå and Becke, 1995; Ruiz *et. al*., 1986; Garcia *et. al*., 1997; Mourik and Gdanitz, 2002; Mourik, 2008).

2.3.1 FORMATION OF EPOXIDE

In most mechanistic studies, the species **A5** (Scheme 2.4 and Fig. 2.1) has been invoked as the direct precursor for epoxide. This species was postulated by Sharpless *et. al.* (Sharpless *et. al.*, 1977) as the immediate precursor of epoxide and by Limberg *et .al*. (1998) as the oxirane adduct intermediate leading to acetaldehyde. Limberg and Köppe (1999) isolated the propylene analogue of **A5** in the reaction between CrO_2Cl_2 and propylene.

Species **A5** could in principle arise from four separate pathways:

(1) a two-step process involving [2+2] addition of ethylene across the Cr=O bond of CrO_2Cl_2

(2) a two-step process involving [3+2] addition of ethylene across the two oxygen atoms of CrO_2Cl_2

(3) a two-step process involving [3+2] addition of ethylene across the oxygen and chlorine atoms of CrO_2Cl_2 (all shown in Scheme 2.4), and

(4) a one-step direct addition of ethylene to one oxygen atom of CrO_2Cl_2.

No transition state was located linking the reactants and the epoxide precursor **A5** through the direct addition pathway on the singlet and triplet PES, despite an exhaustive search of the surfaces. On the basis of this, the direct addition pathway is considered a very unlikely route for epoxide formation. A triplet intermediate **C1/t** which

is 0.12 kcal mol^{-1} endothermic was located and is thought to most likely arise from a direct attack of one of the olefinic carbons on an oxygen atom of CrO_2Cl_2. This intermediate re-arranges through a triplet transition state **TS[C1-A3]**, with an activation barrier of 2.11 kcal mol^{-1}, to the ester complex intermediate **A3/t**. However, the transition state for the formation of **C1/t** has not been located.

Energies of the optimized molecular structures (Figures 2.1 and 2.2) obtained for the formation of epoxide and acetaldehyde precursors in Scheme 2.4 are summarized in the energy profile in Figure 2.3. Table 2.1 provides the imaginary frequencies (in cm^{-1}) of the first-order saddle points found in the suggested mechanism for the formation of the epoxide, acetaldehyde, dichloride and chlorohydrin precursors.

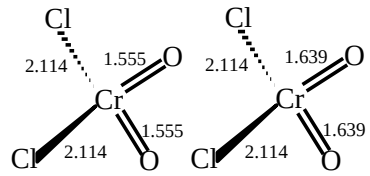

A1

A1/t

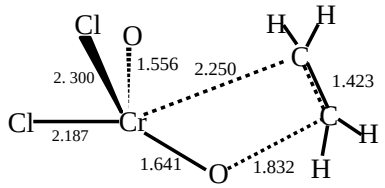

TS(A1-A2)

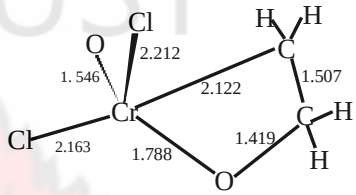

A2

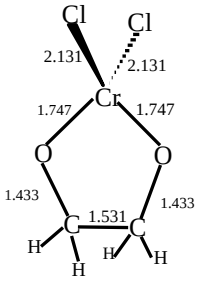

A3

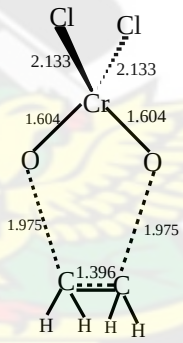

TS(A1-A3)

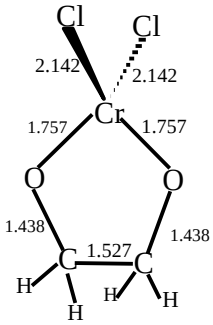

A3/t

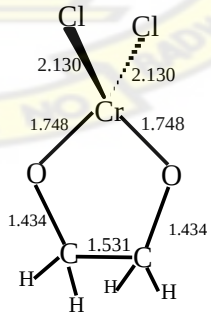

A3/os

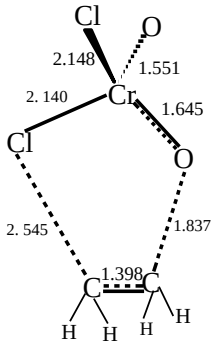

TS(A1-A4)

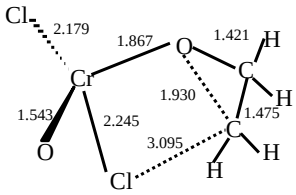

TS[A4-A5]

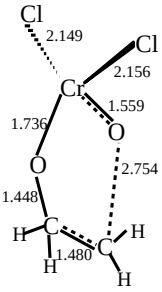

TS[C1-A3]/t

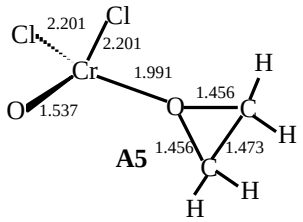

A5

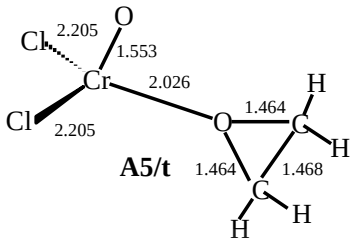

A5/t

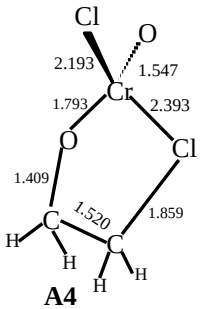

A4

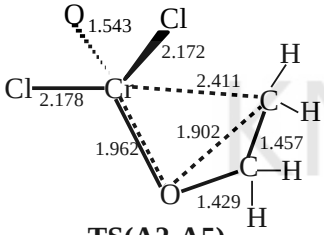

TS(A2-A5)

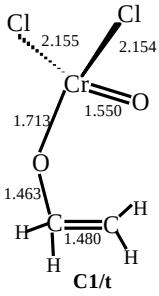

C1/t

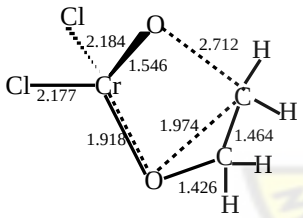

TS(A3-A5)

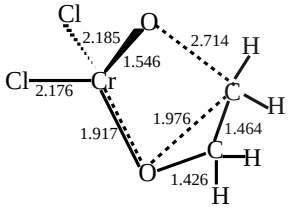

TS(A3-A5)/os

Figure 2.1. Optimized geometrical parameters of the main stationary points involved in the [2+2] and [3+2] addition reaction between CrO_2Cl_2 and ethylene for the formation of the epoxide precursor (t = triplet state, os = open-shell singlet state). Distances in Å and angles in degrees.

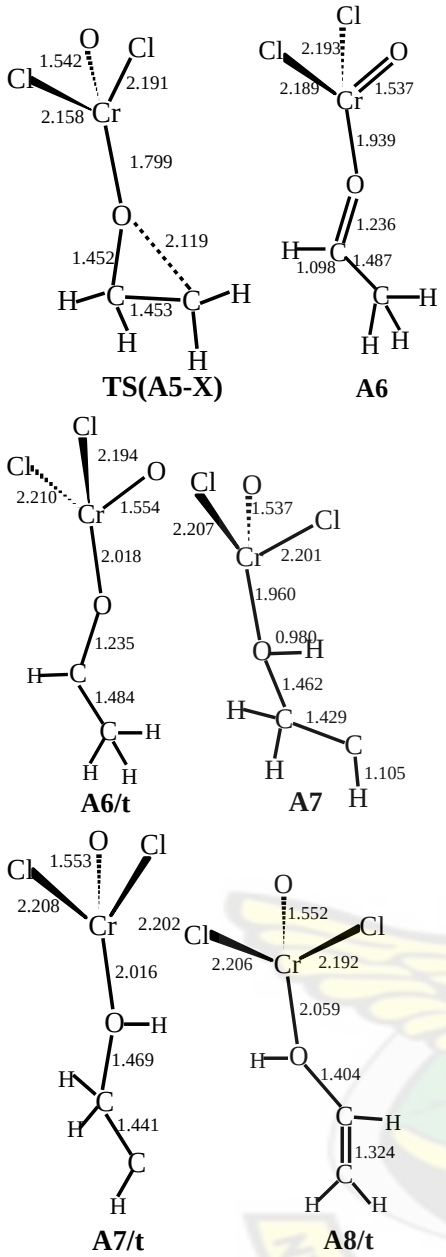

Figure 2.2. Optimized geometrical parameters (in Å) of the stationary points on epoxide ring-opening.

Table 2.1. Imaginary Frequencies (in cm^{-1}) of all First-order Saddle Points Involved in the Suggested Mechanisms for the Formation of Epoxide, Acetaldehyde, Dichloride and Chlorohydrin Precursors.

transition state[a]	freq.
TS[A1-A2]	437.36*i*
TS[A1-A3]	432.39*i*
TS[A1-A4]	421.80*i*
TS[A2-A5]	430.71*i*
TS[A3-A5]	413.40*i*
TS[A4-A5]	402.50*i*
TS[A5-X]	294.23*i*
TS[B1-B2]	421.80*i*
TS[B1-B4]	207.99*i*
TS[B1-B3]	282.89*i*
TS[B4-B3]	332.10*i*
TS[B4-B2]	465.88*i*
TS[B5-B6]	462.07*i*

[a]computed on a singlet PES

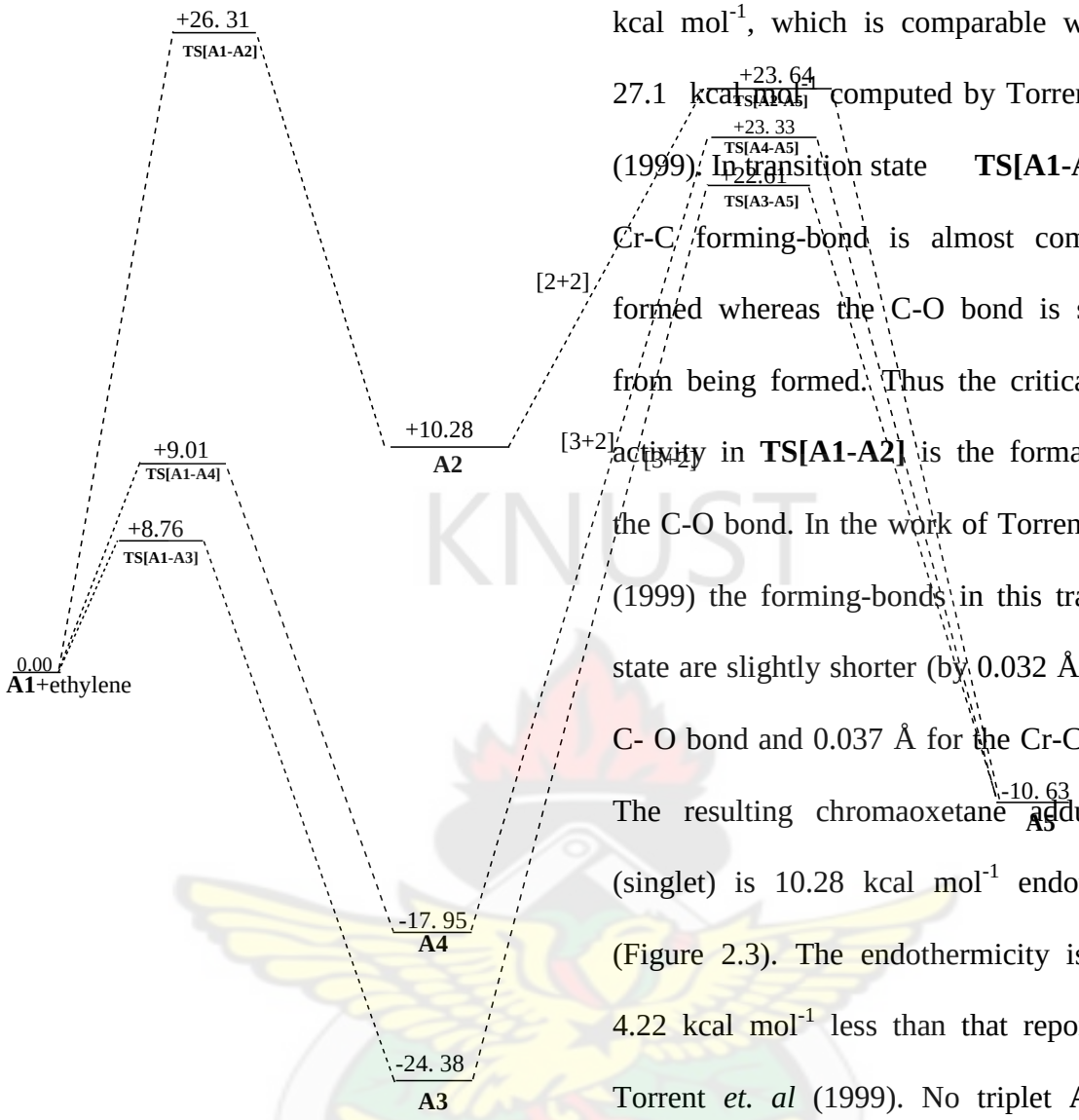

Figure 2.3. Reaction profile of the three suggested mechanisms for the formation of the epoxide precursor from the addition of CrO_2Cl_2 to ethylene on the singlet PES. Energy in kcal mol^{-1}.

The activation barrier for the [2+2] addition of ethylene across the Cr-O bonds of CrO_2Cl_2 leading to the chromaoxetane **A2** through transition state **TS[A1-A2]** is 26.31 kcal mol^{-1}, which is comparable with the 27.1 kcal mol^{-1} computed by Torrent *et.al.* (1999). In transition state **TS[A1-A2]**, the Cr-C forming-bond is almost completely formed whereas the C-O bond is still far from being formed. Thus the critical bond activity in **TS[A1-A2]** is the formation of the C-O bond. In the work of Torrent *et. al.* (1999) the forming-bonds in this transition state are slightly shorter (by 0.032 Å for the C- O bond and 0.037 Å for the Cr-C bond). The resulting chromaoxetane adduct **A2** (singlet) is 10.28 kcal mol^{-1} endothermic (Figure 2.3). The endothermicity is about 4.22 kcal mol^{-1} less than that reported by Torrent *et. al* (1999). No triplet **A2** was located on the surface. The formation of the epoxide precursor **A5** from the chromaoxetane intermediate **A2** through transition state **TS[A2-A5]** has an activation barrier of 13.36 kcal mol^{-1} and an exothermicity of 20.91 kcal mol^{-1}(Figure 2.3). Torrent *et. al.* (1999) found the most viable [2+2] second step pathway through a triplet transition state to be a triplet **A5**, with

an estimated activation barrier of 16.90 kcal mol^{-1} and an exothermicity of just 5.7 kcal mol^{-1}. In this work the triplet **A5** is found to be 19.54 kcal mol^{-1} more stable than the corresponding singlet state. However, the triplet **TS[A2-A5]** was not found.

The transition state **TS[A1-A4]** for the [3+2] addition of ethylene across the oxygen and chlorine atoms of CrO_2Cl_2 is 9.01 kcal mol^{-1} above the reactants. Species **A4** is exothermic by 17.95 kcal mol^{-1}. The formation of **A5** from **A4** transition state **TS[A4-A5]** is 7.32 kcal mol^{-1} endothermic, with an activation barrier of 41.28 kcal mol^{-1}(Figure 2.3). Thus overall, the formation of **A5** by [3+2] addition of ethylene across the oxygen and chlorine atoms of CrO_2Cl_2 cannot compete favorably, both kinetically and thermodynamically, with formation by [2+2] addition.

Along the second [3+2] addition pathway, the transition state **TS[A1-A3]** for the formation of the ester complex intermediate is 8.76 kcal mol^{-1} above the reactants. The geometry of the transition state indicates that the addition is concerted and synchronous. Comparing the C-O bond lengths in the transition state and the product indicates that this is an early transition state. The ester complex intermediate is 24.38 kcal mol^{-1} exothermic. The transition state **TS[A3-A5]** leading to the epoxide precursor from the ester intermediate is 22.61 kcal mol^{-1} above the reactants. Thus, the activation barrier for the formation of the epoxide precursor from the ester complex is 46.99 kcal mol^{-1}. Torrent *et. al.* (1999) calculations found this two-step process involving the [3+2] interaction with activation barrier of 21.9 kcal mol^{-1} more favorable than the two-step [2+2] pathway that required a first step activation energy of 27.1 kcal mol^{-1}.

The present study indicates that even though in the first step of the two-step processes of epoxide precursor formation the [3+2] addition across two Cr=O bonds is the most favorable pathway, the ester

complex intermediate **A3** formed from [3+2] addition is too stable to allow an easy conversion to the reputed epoxide precursor **A5**. The epoxide precursor is, therefore, not likely to be accessible from the ester complex intermediate. The implication of this is that the epoxide is not likely to originate from an ester intermediate formed from [3+2] addition, contrary to the findings of Torrent *et. al*. (1999). On the basis of this, it is concluded that the [2+2] addition pathway is the preferred route for the formation of epoxide through the epoxide precursor (Figure 2.3). This conclusion is based on the assumption that **A3** dissipates its excess energy (exothermicity) from step 1 before it attempts to go over the second barrier. If it does not dissipate the excess energy quickly, then the [3+2] route via **A3** may still be the most favorable route overall.

As a result of Torrent *et. al.*'s (1999) treatment of **A3**, **TS[A3-A5]** and **A5** as triplet ground state species, the triplet PES was explored in relation to these species in this work. Triplet **A3** and **A5** were computed to be 49.87 kcal mol^{-1} and 30.17 kcal mol^{-1} exothermic respectively compared with the exothermicities of 24.3 kcal mol^{-1} and 10.63 kcal mol^{-1} found for the singlet **A3** and **A5** relative to the CrO_2Cl_2 and ethylene reactants. These exothermicities suggest that even the singlet state **A3** and **A5** intermediates should be stable enough to be observed experimentally. However, only **A5** has been observed experimentally by Limberg and Koppé (1999). Torrent *et. al.* (1999) have found the triplet **A3** to be 13.0 kcal mol^{-1} exothermic and the triplet **A5** to be 8.8 kcal mol^{-1} endothermic. Torrent's proposed mechanism for this [3+2] reaction leads from the singlet reactants via a singlet transition state to a triplet [3+2] cycloadduct **A3**, followed by rearrangement of **A3** to a triplet **A5** through a triplet transition state **TS[A3-A5]**. An exhaustive search for a triplet **TS[A3-A5]** in this work yielded no stationary point. Therefore this forbidden spin cross-over path could not be fully explored.

Limber and Koppé (1999) did not observe in their photolytic matrix isolation experiment the intermediates **A3** and **A2** which have been proposed in the formation of the epoxide precursor **A5**, and, asserting that CrO_2Cl_2 also possesses a low-lying triplet state (our calculations found the singlet more stable than the triplet), these workers concluded that if this low-lying triplet state, which was accessible in the photolytic matrix conditions, is responsible for product formation a forbidden spin crossover would not even have to be considered. Consequently the proposed path was a reaction of triplet CrO_2Cl_2 with olefin in close proximity producing either epoxide precursor **A5** or the carbonyl compounds **A6** by independent routes.

In the present work, the species **A3**, **A5**, and **TS[A3-A5]** have also been computed as open-shell singlets and these have been found to be comparable to the closed-shell singlets both in terms of geometry and energetics (relative energies of -24.44, -10.68 and +22.61 kcal mol^{-1} respectively).

2.3.2 FORMATION OF ACETALDEHYDE AND VINYL ALCOHOL

Limberg *et. al*. (1998) have postulated the species **A5** as the oxirane adduct intermediate leading to acetaldehyde, upon opening of the epoxide ring. Attempts were, therefore, made to localize the products of epoxide ring-opening on the potential energy surface (Figure 2.2). The singlet and triplet transition state **TS[A5-X]** for epoxide ring-opening are found to be respectively 12.62 and 1.58 kcal mol^{-1} above the reactants. Animating the motion of the atoms along the reaction coordinate in **TS [A5-X]** on SPARTAN's graphical user interface reveals that in addition to breaking of the C-O bond in the three-membered ring, one of the hydrogen atoms on the carbon atom involved in the bond-breaking appears to be moving towards the oxygen atom in the three-membered ring. This leads to the

formation of a carbene-like species **A7.** Triplet and singlet **A7** are 33.54 and 52.23 kcal mol^{-1} endothermic respectively. A 1,2-hydride shift from the secondary carbon to the terminal carbon of **A7** results in species **A8**, which can undergo Cr-O single bond cleavage to produce vinyl alcohol. Triplet **A8** has been computed to be 38.01 kcal mol^{-1} exothermic while no singlet **A8** could be located. The acetaldehyde precursor **A6** has been obtained in an attempt to optimize **A8** on the singlet PES. Species **A6** has exothermicities of 40.96 and 58.20 kcal mol^{-1} for the singlet and triplet species respectively, making it the global minimum on both the singlet and triplet PES. Limberg *et. al.*(1998) have found **A6** an intermediate in the thermal reaction of ethylene with CrO_2Cl_2 and postulated it as a precursor to the formation of acetaldehyde, upon cleavage of the Cr-O single bond. However, the most plausible pathway to the formation of **A6**, **A7** and **A8** appears to be a direct attack of one of the carbon atoms of ethylene on an oxygen atom of CrO_2Cl_2 to form triplet **C1/t**, followed by re-arrangement. The species **C1/t** and **A8** exist only on the triplet PES. Optimization of **A8** on the singlet PES converges on **A6**. Triplet **A7** (+33.52 kcal mol^{-1}) is considerably more stable than the singlet **A7** (+52.23 kcal mol^{-1}) and its high endothermicity relative to the singlet CrO_2Cl_2 and ethylene reactants suggests that it might be formed from a triplet CrO_2Cl_2 reactant.

2.3.3 FORMATION OF 1,2-CHLOROHYDRIN AND 1,2-DICHLOROETHANE

Sharpless *et. al.* (1977) have suggested that the conversion of olefins into chlorohydrins result from highly selective cis-addition of the elements of HOCl across the olefinic linkage, whereas chlorohydrins resulting from trans-addition were concluded to be secondary products derived by opening of the epoxide. Scheme 2.5 proposes three mechanistic pathways for the formation of the 1,2-chlorohydrin - a one-step process involving [3+2] addition of

ethylene across the oxygen and chlorine atoms of CrO_2Cl_2 to form the chlorohydrin precursor **B2**, a two-step process involving [2+2] addition of ethylene across the Cr-Cl bond of CrO_2Cl_2 to form the alkylchromium intermediate **B4** followed by re-arrangement through **TS[B4-B2]** to **B2**, and a third route involving the formation of **B6**, which could also be considered a chlorohydrin precursor, from **B4**. In their matrix isolation studies of the reaction between CrO_2Cl_2 and ethylene, Limberg *et. al.*(1998) postulated the presence of $CrOCH_2CH_2Cl$ fragments in the Etard complex, which is consistent with the structure of **B6**.

The formation of the chlorohydrin precursor **B2** (closed-shell singlet) has been found to be 17.95 kcal mol^{-1} exothermic. An open-shell singlet **B2** has been found to be 17.96 kcal mol^{-1} exothermic, with geometrical parameters the same as those of the closed-shell singlet minimum. The activation barrier for the formation of **B2** through the [3+2] addition is 9.01 kcal mol^{-1} (Figure 2.5). In addition to the singlet **B2** which is 17.95 kcal mol^{-1} exothermic a triplet state **B2** was computed and found to be 16.20 kcal mol^{-1} more stable than the singlet state **B2**. Torrent *et. al.*(1999) did not report of a singlet state **B2** but found a triplet state **B2** (3.8 kcal mol^{-1} endothermic) formed from a singlet reactant **B1** via a [3+2] singlet transition state **TS[B1-B2]** with an activation barrier of 15.7 kcal mol^{-1} compared with a triplet activation barrier of 37.3 kcal mol^{-1}. In the two-step formation of **B2** the activation barrier for the formation of the alkylchromium intermediate **B4** is 25.61 kcal mol^{-1} (Figure 2.6). The intermediate **B4** has been found to be 1.82 kcal mol^{-1} endothermic.

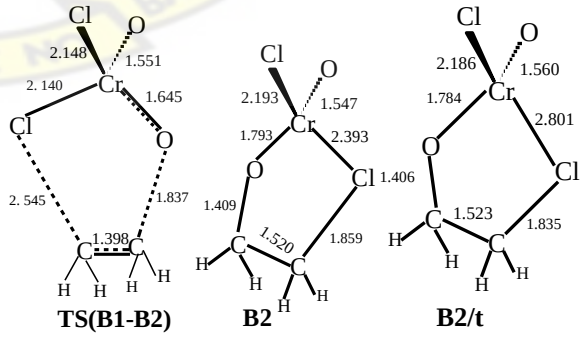

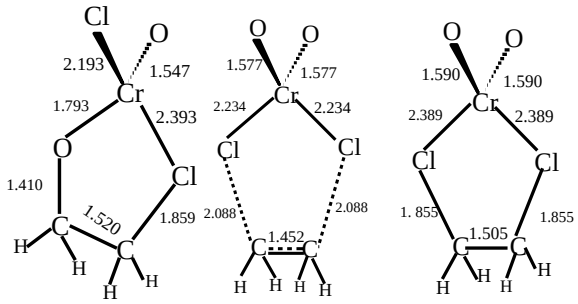

B2/os **TS(B1-B3)** **B3**

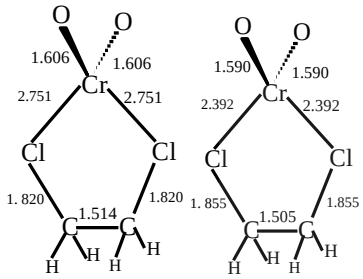

B3/t **B3/os**

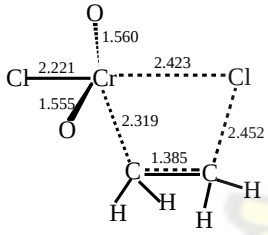

TS(B1-B4)

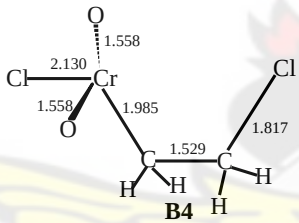

B4

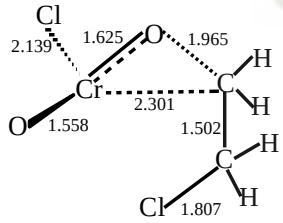

TS[B4-B2]

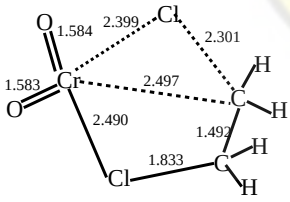

TS(B4-B3)

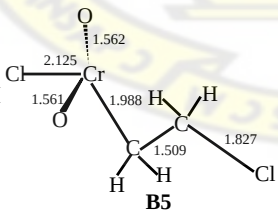

B5

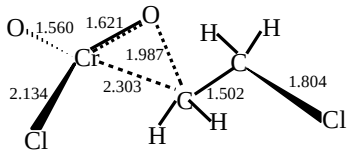

TS(B5-B6)

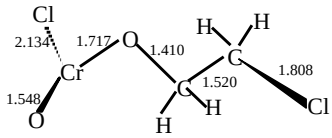

B6

Figure 2.4. Optimized geometrical parameters of the main stationary points involved in the [2+2] and [3+2] addition reaction between CrO_2Cl_2 and ethylene for the formation of chlorohydrin and dichloride precursors (t = triplet state, os = open-shell singlet state). Distances in Å and angles in degrees.

The activation barrier for the formation of **B2** from **B4** is 23.12 kcal mol^{-1}. Along the third proposed pathway for the formation of chlorohydrins (Scheme 2.5), species **B4** undergoes rotation about the C_1-C_2 bond to form species **B5** which is 7.89 kcal mol^{-1} more stable than **B4**. Species **B6**, which generates the chlorohydrin, is formed from **B5** by the breaking of the Cr-C bond and formation of the C-O bond. The energy barrier for this transition through **TS[B5-B6]** is 31.94 kcal mol^{-1}.

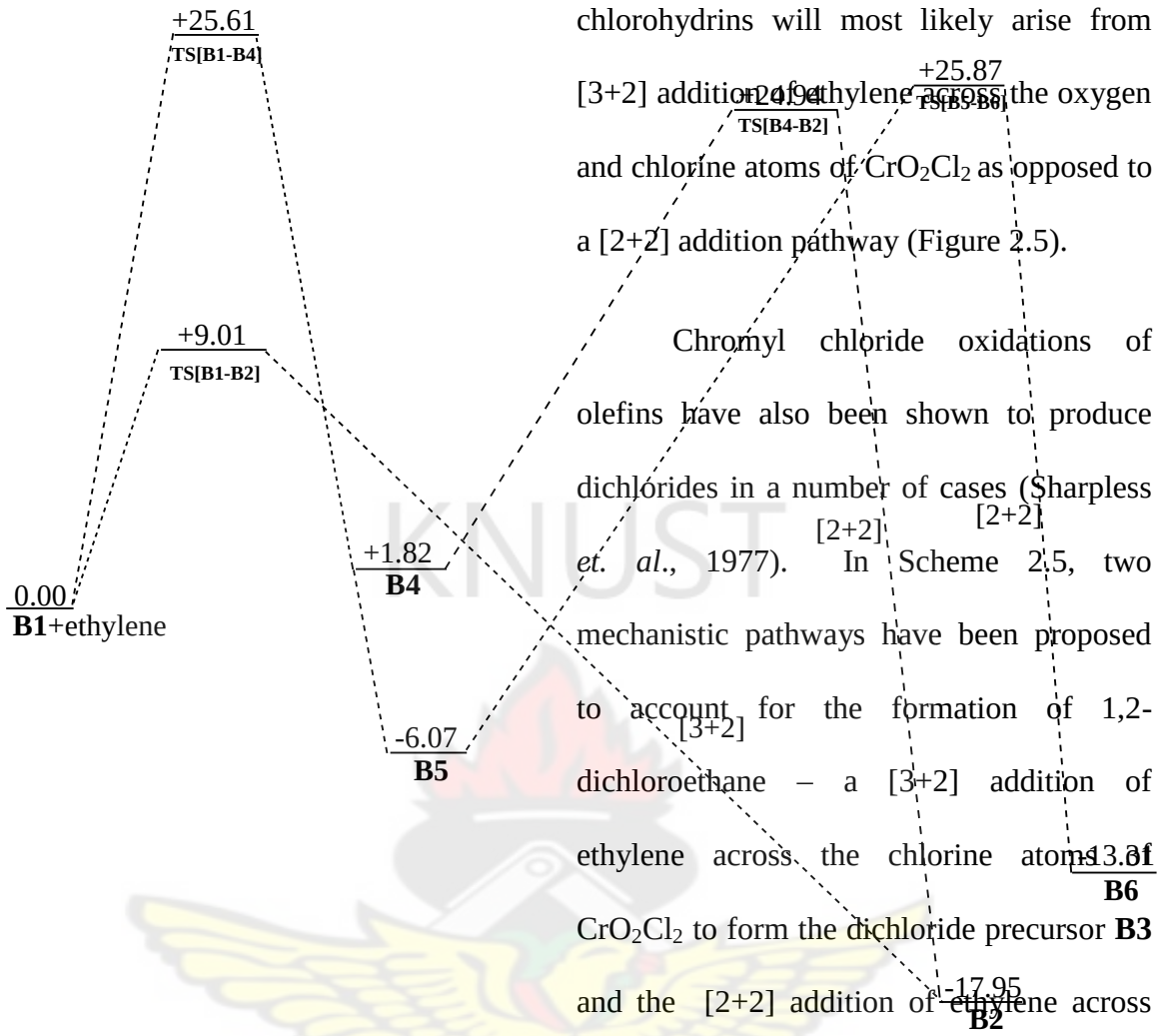

Figure 2.5. Energy profile of the three suggested mechanisms for the formation of the 1,2-chlorohydrin precursor from the addition of CrO_2Cl_2 and ethylene on a singlet PES. Energies in kcal mol^{-1}.

Since the [3+2] pathway leading to the chlorohydrin precursor **B2** has the lowest overall activation barrier and the highest exothermicity, it is concluded that the [3+2] route is the preferred one for the formation of 1,2-chlorohydrin from the reaction of ethylene with CrO_2Cl_2. Thus, 1,2-chlorohydrins will most likely arise from [3+2] addition of ethylene across the oxygen and chlorine atoms of CrO_2Cl_2 as opposed to a [2+2] addition pathway (Figure 2.5).

Chromyl chloride oxidations of olefins have also been shown to produce dichlorides in a number of cases (Sharpless *et. al*., 1977). In Scheme 2.5, two mechanistic pathways have been proposed to account for the formation of 1,2-dichloroethane – a [3+2] addition of ethylene across the chlorine atoms of CrO_2Cl_2 to form the dichloride precursor **B3** and the [2+2] addition of ethylene across one of the Cr-Cl bonds to form the alkylchromium intermediate **B4** followed by re-arrangements through **TS[B4-B3]** to the dichloride precursor **B3**.

In the one-step [3+2] addition for the formation of **B3** through **TS[B1-B3]**, the activation barrier for the formation of **B3** through **TS[B1-B3]** by [3+2] addition is 20.75 kcal mol^{-1}. The dichloride precursor **B3** (closed- shell singlet) has been found to

be 17.22 kcal mol^{-1} endothermic, the open-shell singlet **B3** has also been found to be 17.21 kcal mol^{-1} endothermic while the triplet **B3** has been found to be 10.67 kcal mol^{-1} endothermic. Torrent *et. al.*(1999) reported only a triplet minimum which was 44.7 kcal mol^{-1} endothermic and proposed a mechanism involving singlet reactants through a singlet transition state and intermediate to a triplet dichloride precursor.

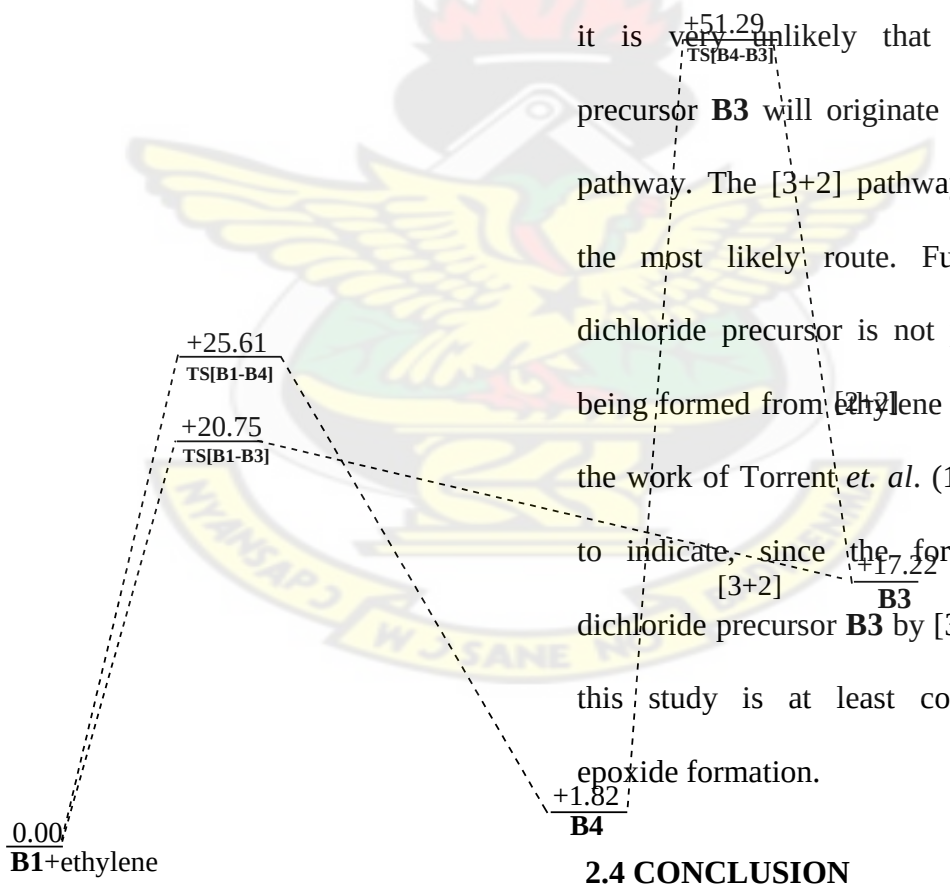

Figure 2.6. Energy profile of the two suggested mechanisms for the formation of the dichloride precursor from addition of CrO_2Cl_2 and ethylene on a singlet PES. Energies in kcal mol^{-1}.

In the two-step [2+2] addition for the formation of B3 through **TS[B4-B3]** the activation barrier for the formation of the alkylchromium intermediate **B4** is 25.61 kcal mol^{-1}. The transition barrier linking **B4** and **B3** is very high (51.29 kcal mol^{-1}). On the basis of this energetic data (Figure 2.6), it is very unlikely that the dichloride precursor **B3** will originate from the [2+2] pathway. The [3+2] pathway is considered the most likely route. Furthermore, the dichloride precursor is not precluded from being formed from ethylene and CrO_2Cl_2 as the work of Torrent *et. al*. (1999) will seem to indicate, since the formation of the dichloride precursor **B3** by [3+2] addition in this study is at least competitive with epoxide formation.

2.4 CONCLUSION

The following conclusions are drawn from the results presented:

1. In the first step of the reaction between CrO_2Cl_2 and ethylene, the [3+2] addition of ethylene across the two oxygen atoms of CrO_2Cl_2 to form the ester complex intermediate has the lowest barrier (8.76 kcal mol^{-1}) compared to the [3+2] addition across the oxygen and chlorine atoms (9.01 kcal mol^{-1}), [3+2] addition across the two chlorine atoms (20.75 kcal mol^{-1}), [2+2] addition across the Cr-Cl bond (25.61 kcal mol^{-1}) and [2+2] addition across the Cr-O bond to form the chromaoxetane (26.31 kcal mol^{-1}).

2. The most favorable pathway for the formation of the epoxide precursor is by initial [2+2] addition of ethylene across the Cr-O bonds of CrO_2Cl_2. The highest barrier along this pathway is 26.31 kcal mol^{-1}. The highest barrier along the [3+2] addition route across the oxygen and chlorine atoms is 41.28 kcal mol^{-1} while that along the [3+2] addition route across the two oxygen atoms is 46.99 kcal mol^{-1}. Thus the epoxide will most likely arise from a [2+2] addition pathway as opposed to a [3+2] pathway as reported by Torrent *et. al.*(1999).

3. There appears to be no direct addition pathway for the formation of the epoxide precursor.

4. The [3+2] addition of ethylene across the oxygen and chlorine atoms of CrO_2Cl_2, which appears to have been ignored as a plausible pathway for epoxide precursor formation in earlier studies, has been found to be favored over the [3+2] addition of ethylene across the two oxygen atoms of CrO_2Cl_2.

5. The formation of 1,2-dichlorohydrin will most likely arise from [3+2]

addition across the oxygen and chlorine atoms of CrO_2Cl_2 and not by [2+2] addition.

6. The formation of 1,2-dichoroethane will most likely proceed by [3+2] addition of ethylene across the two chlorine atoms of CrO_2Cl_2 as opposed to a [2+2] addition.

7. The 1,2-dichoroethane is not precluded from being formed from CrO_2Cl_2 and ethylene as the work of Torrent *et. al.*(1999) may seem to indicate. The formation of dichloride is slightly favored over the formation of epoxide.

8. The acetaldehyde precursor $O{=}CrCl_2{-}OCHCH_3$ formed from optimization of the vinyl alcohol precursor $O{=}CrCl_2{-}(OH)CH{=}CH_2$ is the most stable species on the reaction surface (40.96 kcal mol^{-1} exothermic).

9. The vinyl alcohol precursor $O{=}CrCl_2{-}(OH)CH{=}CH_2$ has been found to exist only on the triplet PES.

10. The inability to locate some key transition states on the triplet PES in this work does not allow a comparison of the viability of the reaction on the singlet PES and that involving the singlet-triplet ground state crossover.

REFERENCES

Clark, M.; Cramer, R. D.; Opdenbosch, N. V. (1989) Validation of the general purpose tripos 5.2 force field. *J. Comp. Chem.* 10: 982 – 1012.

Corey, E. J.; Jardine, P. D.; Virgils, S.; Yuen, P.-W.; Connell, R. D. (1989) Enantioselective vicinal hydroxylation of terminal and E-1,2-disubstituted olefins by a chiral complex of osmium tetroxide. An

effective controller system and a rational mechanistic model. *J. Am. Chem. Soc.* 111: 9243 – 9244.

Corey, E. J.; Noe, M. C.; Sarshar, S. (1993) The origin of high enantioselectivity in the dihydroxylation of olefins using osmium tetraoxide and cinchona alkaloid catalysts. *J. Am. Chem. Soc*. 115: 3828 – 3829.

Criegee, R. (1936) Osmiumsäure-ester als Zwischenprodukte bei Oxydationen. *Justus Liebigs Ann. Chem.* 522: 75 – 96.

Criegee, R.; Marchaand, B.; Wannowius, H. (1942) Zur Kenntnis der organischen Osmium-Verbindungen. II. Mitteilung. *Justus Liebigs Ann. Chem.* 550: 99 – 133.

Dapprich, S.; Ujaque, G.; Maseras, F.; Lledós, A.; Musaev, D. G.; Morokuma, K. (1996) Theory does not support an osmaoxetane intermediate in the osmium-catalyzed dihydroxylation of olefins. *J. Am. Chem. Soc.* 118: 11660 – 11661.

Del Monte, A. J.; Haller, J.; Houk, K. N.; Sharpless, K. B.; Singleton, D. A.; Strassner, T.; Thomas, A. A. (1997) Experimental and theoretical kinetic isotope effects for asymmetric dihydroxylation. Evidence supporting a rate-limiting "(3+2)" CycloadditioN. *J. Am. Chem. Soc.* 119: 9907 – 9908.

Dunning, T. H., Jr.; Hay, P. J. (1976) In: Modern Theoretical Chemistry, H. F. Schaefer, III, Vol. 3; Plenum, New York.

Freeman, F. (1975) possible criteria for distinguishing between cyclic and acyclic activated complexes and among cyclic activated complexes in addition reactions. *Chem. Rev.* 75: 439 – 490.

Gable, K. P.; Phan, T. N. (1994) Extrusion of Alkenes from Rhenium (V) Diolates: Energetics and Mechanism. *J. Am. Chem. Soc*. 116: 833 – 839.

Garcia, A.; Cruz, E. M.; Sarasola, C.; Ugalde, J. M. (1997) Density functional studies of the bπ. aσ charge-transfer complex formed between ethyne and chlorine monofluoride. *J. Phys. Chem. A* 101: 3021 – 3024.

Göbel, T.; Sharpless, K. B. (1993) Temperature Effects in Asymmetric Dihydroxylation: Evidence for a Stepwise Mechanism. *Angew. Chem.; Int. Ed. Engl*. 32: 1329 – 1331.

Goldberg, N.; Ault, B. S. (2006) A matrix isolation study of the reactions of $OVCl_3$ with a series of silanes. *J. Mol. Struct.* 787, 203 – 208.

Hay, P. J.; Wadt, W, R. (1985) *Ab initio* effective core potentials for molecular calculations. Potentials for the transition metal atoms *Sc t*o Hg. *J. Chem. Phys*. 82: 270.

Hay, P. J.; Wadt, W, R. (1985) *Ab initio* effective core potentials for molecular calculations. Potentials for K to Au including the outermost core orbitals. *J. Chem. Phys*. 82: 299.

Hentges, S. G.; Sharpless, K. B. (1980) Asymmetric induction in the reaction of osmium tetroxide with olefins. *J. Am. Chem. Soc*. 102: 4263 – 4265.

Jorgensen, K. A.; Hoffmann, R. W. (1986) Binding of alkenes to the ligands in OsO_2X_2 (X=O and NR) and $CpCo(NO)_2$. A frontier orbital study of the formation of intermediates in the transition-metal-

catalyzed synthesis of diols, amino alcohols, and diamines. *J. Am. Chem. Soc.* 108: 1867 – 1876.

Kristán, S.; Pulay, P. (1994) Can (semi) local density functional theory account for the London dispersion forces? *Chem. Phys. Lett*. 229, 175 – 180.

Limberg, C.; Köppe, R. (1999) Reactive intermediates in olefin oxidations with chromyl chloride. IR-spectroscopic proof for O=$CrCl_2$−epoxide complexes. *Inorg. Chem.* 38: 2106 – 2116.

Limberg, C.; Köppe, R.; Schnöckel, H. (1998) Matrix isolation and characterization of a reactive intermediate in the olefin oxidation with chromyl chloride. *Angew. Chem. Int. Ed*. 37: 496.

Marsden, C. J.; Hedberg, L.; Hedberg, K. (1982) Molecular structure and quadratic force field of chromyl chloride, CrO_2Cl_2. *Inorg. Chem*. 21: 1115.

Mourik, T. V. (2008) assessment of density functionals for intramolecular dispersion-rich interactions. *J. Chem. Theory Comput*. 41610 – 1619.

Mourik, T. V.; Gdanitz, R. J. (2002) A critical note on density functional theory studies on rare-gas dimers. *J. Chem. Phys*. 116: 9620 – 9623.

Nortey, P. O. Becker, H.; Sharpless, K. B. (1996) Toward an understanding of the high enantioselectivity in the osmium-catalyzed asymmetric dihydroxylation. 3. New insights into isomeric forms of the putative osmaoxetane intermediate. *J. Am. Chem. Soc.* 118: 35 – 42.

Nortey, P. O.; Kolb, H. C.; Sharpless, K. B. (1994) Calculations on the reaction of ruthenium tetroxide with olefins using density functional theory (DFT). Implications for the possibility of intermediates in osmium-catalyzed asymmetric dihydroxylation *Organometallics* 13: 344 – 347.

Peréz-Jordá, J. M.; Becke, A. D. (1995) A density-functional study of van der Waals forces: rare gas diatomics. *Chem. Phys. Lett*. 233: 134 – 137.

Pidun, U.; Boeheme, C..; Frenking, G. (1996) Theory Rules Out a [2 + 2] Addition of Osmium Tetroxide to Olefins as Initial Step of the Dihydroxylation Reaction *Angew. Chem.; Int. Ed. Engl*. 35: 2817 – 2820.

Rappé, A. K.; Goddard, W. A., III (1982) Hydrocarbon oxidation by high-valent Group VI oxides. *J. Am. Chem. Soc*. 104: 3287 – 3294.

Rappé, A. K.; Goddard, W. A., III. (1980) Bivalent spectator oxo bonds in metathesis and epoxidation alkenes. *Nature (London)* 285: 311 – 312.

Rappé, A. K.; Goddard, W. A., III. (1980) Mechanism of metathesis and epoxidation in chromium and molybdenum complexes containing methyl-oxo bonds. *J. Am. Chem. Soc.* 102: 5114 – 1515.

Rappé, A. K.; Goddard, W. A., III. (1982) Olefin metathesis - a mechanistic study of high-valent group VI catalysts. *J. Am. Chem. Soc.* 104: 448 – 456.

Ruiz, E.; Salahub, D. R.; Vela, A. (1996) Charge-Transfer Complexes: Stringent tests

for widely used density functionals. *J. Phys. Chem.* 100: 12265 – 12276.

Samsel, E. G.; Srinivasan, K.; Kochi, J. K. (1985) Mechanism of the chromium-catalyzed epoxidation of olefins. Role of oxochromium(V) cations. *J. Am. Chem. Soc*. 107: 7606 – 7617.

Schröder, M. (1980) Osmium tetroxide cis-hydroxylation of unsaturated substrates. *Chem. Rev*. 80: 187 – 213.

Sharpless, K. B.; Teranishi, A. Y.; Bäckvall, J. E. (1977) Chromyl chloride oxidations of olefins. Possible role of organometallic intermediates in the oxidations of olefins by oxo transition metal species. *J. Am. Chem. Soc.* 99: 3120 – 3128.

Spartan, Wavefunction, Inc.; 18401 Von Karman Ave., # 370, Irvine, CA, 92715, USA.

Torrent, M.; Deng, L.; Duran, M.; Solá, M.; Ziegler, T. (1997) Density functional study of the [2+2]- and [3+2]-cycloaddition mechanisms for the osmium-catalyzed dihydroxylation of olefins. *Organometallics* 16: 13 – 19.

Torrent, M.; Deng, L.; Duran, M.; Solá, M.; Ziegler, T. (1999) Mechanisms for the formation of epoxide and chlorine-containing products in the oxidation of ethylene by chromyl chloride: a density functional study. *Can. J. Chem.* 77: 1476 – 1491.

Torrent, M.; Deng, L.; Ziegler, T. (1998) A Density functional study of [3+2] versus [2+2] addition of ethylene to chromium-oxygen bonds in chromyl chloride. *Inorg. Chem.* 37: 1307-1314.

Upton, T. H.; Rappé, A. K. (1985) A theoretical basis for low barriers in transition-metal complex 2π + 2π reactions: the isomerization of the dicyclopentadienyltitanium complex $Cp_2TiC_3H_6$ to $Cp_2TiCH_2(C_2H_4)$. *J. Am. Chem. Soc.* 107: 1206.

Wadt, W. R.; Hay, P. J. (1985) *Ab initio* effective core potentials for molecular calculations. Potentials for main group elements Na to Bi. *J. Chem. Phys*. 82: 284.

Walba, D. M.; DePuy, C. H.; Grabowski, J. J.; Bierbaum, V. M. (1984) Oxidation of alkenes by d^0- transition metal oxo species: a mechanism for the oxidation of ethylene by a dioxochromium (VI) complex in the gas phase. *Organometallics* 3: 498 – 499.

Wallis, J. M.; Kochi, J. K. (1988) Direct osmylation of benzenoid hydrocarbons. Charge-transfer photochemistry of osmium tetraoxide. *J. Org. Chem.* 53: 1679 – 1686.

Wallis, J. M.; Kochi, J. K. (1988) Electron-transfer activation in the thermal and photochemical osmylations of aromatic electron donor-acceptor complexes with osmium (VIII) tetroxide. *J. Am. Chem. Soc.* 110: 8207 – 8223.

Wright, T. C. (1996) Geometric structure of $Ar{\cdot}NO^+$: revisited. A failure of density functional theory. *J. Chem. Phys.* 105, 7579.

Wu, Y.-D.; Wang, Y.; Houk, K. N. (1992) A new model for the stereoselectivities of dihydroxylations of alkenes by chiral diamine complexes of osmium tetroxide. *J. Org. Chem.* 57: 1362 – 1369.

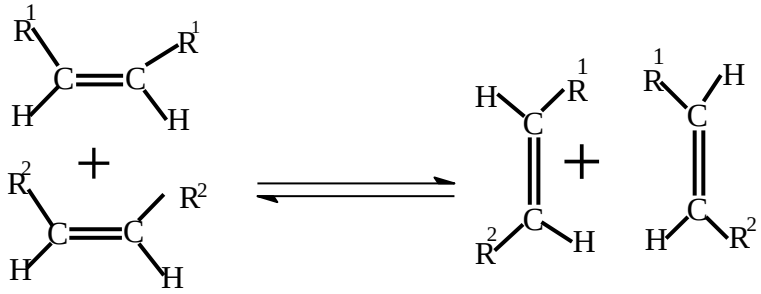

CHAPTER THREE

DENSITY FUNCTIONAL THEORY STUDIES OF THE MECHANISTIC ASPECTS OF OLEFIN METATHESIS REACTIONS

3.1 INTRODUCTION

The very foundation of organic synthesis consists of reactions that can reliably and efficiently form carbon-carbon bonds. In recent years, the olefin metathesis reaction has attracted widespread attention as a versatile carbon-carbon bond-forming method. Metathesis is the metal-catalyzed re-distribution of carbon-carbon double bonds. The reaction describes the apparent interchanges of carbon atoms between two pairs of bonds. Formally, metathesis involves a simultaneous cleavage of two olefin double bonds, followed by the formation of alternate bonds.

Olefin metathesis has become a widely used reaction in organic and polymer chemistry (Kingsbury *et. al*, 1999; Roy and Das, 2000; Maier, 2000) for a number of reasons. First, some olefins are easy to prepare and others require more effort to access. Olefin metathesis allows facile access from the easily prepared olefins to those that are cumbersome to prepare. Second, olefin metathesis reactions either do not generate a by-product or only produce one, such as ethylene, which can be removed by evaporation. Third, olefins are routinely used to interconvert molecules. Olefins are useful largely because they represent the better of two worlds: stability and reactivity. Olefins are stable – they are

typically stored indefinitely without decomposition, and yet they contain a π-bond that is sufficiently reactive to be used in a wide range of transformations.

Olefin metathesis has a variety of applications, including ring-opening metathesis polymerization (ROMP), ring-closing metathesis (RCM), acyclic diene metathesis polymerization (ADMET), ring-opening metathesis (ROM) and cross-metathesis (CM) (Trnka and Grubbs, 2001). Some of the most impressive achievements include the use of ROMP to make functionalized polymers, the syntheses of small to large heterocyclic systems by RCM, and the CM of olefins with pendant functional groups. Olefin metathesis opens up new industrial routes to important petrochemicals, oleochemicals, polymers and specialty chemicals (Mol, 2004).

Since the work of Herrison and Chauvin (Herrison and Chauvin, 1971), it has been generally accepted that metal-alkylidene (carbene) complexes play a pivotal role in transition-metal-catalyzed olefin metathesis. The carbene complex is recognized as the active chain-carrying catalyst that reacts with an olefin to form a metallacyclobutane intermediate that decomposes to form the product olefin. The alkenes add, one at a time, to the metal-alkylidene complex *in situ* to form a metallacyclobutane intermediate, which subsequently leads to an alkylidene-alkene exchange in the propagation stage (Scheme 3.1).

Scheme 3.1: The Herrison-Chauvin Non-pairwise Mechanism of Olefin Metathesis (Herrison and Chauvin, 1971)

Initiation:

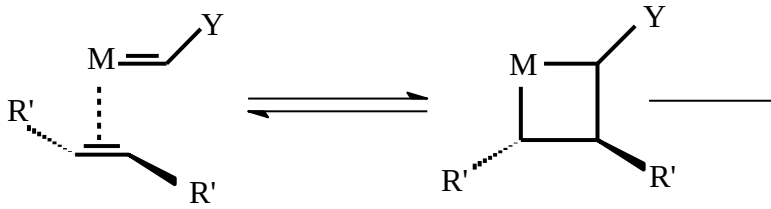

Catalytic Cycle:

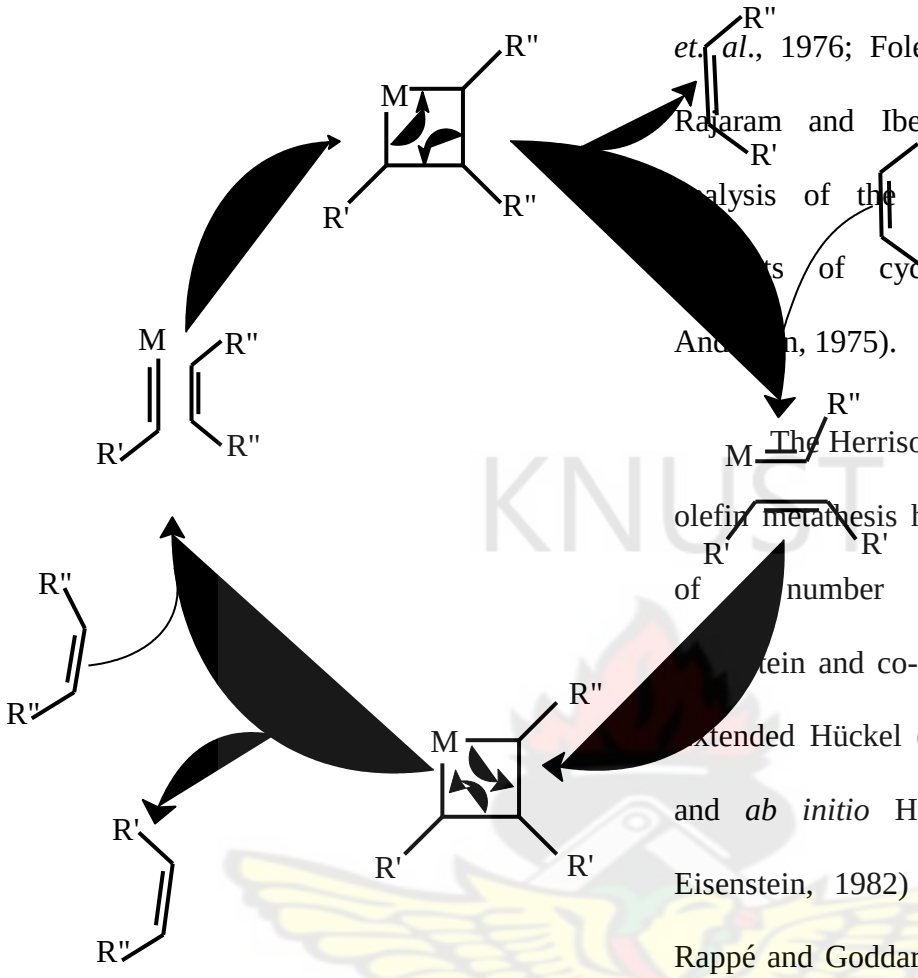

The Herrison-Chauvin mechanism has been established through detailed study of isotopic scrambling (Grubbs *et. al*., 1975; Grubbs *et. al*., 1976; Katz and McGinnis, 1975, Katz *et. al*., 1976), the synthesis of metalloalkylidenes (Schrock, 1974; 1976, Schrock and Sharp, 1978) and metallacyclobutanes (Ephritikhine *et. al*., 1976; Ephritikhine *et. al*., 1977, Puddephat *et. al*., 1976; Foley and Whiteside, 1979; Rajaram and Ibers, 1978) and by the analysis of the character of polymeric products of cyclo-olefins (Casey and Anderson, 1975).

The Herrison-Chauvin mechanism of olefin metathesis has also been the subject of a number of theoretical studies. Eisenstein and co-workers have carried out extended Hückel (Eisenstein *et. al.*, 1981) and *ab initio* Hartree-Fock (Dediu and Eisenstein, 1982) studies on the subject. Rappé and Goddard (1982) have reported a GVB study of the reaction between $Cl_4Mo{=}CH_2$ and ethylene in which the formation of the metallacycle was found to be endothermic. However, when the same reaction was re-calculated using fully optimized geometries, it was found to be exothermic (Anslyn and Goddard, 1989). Rappé and Goddard (1982) have used the results of an *ab initio* theoretical mechanistic study to suggest that the oxo-alkylidene

complex $Cl_2(O)M=CH_2$ would favor formation of metallacycles because of conversion of the double-bond spectator oxo group in the reactant to a triple bond in the product. Rappé and Goddard (1980) have again used the results of *ab initio* GVB and CI theoretical studies to examine the thermochemistry and mechanisms for metathesis of olefins by Cr and Mo complexes and concluded that in activating metal chlorides it is essential to have spectator metal-oxo bonds. Sodupe *et. al*. (1991) performed an *ab initio* Hartree-Fock study of the reaction between the $Cl_4Mo=CH_2$ complex and ethylene and found the formation of the metallacyclobutane to be exothermic. A GVB study found no activation barrier for the interconversion of titanium alkylidene-olefin complex $Cl_2TiC_3H_6$, where the metallacyclobutane was found to be 12 kcal mol^{-1} more stable than the olefin-alkylidene complex (Rappé and Upton, 1984; Upton and Rappé, 1985). Cundari and Gordon (1992) performed an *ab initio* analysis of the electronic structure of high-valent, transition-metal alkylidenes as models for olefin metathesis catalysts and observed that the W-C bond is more polarized in a $M^+=C^-$ fashion for the W methylidene than is the Mo-C bond of the Mo methylidene analogue and concluded that the greater polarization correlates with greater metathesis activity exhibited by the W alkylidene metathesis catalysts when compared to Mo analogues. Cavallo (2002) has carried out density functional theory study of the ruthenium-catalyzed olefin metathesis reactions and found, *inter alia*, that the metallacyclobutane structures represented minimum energy situations along the reaction coordinate, and are of slightly higher energy with respect to the corresponding olefin-bound intermediates in the case of the phosphane-based systems, while they are slightly more stable than the olefin adducts in the case of the NHC-based systems. Bernardi *et. al*. (2003) have carried out a theoretical investigation at the DFT B3LYP level of theory on the mechanism of

the metathesis of ethylene catalyzed by Grubbs' complexes, $Cl_2(PH)_3$-Ru=CH_2 and $Cl_2(PPH_3)_2$Ru=CH_2, and found, among other things, that the primary active catalytic species is the metal-carbene $(PH)_3Cl_2$-Ru=CH_2 and not the carbenoid complex $(PH)_3$Cl-Ru-CH_2Cl which was found to be significantly higher in energy (by 18.45 and 19.26 kcal mol^{-1} for the two model systems), and that cyclopropanation is disfavored compared to metathesis since the former requires the overcoming of larger activation barriers than those found for the latter. Poater *et. al.*(2007) carried out gas phase DFT B3PW91 calculations on the reactivity of ethylene with model systems M(≡NR)(=$CHCH_3$)(X)(Y) [M = Mo, W; R = methyl, phenyl; X = CH_2-CH_3, OCH_3, $OSiH_3$; and Y = CH_2CH_3, OCH_3, $OSiH_3$] and found that the factors controlling the detailed shape of the energy profiles are the energy of distortion of the tetrahedral catalyst and the stability of the metallacycle intermediate, which is controlled by the M-C bond strength. They also found that unsymmetrical catalysts (X ≠Y) were systematically more efficient for all systems (Mo, W, Re) and that overall, the Re complexes were less efficient than the Mo and W catalysts, except when Re is unsymmetrically substituted. Yüksel *et. al.* (2008) investigated a catalytic system consisting of tungsten carbene generated from WCl_6 and atomic carbon for the metathesis of 1-octene at B3LYP/extended LAN2DZ level of theory and found that the formation of the catalytically active heptylidene is energetically favored in comparison to the formation of methylidene, while the degenerative and productive metathesis steps are competitive. They also found that solvent effects on the metathesis reactions were minor and solvation does not cause any change in the directions of the overall metathesis reactions. To date, no olefin metathesis involving hexavalent chromium complexes has been reported, but the reason for this has not been elucidated.

In this work, the mechanisms of the reactions of the complexes Cl_4MCH_2 (M= Cr, Mo, W, Ru, Re) and $Cl_2(O)MCH_2$ (M= Cr, Mo, W, Ru, Re) with ethylene are studied theoretically at the DFT B3LYP/LACVP* level of theory with the aim of elucidating the metathesis activity of these complexes and delineating the factors responsible for any difference in metathesis activity. This has been done by exploring the most favorable reaction routes of these complexes with ethylene *vis-à-vis* the [3+2] and [2+2] addition pathways in an attempt to provide insight into this class of reactions, particularly the reasons for the absence of olefin metathesis in hexavalent chromium complexes and the trends in the reactivity of the metal complexes.

3.2 DETAILS OF CALCULATIONS

All calculations were carried out with the SPARTAN '06 V112 Molecular Modeling program (Wavefunction, 2006) at the DFT B3LYP/LACVP* level of theory. The LACVP* basis set is a relativistic effective core-potential that describes the atoms H – Ar with the 6-31G* basis while heavier atoms are modeled with the LANL2DZ basis set which uses the all-electron valence double zeta basis set (D95V), developed by Dunning (Dunning and Hay, 1976), for first row elements and the Los Alamos ECP plus double zeta basis set developed by Wadt and Hay for the atoms Na – La, Hf – Bi (Hay and Wadt, 1985a; 1985b; Wadt and Hay, 1985).

The starting geometries of the molecular systems were constructed using SPARTAN's graphical model builder and minimized interactively using the sybyl force field (Clark *et. al*, 1989). All geometries were fully optimized without any symmetry constraints. The optimized geometries were subjected to full frequency calculations to verify the nature of the stationary points. Equilibrium geometries

were characterized by the absence of imaginary frequencies. The transition state structures were located by a series of constrained geometry optimizations in which the forming- and breaking-bonds were fixed at various lengths while the remaining internal coordinates were optimized. The approximate stationary points located from such a procedure were then fully optimized using the standard transition state optimization procedure in SPARTAN. All first-order saddle-points were shown to have a Hessian matrix with a single negative eigenvalue, characterized by an imaginary vibrational frequency along the reaction coordinate. All the computations were performed on Dell Precision T3400 Workstation computers.

3.3 RESULTS AND DISCUSSIONS

3.3.1 REACTIONS OF Cl_4MCH_2(Cr, Mo, W, Ru, Re) WITH ETHYLENE

The optimized geometries and relative energies of the main stationary points involved in the reaction between Cl_4CrCH_2 and ethylene are shown in Figures 3.1 and 3.2 respectively. The DFT geometry optimization of Cl_4CrCH_2 on the singlet potential energy surface (PES) with RB3LYP yielded three minima: a trigonal bipyramid carbene structure $Cl_4Cr{=}CH_2$ (**R1**) of C_{2v} symmetry in which the methylene ligand occupies an equatorial position on the metal center with the hydrogen atoms in the trigonal planes, a carbenoid complex Cl_3CrCH_2-Cl (**R2**), which was obtained in an attempt at optimizing the axial methylidene intermediate, and a bridged compound **R3**. The axial Cr-Cl bonds of **R1** were found to be 0.194 Å longer than the equatorial bonds. No alkylidene minimum with the methylene ligand occupying the axial position was found on the reaction surface.

The carbenoid **R2** minimum is 42.39 kcal mol^{-1} and 26.66 kcal mol^{-1} more stable

than the carbene complex **R1** and the bridged complex **R3** respectively. It is found that **R2** can be transformed to **R3** through transition state **TS3**, but this conversion, which has an activation barrier of 44.66 kcalmol^{-1}, is not competitive with the formation of **pdt2** from **R2** , a reaction which requires an activation energy of 31.53 kcal mol^{-1} (*vide infra*).

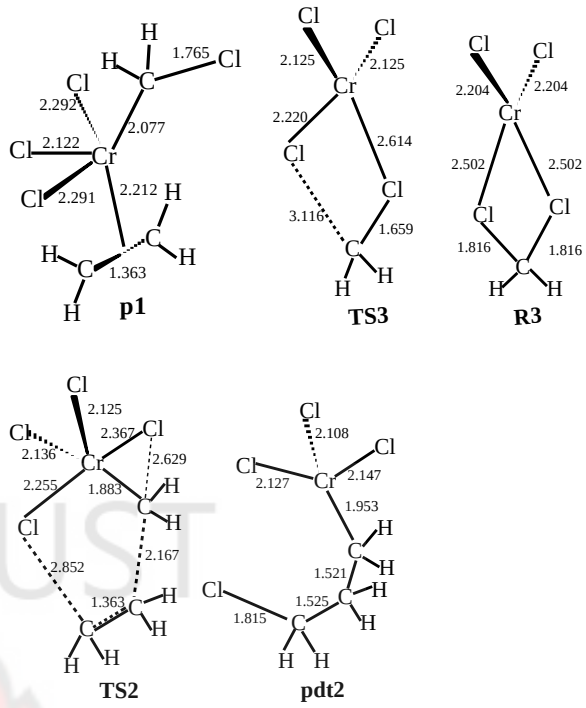

Figure 3.1 Optimized geometries of the main stationary points involved in the reaction of Cl_4CrCH_2 with ethylene. Distances in Å and angles in degrees.

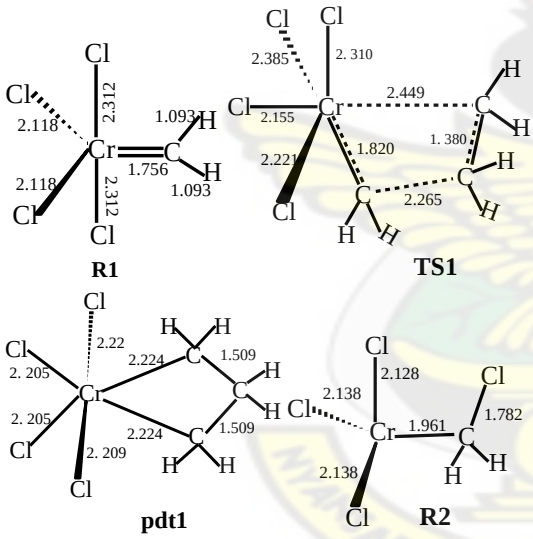

Attempts at locating the reactant **R1** on the triplet and quartet PESs yielded no minima while an open-shell singlet carbene complex located turned out to be an exact replica of the closed-shell **R1** in terms of geometry and energy. A triplet carbenoid (**R2/t**) was found to be 31.80 kcal mol^{-1} more stable than the singlet carbenoid **R2**.

A search of the reaction surface for a Cr carbene-ethylene π-bonded complex

yielded no stationary point. A singlet π-bonded complex **p1** optimized from the interaction of the carbenoid and ethylene is 2.13 kcal mol^{-1} less stable than the separated carbenoid (**R2**) and ethylene reactants, but 32.51 kcal mol^{-1} more stable than the separated carbene and ethylene reactants. A triplet counterpart of **p1** was found to be 32.15 kcal mol^{-1} more stable than the singlet **p1**.

The formation of the metallacyclobutane **pdt1** through the transition state **TS1** by [2+2] addition of ethylene across the Cr-C bond of the carbene complex is 11.52 kcal mol^{-1} exothermic and has an activation barrier of 5.68 $kcalmol^{-1}$. The metallacyclobutane **pdt1** formed is symmetric with respect to the Cr-C and C-C bonds, and has a Cr-C-C-C dihedral angle of 6.88^{o}. This places the two Cr-C bonds in almost the same plane. The Cr=C bond increases from 1.756 Å in the reactant (**R1**) to 1.820 Å in the transition state (**TS1**) while the ethylene C=C bond increases from 1.331 Å in the reactant olefin to 1.380 Å in the transition state. In transition state **TS1**, the Cr-C-C-C dihedral angle is 9.22^{o}, giving the four reacting atoms an almost planar four-center geometry which is typical for olefin insertion into M-C σ bonds (Lohrenz *et. al*., 1995; Deng *et. al*., 1997; Yoshida *et. al*., 1995). Triplet state structures for transition state **TS1** and product **pdt1** were found not to exist on the reaction surface while an open-shell singlet **pdt1** which was found turned out to be the same as the closed-shell singlet **pdt1** with regard to its energy and geometry.

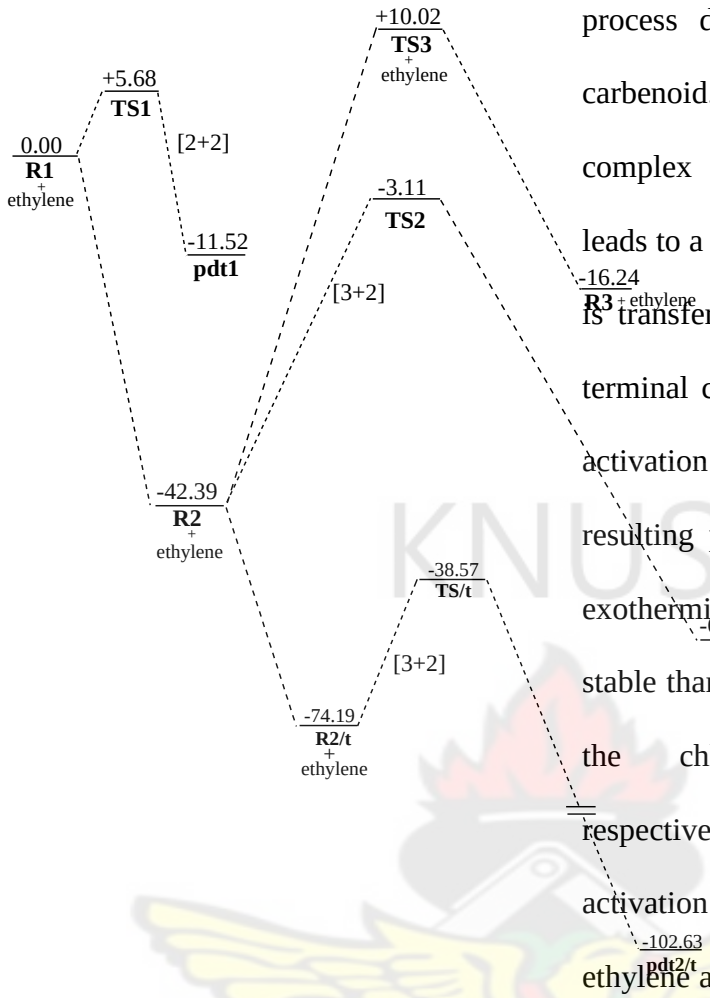

Figure 3. 2. Energetics of the reactions of Cl_4CrCH_2 with ethylene (t = triplet state). Relative energies in kcalmol^{-1}.

The [3+2] addition of ethylene across the Cr-C and Cr-Cl bonds of Cl_4CrCH_2 does not seem to proceed from the carbene reactant since no transition state was located for this reaction step. The process does however proceed from the carbenoid. The addition across the carbenoid complex **R2** through transition state **TS2** leads to a product **pdt2** in which the Cl atom is transferred from the metal center to the terminal carbon atom. This reaction has an activation barrier of 39.28 kcal mol^{-1} and the resulting product **pdt2** is 64.83 kcal mol^{-1} exothermic; 53.31 and 48.59 kcal mol^{-1} more stable than the metallacyclobutane **pdt1** and the chlorine-bridged complex **R3** respectively. On the triplet PES, the activation barrier for the [3+2] addition of ethylene across the Cr-C and Cr-Cl bonds of the triplet carbenoid (**R2/t**) through triplet transition state **TS2/t** is 35.62 kcalmol^{-1}. The resulting triplet product (**pdt2/t**) is very stable (-102.63 kcalmol^{-1}), making it the global minimum on the portions of the reaction surface explored.

Attempts at locating a transition state linking the carbenoid **R2** or the carbenoid-ethylene π-complex **p1** to the metallacyclobutane product **pdt1** was not

successful, suggesting that the formation of the metallacyclobutane, which is the first step of the olefin metathesis reaction according to the Herrison-Chauvin mechanism, may not proceed from the carbenoid complex. Thus the most likely active species for any olefin metathesis in the Cr complex is the carbene complex $Cl_4Cr{=}CH_2$. Even though Figure 3.2 shows that the [2+2] addition of ethylene across the Cr-C bond of $Cl_4Cr{=}CH_2$ to form the metallacyclobutane intermediate **pdt1** has a lower activation barrier than the [3+2] addition pathway, olefin metathesis is not likely to occur with the Cl_4CrCH_2 complex because the existence of a lower-energy carbenoid Cl_3CrCH_2Cl complex (**R2** and **R2/t**) will most likely deplete the reaction surface of the active carbene species **R1** for the process (*vide supra*). This is consistent with the fact that no olefin metathesis reaction has been reported with Cr complexes of this nature to date.

Table 3.1 gives the relative energies of the main stationary points involved in the reaction of Cl_4MCH_2(M= Cr, Mo, W, Ru, Re) complexes with ethylene.

Table 3.1. Calculated Relative Energies (in kcalmol^{-1}) of the Main Stationary Points for the [2+2] and [3+2] Addition of Cl_4MCH_2(M=Cr, Mo, W, Ru, Re) Complexes to Ethylene [a]

complex	carbene+olefin	carbenoid+olefin	TS [2+2]	TS [3+2]	pdt [2+2]	pdt [3+2]
Cl_4CrCH_2	0.00	-42.39	+5.68	-3.11[b]	-11.52	-64.83
Cl_4MoCH_2	0.00	+7.68	+5.33	+6.91	-12.26	-26.77
Cl_4WCH_2	0.00	+31.23	+2.93	+13.65	-13.31	-5.32
Cl_4RuCH_2	0.00	-33.40	+0.48	-4.02[b]	-16.76	-65.54
Cl_4ReCH_2[c]	0.00	+5.15	+2.58	+6.64	-13.74	-27.77

[a] Energies calculated relative to the respective separated carbene and ethylene reactants. [b]In Cl_4CrCH_2 and Cl_4RuCH_2 the [3+2] addition pathway involves the carbenoid complex and not the carbene complex. Thus the activation barrier for [3+2] addition in these complexes are 31.53 and 29.38 kcal mol^{-1} respectively. [c]The Re complex has a doublet ground state electronic structure.

The optimized geometries and relative energies of the main stationary points involved in the reaction of Cl_4MoCH_2 with ethylene are shown in Figures 3.3 and 3.4 respectively. A geometry optimization of the Mo complex Cl_4MoCH_2 on the closed-shell singlet PES yielded two trigonal bipyramid carbene conformers: one in which the CH_2 ligand is in the axial position (**R4$_{ax}$**) and the other in which the methylene ligand occupies the equatorial position (**R4$_{eq}$**). A third minimum has been located on the reaction surface corresponding to a carbenoid Cl_3MoCH_2-Cl species (**R5**). The equatorial carbene **R4$_{eq}$** is 12.89 kcal mol^{-1} and 7.68 kcal mol^{-1} more stable than the axial carbene conformer **R4$_{ax}$** and carbenoid complex **R5** respectively. The axial Mo-Cl bonds are 0.12 - 0.15 Å longer than the corresponding equatorial bonds. The triplet structure of **R4$_{eq}$** has been found to be 11.60 kcal mol^{-1} less stable than the singlet reactant whiles the open-shell singlet structure located is the exact replica of the closed-shell singlet structure. The triplet carbenoid is 28.00 kcal mol^{-1} more stable than the triplet carbene.

A carbene-ethylene π-bonded complex (**pi-comp1**) optimized from the interaction of the equatorial conformer of the carbene complex with ethylene is found to be 5.66 kcal mol^{-1} less stable than the separated reactants. The singlet π-complex **p2** obtained from the interaction of the carbenoid (**R5**) and ethylene is 22.67 kcal mol^{-1} more stable than the separated carbenoid and ethylene reactants and 14.99 kcal mol^{-1} more stable than the carbene and ethylene reactants. The triplet **p2** is 0.20 kcal mol^{-1} less stable than the separated triplet carbenoid and ethylene reactants. The Mo-C bond is 0.164 Å longer in the triplet carbene than the singlet carbene.

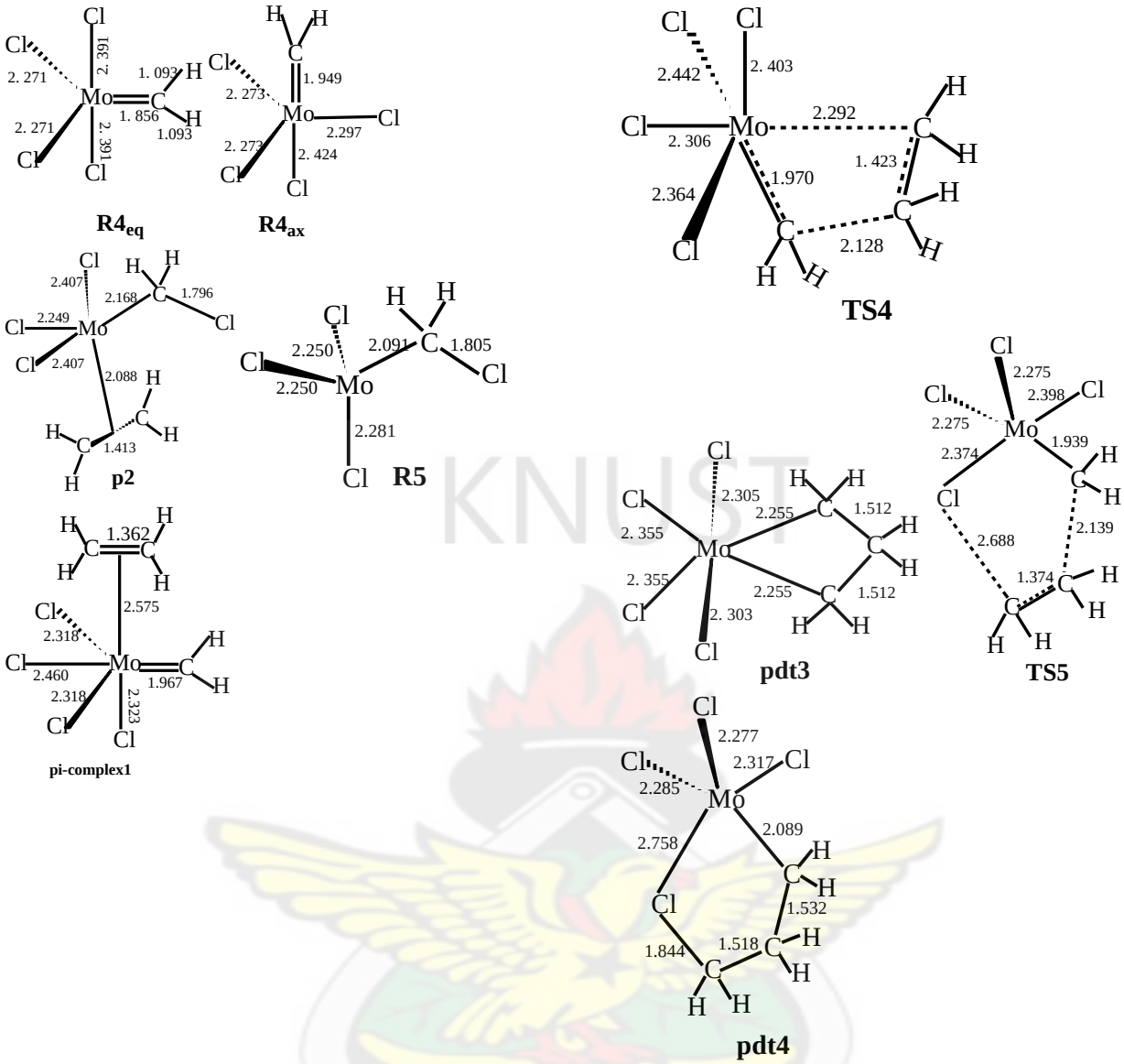

Figure 3.3 Optimized geometries of the main stationary points involved in the reaction of Cl_4MoCH_2 with ethylene. Distances in Å and angles in degrees.

The formation of metallacyclobutane **pdt3** through transition state **TS4** by [2+2] addition of ethylene across the Mo-C bond of Cl_4MoCH_2 has an activation barrier of

5.33 kcal mol^{-1} and exothermicity of 12.26 kcalmol^{-1}. The geometries of the Mo metallacyclobutane intermediate and transition state are very similar to the geometries of the corresponding structures in the Cr complex. The metallacyclobutane is symmetric with respect to the Mo-C and C-C bonds. In transition state **TS4** the Mo-C-C-C dihedral angle is 4.39^{o}, giving the four reacting atoms an almost planar four-center geometry. However, in the metallacyclobutane **pdt3** the four-membered ring is distorted out of plane by 12.54^{o} compared to the Cr metallacyclobutane **pdt1**. The exothermicity of the Mo and Cr products is also comparable; the Mo metallacyclobutane complex is just 0.74 kcal mol^{-1} more stable than the Cr complex.

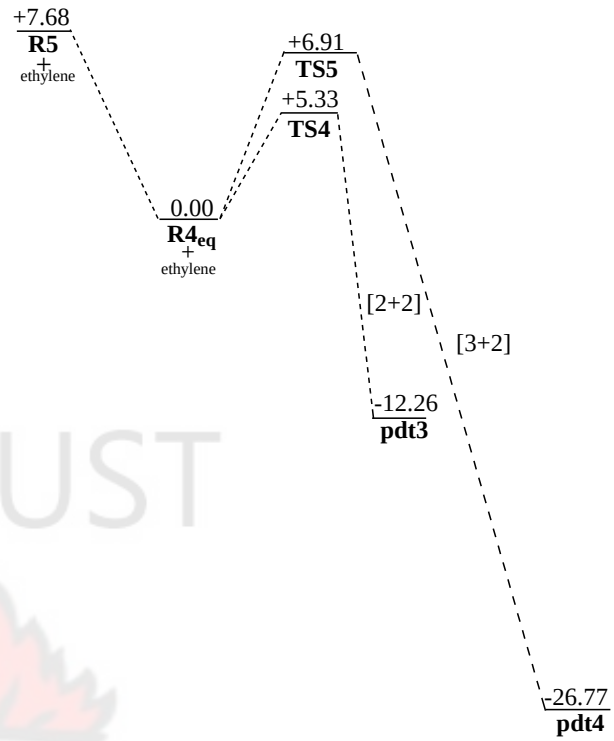

Figure 3.4 Energetics of the reactions of Cl_4MoCH_2 with ethylene. Relative energies in kcalmol^{-1}.

On the triplet PES, the **pdt3** is 30.23 kcal mol^{-1} exothermic; 17.97 kcal mol^{-1} more exothermic than the singlet **pdt3**. The triplet transition state for the formation of **pdt3** is 12.43 kcal mol^{-1} above the singlet reactants and 0.83 kcal mol^{-1} above the triplet reactants. The two Mo-C bonds of the triplet metallacyclobutane are 0.297 Å longer than those of the singlet species while

the Mo-C-C-C dihedral angle in the triplet product is 9.6^{o} compared to the angle of 16.93^{o} in the singlet species. Thus the metallacyclobutane ring is more planar in the triplet species than in the singlet species.

A [3+2] addition of ethylene across the Mo-C and Mo-Cl bonds of the singlet carbene complex leading to the singlet product **pdt4**, which is 26.77 kcal mol^{-1} exothermic, has an activation barrier of 6.91 kcal mol^{-1} through the singlet transition state **TS5**. The triplet **pdt4** has been found to be 21.95 kcal mol^{-1} more stable than the singlet **pdt4**. The triplet transition state **TS5** is not found on the reaction surface.

The olefin metathesis reaction in Mo is not likely to proceed from the carbenoid complex **R5** or the carbenoid π-complex **p2** since attempts at locating a transition state linking the carbenoid complex and metallacyclobutane product yielded no stationary point. Thus the most likely active species for the olefin metathesis is the carbene complex $Cl_4Mo{=}CH_2$. As Fig.3.4 and Table 3.1 show the [2+2] addition pathway is favored kinetically over the [3+2] route, indicating that olefin metathesis will most likely occur in the Mo system. However, the kinetic preference of the [2+2] pathway is only marginal and, given the much higher exothermicity of the [3+2] route, the [3+2] addition pathway is likely to be competitive with the [2+2] addition route. If the kinetics of **p2** formation, which could not be determined in this work, turns out to be favorable and **p2** becomes accessible in the reaction mixture, then the population of the active species will decrease as a result since **p2** is more stable than the separated carbene and ethylene. This might decrease the activity of the Mo catalyst in the olefin metathesis reaction.

On the singlet tungsten (W) reaction surface, two carbene complex minima are located: an equatorial $\mathbf{R6_{eq}}$ and axial $\mathbf{R6_{ax}}$ conformer (Figure 3.5). The equatorial conformer is 13.36 kcal mol^{-1} more stable than the axial conformer. The W=C

bond is marginally shorter (by 0.072 Å) in the equatorial carbene conformer than in the axial conformer. The triplet state **R6$_{eq}$** is 19.52 kcal mol^{-1} less stable than the singlet species and the W-C bond is 0.109 Å longer in the triplet carbene than in the singlet carbene. A carbenoid minimum (**R7**) is also located on the surface but is 31.23 kcal mol^{-1} and 17.89 kcal mol^{-1} less stable than the equatorial and axial carbene complexes respectively. The C-Cl bond in the tungsten carbenoid **R7** is 0.034 and 0.064 Å longer than that in the Mo carbenoid (**R5**) and Cr carbenoid (**R2**) respectively. The bond lengths for the W axial and equatorial carbene complexes (**R6$_{eq}$** and **R6$_{ax}$**) are systematically shorter by between 0.094 and 0.253 Å compared to those reported by Sodupe et. *al*. (1989) in an *ab initio* Hartree-Fock study of this system.

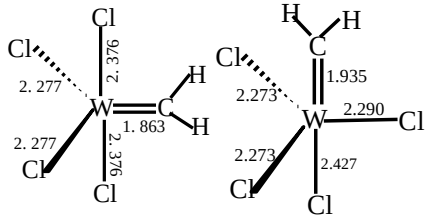

R6$_{eq}$ **R6$_{ax}$**

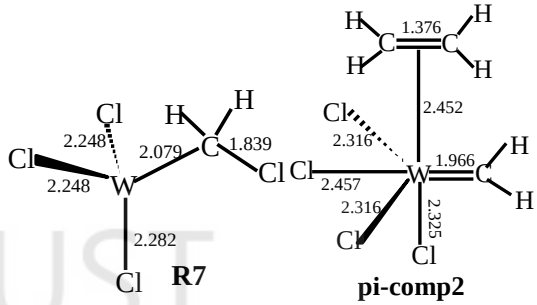

R7 **pi-comp2**

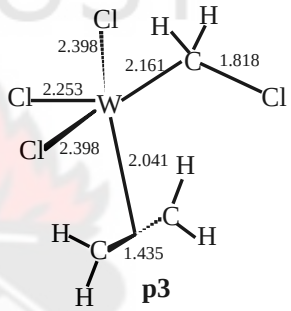

p3

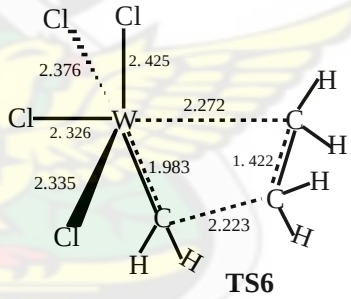

TS6

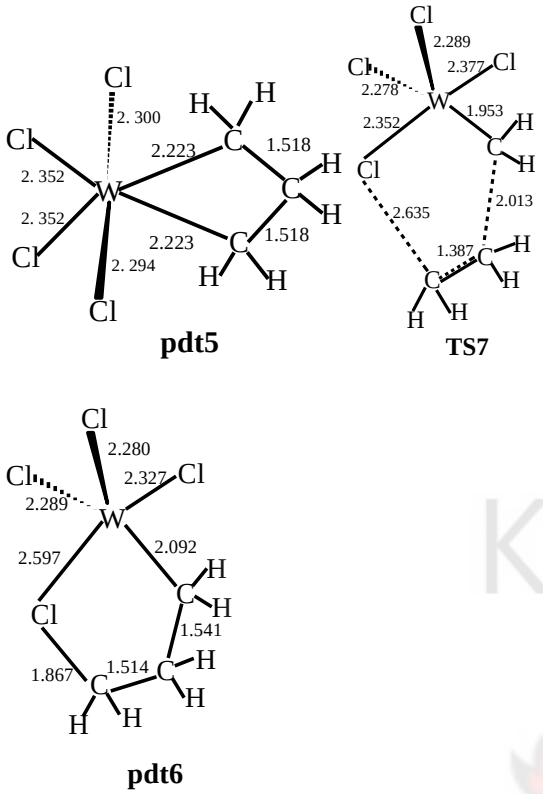

Figure 3.5 Optimized geometries of the main stationary points involved in the reaction of Cl_4WCH_2 with ethylene. Distances in Å and angles in degrees.

The π-complex (**pi-comp2**) that has been optimized from the interaction between the equatorial carbene and ethylene is 9.44 kcal/mol less stable than the separated reactants. The olefinic C-C bond is 0.014 Å longer in the W π-complex than in the Mo π-complex. The π-complex **p3** formed from the interaction of the carbenoid and ethylene is 34.79 kcamol^{-1} more stable than the carbenoid and ethylene reactants, and 3.56 kcal mol^{-1} more stable than the carbene and ethylene reactants. It appears that the π-complex **p3** might be in equilibrium with the carbene and ethylene reactants. The triplet state π-complex **p3** is 9.94 kcal mol^{-1} less stable than the singlet species. The most likely active species for the olefin metathesis appears to be only the carbene complex $Cl_4W{=}CH_2$ and not the carbenoid since no transition state was located linking the carbenoid complex **R7** or the carbenoid π-complex **p3** and the metallacyclobutane intermediate.

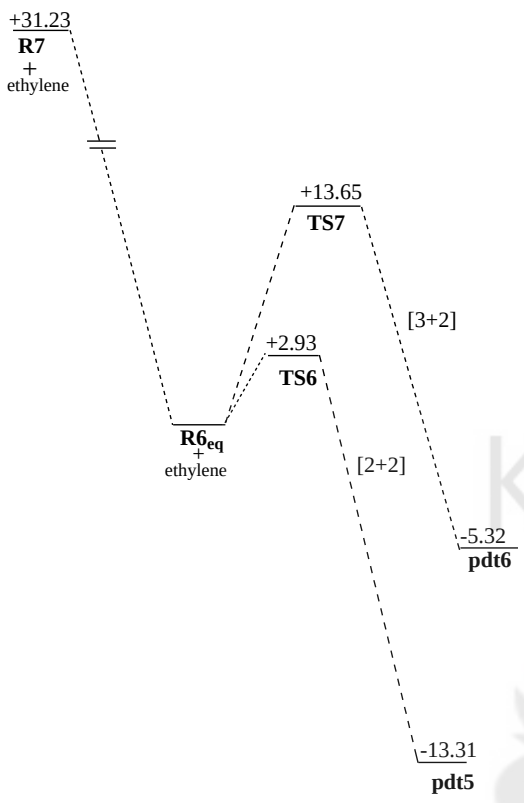

Figure 3.6 Energetics of the reactions of Cl_4WCH_2 with ethylene. Relative energies in kcalmol^{-1}.

The activation barrier for the [2+2] addition of ethylene across the W-C bond of the carbene complex through transition state **TS6** is 2.93 kcalmol^{-1}. The resultant metallacyclobutane **pdt5** is 13.31 kcal mol^{-1} exothermic. This activation barrier is lower than that computed for the corresponding reactions in the Cr and Mo systems, while the formation of the W metallacyclobutane is slightly more exothermic than the formation of the Cr and Mo metallacyclobutanes. The metallacyclobutane is also symmetric with respect to the W-C and C-C bonds as is the case for the Cr and Mo species. The W-C-C-C dihedral angle of 3.08^o in the transition state becomes distorted by 15.74^o in the metallacyclobutane **pdt5**.

The triplet state transition state **TS6** is 17.89 kcal mol^{-1} higher in energy than the singlet species. The newly-forming W-C bond is 0.291 Å longer in the triplet transition state than in the singlet transition state while the newly-forming C-C bond is marginally shorter (by 0.031 Å) in the triplet species than in the singlet species. The resulting triplet metallacycle is 17.73 kcal mol^{-1} less stable than the singlet **pdt5**. With a W-C-C-C dihedral angle of 0.88^o, the triplet metallacycle ring is much more planar than the singlet metallacycle. An open-shell singlet **pdt5** turns out to be exactly like the

closed-shell singlet species in terms of energy and geometry.

Along the [3+2] addition pathway, ethylene adds across the W-C and W-Cl bonds of the carbene complex through transition state **TS7**, with a barrier of 13.65 kcal mol^{-1}, to form species **pdt6** which is 5.32 kcal mol^{-1} exothermic on the singlet PES and 22.98 kcal mol^{-1} exothermic on the triplet PES, the W-Cl forming bond being 0.174 Å longer in the triplet structure than in the singlet structure. Thus the [2+2] addition reaction pathway to form the metallacyclobutanes is more favorable, kinetically and thermodynamically, than the [3+2] addition reaction pathway and therefore the W complex should be able to catalyze metathesis. The energetic preference of the [2+2] over the [3+2] pathway is unambiguous in the W system, unlike in the Mo system where the [3+2] pathway is likely to be competitive with the [2+2] pathway. Also there is no low-energy carbenoid reaction path that might compete with the metathesis process. These results are consistent with earlier suggestions that the W alkylidene catalyst has a greater metathesis activity than the Mo species (Cundari and Gordon, 1992). A Mulliken population analysis of the carbene complexes reveals that the order of polarization of the M-C bond in a $M^{+}=C^{-}$ fashion is in the order: W > Mo > Cr. This observation supports the finding by Cundari and Gordon (1992) that the W-C bond is more polarized than the Mo-C bond in the methylidene complexes. The extent of polarization has been found to be comparable in the Mo and W carbenoid complexes.

On the singlet Ru reaction surface an equatorial carbene conformer $Cl_4Ru=CH_2$ **R8$_{eq}$** and a carbenoid Cl_3Ru-CH_2-Cl **R9** structure (Figures 3.7 and 3.8) are located. The carbenoid complex is 33.46 kcal mol^{-1} more stable than the carbene complex. In contrast, DFT B3LYP studies by Bernardi et. *al.* (2003) on olefin metathesis catalyzed

by Grubbs' ruthenium complexes found the equatorial carbenic complex $Cl_2(PH_3)_2Ru{=}CH_2$ to be 18.45 kcal mol^{-1} more stable than the carbenoid $Cl_2(PH_3)Ru$-$CH_2(PH_3)$ species. The triplet carbene complex has been found to be 12.77 kcal mol^{-1} more stable than the singlet carbene whiles the triplet carbenoid is 0.86 kcal mol^{-1} less stable than the singlet carbenoid.

Attempts at locating the axial carbene conformer and a carbene-ethylene π-bonded complex on the reaction surface were not successful. An ethylene π-bonded carbenoid complex **p4** optimized from the interaction of the carbenoid and ethylene has been found to be 6.74 kcal mol^{-1} more stable than the singlet carbenoid and ethylene reactants, and 40.16 kcal mol^{-1} more stable than the carbene and ethylene reactants. The triplet carbenoid-ethylene π-complex is 2.68 kcal mol^{-1} more stable than the singlet π-complex. The distance between the Ru center and the olefinic C-C centroid is 0.330 Å longer in the triplet π-complex than in the singlet π-complex.

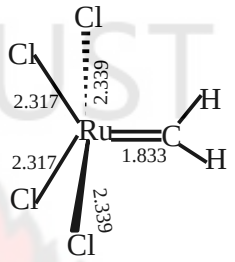

R8$_{eq}$

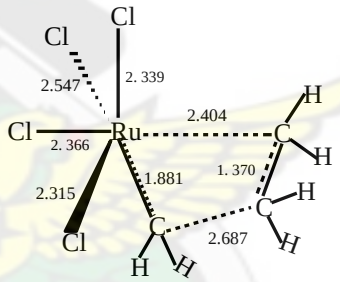

TS8

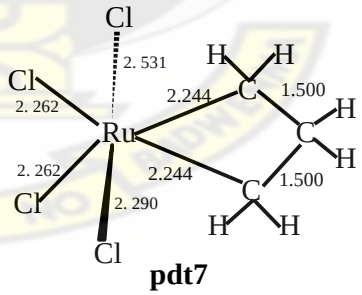

pdt7

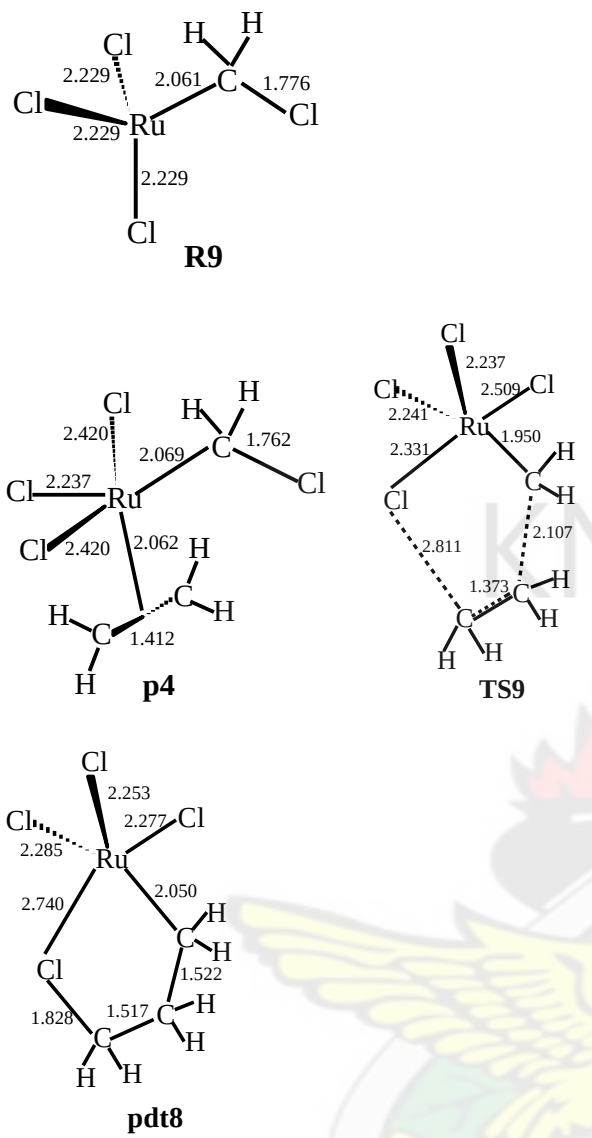

Figure 3.7 Optimized geometries of the main stationary points involved in the reaction of Cl_4RuCH_2 with ethylene. Distances in Å and angles in degrees.

The activation barrier through transition state **TS8** for the [2+2] addition of ethylene across the Ru-C bond of the carbene is 0.48 kcalmol^{-1}, which is smaller than the barriers of 9.7 and 9.6 kcal mol^{-1} for norbonene and 1-butene respectively found by Cavallo (2002) in the study of the mechanism of metathesis reactions of 1-butene and norbonene catalyzed by model Grubbs Ru catalysts. The resultant metallacyclobutane (**pdt7**), which is 16.76 kcal mol^{-1} exothermic, is symmetric with respect to the Ru-C and C-C bonds. The Ru-C-C-C dihedral angle is 5.50^{o} in transition state **TS8** and 5.54^{o} in the metallacyclobutane **pdt7**. Thus there is no considerable distortion of the planar geometry of the forming ring during the formation of the metallacyclobutane from the transition state. The activation barrier for the [2+2] addition of ethylene across the Ru-C bond of triplet carbene through a triplet transition state **TS8/t** is 3.58 kcalmol^{-1}. The newly-forming Ru-C and C-C bonds are 0.317 Å and 0.639 Å respectively longer in the triplet transition state than in the singlet transition state.

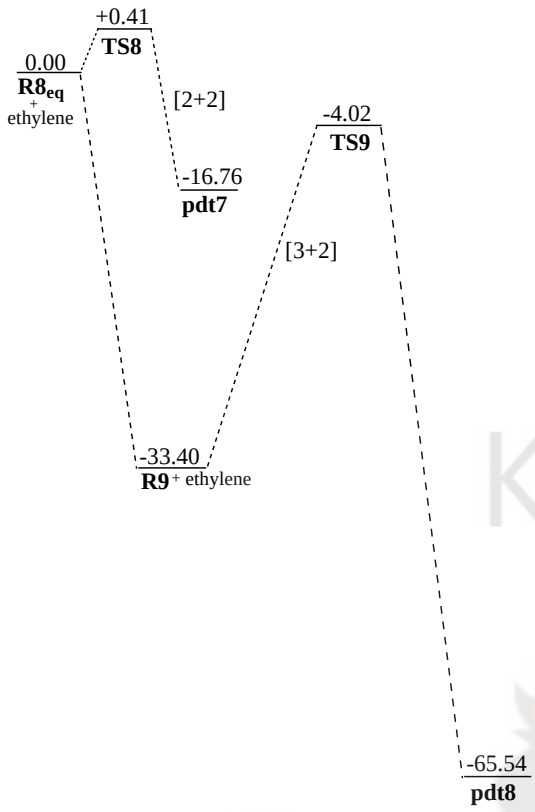

Figure 3.8 Energetics of the reactions of Cl_4RuCH_2 with ethylene. Relative energies in kcalmol^{-1}.

Just as was observed for the Cr complex, the [3+2] addition of ethylene across the Ru-C and Ru-Cl bonds of Cl_4RuCH_2 does not proceed from the carbene complex but rather from the carbenoid. The [3+2] addition of ethylene across the Ru-C and Ru-Cl bonds of carbenoid **R9** through transition state **TS9** has a barrier of 29.38 kcalmol^{-1}, leading to a very exothermic (-65.54 kcalmol^{-1}) product **pdt8**.

It is being concluded that a metallacyclobutane may not originate from the carbenoid complex, since no transition state was located linking the carbenoid and the metallacycle. Thus the active species for any olefin metathesis in the Ru complex should be the carbene complex. Even though the [2+2] addition pathway has a very low transition barrier, the reaction surface is likely to be populated by the carbenoid complex reactant and not the carbene complex as Table 3.1 shows. Thus the formation of **pdt7**, which will ultimately lead to olefin metathesis, may not occur since the reaction surface may be depleted of the active species for metathesis.

The optimized geometries and relative energies of the main stationary points involved in the reaction of Cl_4ReCH_2 with ethylene are shown in Figure 3.9 and Figure 3.10 respectively. No stationary points could be located on the singlet and

triplet PESs. The reactant minima **R10$_{eq}$/d** and **R10$_{eq}$/q** were located on the doublet and quartet PESs; the doublet structure being 12.40 kcal mol^{-1} more stable than the quartet structure. The Re-C double bond is 0.112 Å longer in the quartet species than in the doublet species. A carbenoid species **R11/d** located on the doublet surface is 5.15 kcal mol^{-1} less stable than the doublet carbene whiles a quartet carbenoid is 2.93 kcal mol^{-1} more stable than the doublet carbene. π-complexation of the doublet and quartet carbenoids with ethylene stabilizes the system by 21.55 and 8.49 kcal mol^{-1} respectively relative to the separated reactants. This contrasts with π-complexation of the doublet carbene with ethylene which destabilizes the system by only 1.11 kcal mol^{-1} relative to the separated reactants.

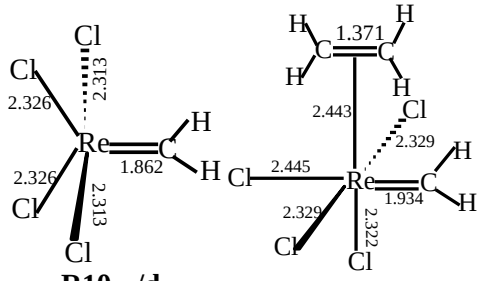

R10$_{eq}$/d

pi-comp4

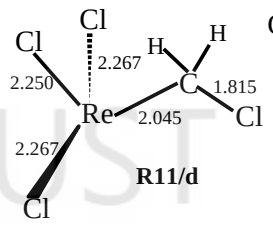

R11/d

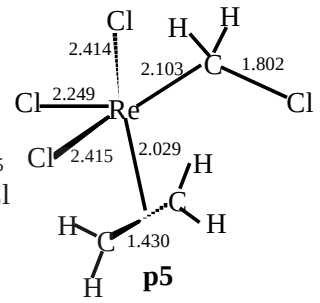

p5

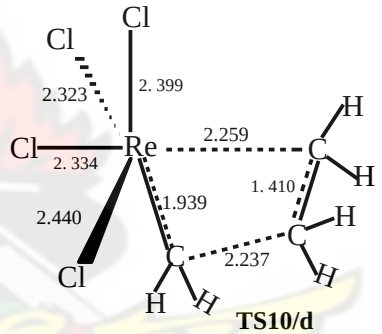

TS10/d

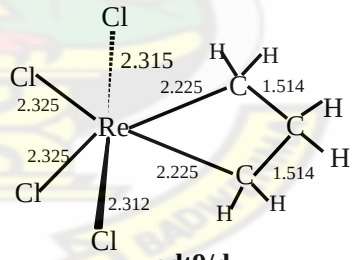

pdt9/d

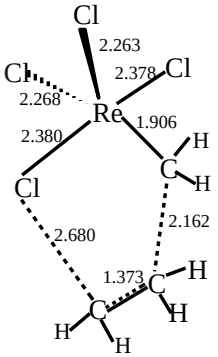

TS11/d

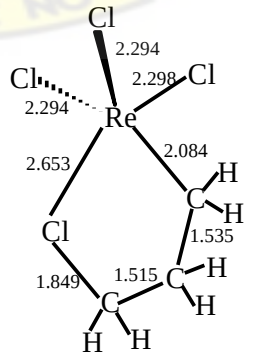

pdt10

Figure 3.9 Optimized geometries of the main stationary points involved in the reaction of Cl_4ReCH_2 with ethylene. Distances in Å and angles in degrees.

The doublet transition state **TS10/d** that connects the carbene reactant **R10eq/d** to the doublet product **pdt9/d** in the [2+2] addition of ethylene across the Re-C bond of Cl_4ReCH_2 is 2.58 kcal mol^{-1} above the doublet carbene and ethylene reactants on the potential energy profile. The product resulting from this addition is 13.74 kcal mol^{-1} exothermic. The Re-C-C_1-C_2 dihedral angle (where C_1 and C_2 are the olefinic carbons) of 4.52^o in transition state **TS10** increases to 14.15^o in the product **pdt9**.

The activation barrier for the [3+2] addition of ethylene across the Re-C and Re-Cl bonds of doublet Cl_4ReCH_2 through the doublet transition state **TS11** is 6.64 $kcalmol^{-1}$. The product formed, which is also a doublet species, is 27.77 kcal mol^{-1} exothermic. No quartet state **TS10** and **TS11** were located on the PESs.

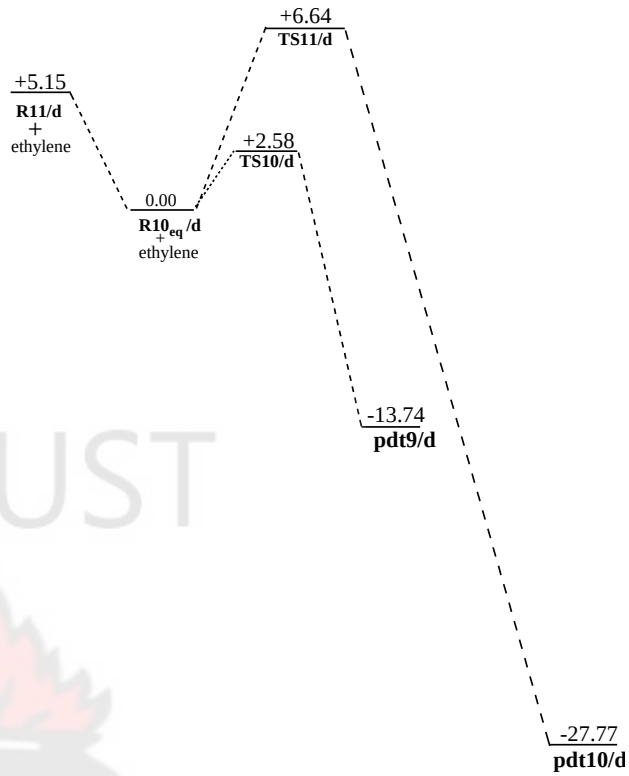

Figure 3.10 Energetics of the reactions of Cl_4ReCH_2 with ethylene. Relative energies in $kcalmol^{-1}$.

Since the activation barrier of the formation of the metallacyclobutane is lower than the barrier for the formation of product of [3+2] addition, the Re complex is likely to be able to catalyze metathesis.

Figure 3.11 is a summary of the possible paths for the reactions of the complexes Cl_4MCH_2 (M=Cr, Mo, W, Ru,

Re) with ethylene. The Mo, W, and Re complexes can follow two reaction paths: **1** → **4** → **5** and **1** → **6**→ **8**, but the former route is preferred over the latter. The preference for the **1** → **4** → **5** route over **1** → **6** → **8** is clearly unambiguous in W, whereas in Mo the latter route is likely to be competitive with the former. The Cr and Ru complexes can also follow paths: **1** → **4** → **5** and **2** → **7** → **8**, but the latter path is preferred over the former.

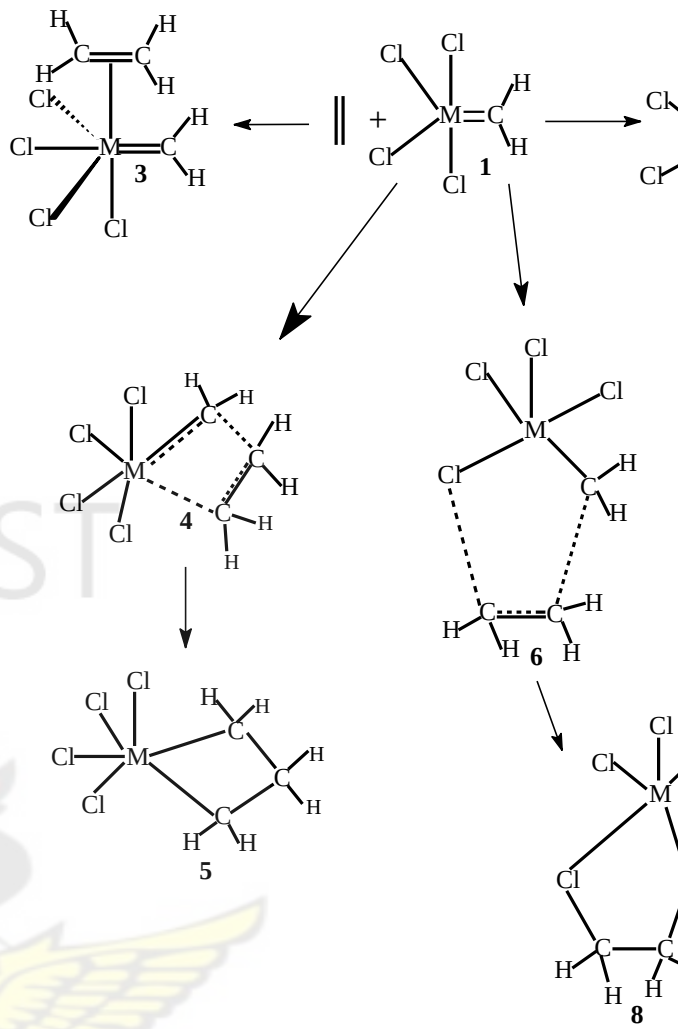

reaction route	metal complex
1 → **4** → **5**[a]	Cr, Mo, W, Ru, Re
1 → **6** → **8**	Mo, W, Re
2 → **7**→ **8**[b]	Cr, Ru
1 → **3**	Mo, W, Ru, Re
2 → **9**	Cr, Mo, W, Ru, Re

[a] **1** → **4** → **5** is preferred

route in Mo, W, Re

[b]**2** → **7**→ **8** is preferred

route in Cr, Ru

Figure 3.11 Summary of the possible reaction paths for the reaction of Cl_4MCH_2 (M=Cr, Mo, W, Ru, Re) with ethylene.

The energy profiles (Figures 3.2, 3.4, 3.6, 3.8 and 3.10) indicate that the reaction of carbene complexes $Cl_4M{=}CH_2$ with ethylene to form a metallacyclobutane is a low-barrier process for each of the metal complexes studied, the highest barrier being 5.68 kcal mol^{-1} for the Cr complex and the lowest being 0.48 kcal mol^{-1} for the Ru complex. The activation barriers of the complexes studied were found to decrease in the order: Cr > Mo > W ≈ Re > Ru while the exothermicities decrease in the order: Ru (16.76 $kcalmol^{-1}$) > Re ≈ W > Mo > Cr (11.52 $kcalmol^{-1}$).

Attempts at locating a transition state linking the metallacyclobutane product and the carbenoids in each of the systems studied yielded no stationary point, indicating that the formation of the metallacyclobutane is not likely to proceed from the carbenoid complexes. Therefore the active species for the metathesis reaction in each of these complexes are carbene complexes as opposed to carbenoids.

One key factor has been found to be responsible for the difference in metathesis activity in the complexes studied: the stability of the carbenoid complexes relative to the carbenes. In Cr and Ru, the carbenoid complexes are more stable than the carbenes and thus Cl_4CrCH_2 and Cl_4RuCH_2 are likely to exist in the lower-energy carbenoid Cl_3MCH_2Cl form as opposed to the carbene $Cl_4M{=}CH_2$ form. This is likely to deplete the reaction surface of the active species of the process, making Cl_4MCH_2(M=Cr, Ru) not suitable for olefin metathesis. This suggests that whereas Cl_4MCH_2 (M = Mo, W, Re) may catalyze olefin metathesis, Cl_4MCH_2 (M = Cr, Ru) may not. The kinetic and thermodynamic preference of the [2+2] pathway over the [3+2] pathway is unambiguous in $Cl_4W{=}CH_2$ whereas in Cl_4MoCH_2 the [3+2] pathway and the formation of carbenoid complexes may be competitive with the [2+2] pathway. The

kinetics of metallacyclobutane formation also indicates that the W and Re complexes may have a greater metathesis activity than the Mo complex.

The Cr and Ru carbene complexes do not seem to form π-complexes while the carbene-ethylene π-complexes located for the Mo, W and Re complexes are all higher-energy species relative to the reactants. This must be considered in relation to the well-known difficulties for DFT methods to describe weak interactions (Kristán and Pulay, 1994; Wright, 1996; Peréz-Jordá and Becke, 1995; Ruiz *et. al*., 1996; Garcia *et. al*., 1997). The B3LYP functional in particular does not describe dispersion, and therefore underestimate the interaction energies of π-bonded systems. This may well result in a repulsive interaction (Mourik and Gbanitz, 2002; Mourik, 2008). Given these difficulties, it is difficult to assess the role of the π-complex in the mechanism of the reactions.

Some of the minima and transition states located in this work display multiple spin ground states. For the Cr and Ru complexes, inclusion of the triplet state structures actually increases the stability of the carbenoid relative to the carbenes and this worsens the inability of the Cl_4CrCH_2 complex to catalyze metathesis. For the Re complex, the doublet ground state is more favored over the quartet ground state. The Re complex appears not to have a singlet or triplet ground state. Finally the reaction patterns of the Cr and Ru complexes are similar whiles those of the Mo and W are also similar.

3.3.2 REACTIONS OF $Cl_2(O)MCH_2$ (Cr, Mo, W, Ru, Re) WITH ETHYLENE

Rappé and Goddard (1982) have used the results of an *ab initio* theoretical mechanistic study to suggest that the oxo-

alkylidene complex $Cl_2(O)M{=}CH_2$ would favor formation of metallacycles because of conversion of the double-bond spectator oxo group in the reactant to a triple bond in the product. These intermediates have therefore been studied in this work as potential active chain-carrying catalysts that could react with an olefin to form metallacyclobutanes in olefin metathesis. Various possible modes of reaction of ethylene with metal oxo-alkylidenes are considered in the study.

The optimized geometries of the main stationary points involved in the reaction between Cl_2OCrCH_2 and ethylene are shown in Figure 3.12. The Cr oxo-methylidene complex **R12** as optimized at the DFT B3LYP/LACVP* level has a Cs symmetry. The Cr=O and Cr=C bond lengths are 1.536 Å and 1.761 Å respectively while the two Cr-Cl bond lengths are equal (2.150 Å). A carbenoid minimum **R13** is also located on the reaction surface and is found to be 3.60 kcal mol^{-1} less stable than the carbene minimum.

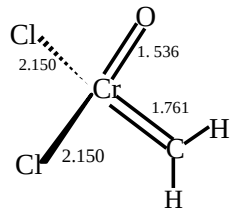

R12

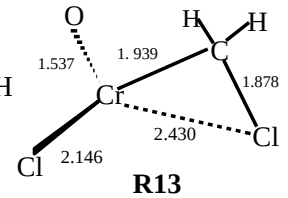

R13

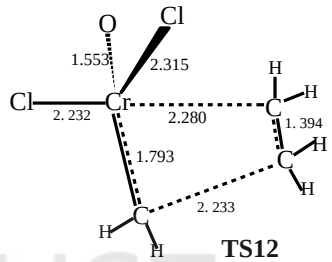

TS12

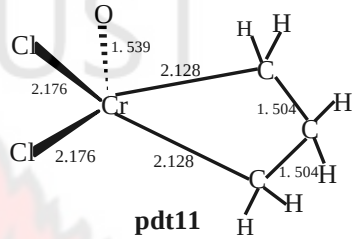

pdt11

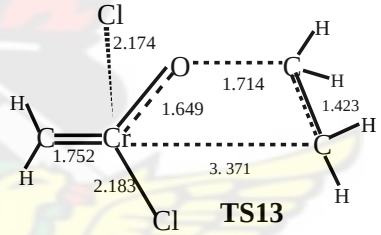

TS13

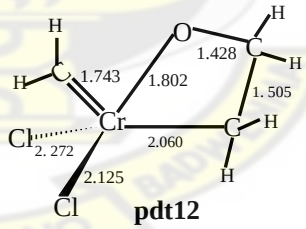

pdt12

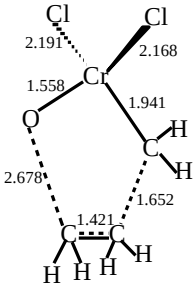

TS14

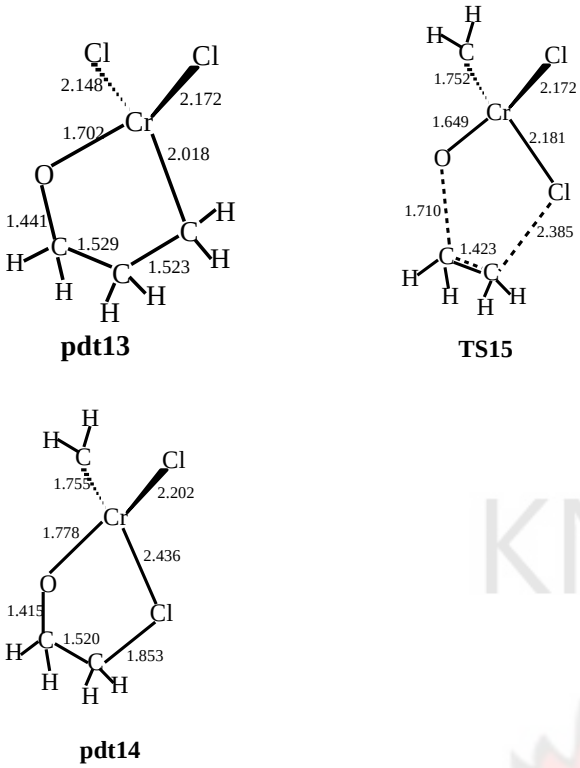

Figure 3.12 Optimized geometries of the main stationary points involved in the reaction of $Cl_2(O)CrCH_2$ with ethylene. Distances in Å and angles in degrees.

The formation of the product **pdt11** by [2+2] addition of ethylene across the Cr-C bond of **R12** through transition state **TS12** has an activation barrier of 12.10 kcamol^{-1} and exothermicity of 14.30 kcal mol^{-1} (Figure 3.13). The metallacycle is symmetric with respect to the C-C and Cr-C bonds. Rappé and Goddard (*ibid.*) had found, by *ab initio* GVB calculations, that the formation of **pdt11** is exothermic by 20 kcalmol^{-1}.

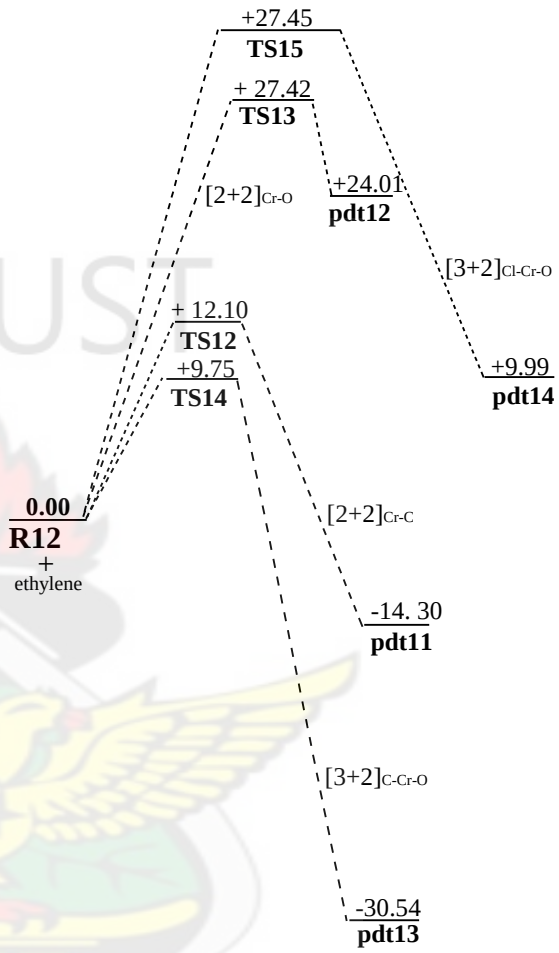

Figure 3.13. Energetics of the reactions of $Cl_2(O)CrCH_2$ with ethylene. Relative energies in kcalmol^{-1}.

The formation of product **pdt12** by [2+2] addition of ethylene across the Cr-O bond of **R12** through transition state **TS13** has a barrier of 27.42 kcal mol^{-1} and

endothermicity of 24.01 kcalmol^{-1}. Thus the [2+2] addition of ethylene across the Cr-C bond is more favorable, both kinetically and thermodynamically, over addition across the Cr-O bond. The early transition state **TS13** is a highly asynchronous one. In the work of Rappé and Goddard (1982) this reaction is reported to be 12 kcal mol^{-1} endothermic.

The [3+2] addition of ethylene across the Cr-O and Cr-C bonds of **R12** involves transition state **TS14**, with a barrier of 9.75 kcalmol^{-1}, to form **pdt13** which is 30.54 kcal mol^{-1} exothermic (Figure 3.13). The [3+2] addition across the Cr-O and Cr-Cl bonds has a much higher activation barrier of 27.45 kcal mol^{-1} and the resulting product **pdt14** is 9.99 kcal mol^{-1} endothermic.

The most favorable pathway, kinetically and thermodynamically, is the [3+2] addition of ethylene across the Cr-O and Cr-C bonds of **R12**. Since the [3+2] addition is more favorable than the [2+2] addition across the Cr-C bond of **R12** (Figure 3.13), the first step of the olefin metathesis reaction, olefin metathesis reaction may not occur in the $Cl_2(O)CrCH_2$ complex. However, since the activation barrier of the metallacyclobutane formation is only 2.35 kcal mol^{-1} higher than the barrier of the [3+2] pathway, the metathesis reaction is not too disfavored and may occur to some extent.

Table 3.2 Activation Barriers (in kcalmol^{-1}) of the Various Pathways in the Reaction of $Cl_2(O)MCH_2$ (M=Cr, Mo, W, Ru, Re) with Ethylene

complex	[2+2](M-C)	[2+2](M-O)	[3+2](O-M-C)	[3+2](O-M-Cl)
$Cl_2(O)CrCH_2$	12.10	27.42	9.75	27.45
$Cl_2(O)MoCH_2$	5.38	30.67	26.68	44.43
$Cl_2(O)WCH_2$	0.38	26.25	39.48	-
$Cl_2(O)Ru$			-	

CH_2	13.78	17.00		10.17
$Cl_2(O)Re$				
CH_2	7.80	26.66	11.34	38.71

On the Mo reaction surface, the reactant oxo-alkylidene (**R14** in Figure 3.14) has a Mo=O bond length of 1.681 Å, Mo=C bond length of 1.883 Å and the two Mo-Cl bond lengths at 2.303 Å each. No carbenoid minimum could be located on the surface.

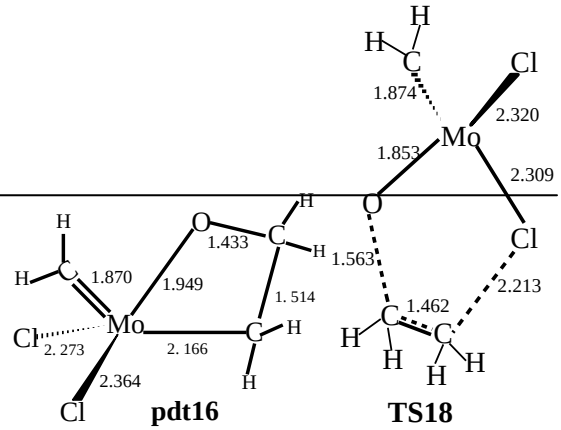

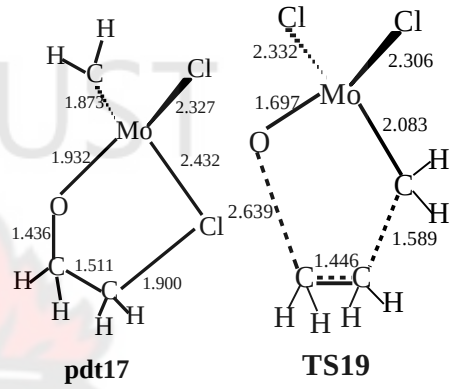

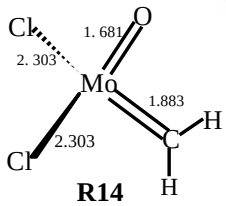

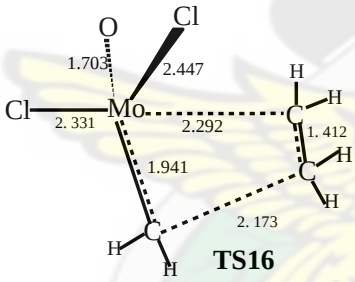

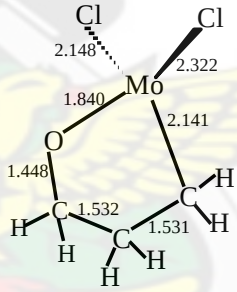

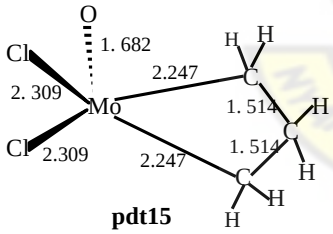

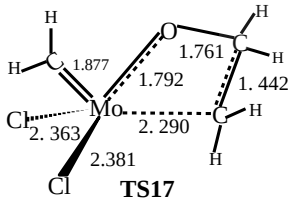

Figure 3.14 Optimized geometries of the main stationary points involved in the reaction of $Cl_2(O)MoCH_2$ with ethylene. Distances in Å and angles in degrees.

The transition barrier for [2+2] addition of ethylene across the Mo-C bond of **R14** through transition state **TS16** is 5.38 kcalmol^{-1}, leading to the metallacycle **pdt15**

which is 11.38 kcal mol^{-1} exothermic. Rappé and Goddard (1982) found this reaction to be 24 kcal mol^{-1} exothermic. Compared with the corresponding Cr-system this reaction is more favorable kinetically, but slightly less so thermodynamically. The [2+2] addition of ethylene across the Mo-O bond of **R14** has a barrier of 30.67 kcal mol^{-1} which is about six times higher than the barrier for addition across the Mo-C bond. The resulting metallacycle **pdt16** is 18.86 kcal mol^{-1} endothermic. Thus addition across the Mo-C bond is more favorable, both kinetically and thermodynamically, than addition across the Mo-O bond.

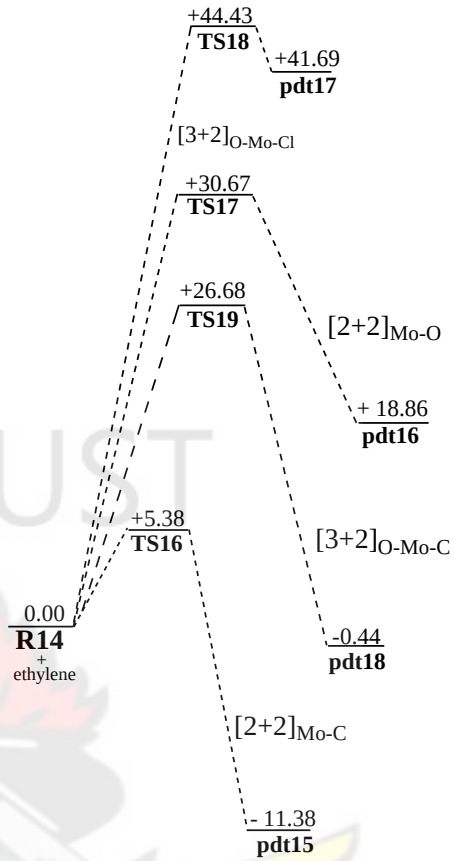

Figure 3.15 Energetics of the reactions of $Cl_2(O)MoCH_2$ with ethylene. Relative energies in kcalmol^{-1}.

The [3+2] addition across the Mo-C and Mo-O bonds through transition state **TS19** has a barrier of 26.68 kcalmol^{-1}, leading to a five-membered product **pdt18** which is 0.44 kcal mol^{-1} exothermic while the [3+2] addition across the Mo-O and Mo-Cl bonds of **R14** through transition state **TS18** has a much higher barrier of 44.43

kcalmol^{-1}, leading to product **pdt17** which is very endothermic (+41.69 kcalmol^{-1}). Thus in the Mo complex the [2+2] addition of ethylene across the Mo-C bond of **R14**, which is the first step of the olefin metathesis reaction, is the most favorable reaction pathway. The preference of the metallacyclobutane formation pathway over the side-reactions is clearly unambiguous. The side reactions are therefore not likely to be competitive with the olefin metathesis reaction (Figure 3.15). Olefin metathesis will therefore be favored to occur in the Mo complex.

The W oxo-alkylidene reactant (**R15** in Figure 3.16) has a W=O bond length of 1.688 Å, a W=C bond length of 1.886 Å and the two W-Cl bond lengths at 2.299 Å each.

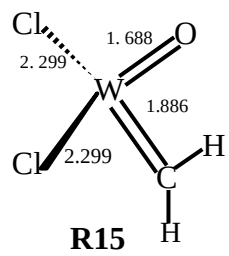

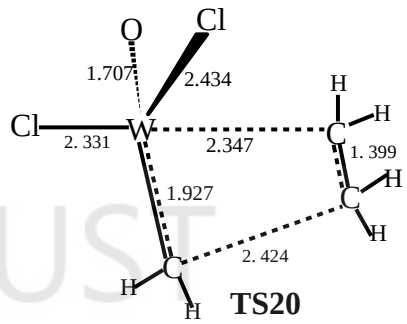

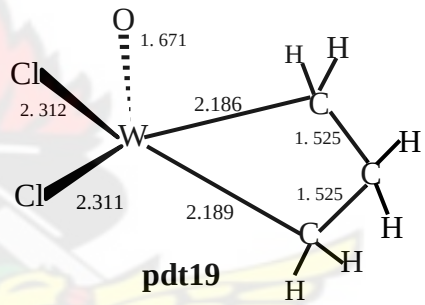

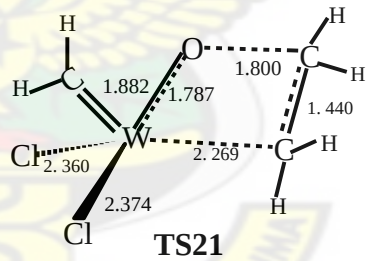

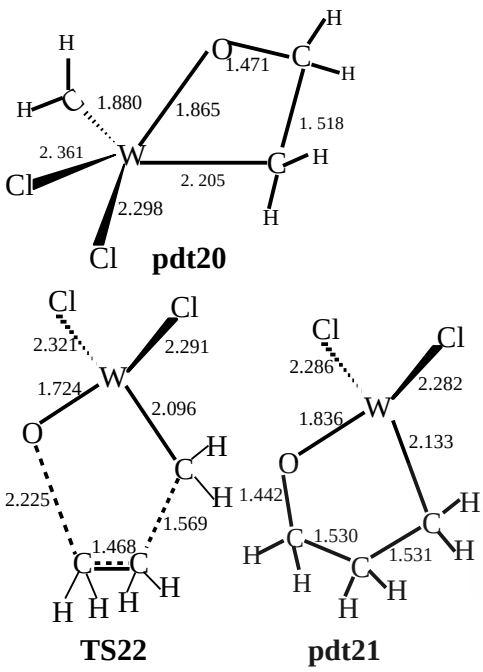

Figure 3.16 Optimized geometries of the main stationary points involved in the reaction of $Cl_2(O)WCH_2$ with ethylene. Distances in Å and angles in degrees.

The activation barrier for the formation of metallacyclobutane **pdt19**, which is 16.49 kcal mol^{-1} exothermic, by [2+2] addition of ethylene across the W-C bond of **R15** through transition state **TS20** is 0.38 kcalmol^{-1}. The resulting metallacycle **pdt19** is 16.49 kcal mol^{-1} exothermic. In the work of Rappé and Goddard (1982) this reaction is found to be 18 kcal mol^{-1} exothermic. The activation energy for [2+2] addition across the W-O bond of **R15** through transition state **TS21** is 26.25 kcalmol^{-1}, resulting in a metallacycle **pdt20** which is 19.83 kcal mol^{-1} endothermic. Thus addition across the W-C is far more favored, both kinetically and thermodynamically, than addition across the W-O bond.

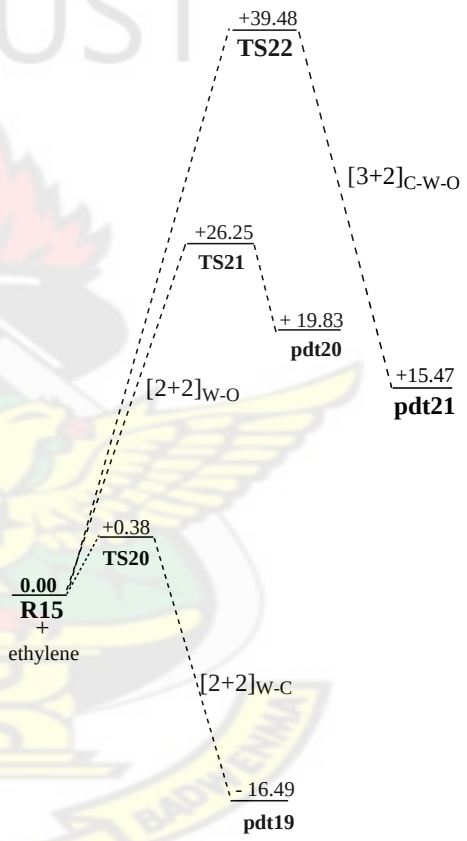

Figure 3.17 Energetics of the reactions of $Cl_2(O)WCH_2$ with ethylene. Relative energies in kcalmol^{-1}.

Along the [3+2] pathway, addition across the W-O and W-C bonds of **R15**

through **TS22** has a barrier of 39.48 kcalmol^{-1}, leading to a five-membered ring product **pdt21** which is 15.47 kcal mol^{-1} endothermic. No product or transition state could be located for the [3+2] addition across the W-O and W-Cl bonds.

Of the three possible addition pathways, the [2+2] addition of ethylene across the W-C bond, which is the first step of the olefin metathesis reaction, is the most favorable one. The possible side reactions are therefore not competitive with the olefin metathesis reaction, just as has been observed for the Mo system.

DFT optimization of the Ru oxo-alkylidene intermediate gave structure **R16**, which has a Ru-C bond length of 1.844 Å, Ru-O bond length of 1.685 Å and the two Ru-Cl bond lengths at 2.292Å each. A carbenoid minimum **R17** and is 4.07 kcal mol^{-1} less stable than the carbene. The activation barrier for the formation of metallacyclobutane **pdt22** by [2+2] addition of ethylene across the Ru-C bond of **R16** through transition state **TS23** has an activation barrier of 13.78 kcal mol^{-1} and an exothermicity of 31.45 kcalmol^{-1}. The barrier for [2+2] addition across the Ru-O bond of **R16** through **TS24** is 17.00 kcalmol^{-1}, leading to a metallacyclobutane **pdt23** which is 2.70 kcal mol^{-1} exothermic. Thus, of the [2+2] addition pathways, addition across the Ru-C bond is more favorable, both kinetically and thermodynamically, than addition across the Ru-O bond.

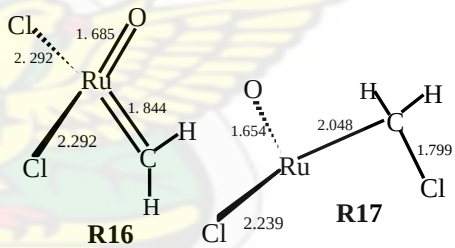

R16 **R17**

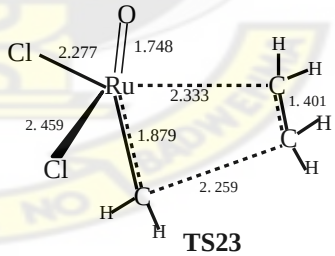

TS23

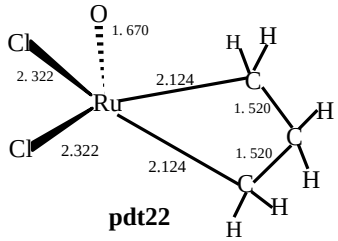

pdt22

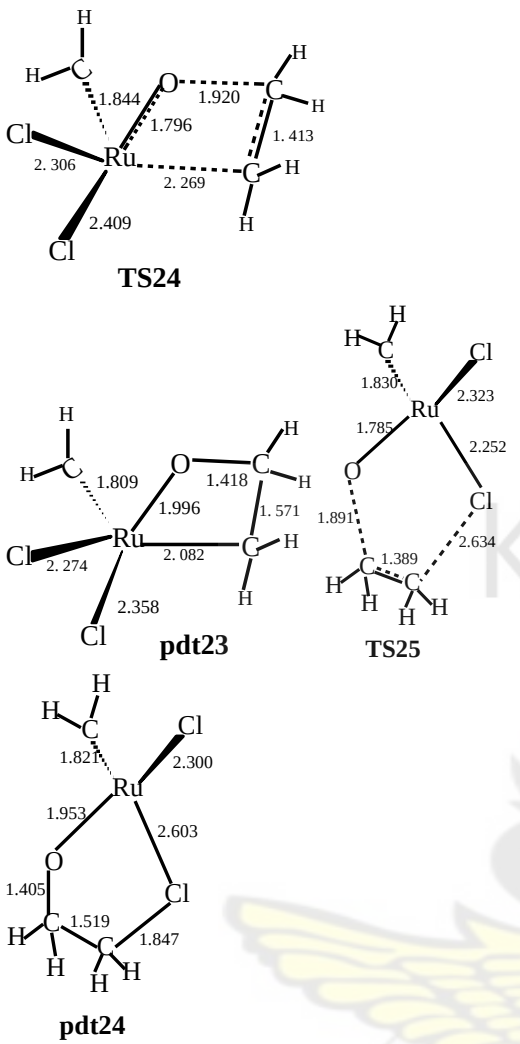

Figure 3.18 Optimized geometries of the main stationary points involved in the reaction of $Cl_2(O)RuCH_2$ with ethylene. Distances in Å and angles in degrees.

Along the [3+2] pathway, addition of ethylene across the Ru-O and Ru-Cl bonds of **R16** has a barrier of 10.17 kcalomol^{-1} with the resulting product **pdt24** being 16.33 kcal mol^{-1} exothermic. The [3+2] addition pathway is slightly more favorable kinetically than the [2+2] addition across the Ru-C bond of **R16**. Thus this reaction might interfere with the olefin metathesis reaction. Attempts at locating the transition state or product corresponding to the [3+2] addition across the Ru-O and Ru-C bonds on the surface was not successful.

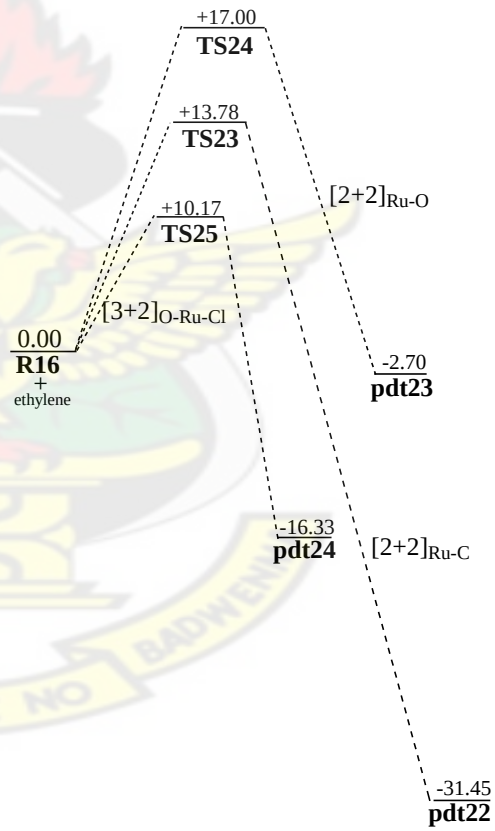

Figure 3.19 Energetics of the reactions of $Cl_2(O)RuCH_2$ with ethylene. Relative energies in kcalmol^{-1}.

The optimized geometries and relative energies of the main stationary points involved in the reaction of the Re oxo-methylidene complex $Cl_2(O)ReCH_2$ with ethylene are shown in Figures 3.20 and 3.21 respectively. The Re complex display a doublet electronic ground state electronic structure rather than a singlet structure. It also displays a quartet structure but this is of higher energy than the doublet structure. The doublet oxo-methylidene reactant **R18** has the two Re-Cl bond lengths of 2.298 Å, the Re-O bond at 1.690 Å and the Re-C bond at 1.865 Å. The quartet reactant which displays slightly longer bonds than the doublet structure is 77.33 kcal mol^{-1} less stable than the doublet structure. An oxo-carbenoid **R19** that has been optimized is found to be 29.33 kcal mol^{-1} less stable than the carbene reactant.

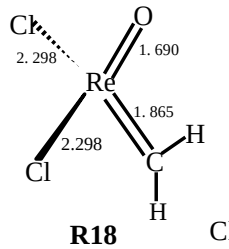

R18

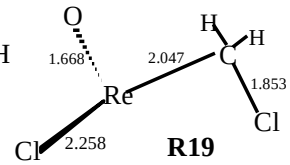

R19

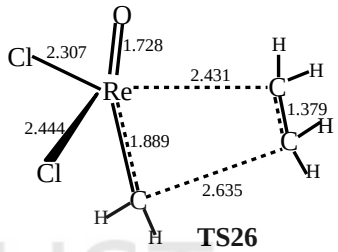

TS26

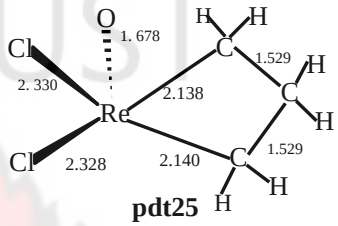

pdt25

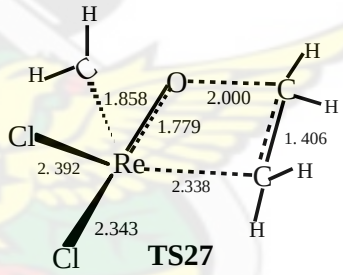

TS27

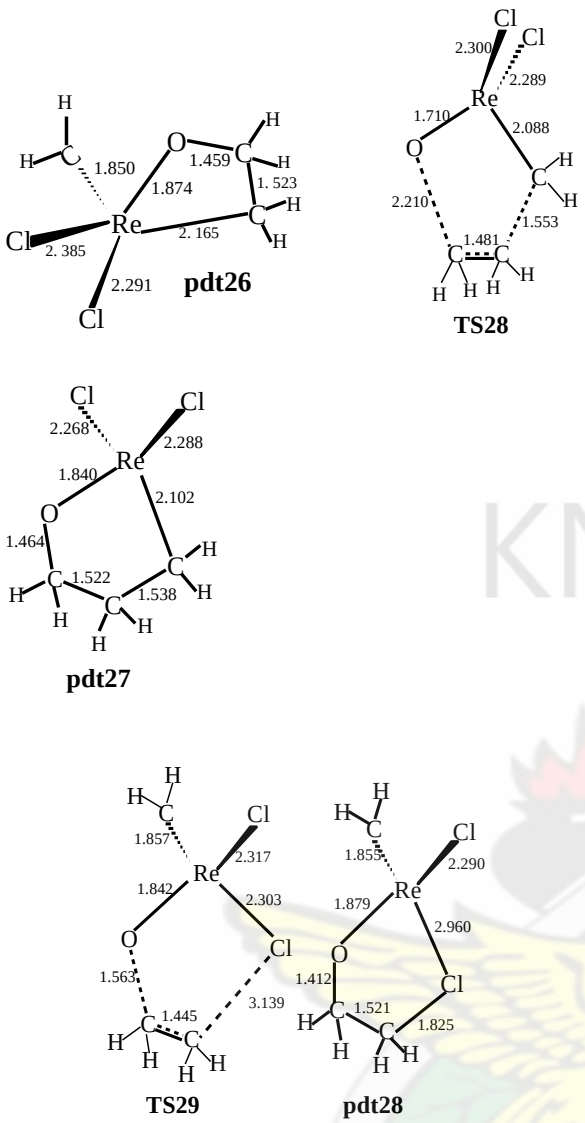

Figure 3.20 Optimized geometries of the main stationary points involved in the reaction of $Cl_2(O)ReCH_2$ with ethylene. Distances in Å and angles in degrees.

The formation of the product **pdt25** by [2+2] addition of ethylene across the Re-C bond of $Cl_2(O)ReCH_2$ through transition state **TS26** has an activation barrier of 7.80 kcal mol^{-1} and an exothermicity of 25.70 $kcalmol^{-1}$. This barrier is lower than the corresponding barriers for the Cr (12.10 $kcalmol^{-1}$) and Ru (13.78 $kcalmol^{-1}$) complexes, comparable with the Mo barrier (5.38 $kcalmol^{-1}$) but higher than the W barrier (0.38 $kcalmol^{-1}$). The exothermicity is also higher than the corresponding exothermicities for all the complexes except for Ru. The Re-O bond length in the reactant does not undergo any change in the formation of the metallacyclobutane product.

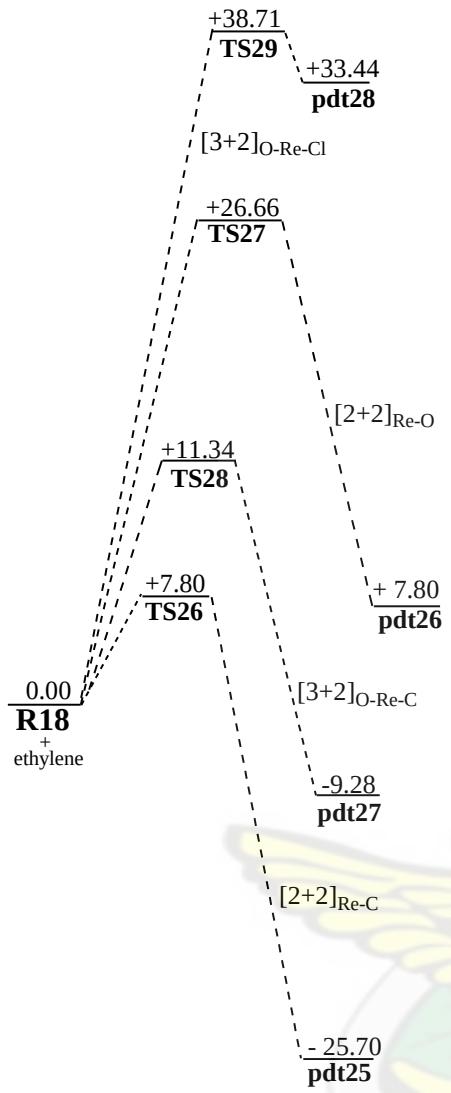

Figure 3.21 Energetics of the reactions of $Cl_2(O)ReCH_2$ with ethylene. Relative energies in kcalmol^{-1}.

The formation of product **pdt26** by [2+2] addition of ethylene across the Re-O bond of $Cl_2(O)Re{=}CH_2$ through transition state **TS27** is 7.80 kcal mol^{-1} endothermic and has an activation barrier of 26.66 kcamol^{-1}. This barrier is comparable with the barriers of 27.42, 30.67, and 26.25 kcal mol^{-1} found for the corresponding reactions in the Cr, Mo, and W complexes respectively but higher than the barrier of 17.00 kcal mol^{-1} found for the Ru complex. The product is also more stable than the corresponding products in the Cr, Mo, and W complexes but 10.50 kcal mol^{-1} less stable than the Ru product.

The activation barrier for [3+2] addition of ethylene across the Re-C and Re-O bonds of $Cl_2(O)ReCH_2$ through transition state **TS28** is 11.34 kcalmol^{-1}. In transition state **TS28** the newly-forming C-C bond is almost formed and thus the critical activity is the forming of the C-O bond. The resulting product **pdt27** is 9.28 kcal mol^{-1} exothermic. The [3+2] addition across the Re-O and Re-Cl bonds has a much higher of 38.71 kcal mol^{-1} through transition state **TS29** and the resulting product **pdt28** is 33.44 kcal mol^{-1} endothermic.

Since the formation of the metallacyclobutane **pdt25** has a lower barrier than all the potential side-reactions, olefin metathesis may be favorable in the Re complex. However, the barrier for the formation of the metallacyclobutane in this case is about thrice the corresponding barrier in the reaction of Cl_4ReCH_2 with ethylene. Thus the Cl_4ReCH_2 complex may be a better metathesis catalyst than the $Cl_2(O)ReCH_2$ complex

For the reaction of $Cl_2(O)MCH_2$(M=Mo, W, Re) complexes with ethylene, the pathway leading to the formation of the metallacyclobutane is the most favorable course of reaction whereas in $Cl_2(O)MCH_2$(M = Cr, Ru) this pathway is less favorable compared to the side reactions. Thus the metathesis reaction will occur preferentially in the Mo, W, and Re complexes where as in the Cr and Ru complexes, the metathesis reaction pathway is not the most preferred pathway. Using the barrier of formation of the metallacyclobutane and the preference of the metallacyclobutane formation over the side-reactions as the criteria for determining metathesis activity, it is seen that the W complex is the best complex for olefin metathesis reactions as it has the lowest barrier among the Mo, W, and Re complexes, and the preference of the metathesis pathway over the side reactions is clearly unambiguous.

The results indicate that replacing Cl_4MCH_2 with $Cl_2(O)MCH_2$ as models of the carbene complex raises the activation barriers for the metallacyclobutane formation reaction in the Cr, Ru and Re complexes, but lowers it in the W complexes. There is no significant change in activation barriers in the Mo complex. Thus this replacement does not necessarily increase metathesis activity. The M-O bond lengths in the reactants and the products of [2+2] addition of ethylene to the M-C bonds of $Cl_2(O)MCH_2$ are not significantly different. This is contrary to the conclusions

of Rappé and Goddard that the spectator oxo-group double-bond in the reactant is converted to a triple bond in the product (Rappé and Goddard, 1982), since such a conversion will lead to a decrease in the Cr-O bond length.

3.4 CONCLUSION

From the foregoing, the following conclusions are drawn:

1. The formation of the metallacyclobutane through formal [2+2] addition, the first step in the olefin metathesis reaction, is a low-barrier process for each of the methylidene and oxo-methylidene complexes studied.

2. The active species for the formation of the metallacyclobutanes in the Cl_4MCH_2 complexes is a carbene $Cl_4M{=}CH_2$ and not a carbenoid Cl_3MCH_2-Cl.

3. In the Cl_4MCH_2 complexes one key factor has been found to be responsible for the difference in metathesis activity: the stability of the carbenoid complexes relative to the carbenes. In Cr and Ru, the carbenoid complexes are more stable than the carbenes and thus Cl_4CrCH_2 and Cl_4RuCH_2 are likely to exist in the lower-energy carbenoid Cl_3MCH_2Cl form as opposed to the carbene $Cl_4M{=}CH_2$ form. This is likely to deplete the reaction surface of the active species of the process, making Cl_4MCH_2(M=Cr, Ru) not suitable for olefin metathesis. This suggests that whereas Cl_4MCH_2 (M = Mo, W, Re) may catalyze olefin metathesis, Cl_4MCH_2 (M = Cr, Ru) may not.

4. In $Cl_2(O)MCH_2$(M=Cr, Ru), the potential chain-terminating side reactions are more favorable than the olefin metathesis reaction whereas in $Cl_2(O)MCH_2$ (M=Mo, W, Re) olefin

metathesis is the most favorable reaction.

5. Replacing $Cl_4M{=}CH_2$ with $Cl_2(O)M{=}CH_2$ as models of the carbene complex raises the activation barrier of the first step of metathesis in Cr, Ru and Re complexes but lowers it in W complexes. There is no significant change in Mo.

6. The W carbene complexes were found to be the best complexes for olefin metathesis reactions as these complexes have the lowest barriers among the Mo, W, and Re complexes and the most unambiguous preference for the metathesis pathway over the side reactions.

REFERENCES

Anslyn, E. V.; Goddard, W. A., III (1989) Structures and reactivity of neutral and cationic molybdenum methylidene complexes. *Organometallics* 8: 1550 – 1558.

Bernandi, F.; Bottoni, A.; Miscione, G. P. (2003) DFT study of the olefin metathesis catalyzed by ruthenium complexes**.** *Organometallics* 22: 940 – 947.

Casey, C. P.; Anderson, R. L. (1975) Thermolysis of (2-oxacyclopentylidene)pentacarbonyl chromium (0): evidence against free carbenes in thermal decomposition of metal–carbene complexes. *J. Chem. Soc., Chem. Comm*. 895 – 896.

Cavallo, L. (2002) Mechanism of ruthenium-catalyzed olefin metathesis reactions from a theoretical perspective. *J. Am. Chem. Soc.*124: 8965 – 8973.

Clark, M.; Cramer, R. D.; Opdenbosch, N. V. (1989) Validation of the general purpose tripos 5.2 force field. *J. Comp. Chem*. 10: 982 – 1012.

Cundari, T. R.; Gordon, M. S. (1992) Theoretical investigations of olefin metathesis catalysts. *Organometallics* 11: 55 – 63.

Dediu, A.; Einsenstein, O. (1982) Metallacyclobutanes: Are they distorted? A theoretical *ab initio* study. *Nouv. J. Chim.* 6: 337 – 339.

Deng, L.; Woo, T. K.; Cavallo, L.; Margl, P. M.; Ziegler, T. (1997) The Role of Bulky substituents in Brookhart-type Ni(ii) diimine catalyzed olefin polymerization: A combined density functional theory and molecular mechanics study. *J. Am. Chem. Soc*. 119: 6177 – 6186.

Dunning, T. H., Jr.; Hay, P. J. (1976) In: Modern Theoretical Chemistry, H. F. Schaefer, III, Vol. 3; Plenum, New York.

Eisenstein, O.; Hoffman, R.; Rossi, A. R. (1981) Some geometrical and electronic features of the intermediate stages of olefin metathesis. *J. Am. Chem. Soc.* 103: 5582 – 5584.

Ephritikhine, M.; Francis, B. R.; Green, M. L. H.; MacKenzie, R. E.; Smith, M. J. (1977) Bis(η-cyclopentadienyl)-molybdenum and -tungsten chemistry: σ- and η -allylic and metallacyclobutane derivatives. *J. Chem. Soc., Dalton Trans*. 1131 – 1135.

Ephritikhine, M.; Green, M. L. H.; MacKenzie, R. E. (1976) Some η^1 and η^3 -allylic and metallocyclobutane derivatives of molybdenum and tungsten. *J. Chem. Soc., Chem. Comm*. 619.

Foley, P.; Whitesides, G. M. (1979) Thermal generation of bis(triethylphosphine)-3,3-dimethylplatinacyclobutane from dineopentylbis(triethylphosphine) platinum(II). *J. Am. Chem. Soc.* 101: 2732 – 2733.

Garcia, A.; Cruz, E. M.; Sarasola, C.; Ugalde, J. M. *(*1997) Density functional studies of the bπ. aσ charge-transfer complex formed between ethyne and chlorine monofluoride. *J. Phys. Chem. A* 101: 3021 – 3024.

Grubbs, R. H.; Burke, P. L.; Carr, D. D. (1975) Mechanism of the olefin metathesis reaction. *J. Am. Chem. Soc.* 97: 3265 - 3267.

Grubbs, R. H.; Carr, D. D.; Hoppin, C.; Burke, P. L. (1976) Consideration of the mechanism of the metal catalyzed olefin metathesis reaction. *J. Am. Chem. Soc.* 98: 3478 – 3483.

Hay, P. J.; Wadt, W, R. (1985) *Ab initio* effective core potentials for molecular calculations. Potentials for the transition metal atoms Sc to Hg. J. *Chem. Phys*. 82: 270.

Hay, P. J.; Wadt, W, R. (1985) *Ab initio* effective core potentials for molecular calculations. Potentials for K to Au including the outermost core orbitals. *J. Chem. Phys*. 82: 299.

Hérisson, J.-L.; Chauvin, Y. (1971). Catalyse de transformation des oléfines par les complexes du tungstène. II. Télomérisation des oléfines cycliques en présence d'oléfines acycliques. *Makromol. Chem.* 141: 161.

Katz, T. J.; McGinnis, J. (1975) Mechanism of the olefin metathesis reaction. *J. Am. Chem. Soc.* 97: 1592 – 1594.

Katz, T. J.; McGinnis, J.; Altus, C. (1976) Metathesis of a cyclic trisubstituted alkene. Preparation of polyisoprene from 1-methylcyclobutene. *J. Am. Chem. Soc.* 98: 605 – 606.

Kingsbury, C. L.; Mehrman, S. J.; Takacs, J. M. (1999) Comprehensive review of the applications of transition metal-catalyzed

reactions to solid phase synthesis. *Curr. Org. Chem*. 3, 497 – 555.

Kristyán, S.; Pulay, P. (1994) Can (semi)local density functional theory account for the London dispersion forces? *Chem. Phys. Lett*. 229: 175 – 180.

Lohrenz, J. W.; Woo, T. K.; Ziegler, T. (1995) A density functional study on the origin of the propagation barrier in the homogeneous ethylene polymerization with Kaminsky-type catalysts. *J. Am. Chem. Soc.* 117: 12793 – 12800.

Maier, M. E. (2000) Synthesis of medium-sized rings by the ring-closing metathesis reaction. *Angew. Chem., Int. Ed.* 39: 2073 - 2077.

Mol, J. C. 2004) Industrial applications of olefin metathesis. *J. Mol. Catal. A: Chemical* 213: 39 - 45.

Mourik, T. V. (2008) Assessment of Density Functionals for Intramolecular Dispersion-Rich Interactions. *J. Chem. Theory Comput*. 41610 – 1619.

Mourik, T. V.; Gdanitz, R. J. (2002) A critical note on density functional theory studies on rare-gas dimers. *J. Chem. Phys*. 116: 9620 – 9623.

Peréz-Jordá, J. M.; Becke, A. D. (1995) A density functional study of van der Waals forces: rare gas diatomics. *Chem. Phys. Lett*. 233: 134.

Poater, A.; Solans-Monfort, X.; Clot, E.; Coperet, C.; Eisenstein (2007) Understanding d^0-Olefin Metathesis Catalysts: Which Metal, Which Ligands? *J. Am. Chem. Soc*. 129: 8207 – 8216.

Puddephat, R. J.; Quyser, M. A.; Tippar, C. F. H. (1976) Easy isomerisation of a metallocyclobutane complex, and its relevance to the mechanism of olefin metathesis. *J. Chem. Soc., Chem. Comm*. 626 – 627.

Rajaram, R.; Ibers, J. A., Rajaram (1978) Metallocenes. Preparation and structural characterization of the products of insertion of (ethylene)bis (triphenylphosphine) platinum into 1,1,2,2,-tetracyano-3-phenylcyclopropane and 1-carboethoxy-1,2, 2-tricyano-trans-3-phenylcyclopropane. *J. Am. Chem. Soc.* 100: 829 – 838.

Rappé, A. K.; Goddard, W. A., III (1980) Mechanism of metathesis and epoxidation in chromium and molybdenum complexes containing methyl-oxo bonds. *J. Am. Chem. Chem. Soc.* 102: 5114 -5115.

Rappé, A. K.; Goddard, W. A., III (1982) Olefin metathesis - a mechanistic study of high-valent Group VI catalysts. *J. Am. Chem. Soc.* 104: 448 – 456.

Rappé, A. K.; Upton, T. H. (1984) Reaction energetics of a dissociative olefin metathesis mechanism for dichlorotitanacyclobutane. *Organometallics* 3: 1440 – 1442.

Roy, R.; Das, S. K. (2000) Recent applications of olefin metathesis and related reactions in carbohydrate chemistry. *Chem. Commun.* 519 – 529.

Ruiz, E.; Salahub, D. R.; Vela, A. (1996) Charge-Transfer Complexes: Stringent Tests for Widely Used Density Functionals. *J. Phys. Chem.* 100: 12265 – 12276.

Schrock, R. R. (1974) Alkylcarbene complex of tantalum by intramolecular α-

hydrogen abstraction. *J. Am. Chem. Soc.* 96: 6796 – 6797.

Schrock, R. R. (1976) Multiple metal-carbon bonds. 5. The reaction of niobium and tantalum neopentylidene complexes with the carbonyl function. *J. Am. Chem. Soc.* 98, 5399 – 5400.

Schrock, R. R.; Sharp, P. R. (1978) Multiple metal-carbon bonds. 7. Preparation and characterization of Ta (η^5-$C_5H_5)_2(CH_2)(CH_3)$, a study of its decomposition, and some simple reactions. *J. Am. Chem. Soc.* 100: 2389 – 2399.

Sodupe, M.; Lluch, J. M.; Olivia, A.; Bertrán, J. (1989) Theoretical study of the conformational preferences in the Cl4W:CH2 complex. *Organometallics* 8: 1837-1841.

Sodupe, M.; Lluch, J. M.; Olivia, A.; Bertrán, J. (1991) *Ab initio* study of the reaction between methylenemolybdenum tetrachloride ($Cl_4Mo:CH_2$) and ethylene, New Journal of Chemistry. *New J. Chem*. 15: 321.

Spartan, Wavefunction, Inc.; 18401 Von Karman Ave., # 370, Irvine, CA, 92715, USA.

Trnka, T. M.; Grubbs, R. H. (2001) The Development of L_2X_2Ru=CHR Olefin Metathesis Catalysts: An Organometallic Success Story. *Acc. Chem. Res*. 34: 18 – 29.

Upton, T. H.; Rappé, A. K. (1985) A theoretical basis for low barriers in transition-metal complex 2π + 2π reactions: the isomerization of the dicyclopentadienyl titanium complex $Cp_2TiC_3H_6$ to $Cp_2TiCH_2(C_2H_4)$. *J. Am. Chem. Soc.* 107: 1206 – 1218.

Wadt, W. R.; Hay, P. J. Hay (1985) *Ab initio* effective core potentials for molecular calculations. Potentials for main group elements Na to Bi. *J. Chem. Phys*. 82: 284.

Wright, T. C. (1996) Geometric structure of $Ar{\cdot}NO^+$: revisited. A failure of density functional theory. *J. Chem. Phys.* 105: 7579.

Yoshida, T.; Koga, N.; Morokuma, K. (1995) *Ab Initio* theoretical study on ethylene polymerization with homogeneous silylene-bridged group 4 metallocene catalysts. Ethylene insertion and β-elimination**.** *Organometallics* 14: 746 – 758.

Yüksel, D.; Düz, B.; Sevin, F. (2008) DFT study of the 1-octene metathesis reaction mechanism with WCl_6/C catalytic system. *J. Phys. Chem. A* 112: 4636 – 4643.

CHAPTER FOUR

DENSITY FUNCTIONAL THEORY STUDIES OF THE MECHANISTIC ASPECTS OF TRANSITION-METAL-

ASSISTED FORMATION OF 1, 2-DINITROSOALKANES

4.1 INTRODUCTION

Brunner and Loskot (Brunner, 1968; Brunner and Loskot, 1971; 1973) have reported that the cobalt nitrosyl dimmer $[CpCoNO]_2$, prepared by nitrosating $CpCo(CO)_2$, reacted, in the presence of additional NO, with moderately strained bicyclic alkenes such as norbonene to give cis- exo complexes (1,2-dinitrosoalkanes). Reactions of this type have a number of practical advantages, the most important being attenuation of steric problems associated with direct approach to the metal center, more efficient complexation of electron-rich alkenes, and high retention of stereochemistry at the alkene.

Bergman and co-workers (Becker *et. al*., 1980) investigated the scope and mechanism of the reaction and found it to proceed well with a wide range of alkenes, including even those which were substituted with several electron-donating alkyl groups. They also found that the dinitrosoalkanes formed in these reactions were in some cases isolable and in all cases could be reduced with $LiAlH_4$, thus providing a general method for converting alkenes into vicinal, primary diamines (Becker *et. al*., 1980). Indeed, this procedure has been shown to work satisfactorily for terminal, E and Z, di-, tri-, and at least some tetra-substituted alkenes and leads to various aliphatic 1,2- diamines (Le Gall *et. al*., 1998). Compounds incorporating the 1,2-diamino functionality have important biological properties (Michalson and Szuskovicz, 1989). In recent years several synthetic 1,2-diamines such as 1,2-diaminoplatinum complexes have been employed as medicinal agents, in particular in chemotherapy (Le Gall *et. al*., 1998). Vicinal diamine derivatives also find increasing utilization in synthesis, either as chiral auxiliaries or as metallic ligands, especially in the field of catalytic asymmetric synthesis (*ibid*.). Schomaker *et. al.* (2008) have reported the use of the

ligand-based reactivity of a series of cobalt dinitrosyl complexes for the C-H functionalization of alkenes. Schomaker *et. al*. (2009) have also demonstrated the utility of the cobalt dinitrosyl complexes for the [3+2] annulation of alkenes with unsaturated enones and ketimines. Reactions of a series of cobalt dinitrosyl/alkene adducts with conjugate acceptors in the presence of $Sc(OTf)_3$/LHMDS formed two new C-C bonds at the carbons α to the nitrosyl groups of the substrate, leading to unusual tri- and tetra-cycles, retrocycloaddition of which in the presence of norbomadiene yielded functionalized tetrasubstituted bicyclic olefins.

The requirement for NO in the adduct-forming step led Bergman *et. al*. (Becker *et. al.*, 1980) to suggest that $CpCo(NO)_2$ may be the initially formed intermediate; they subsequently provided kinetic and spectroscopic evidence for $CpCo(NO)_2$ as a reactive intermediate (Becker and Bergman, 1983).

Some mechanistic questions surrounding the reaction of the cobalt dinitrosyl complex ($CpCo(NO)_2$) intermediate with alkenes to form dinitrosoalkanes have not been clearly resolved. Bergman *et. al.* (Becker and Bergman, 1983) measured the absolute and relative bimolecular rate constants for the reaction of $CpCo(NO)_2$ with various olefins in cyclohexane at 20 ^oC and observed that 2,3-dimethyl-2-butene reacted fastest of all the isomeric hexenes studied. In contrast, it has been noted that transition-metal reactions involving olefin coordination usually follow the rate sequence $RCH=CH_2$ >> (Z)-RCH=CHR > (E)-RCH=CHR, while tri- and tetra- substituted olefins often show little tendency to react at all (Biellman *et. al*, 1970). Therefore, that 2,3-dimethyl-2-butene (a tetrasubstituted olefin) reacted at all, and that , except for 1-hexene, the trend in olefin reactivity is completely opposite to the noted trend for $CpCo(NO)_2$, has been considered by Becker and Bergman (1983) as strong evidence that this cyclization

reaction does not take place via initial olefin coordination to the cobalt atom. These workers, therefore, suggested that the reaction takes place directly - probably in a concerted fashion - between the nitrogen atoms of the nitrosyl group and the π- bond of the olefin (Scheme 4.1), in analogy to the classical mechanism for osmium tetraoxide olefin oxidation (Schröder, 1980; Schröder and Constable, 1982; Casey, 1983).

Scheme 4.1: Bergman's Proposed Mechanism for the Formation of 1,2-Dinitrosoalkanes.

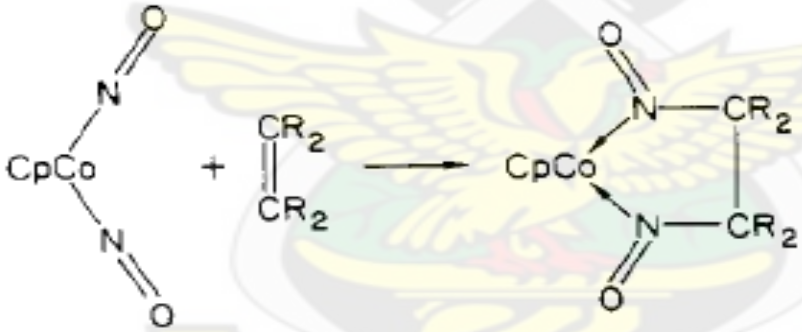

However, using ECP Hartree-Fock and GVB calculations and Pauli Principle (Upton and Rappé, 1984) arguments, Upton and Rappė (1985) have suggested that in general (given thermodynamic accessibility) a 2+2 4π-electron reaction where one of the component electrons is in a d-orbital will occur with very small barriers. These workers showed that the participation of a 3d-orbital allows satisfaction of the Pauli Principle constraints in a unique way that avoids the unfavorable transition-state bonding interactions that are usually the source of a high barrier. These workers therefore proposed a reaction sequence involving the concerted addition of a single metal-nitrogen π-bond across the olefin π-bond, followed by a rapid reductive elimination involving the second metal-nitrogen π- bond to form the observed 1,2-dinitrosoalkane (Scheme 4.2), since the addition of an olefin across a metal-ligand π-bond will occur with a small barrier (on the order of 2

kcal/mol) and reductive elimination reactions are documented to occur with small barriers (Norton, 1979).

Scheme 4.2: Rappé's Proposed Mechanism of 1,2-Dinitrosoalkane Formation

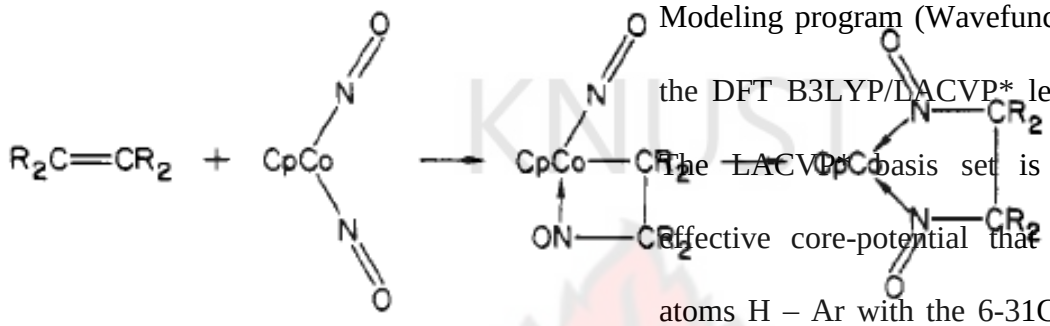

This work aims at exploring theoretically the potential energy surface of the reactions of $CpM(NO)_2$(M=Co, Rh, Ir) with some olefins (ethylene, 2-norbonene, trans-1-phenylpropene, cyclopentene, cyclohexene and 2,3-dimethyl-2-butene) at the DFT B3LYP/LACVP* level of theory. The geometries and relative energies of the relevant structures (reactants, transition states, intermediates and products) along the two proposed reaction pathways (Schemes 4.1 and 4.2) are computed to provide some understanding of the plausible mechanistic channels of the formation of 1,2-dinitrosoalkanes.

4.2 DETAILS OF CALCULATIONS

All calculations were carried out with the SPARTAN '06 V112 Molecular Modeling program (Wavefunction, 2006) at the DFT B3LYP/LACVP* level of theory. The LACVP* basis set is a relativistic effective core-potential that describes the atoms H – Ar with the 6-31G* basis while heavier atoms are modeled with the LANL2DZ basis set which uses the all-electron valence double zeta basis set (D95V), developed by Dunning, for first row elements (Dunning and Hay, 1976) and the Los Alamos ECP plus double zeta basis set developed by Wadt and Hay for the atoms Na – La, Hf – Bi (Hay and Wadt, 19785a; 1985b; Wadt and Hay, 1985).

The starting geometries of the molecular systems were constructed using SPARTAN's graphical model builder and minimized interactively using the sybyl

force field (Clark *et. al*, 1989). All geometries were fully optimized without any symmetry constraints. The optimized geometries were subjected to full frequency calculations to verify the nature of the stationary points. Equilibrium geometries were characterized by the absence of imaginary frequencies. The transition state structures were located by a series of constrained geometry optimizations in which the forming- and breaking-bonds were fixed at various lengths while the remaining internal coordinates were optimized. The approximate stationary points located from such a procedure were then fully optimized using the standard transition state optimization procedure in SPARTAN. All first-order saddle-points were shown to have a Hessian matrix with a single negative eigenvalue, characterized by an imaginary vibrational frequency along the reaction coordinate. All the computations were performed on Dell Precision T3400 Workstation computers.

4.3 RESULTS AND DISCUSSION

4.3.1 REACTIONS OF $CpM(NO)_2$ (M= Co, Rh, Ir) WITH ETHYLENE

The density functional theory (DFT) optimized geometries of the $CpM(NO)_2$ reactant structures are shown in Figure 4.1a. Optimization of the $CpCo(NO)_2$ reactant yielded four minima, labeled **R1**, **R2**, **R3** and **R4** in Figure 4.1a. Structure **R1** is the most stable structure. It has the two Co-N-O angles at 136.85^o, the N-Co-N angle at 100.69^o and the oxo groups pointing outward. This structure has the shortest Cp-Co bond length (1.743 Å) and the longest Co-N bond length (1.719 Å) of all the optimized Co reactant structures. Structure **R2** which has the two C-N-O angles at 171.48^o and 124.97^o and the oxo groups pointing inwards, is 0.96 kcalmol^{-1}less stable than **R1**.

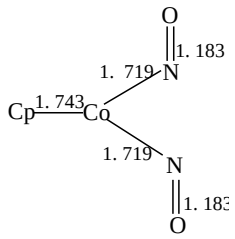

R1

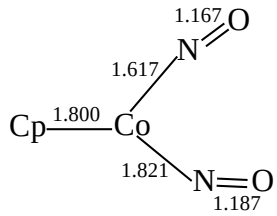

R2

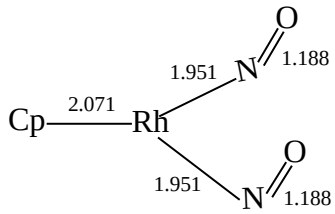

R8

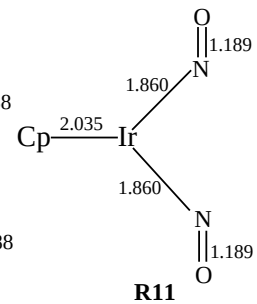

R11

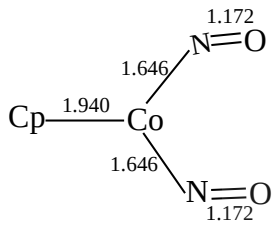

R3

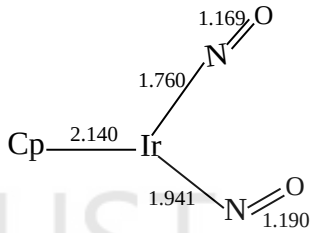

R9

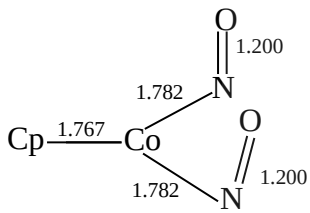

R4

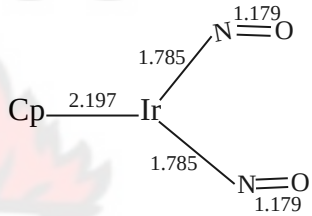

R10

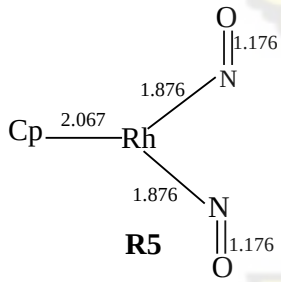

R5

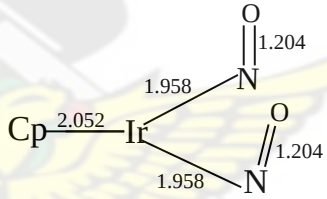

R12

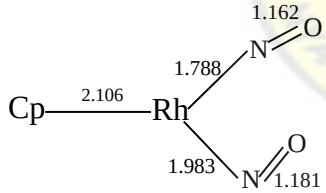

R6

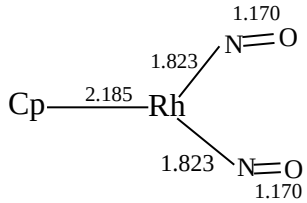

R7

Figure 4.1a Optimized geometries of the $CpM(NO)_2$ (M = Co, Rh, Ir) reactant minima. Bond lengths in Å.

Unlike in **R1**, the two Co-N bond lengths in **R2** are unequal. The Cp-Co bond in structure **R2** is 0.06 Å longer than it is in structure **R1**. Structure **R3** has the two Co-N-O angles at 150.28^{o} and the oxo groups pointing inwards. It has the shortest Co-N bond (1.646 Å) and the longest Cp-Co bond

(1.940 Å) of all the Co reactant structures and is 6.88 kcal mol^{-1} less stable than **R1**. Structure **R4** has the two N-O bonds sticking out of the N-Co-N plane by 99.18^o and is the least stable of all the reactant minima. It has the smallest N-Co-N angle of 96.56^o which is 4.13^o smaller than the corresponding angle in **R1** and is 13.05 kcal mol^{-1} less stable than **R1**. In **R1**, **R2**, and **R3**, the two N-O and Co-N bonds all lie in the same plane while in **R4**, the two N-O bonds are almost perpendicular (99.18^o) to the N-Co-N plane.

Four reactant minima, labeled **R5**, **R6**, **R7** and **R8** in Figure 4.1a, have also been located for the Rh system. Structure **R5** which is the most stable minimum has the two Rh-N bond lengths at 1.876 Å, Rh-N-O angles at 133.30^o, an N-Rh-N angle of 97.85^o and the Rh-Cp distance of 2.067 Å. This structure is geometrically very similar to structure **R1** which is the most stable structure among the Co reactant structures but the the N-Rh-N angle is 2.84^o smaller in **R5** than in **R1**. Structure **R6** is the second most stable structure and is 2.86 kcal mol^{-1} less stable than **R5**, the most stable structure. Structure **R6** closely resembles **R2**, the second most stable structure among the Co reactant minima. Structure **R6** is 2.86 kcal mol^{-1} less stable than **R5** while structures **R7** and **R8** are 5.08 kcal mol^{-1} and 12.59 kcal mol^{-1} less stable than **R5** respectively. In general, the optimized $CpRh(NO)_2$ reactant geometries are similar to the corresponding optimized $CpCo(NO)_2$ reactant geometries except that the Cp-Rh bonds are longer than the Cp-Co bonds and the N-Rh-N angles are smaller than the N-Co-N angles.

Optimization of the $CpIr(NO)_2$ reactant structures gave **R9**, **R10**, **R11** and **R12**, whose geometrical parameters are similar to those of Co and Rh complexes. The relative energies of the conformers are however different. Whereas **R2** and **R6** are the second most stable reactant minima for the Co and Rh complexes respectively,

structure **R9** which has the closest geometrical resemblance to **R2** and **R6** is the most stable among the Ir reactant minima; also **R11** which has the closest geometrical resemblance to **R1** and **R5** is the third most stable species among the Ir reactant minima.

The π-complexes optimized from the interaction of the $CpM(NO)_2$ with ethylene are shown in Figure 4.1b. The π-complex (**pi-comp1**) formed from the interaction between $CpCo(NO)_2$ and ethylene is 7.02 kcal mol^{-1} above the reactants on the energy profile while the $CpRh(NO)_2$-ethylene π-complex (**pi-comp2**) is 0.65 kcal mol^{-1} above the reactants. The geometric features of **pi-comp1** and **pi-comp2** are very similar. However, the two Rh-N bond lengths are practically the same (differ only by 0.003 Å) in the Rh complex while the two Co-N bonds lengths differ by 0.101 Å. Thus the Rh π-complex is more symmetric than the Co π-complex. The Ir π-complex (**pi-comp3**) formed from the interaction of **R9** with ethylene is 3.78 kcal mol^{-1} above the reactant. Thus the order of stability of the π-complexes formed from the interaction of ethylene with the $CpM(NO)_2$(M=Co, Rh, Ir) complexes is Rh > Ir > Co.

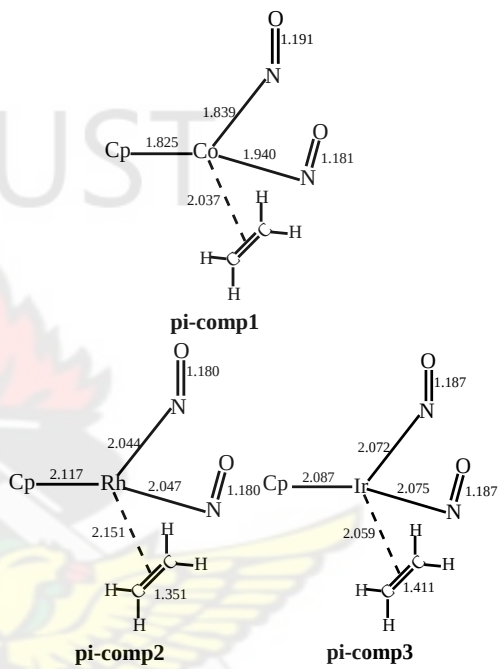

Figure 4.1b Optimized geometries of the π-complexes formed from the interaction of $CpM(NO)_2$ (M = Co, Rh, Ir) with ethylene. Bond lengths in Å.

The energetics of the π-complexes reported here must be considered in relation to the well-known difficulties for DFT methods to describe weak interactions (Kristán and Pulay, 1994; Wright, 1996; Peréz-Jordá and Becke, 1995; Ruiz *et. al.*,

1996; Garcia *et. al*., 1997). The B3LYP functional in particular does not describe dispersion, and therefore underestimates the interaction energies of π-bonded systems. This may well result in a repulsive interaction (Mourik and Gdanitz, 2002; Mourik, 2008). However, Goddard *et. al*. (2002) used the same functional to study copolymerization of polar monomers catalyzed by model Brookhart Pd and Ni catalysts and found all the π-complexes to be lower in energy than the reactants.

The optimized geometries of the transition states and products involved in the [3+2] addition of ethylene across the M-N bonds of $CpM(NO)_2$ are shown in Figure 4.1c. The [3+2] addition of ethylene across the two Co-N bonds of **R1** through transition state **TS1** leads to product **pdt1** (Figure 4.1c). Transition state **TS1** has been found to be 0.33 kcal mol^{-1} below the reactants on the energy profile (Figure 4.1d). Attempts at locating an intermediate connecting the reactants and this transition state were unsuccessful. The resulting product **pdt1** is 34.88 kcal mol^{-1} exothermic. The Cp-Co bond length decreases by only 0.011 Å in going from the reactant to the transition state and a further 0.023 Å to the final product. The geometry of transition state **TS1** suggests that the formation of **pdt1** proceeds by a concerted and synchronous pathway.

The [3+2] addition of ethylene across the two Rh-N bonds of **R5** through transition state **TS4** leads to product **pdt2**, with a barrier of 0.59 kcal mol^{-1} and exothermicity of 29.67 $kcalmol^{-1}$. This transition state also suggests a synchronous pathway but transition state **TS4** occurs slightly later than **TS1**. The differences between the N-C forming bonds in the transition states and the products are 0.79 Å and 0.90 Å for Rh and Co complexes respectively. The transition state **TS7** for the [3+2] addition of ethylene across the two Ir-N bonds of **R9** is 5.0 kcal mol^{-1} above the reactants on the energy profile. Transition

state **TS7** is an early transition state compared with the corresponding transition states in Co (**TS1**) and Rh (**TS4**) complexes. The differences between the N-C forming-bond lengths in the transition state and the product is 1.39 Å in Ir (**TS7)**, 0.90 Å in Co (**TS1**) and 0.79 Å in Rh (**TS4**). The geometry of transition state **TS7** is also indicative of a synchronous reaction pathway. The resulting product **pdt3** is 31.52 kcal mol^{-1} exothermic. The formation of this product is thus slightly more exothermic than the formation of the corresponding product in the Rh complex (-29.67 $kcalmol^{-1}$) but slightly less exothermic than the formation of the corresponding product in the Co complex (-34.52 $kcalmol^{-1}$). Thus the observed trend in the exothermicity of the [3+2] reaction step with respect to metal complex is Co >Ir > Rh, which turns out to be the reverse of the order of the stability of the π-complexes.

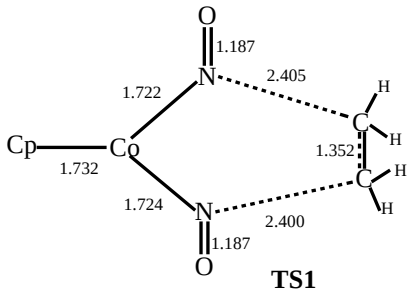

TS1

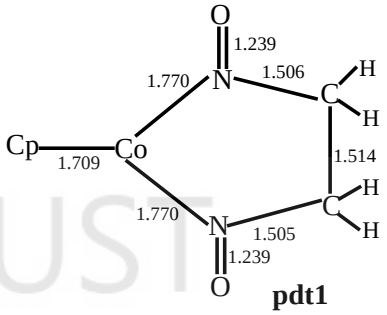

pdt1

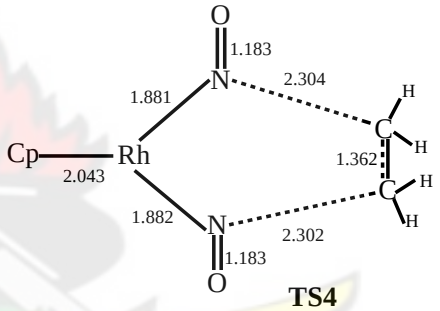

TS4

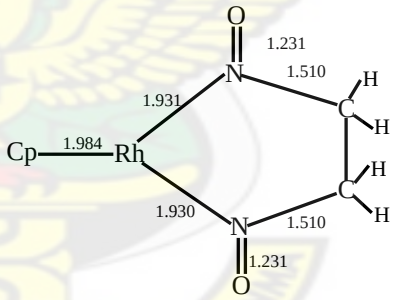

pdt2

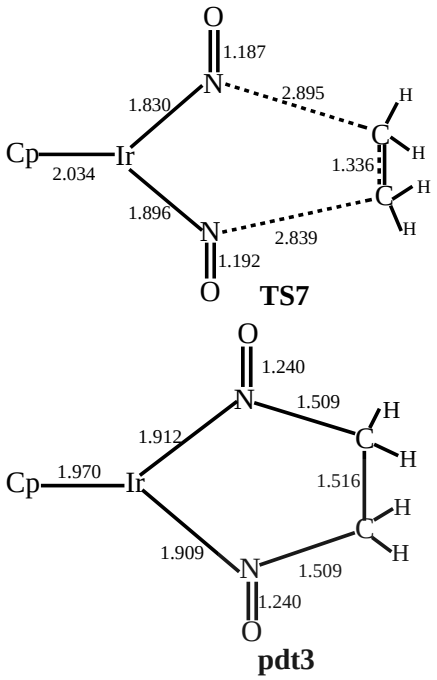

Figure 4.1c Optimized geometries of the transition states and products formed from [3+2] addition of $CpM(NO)_2$ (M = Co, Rh, Ir) with ethylene. Bond lengths in Å.

The [2+2] addition of ethylene across the Co-N bond of **R1** proceed through transition states **TS2** and **TS3** (Figure 4.1d), with barriers of 30.15 and 33.11 kcal mol^{-1} (Figure 4.1d), to form intermediates **I1** and **I2** which are 0.58 and 2.97 kcal mol^{-1} exothermic respectively. In **TS2** the oxygen atom of the spectator NO group points towards the hydrogens in the four-membered ring, an orientation which is indicative of hydrogen bonding, while in **TS3** the oxygen points away. **TS2** is about 3 kcal mol^{-1} more stable than **TS3**, which is due to stabilization of **TS2** by hydrogen bonding relative to **TS3**. In **TS3**, the Co-C forming bonds are almost completely formed (2.184 Å in the transition state compared to 2.000 Å in the product) whereas the N – C bond is still far from being formed (2.16 Å in the transition state compared to 1.48 Å in the product). The Co-C bond length of 2.227 Å in transition state **TS2** decreases to 1.981 Å in the product while the N-C bond length of 2.174 Å decreases to 1.479 Å in the product. The orientation of the oxygen atoms in the transition states are maintained in their respective products. The hydrogen bonding interaction is thus maintained in **I1**, making it 2.38 kcal mol^{-1} more stable than **I2**. The Cp-Co bond length increases from 1.743 Å in the reactant to 1.818 Å in **TS2** and then decreases to 1.787 Å in **I1**.

The [2+2] addition of ethylene across the Rh-N bonds of $CpRh(NO)_2$ (**R5**)

leads to two products **I3** and **I4** through transition states **TS5** and **TS6** respectively (Figure 4.1e). The lower-energy transition state, **TS5**, which is 29.96 kcal mol^{-1} above the reactants (Figure 4.1d), has the oxygen atom pointing towards the four-membered ring and is 2.12 kcal mol^{-1} below **TS6** in which the nitroso oxygen points away. These barriers are comparable with those found for the [2+2] reaction involving the Co complex. The oxygen-in conformer (**I3**), which is 0.54 kcal mol^{-1} exothermic, is 1.99 kcal mol^{-1} more stable than the oxygen-out conformer (**I4**). This contrasts with the case involving the Co complex in which both conformations are slightly exothermic.

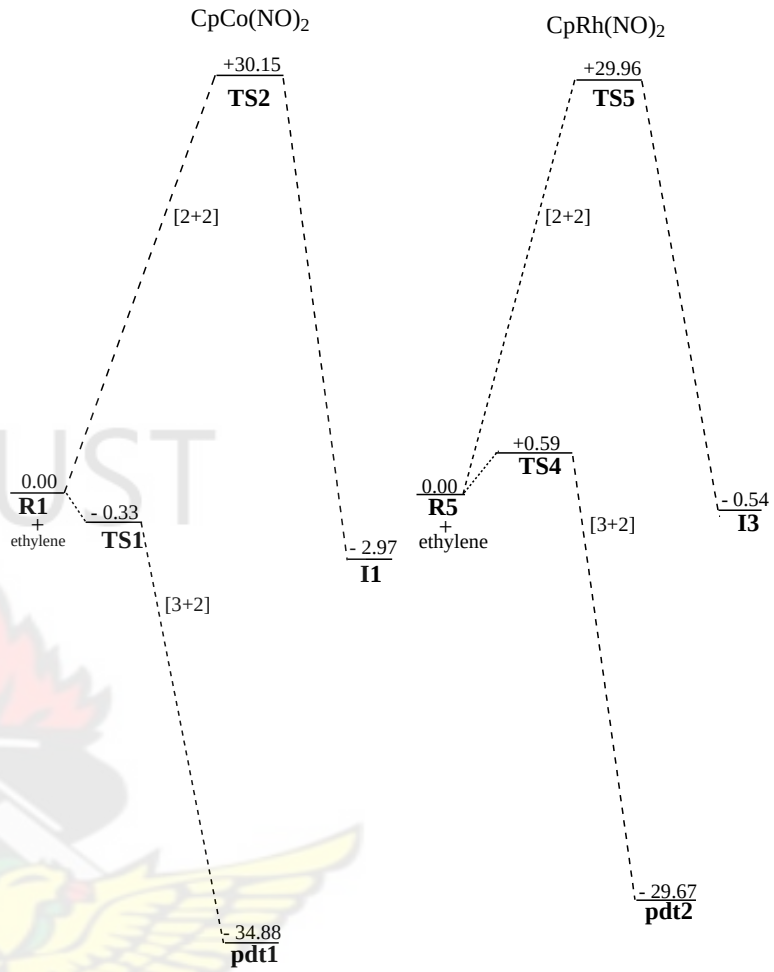

Figure 4.1d Energy profiles of the [3+2] and [2+2] addition reaction of CpM(NO)$_2$ (M = Co, Rh, Ir) with ethylene. Relative energies in kcalmol^{-1}.

Two transition states **TS8** and **TS9** have also been located for the [2+2] addition of ethylene across the Ir-N bond of **R9** to form intermediates **I5** and **I6** (Figure 4.1d). The geometrical features of these transition states are very similar to those located for the corresponding reactions involving the

Co and Rh complexes. Transition state **TS9** which is 32.50 kcal mol^{-1} above the reactants (Figure 4.1d) is 1.86 kcal mol^{-1} lower than transition state **TS8**.

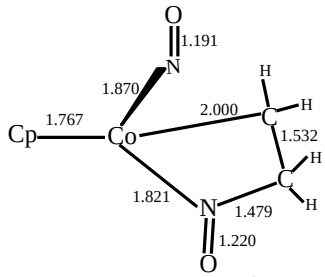

I2

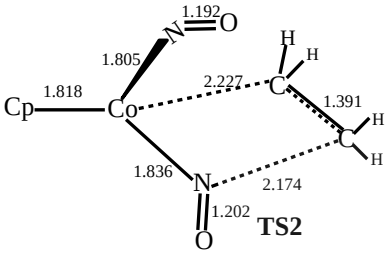

TS2

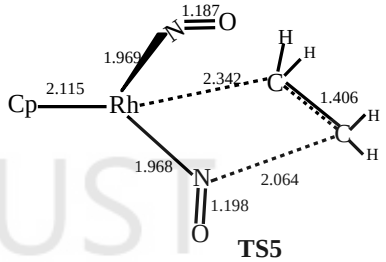

TS5

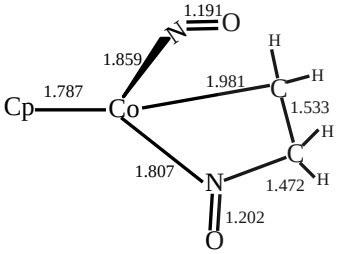

I1

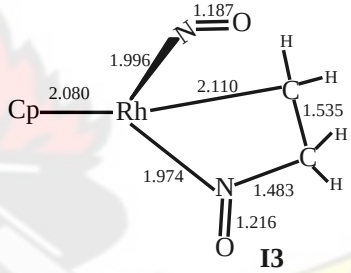

I3

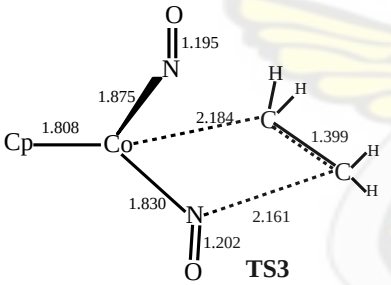

TS3

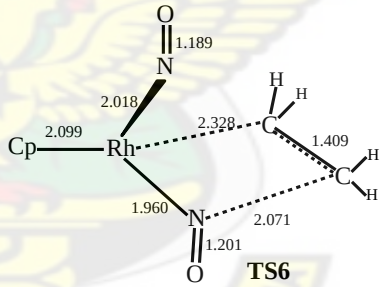

TS6

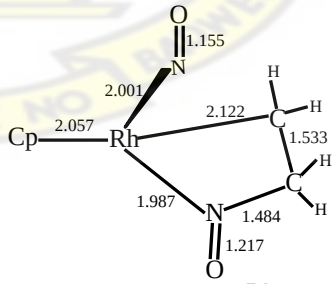

I4

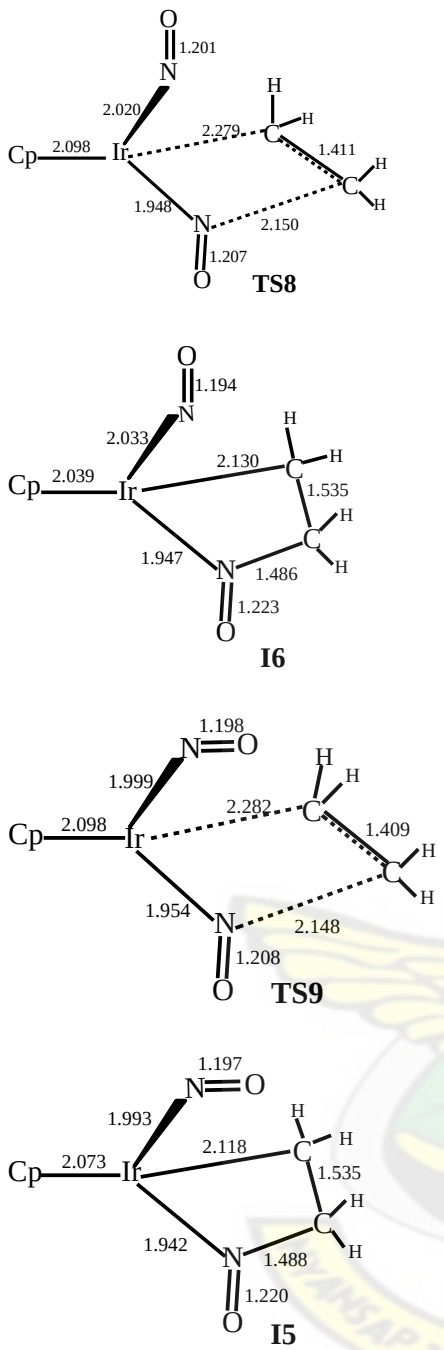

Figure 4.1e Optimized geometries of the stationary points involved in the [2+2] addition of ethylene to $CpM(NO)_2$ (M = Co, Rh, Ir). Bond lengths in Å.

Table 4.1: Relative Energies (in $kcalmol^{-1}$) of the Transition States Formed From [3+2] and [2+2] Addition of Olefins to $CpM(NO)_2$ (M=Co, Rh, Ir)[a]

	Co		Rh
olefin	TS[3+2]	TS[2+2]	TS[3+2]
ethylene	- 0.33	+ 30.15	+ 0.59
2-norbonene	- 1.02	+ 30.63	- 0.65
trans-1-phenyl-propene	- 0.39	+32.46	+1.70
cyclopentene	-0.78	+30.22	- 0.44
cyclohexene	+ 1.29	+38.00	+2.99
2,3-dimethyl-2-butene	-1.56	+32.21	+ 0.81

[a] Energies calculated relative to the respective reactants

For each of the complexes the activation barrier for the [3+2] addition is far lower than the barrier for [2+2] addition (Figure 4.1d and Table 4.1). An attempt to locate a transition state for the re-arrangement of the products of [2+2] addition to the products corresponding to [3+2] addition was unsuccessful, indicating that the re-arrangement of the product of [2+2] addition by reductive elimination involving the second metal-nitrogen π-bond to form the observed 1,2-dinitrosoalkane

may not be possible. Therefore, for the ethylene olefin the one-step [3+2] pathway for the formation of 1,2-dinitrosoalkanes proposed by Becker and Bergman (1983) has been found to be more plausible than the stepwise path proposed by Upton and Rappé (1985).

4.3.2 REACTIONS OF $CpM(NO)_2$ (M= Co, Rh, Ir) WITH 2-NORBONENE

A π-complex (**pi-comp4**) (Figure 4.2a) that has been optimized from the interaction of **R1** with 2-norbonene is 11.54 kcal mol^{-1} endothermic. This $CpCo(NO)_2$-norbonene π-bonded complex is 4.52 kcal mol^{-1} less stable than the $CpCo(NO)_2$-ethylene π-bonded complex. A π-bonded complex (**pi-comp5**) has also been optimized from the interaction of $CpRh(NO)_2$ with 2-norbonene and is found to be 3.94 kcal mol^{-1} endothermic. This π-complex is therefore 7.60 kcal mol^{-1} less stable than **pi-comp4**. The olefinic C-C bond of 2-norbonene is 0.049 Å longer in the π-complex than in the reactant. The π-complex (**pi-comp6**) optimized from the interaction of $CpIr(NO)_2$ with 2-norbone is 9.11 kcal mol^{-1} endothermic. This π-complex is more endothermic than the $CpRh(NO)_2$-norbonene π-complex but less endothermic than the $CpCo(NO)_2$-norbonene π-complex. Thus the order of stability of the π-complexes formed from the reaction of 2-norbonene with the $CpM(NO)_2$(M=Co, Rh, Ir) complexes is Rh > Ir > Co.

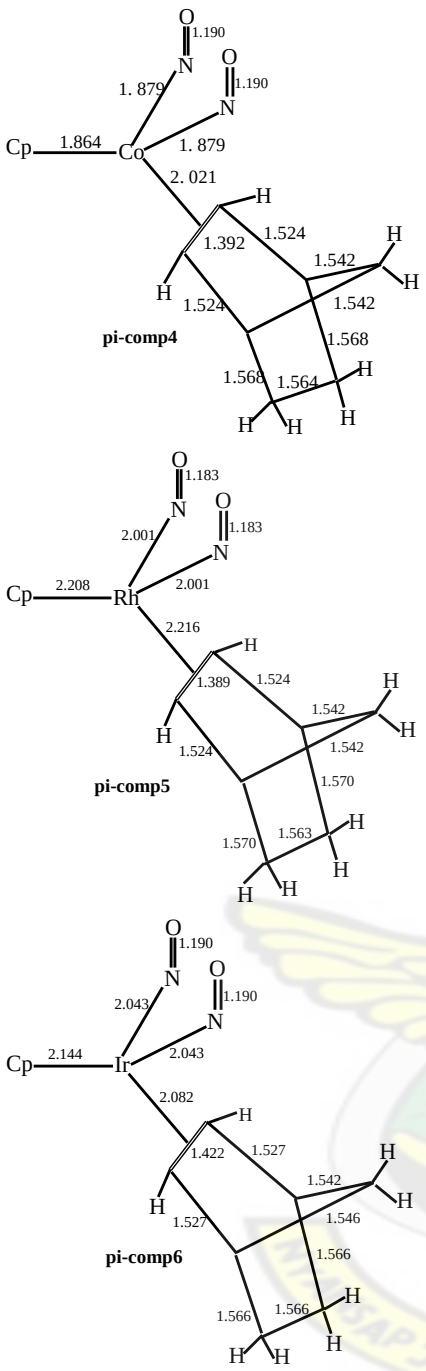

Figure 4.2a Optimized geometries of the π-complexes formed from the interaction of $CpM(NO)_2$ (M = Co, Rh, Ir) with 2-norbonene. Bond lengths in Å.

The optimized geometries of the stationary points involved in the [3+2] addition of 2-norbonene across the M-N bonds of $CpM(NO)_2$(M=Co, Rh, Ir) are shown in Figure 4.2b. The [3+2] addition of the olefinic C-C bond of 2-norbonene across the two Co-N bonds of $CpCo(NO)_2$ leads to two products, **pdt4** (the exo isomer) and **pdt5** (the endo isomer), which are 42.09 and 39.01 kcal mol^{-1} exothermic respectively. Species **pdt4**, the isomer isolated in the work of Brunner and Loskot *(vide supra)*, is found to be 3.08 kcal mol^{-1} more stable than the endo isomer. The products **pdt4** and **pdt5** are 7.21 and 4.13 kcal mol^{-1} respectively more exothermic than **pdt1** which is formed from the reaction of $CpCo(NO)_2$ with ethylene. The transition state **TS10** for the formation of the exo product **pdt4** is found to be 1.02 kcal mol^{-1} below the reactants. The formation of **pdt4** from the reactants apparently occurs in only one step as attempts at locating an intermediate were unsuccessful. The transition state **TS10** is an early transition

state compared to the corresponding ethylene addition in **TS1**.

The [3+2] addition of norbonene across the two Rh-N bonds of $CpRh(NO)_2$ leads to two products, **pdt9** (the exo isomer) and **pdt10** (the endo isomer) (Figure 4.2b), which are 36.38 and 33.84 kcal mol^{-1} exothermic respectively. Products **pdt9** and **pdt10** are respectively 5.71 kcal mol^{-1} and 5.17 kcal mol^{-1} less exothermic than **pdt4** which is formed from the reaction of 2-norbonene with $CpCo(NO)_2$. The transition state **TS13** for the formation of **pdt9** is 0.65 kcal mol^{-1} below the reactants (Figure 4.2c).

The products of [3+2] addition of norbonene across the two Ir-N bonds of $CpIr(NO)_2$ are 38.39 and 34.88 kcal mol^{-1} exothermic respectively for the exo (**pdt15**) and endo(**pdt16**) isomers (Figure 4.2b). These exothermicities are higher than those found for the reaction of norbonene with the Rh complex but lower than those found for the reaction of norbonene with the Co complex. The activation barrier for the formation of **pdt15** through transition state **TS16** is 4.77 $kcalmol^{-1}$. This barrier is higher than that found for the formation of the corresponding product in the Co and Rh complexes. The geometrical features of **pdt15** are similar to those of **pdt3** obtained from the addition of ethylene to $CpIr(NO)_2$) with respect to the N-C forming-bond lengths, which are 1.51 Å in both cases, even though **pdt15** is 6.87 kcal mol^{-1} more exothermic than **pdt3**. Thus changing the olefin from ethylene to norbonene increases the exothermicity of the reaction. The change however has not had any marked effect on the N-C forming-bonds and the activation barrier of the reaction, which only decreases slightly from 5.05 to 4.77 $kcalmol^{-1}$. The N-C forming-bond lengths are also comparable in the transition states involving ethylene and norbonene.

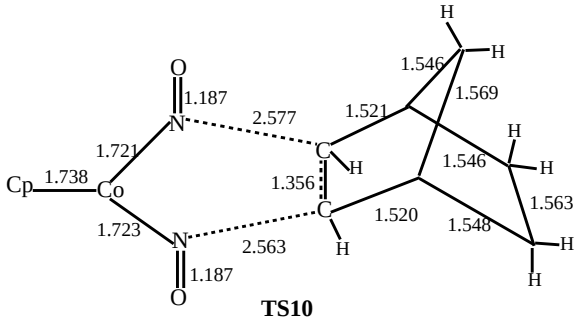

TS10

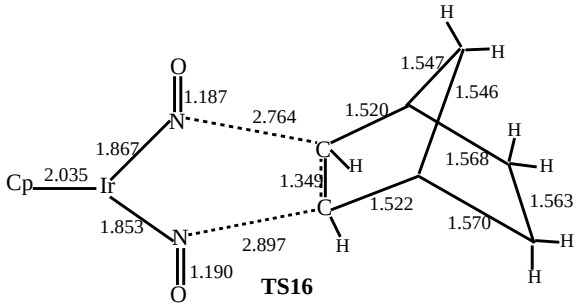

TS16

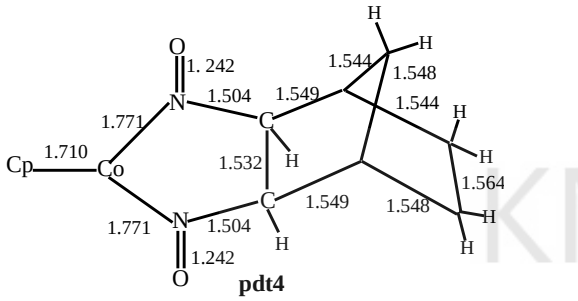

pdt4

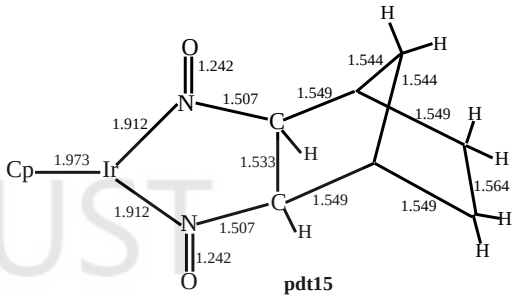

pdt15

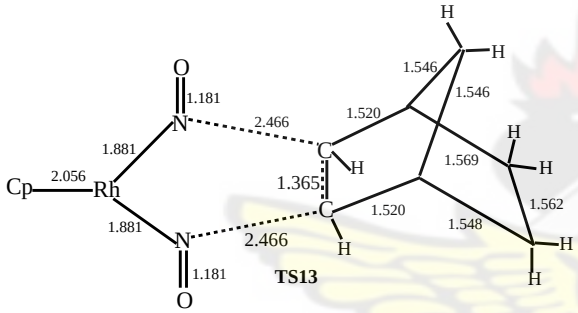

TS13

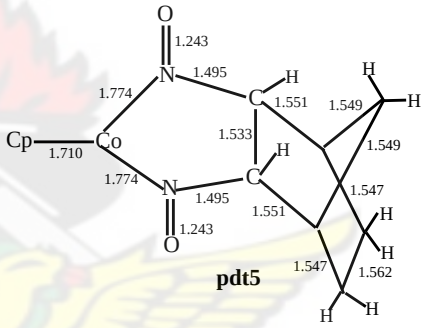

pdt5

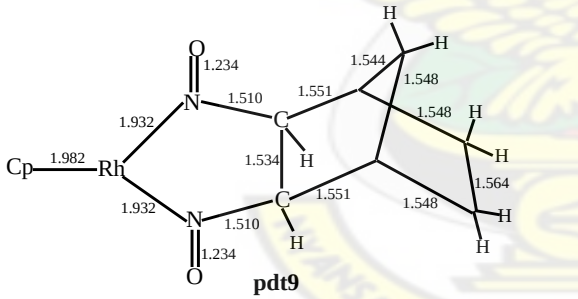

pdt9

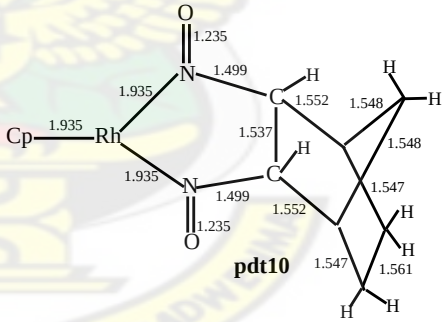

pdt10

Figure 4.2b Optimized geometries of the stationary points involved in the [3+2] reaction of $CpM(NO)_2$ (M = Co, Rh, Ir) with 2-norbonene. Bond lengths in Å.

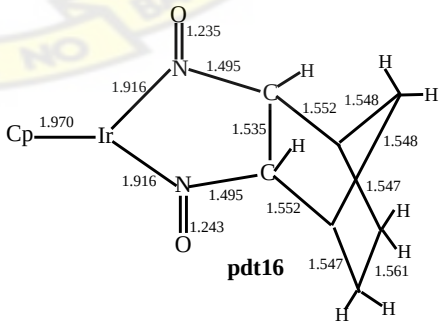

pdt16

Figure 4.2b (*Continued*) Optimized geometries of the stationary points involved in the [3+2] reaction of $CpM(NO)_2$ (M = Co, Rh, Ir) with 2-norbonene.

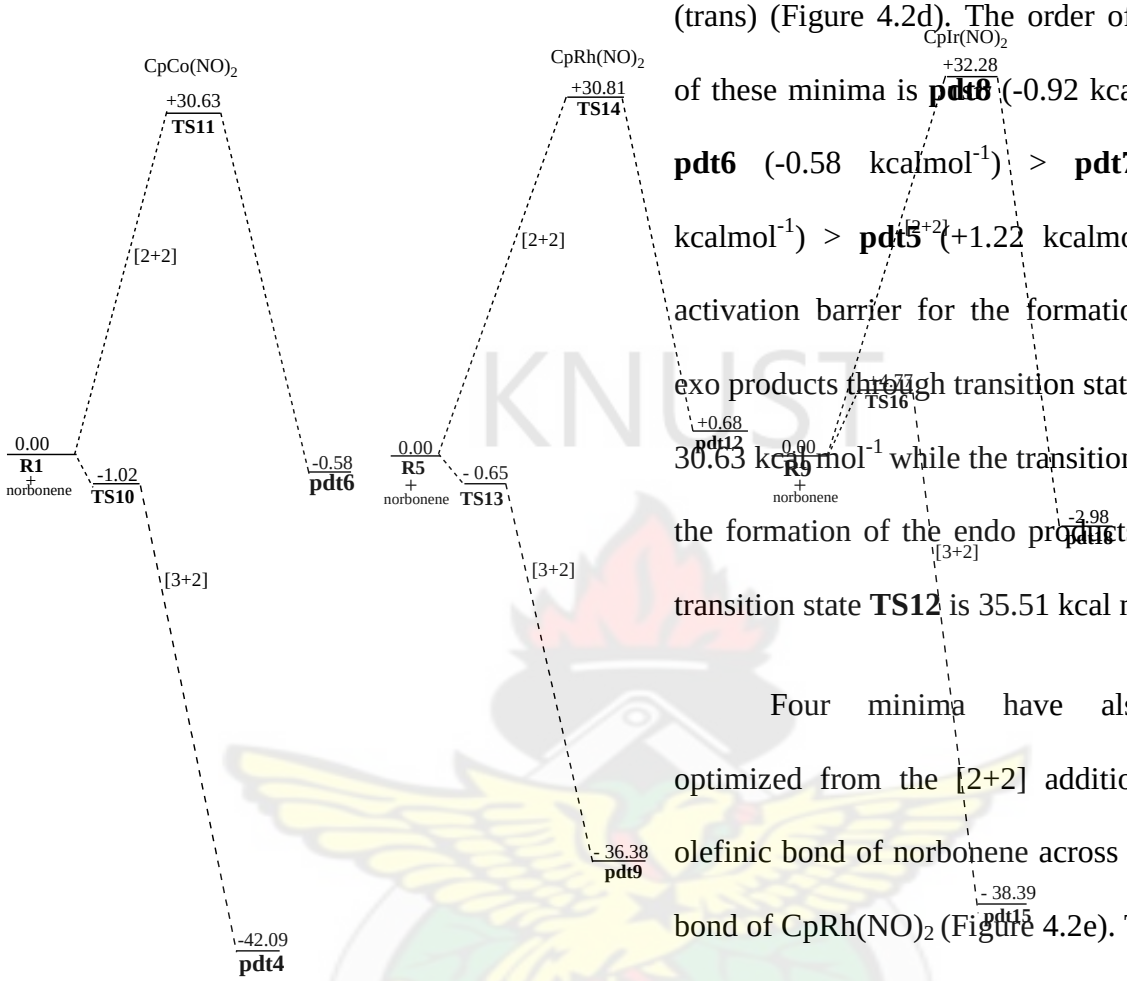

Figure 4.2c Energy profiles of the [3+2] and [2+2] addition reaction of $CpM(NO)_2$ (M = Co, Rh, Ir) with 2-norbonene. Relative energies in $kcalmol^{-1}$.

Four different minima are optimized from the [2+2] addition of the olefinic C-C bond of norbonene across the Co-N bond of $CpCo(NO)_2$ - two isomers (exo and endo) and two conformers depending on whether the nitroso oxygen points towards the norbonene moiety (cis) or away from it (trans) (Figure 4.2d). The order of stability of these minima is **pdt8** (-0.92 $kcalmol^{-1}$) > **pdt6** (-0.58 $kcalmol^{-1}$) > **pdt7** (+1.13 $kcalmol^{-1}$) > **pdt5** (+1.22 $kcalmol^{-1}$). The activation barrier for the formation of the exo products through transition state **TS11** is 30.63 $kcal\ mol^{-1}$ while the transition state for the formation of the endo products through transition state **TS12** is 35.51 kcal mol^{-1}.

Four minima have also been optimized from the [2+2] addition of the olefinic bond of norbonene across the Rh-N bond of $CpRh(NO)_2$ (Figure 4.2e). The order of stability of these structures is: **pdt13** (-0.47 $kcalmol^{-1}$) > **pdt12** (+0.60 kcal mol^{-1}) > **pdt11** (+1.51 kcal mol^{-1}) > **pdt14** (+2.04 kcal mol^{-1}). The activation barrier for the formation of the exo intermediate through transition state **TS14** is 30.81 kcal mol^{-1} while that for the formation of the endo intermediate through transition state **TS15** is 35.32 $kcalmol^{-1}$. These barriers are

comparable with the barriers found for the corresponding reactions involving the Co complex (30.63 and 35.51 kcal mol^{-1} for the exo and endo isomers respectively). The Rh-C forming-bond is 0.149 Å longer in transition state **TS14** than in product **pdt12** while the N-C forming-bond is 0.637 Å longer in transition state **TS14** than in product **pdt12**. The corresponding differences in the Co complex are 0.138 Å and 0.691 Å respectively. For the endo intermediate, the Rh-C forming-bond is 0.136 Å longer in the transition state **TS15** than in the intermediate **pdt14** while the N-C forming bond is 0.759 Å longer in the transition state **TS15** than in the intermediate **pdt14**. The corresponding differences in the Co complex are 0.133 Å and 0.857 Å respectively.

Four minima have been optimized from the [2+2] addition of the olefinic C-C bonds of norbonene to the Ir-N bonds of $CpIr(NO)_2$ (**R9**) (Figure 4.2f). The order of stability of these minima is **pdt20** (-4.78 kcalmol^{-1}) > **pdt18** (-2.98 kcalmol^{-1}) > **pdt17** (-2.59 kcalmol^{-1}) > **pdt19** (-1.92 kcalmol^{-1}).

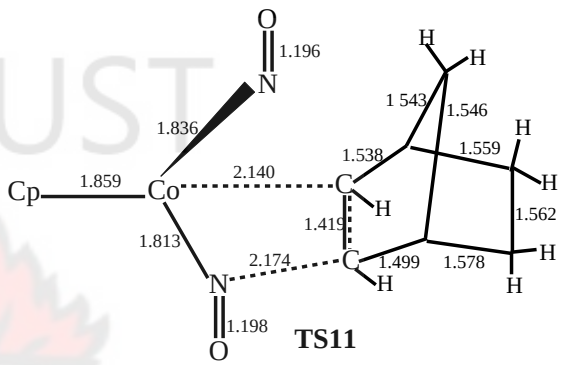

TS11

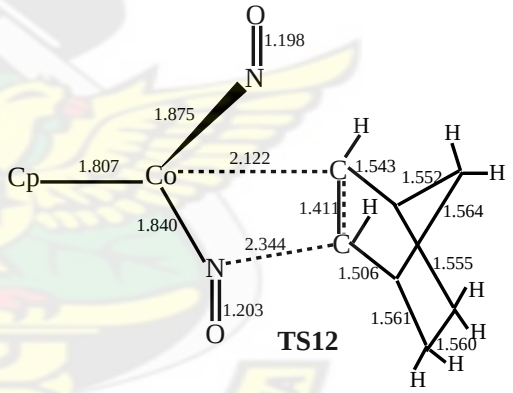

TS12

Figure 4.2d Optimized geometries of the stationary points involved in the [2+2] addition reaction between $CpCo(NO)_2$ and 2-norbonene. Bond lengths in Å.

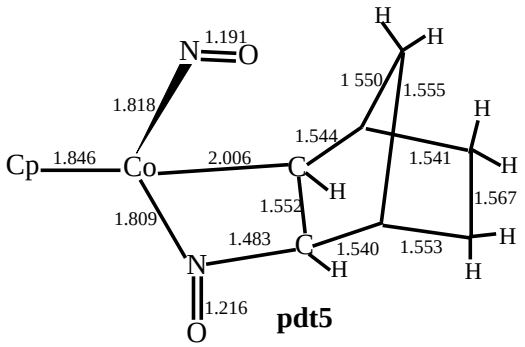

pdt5

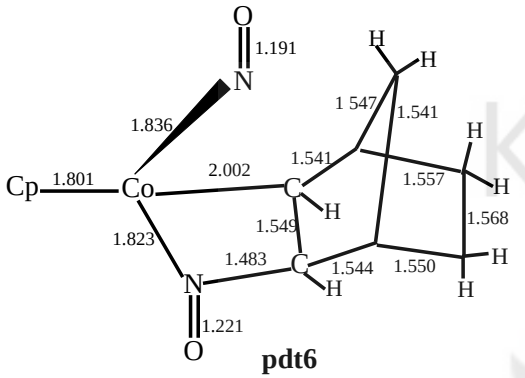

pdt6

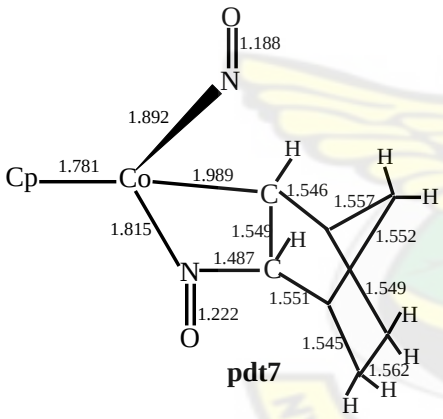

pdt7

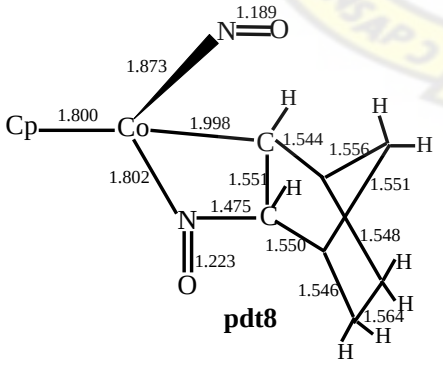

pdt8

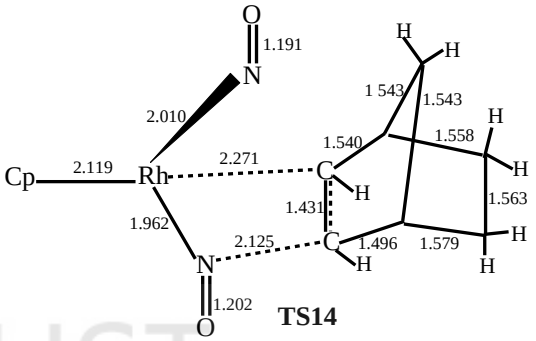

TS14

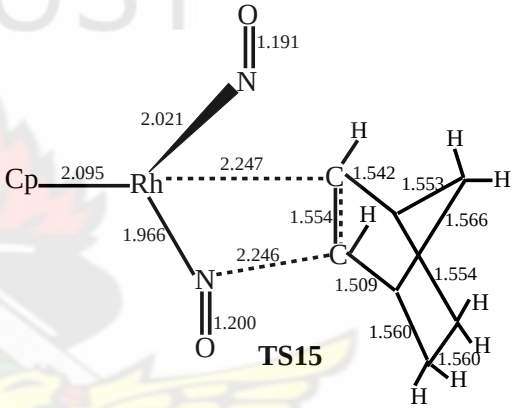

TS15

Figure 4.2e Optimized geometries of the stationary points involved in the [2+2] addition reaction between $CpRh(NO)_2$ and 2-norbonene. Bond lengths in Å.

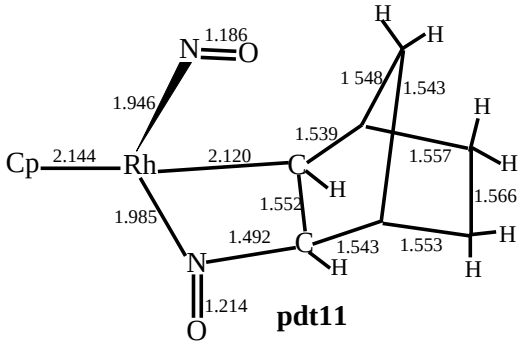

pdt11

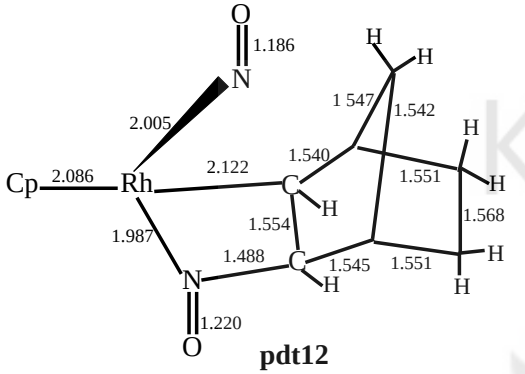

pdt12

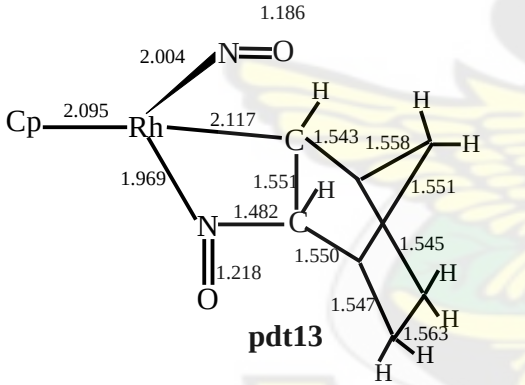

pdt13

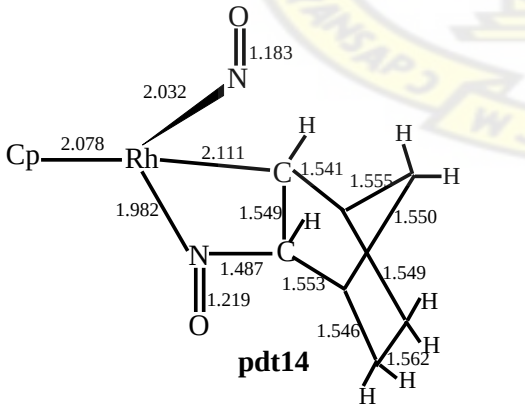

pdt14

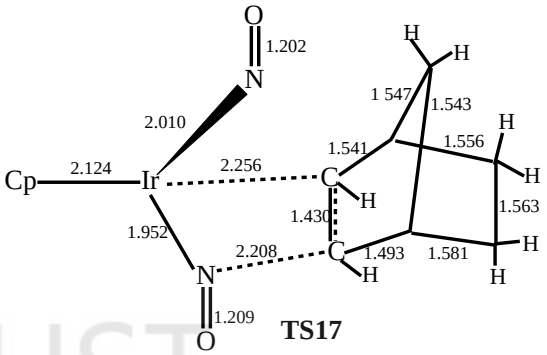

TS17

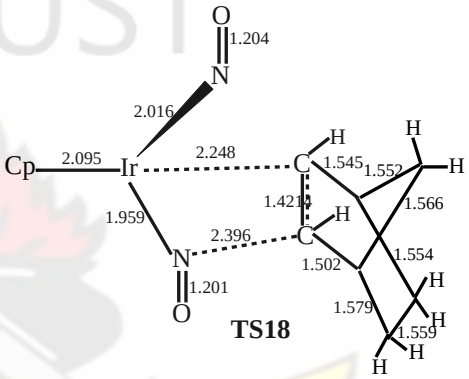

TS18

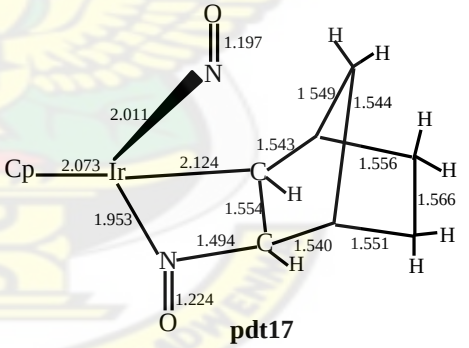

pdt17

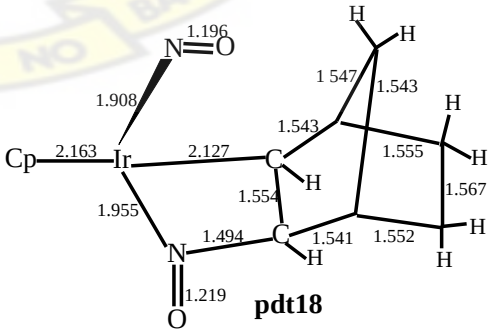

pdt18

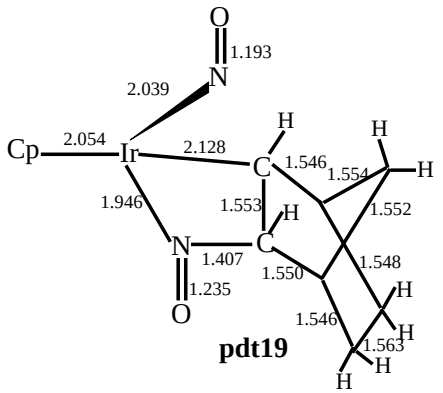

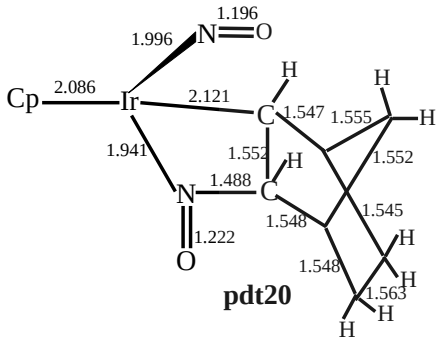

Figure 4.2f Optimized geometries of the stationary points involved in the [2+2] addition reaction between $CpIr(NO)_2$ and 2-norbonene. Bond lengths in Å.

The geometrical parameters of these minima are similar with respect to the forming and breaking bonds. The activation barrier for the formation of the exo and endo intermediates through transition states **TS17** and **TS18** are respectively 32.28 and 36.61 $kcalmol^{-1}$. These barriers are comparable with the barriers found for the corresponding reactions involving the Co and Rh complexes (see Figure 4.2c). They are also comparable with the barriers for the formation of the corresponding products in the reaction of $CpIr(NO)_2$ with ethylene(compare Figures 4.1d and 4.2c).

It is seen that the activation barriers for the [3+2] addition are very low compared to the barriers for the [2+2] addition (Figure 4.2c). A transition state for the re-arrangement of the products of [2+2] addition to the products corresponding to [3+2] addition could not be located, indicating that the re-arrangement of the product of [2+2] addition by reductive elimination involving the second metal-nitrogen π-bond to form the observed 1,2-dinitrosoalkane may not be possible. Therefore, for the 2-norbonene olefin the one-step [3+2] pathway for the formation of 1,2-dinitrosoalkanes proposed by Becker and Bergman (1983) has been found to be more plausible than the stepwise path proposed by Upton and Rappé (1985).

4.3.3 REACTIONS OF $CpM(NO)_2$ (M= Co, Rh, Ir) COMPLEXES WITH TRANS-1-PHENYLPROPENE

A π-complex (**pi-comp7**) (Figure 4.3a) has been optimized from the addition of $CpCo(NO)_2$ (**R1**) with trans-1-phenylpropene and is found to be 15.63 kcal mol^{-1} endothermic. This π-complex is 8.61 kcal mol^{-1} and 4.09 kcal mol^{-1} less stable than **pi-comp1** (where ethylene is the olefin) and **pi-comp4** (when norbonene is the olefin) respectively. The distance between the Co and the olefin C-C centroid in **pi-comp7** is computed to be 2.053 Å, which is close to the distance of 2.037 Å found in **pi-comp1**. A π-complex (**pi-comp8**) has also been optimized from the interaction of $CpRh(NO)_2$ (**R5**) with trans-1-phenylpropene and is 5.69 kcal mol^{-1} endothermic. This endothermicity contrasts with the $CpRh(NO)_2$-ethylene π-complex endothermicity of 0.65 kcal mol^{-1} and the $CpRh(NO)_2$-norbonene π-complex endothermicity of 3.94 $kcalmol^{-1}$. The distance between the metal center and the olefinic C-C centroid in **pi-comp8** is 0.139 Å longer than the corresponding distance in **pi-comp7**. A π-complex **(pi-comp9)** optimized from the interaction of $CpIr(NO)_2$ (**R9**) with trans-1-phenylpropene is 11.19 kcal mol^{-1} endothermic. This π-complex is 7.4 kcal mol^{-1} less stable than the $CpIr(NO)_2$-ethylene π-complex. The order of stability of the π-complexes formed from the interaction of trans-1-phenylpropene with the $CpM(NO)_2$(M=Co, Rh, Ir) complexes is Rh > Ir > Co.

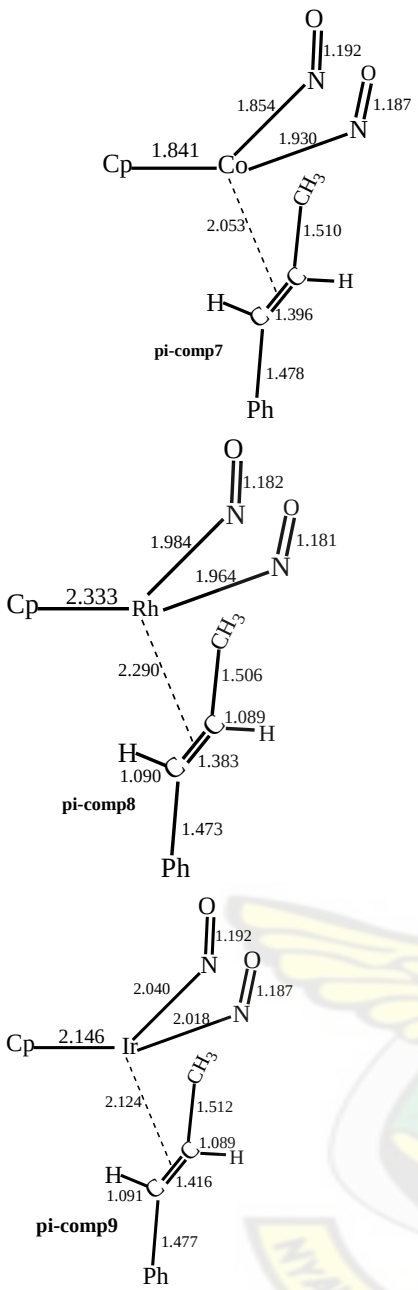

Figure 4.3a Optimized geometries of the π-complexes formed from the interaction of $CpM(NO)_2$ (M = Co, Rh, Ir) with trans-1-phenylpropene. Bond lengths in Å.

The product of [3+2] addition of the olefinic bond of trans-1-phenylpropene across the Co-N bonds of $CpCo(NO)_2$ (**pdt21**) (shown in Figure 4.3b) is found to be 27.93 kcal mol^{-1} exothermic. Thus the exothermicity of the reaction decreases by 6.95 kcal mol^{-1} when trans-1-phenylpropene is used as olefin instead of ethylene. The transition state **TS19** connecting the reactants and **pdt21** is found to be 0.39 kcal mol^{-1} below the reactants. This is consistent with what has been observed in the reaction of $CpCo(NO)_2$ with ethylene and with 2-norbonene. The [3+2] addition of the olefinic C-C bond of trans-1-phenylpropene across the two Rh-N bonds of $CpRh(NO)_2$ (**R5**) leads to the product **pdt27** (Figure 4.3b) which is 22.05 kcal mol^{-1} exothermic; 5.88 kcal mol^{-1} less exothermic than **pdt21** formed from the corresponding reaction involving the Co complex. The transition state **TS24** for the formation of **pdt27** is 1.70 kcal mol^{-1} above the reactants. This transition state contrasts with the transition state of the corresponding reaction involving the Co complex which is 0.39 kcal mol^{-1} below the reactants.

The product **pdt29** (Figure 4.3b) formed from [3+2] addition of the olefinic bond of trans-1-phenylpropene to the Ir-N bonds of **R9** is found to be 23.90 kcal mol^{-1} exothermic. The exothermicity of this reaction is comparable with the exothermicity of the reaction between $CpRh(NO)_2$ with trans-1-phenylpropene to form **pdt27** (22.05kcalmol^{-1}) but 4.03 kcal mol^{-1} less than the exothermicity of the reaction of $CpCo(NO)_2$ with trans-1-phenylpropenene to form **pdt21**. The activation barrier for the formation of **pdt29** through transition state **TS27** is 5.63 kcalmol^{-1}. This reaction thus has a higher barrier compared with the barrier of the corresponding reactions involving the Co complex (formation of **pdt21**) and the Rh complex (formation of **pdt27**).

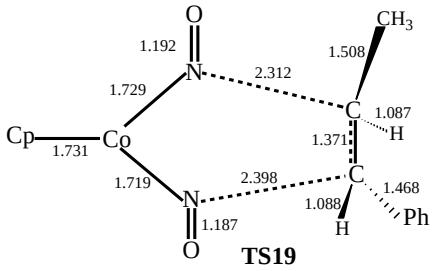

TS19

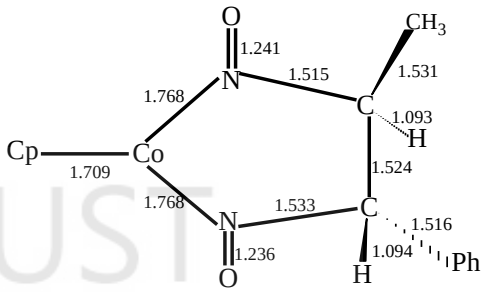

pdt21

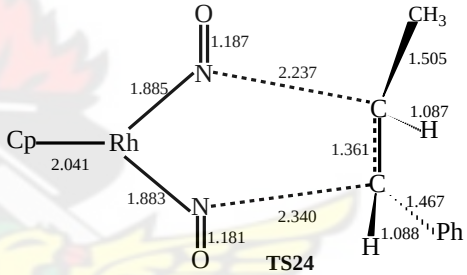

TS24

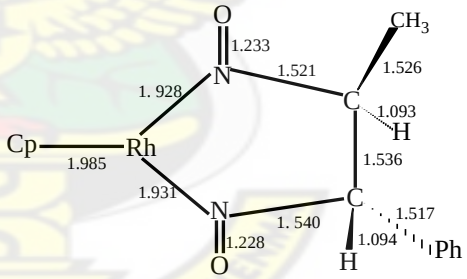

pdt27

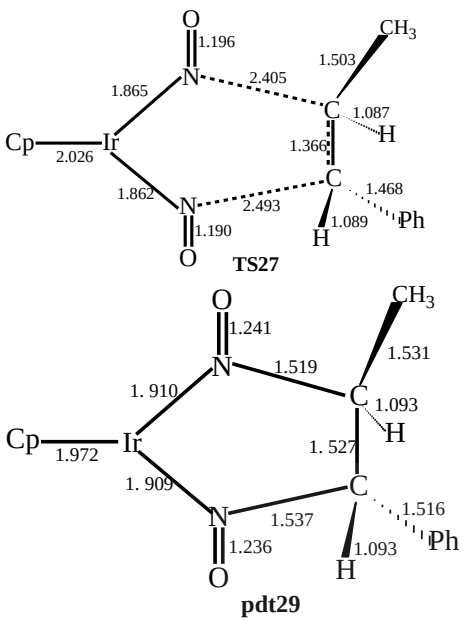

Figure 4.3b Optimized geometries of the stationary points involved in the [3+2] addition reaction of $CpM(NO)_2$ (M = Co, Rh, Ir) with trans-1-phenylpropene. Bond lengths in Å.

The formation of product **pdt23** (Figure 4.3c) from [2+2] addition of the olefinic C-C bond of trans-1-phenylpropene across the Co-N bond of $CpCo(NO)_2$ proceed through a stepwise pathway. The first step involves the formation of **pdt22** which has an endothermicity of 16.50 kcalmol^{-1}, through transition state **TS20** with an activation barrier of 16.73 kcalmol^{-1}, and the second step involves the formation of **pdt23**, which has an endothermicity of 5.14 kcalmol^{-1}, from **pdt22**, through either transition state **TS21** or **TS22** (depending on the stereochemical orientation of the substituents on the olefin at the critical point), with an activation barrier of 15.96 kcal mol^{-1} or 17.69 kcal mol^{-1} (Figure 4.3d). The species **pdt24**, which is 10.77 kcal mol^{-1} exothermic, is a higher-energy conformer of **pdt23**. The species **pdt25** and **pdt26** are formed through transition state **TS23** with a barrier of 41.28 kcalmol^{-1}.

The transition state **TS25** (Figure 4.3c) for the [2+2] addition of the olefinic C-C bond of trans-1-phenylpropene across the Rh-N bond of $CpRh(NO)_2$ is 36.61 kcalmol^{-1}, leading to product **pdt28** which is 12.04 kcal mol^{-1} endothermic (Figure 4.3d). The activation barrier for the [2+2] addition of the olefinic C-C bond of trans-1-phenylpropene across the Ir-N bond of $CpIr(NO)_2$ through transition state **TS28** is 37.12 kcalmol^{-1}, leading to a product **pdt30** which is 7.69 kcal mol^{-1} endothermic.

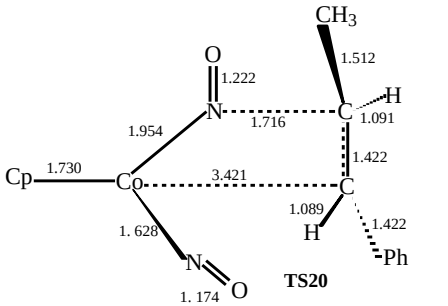

TS20

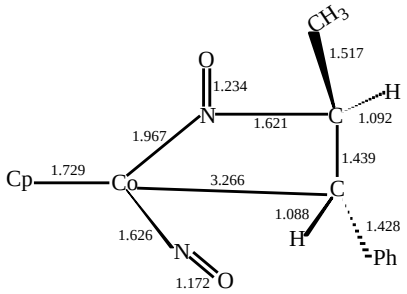

pdt22

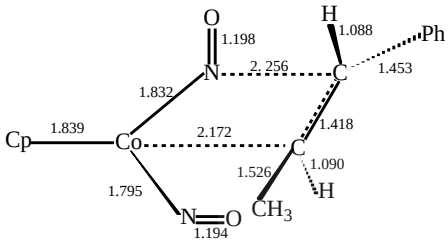

TS21

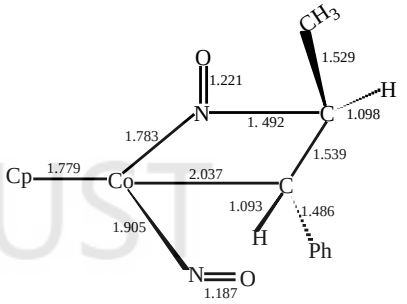

pdt25

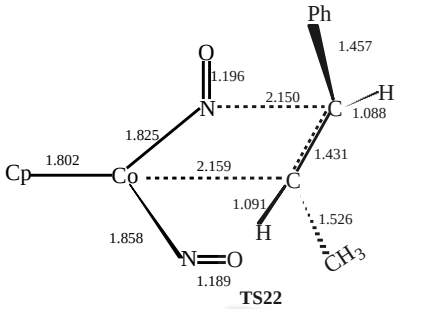

TS22

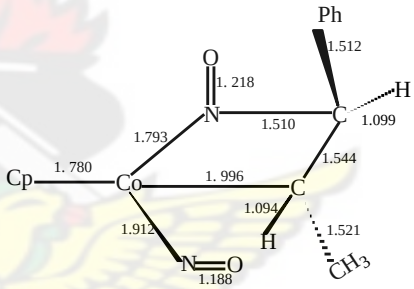

pdt24

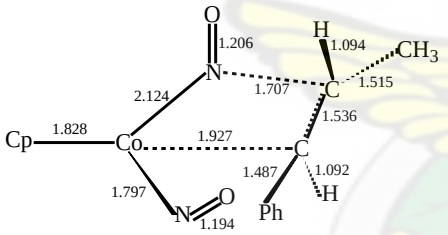

TS23

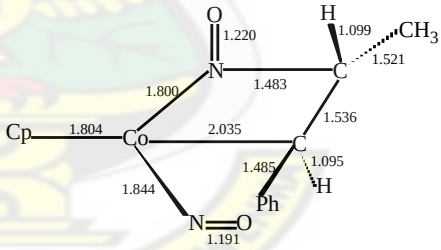

pdt26

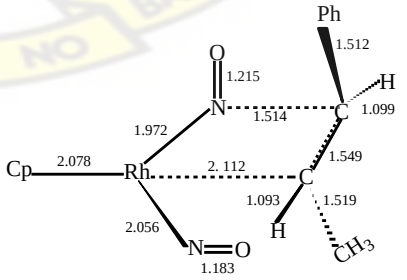

TS25

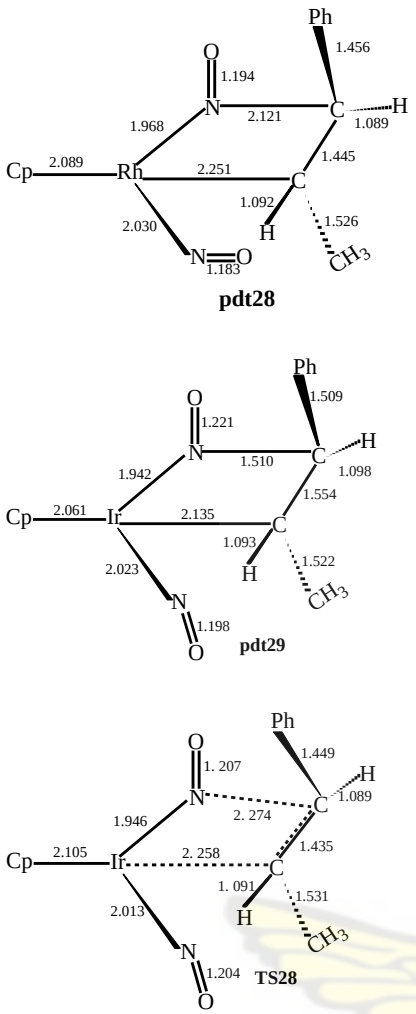

Figure 4.3c Optimized geometries of the stationary points involved in the [2+2] addition reaction of $CpM(NO)_2$ (M = Co, Rh, Ir) with trans-1-phenylpropene. Bond lengths in Å.

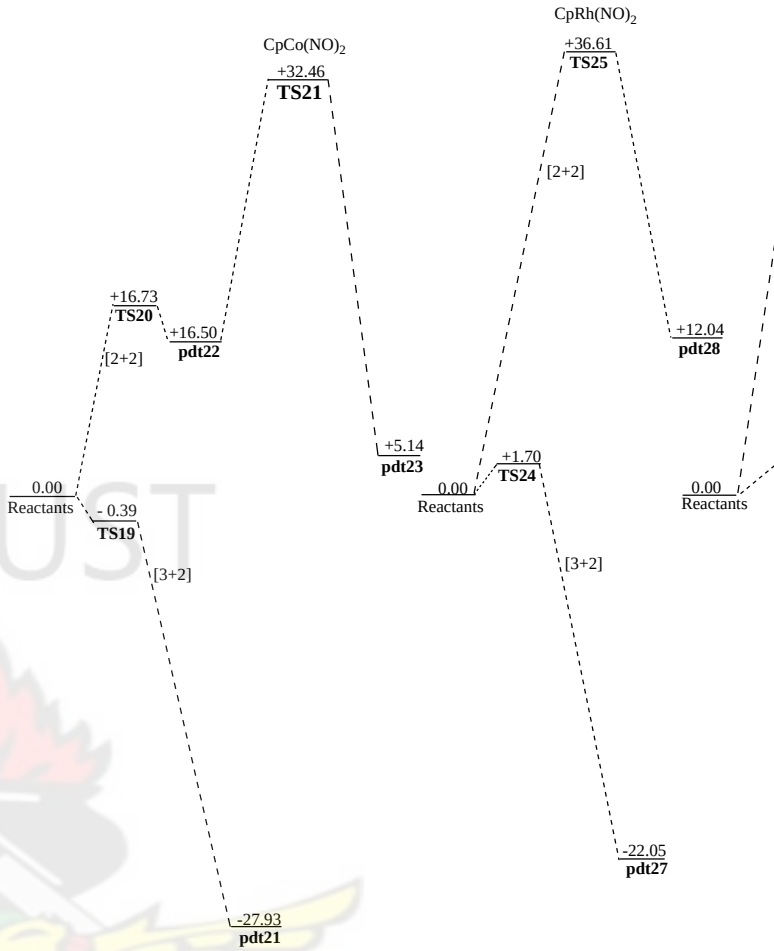

Figure 4.3d Energy profiles of the [3+2] and [2+2] addition reaction of $CpM(NO)_2$ (M = Co, Rh, Ir) with trans-1-phenylpropene. Relative energies in $kcalmol^{-1}$.

Figure 4.3d shows that the activation barrier for the [2+2] addition pathways are higher than those for the [3+2] addition pathway. A transition state for the re-arrangement of the products of [2+2] addition to the products corresponding to

[3+2] addition could not be located, indicating that the re-arrangement of the product of [2+2] addition by reductive elimination involving the second metal-nitrogen π-bond to form the observed 1,2-dinitrosoalkane may not be possible. Therefore, for the trans-1-phenylpropene olefin the one-step [3+2] pathway for the formation of 1,2-dinitrosoalkanes proposed by Becker and Bergman (1983) has been found to be more plausible than the stepwise path proposed by Upton and Rappé (1985).

4.3.4 REACTIONS OF $CpM(NO)_2$ (M= Co, Rh, Ir) WITH CYCLOPENTENE

A π-complex **(pi-comp10)** (Figure 4.4a) optimized from the interaction of cyclopentene and $CpCo(NO)_2$ (**R1**) is 13.30 kcal mol^{-1} endothermic. This π-complex is 6.28 kcal mol^{-1} less stable than **pi-comp1** which is formed from the interaction of **R1** with ethylene. The π-complex **(pi-comp11)** optimized from the interaction of $CpRh(NO)_2$ with cyclopentene is 4.80 kcal mol^{-1} endothermic. It is thus 8.50 kcal mol^{-1} more stable than the $CpCo(NO)_2$ -cyclopentene π-complex but 4.15 kcal mol^{-1} less stable than the $CpRh(NO)_2$-ethylene π-complex. The π-complex **pi-comp12** formed from the interaction of $CpIr(NO)_2$ (**R9**) with cyclopentene is 10.53 kcal mol^{-1} endothermic. This π-complex is 2.87 kcal mol^{-1} more stable than the $CpCo(NO)_2$-cyclopentene π-complex but 5.73 kcal mol^{-1} less stable than the $CpRh(NO)_2$-cyclopentene π-complex.

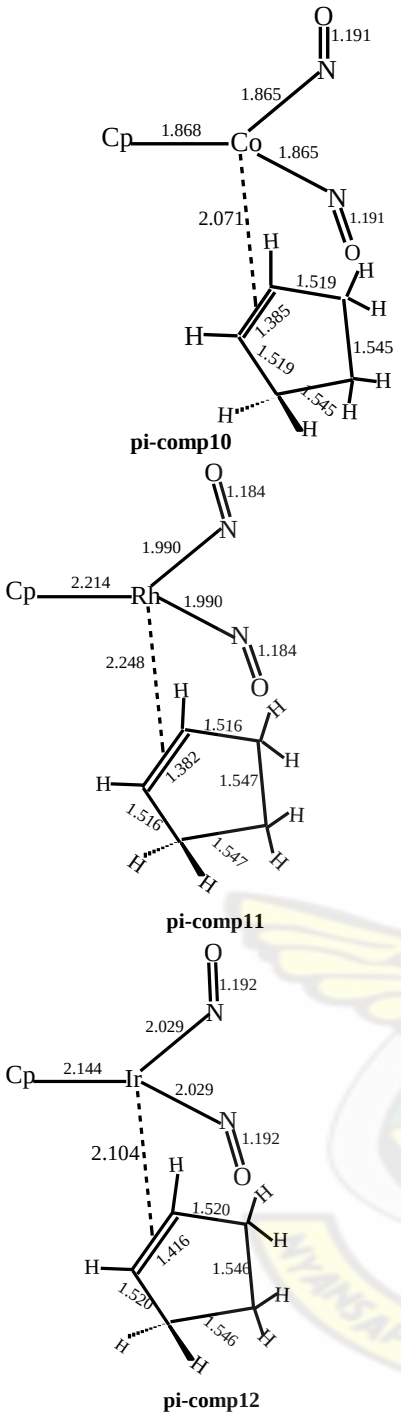

Figure 4.4a Optimized geometries of the π-complexes formed from the interaction of $CpM(NO)_2$ (M = Co, Rh, Ir) with cyclopentene. Bond lengths in Å.

The product **pdt31** (Figure 4.4b) formed from [3+2] addition of the olefinic bond of cyclopentene across the two Co-N bonds of $CpCo(NO)_2$ is 35.32 kcal mol^{-1} exothermic (Figure 4.4d). The exothermicity of this reaction is comparable with the exothermicity of 34.88 kcal mol^{-1} found for the reaction between $CpCo(NO)_2$ (**R1**) and ethylene. The two N-C forming-bonds in the product structures in the two cases (**pdt1** and **pdt31**) are comparable, as are the N-Co-N bond angles. The transition state **TS29** for the formation of product **pdt31** is 0.78 kcal mol^{-1} below the reactants on the energy profile. The geometrical features of transition state **TS29** are comparable with those of **TS1** optimized from the reaction of $CpCo(NO)_2$ with ethylene.

The formation of product **pdt32** by [3+2] addition of the olefinic C-C bond of cyclopentene across the Rh-N bonds of $CpRh(NO)_2$ (**R5**) is 29.67 kcal mol^{-1} and the transition state for this step (**TS31**) is 0.44 kcal mol^{-1} below the reactants on the energy profile. This exothermicity is 5.63 kcal mol^{-1} less than the exothermicity for the formation

of **pdt31**. The activation barrier for the formation of **pdt35** by [3+2] addition of the olefinic bond of cyclopentene across the two Ir-N bonds of $CpIr(NO)_2$ through transition state **TS33** is 4.42 kcalmol^{-1}. This barrier is higher than the barrier of the corresponding reactions in the Co complex (-0.78 kcalmol^{-1}) and Rh complex (-0.44 kcalmol^{-1}). The resulting product **pdt35** is 31.91 kcal mol^{-1} exothermic. Thus product **pdt35** is 3.41 kcal mol^{-1} less stable than **pdt31** formed from the reaction of cyclopentene with $CpCo(NO)_2$, but 2.23 kcal mol^{-1} more stable than **pdt33** formed from the reaction of cyclopentene with $CpRh(NO)_2$.

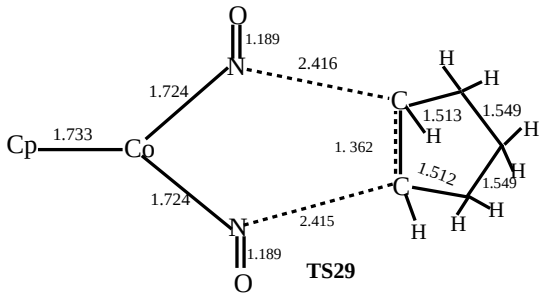

TS29

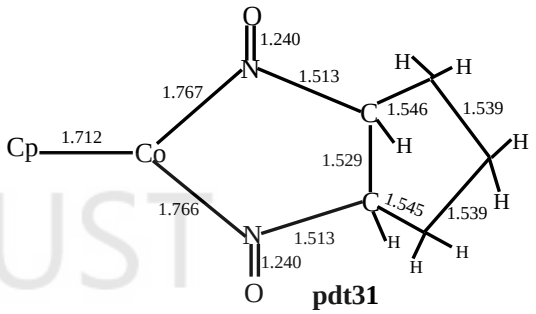

pdt31

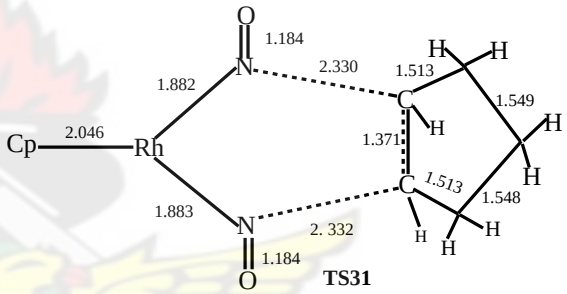

TS31

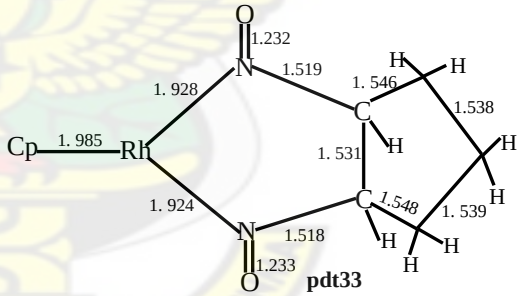

pdt33

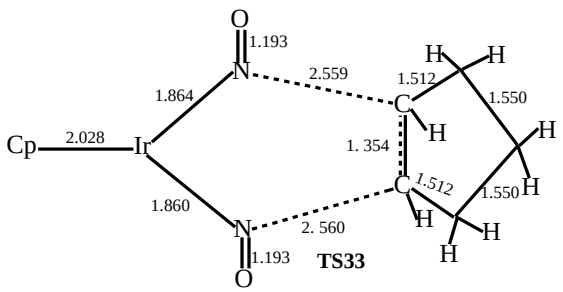

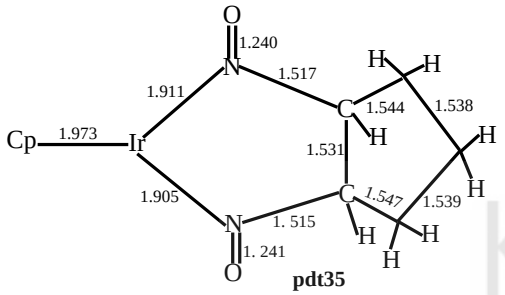

Figure 4.4b Optimized geometries of the stationary points involved in the [3+2] addition reaction of $CpM(NO)_2$ M = Co, Rh, Ir) with cyclopentene. Bond lengths in Å.

The formation of product **pdt32** (Figure 4.4c) by [2+2] addition of the olefinic C-C bond of cyclopentene across the Co-N bond of $CpCo(NO)_2$ through transition sate **TS30** is 2.81 kcal mol^{-1} endothermic and has an activation barrier of 30.22 kcal mol^{-1} while the formation of product **pdt34** by [2+2] addition through transition state **TS32** is 4.78 kcal mol^{-1} endothermic and has an activation barrier of 29.86 $kcalmol^{-1}$. The activation barrier for the formation of product **pdt36** by [2+2] addition of the olefinic bond of cyclopentene across the Ir-N bond of $CpIr(NO)_2$ is 31.41 $kcalmol^{-1}$, and the product is 0.41 kcal mol^{-1} exothermic (Figure 4.4d).

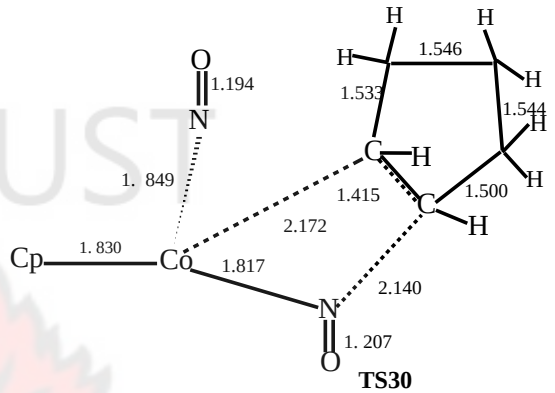

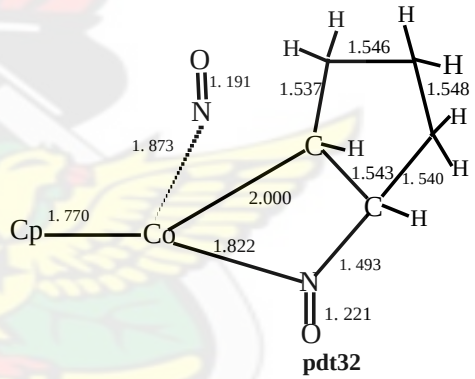

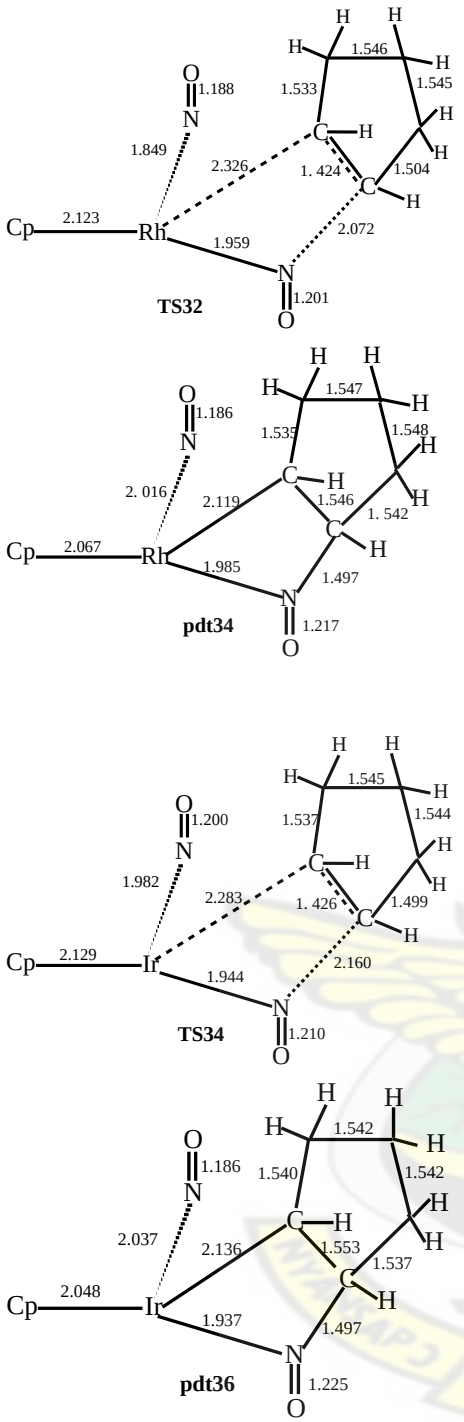

Figure 4.4c Optimized geometries of the stationary points involved in the [2+2] addition reaction of $CpM(NO)_2$ M = Co, Rh, Ir) with cyclopentene. Bond lengths in Å.

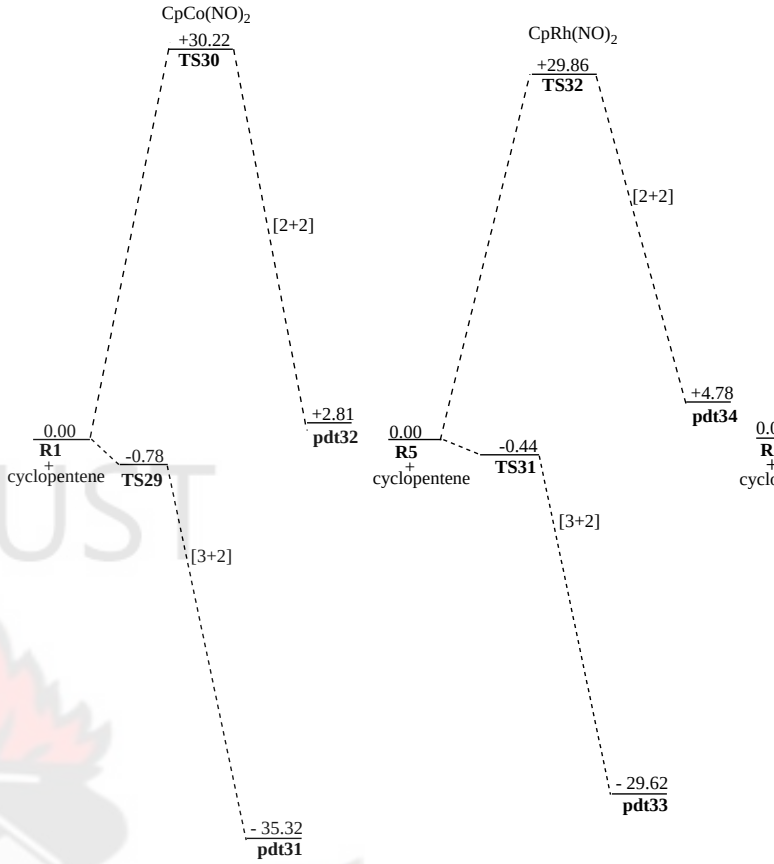

Figure 4.4d Energy profiles of the [3+2] and [2+2] addition reaction of $CpM(NO)_2$ M = Co, Rh, Ir) with cyclopentene. Relative energies in $kcalmol^{-1}$.

As seen in Figure 4.4d, the activation barrier for the [3+2] addition is far lower than the barrier for the [2+2] addition. An attempt to locate a transition state for the re-arrangement of the products of [2+2] addition to the products corresponding to [3+2] addition was unsuccessful, indicating

that the re-arrangement of the product of [2+2] addition by reductive elimination involving the second metal-nitrogen π-bond to form the observed 1,2-dinitrosoalkane may not be possible. Therefore, for the cyclopentene the one-step [3+2] pathway for the formation of 1,2-dinitrosoalkanes proposed by Becker and Bergman (1983) may be more plausible than the stepwise path proposed by Upton and Rappé (1985).

4.3.5 REACTIONS OF $CpM(NO)_2$ (M= Co, Rh, Ir) WITH CYCLOHEXENE

The π-complex **pi-comp13** (Figure 4.5a) formed from the interaction between $CpCo(NO)_2$(**R1**) and cyclohexene is 15.88 kcal mol^{-1} endothermic, which is 8.86 kcal mol^{-1} less stable than the $CpCo(NO)_2$-ethylene π-complex. The π-complex **pi-comp14** formed from the interaction of $CpRh(NO)_2$ with cyclohexene is 3.95 kcal mol^{-1} endothermic, which is 11.93 kcal mol^{-1} more stable than the $CpCo(NO)_2$-cyclohexene π-complex and 3.30 kcal mol^{-1} less stable than the $CpRh(NO)_2$-ethylene π-complex while the π-complex **pi-comp15** formed from the interaction of $CpIr(NO)_2$ with cyclohexene is 6.44 kcal mol^{-1} endothermic, which is 8.64 kcal mol^{-1} more stable than the $CpCo(NO)_2$-cyclohexene π-complex but 2.49 kcal mol^{-1} less stable than the $CpIr(NO)_2$-cyclohexene π-complex. Thus the order of stability of the π-complexes resulting from the interaction of $CpM(NO)_2$ (M=Co, Rh, Ir) with cyclohexene is Rh > Ir > Co.

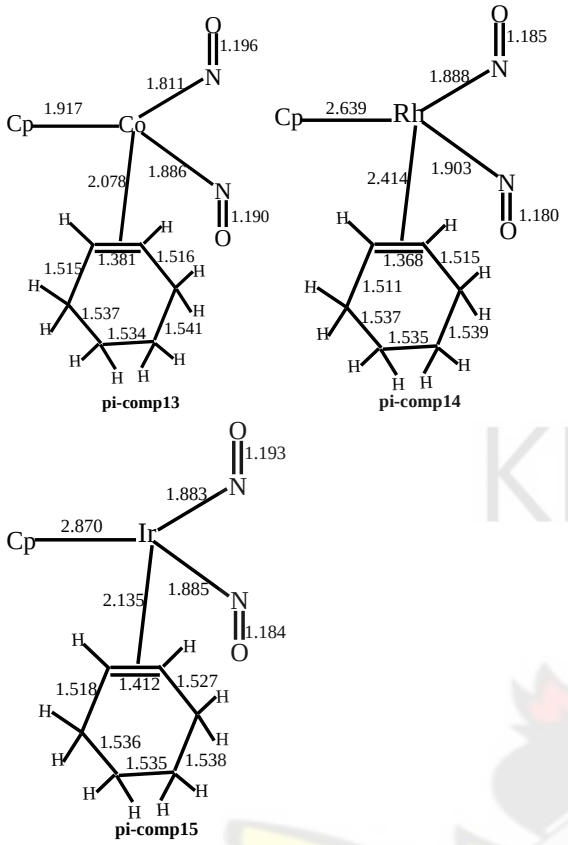

Figure 4.5a Optimized geometries of the π-complexes formed from the interaction of $CpM(NO)_2$ (M = Co, Rh, Ir) with cyclohexene. Bond lengths in Å.

The [3+2] addition of cyclopentene across the Co-N bonds of $CpCo(NO)_2$ (**R1**) leads to two products - an exo isomer (**pdt37**) and an endo isomer (**pdt38**) - which are 29.84 kcal mol^{-1} and 29.94 kcal mol^{-1} exothermic respectively. These exothermicities are comparable with the exothermicity of 34.88 kcal mol^{-1} found for **pdt1** formed from the reaction of $CpCo(NO)_2$ with ethylene. The exo product **pdt37** is more symmetric than the endo product **pdt38** with respect to the forming-bonds. The activation barriers for the formation of the exo product **pdt37** and the endo product **pdt38** through transition states **TS35** and **TS36** are 6.99 kcal mol^{-1} and 1.29 kcal mol^{-1} respectively. The transition state **TS35** is more symmetric than **TS36**.

The [3+2] addition of the olefinic C-C bond of cyclohexene across the two Rh-N bonds of $CpRh(NO)_2$ forms products **pdt40** (exo) and **pdt41**(endo) which are 24.08 and 23.99 kcal mol^{-1} exothermic respectively. The products **pdt40** and **pdt41** are also respectively 5.59 and 5.68 kcal mol^{-1} less stable than **pdt9** which is formed from the reaction of $CpRh(NO)_2$ with ethylene. The activation barriers for the formation of **pdt40** and **pdt41** through transition states **TS38** and **TS39** are 7.71 kcal mol^{-1} and 2.99 kcal mol^{-1} respectively.

The product endo **pdt43** formed from [3+2] addition of the olefinic C-C bond

of cyclohexene across the Ir-N bond of $CpIr(NO)_2$ is 26.10 kcal mol^{-1} exothermic. No exo product could be located on the potential energy surface for the Ir complex. Product **pdt43** is 3.84 kcal mol^{-1} less stable than **pdt38** formed from the reaction of $CpCo(NO)_2$ with cyclohexene but 2.11 kcal mol^{-1} more stable than **pdt41** formed from the reaction of $CpRh(NO)_2$ with cyclohexene. The activation barrier for the formation of **pdt43** through transition state **TS41** is 6.45 kcal mol^{-1}.

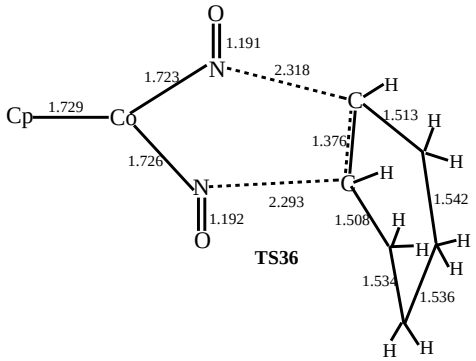

TS36

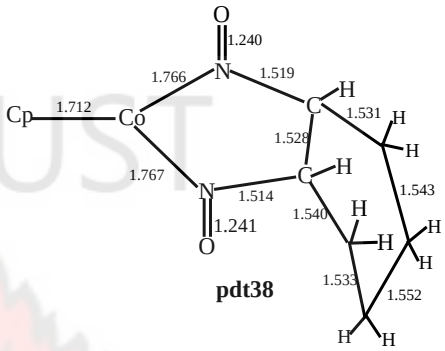

pdt38

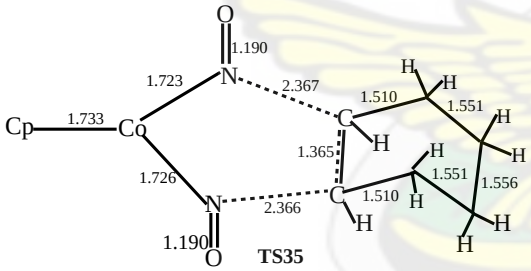

TS35

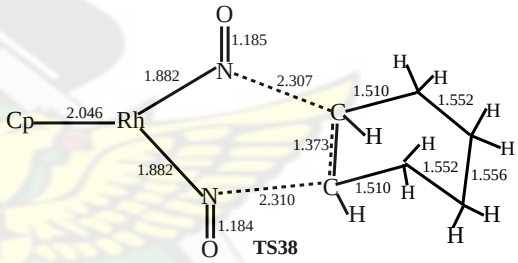

TS38

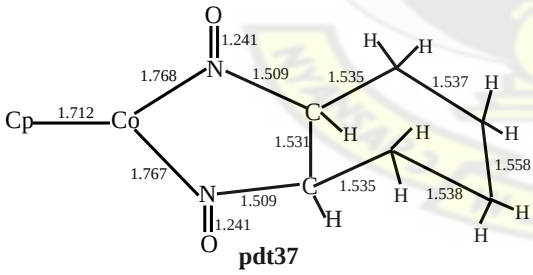

pdt37

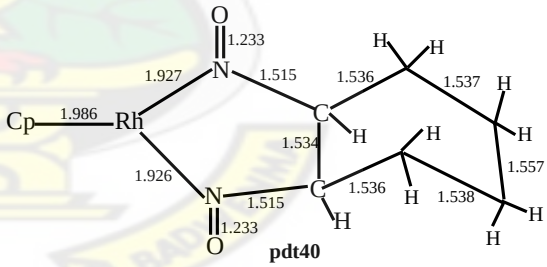

pdt40

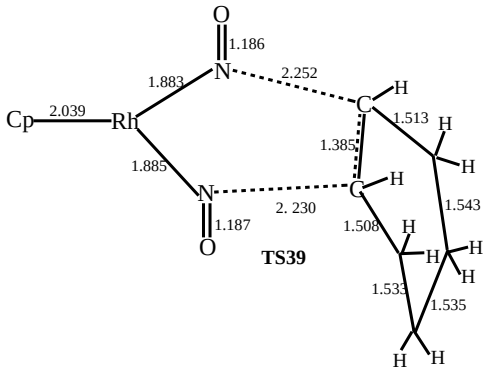

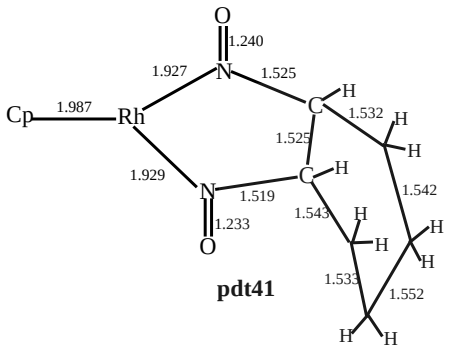

Figure 4.5b Optimized geometries of the stationary points involved in the [3+2] addition reaction of $CpM(NO)_2$ (M = Co, Rh, Ir) with cyclohexene. Bond lengths in Å.

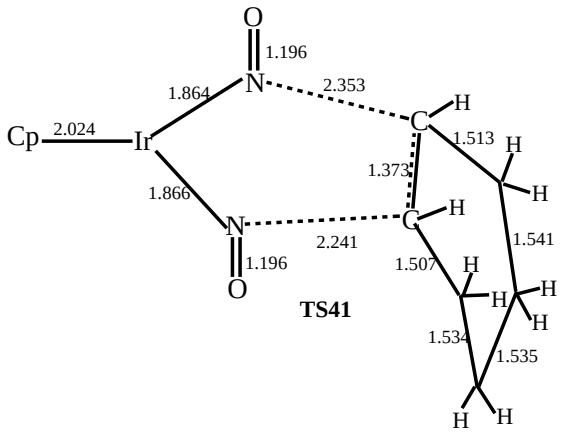

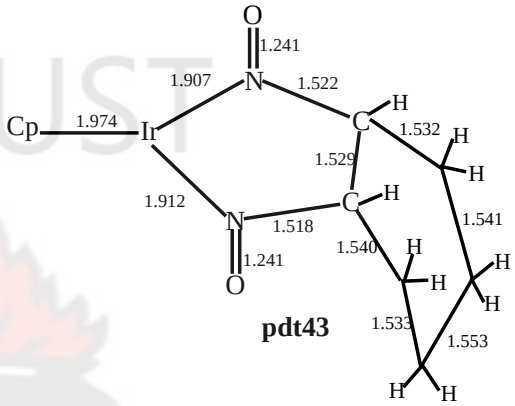

Figure 4.5b (*continued)* Optimized geometries of the stationary points involved in the [3+2] addition reaction of $CpM(NO)_2$ (M = Co, Rh, Ir) with cyclohexene. Bond lengths in Å.

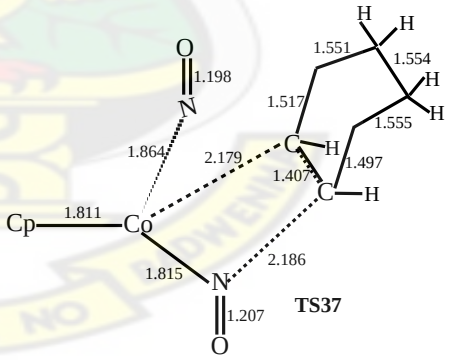

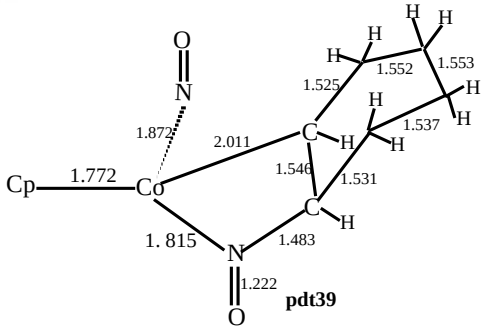

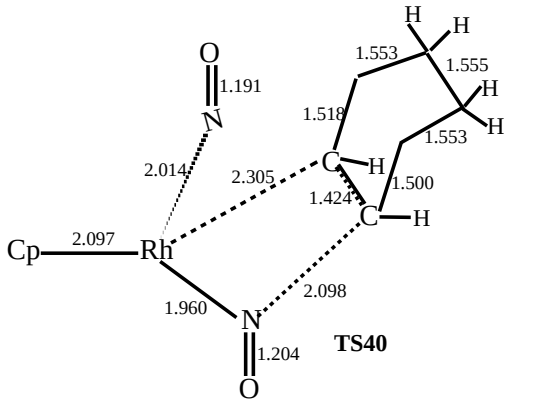

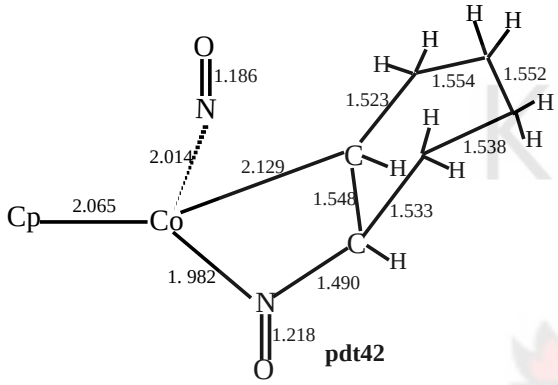

Figure 4.5c Optimized geometries of the stationary points involved in the [2+2] addition reaction of $CpM(NO)_2$ (M = Co, Rh, Ir) with cyclohexene. Bond lengths in Å.

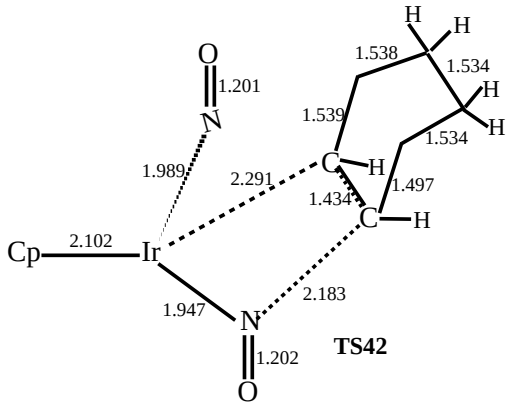

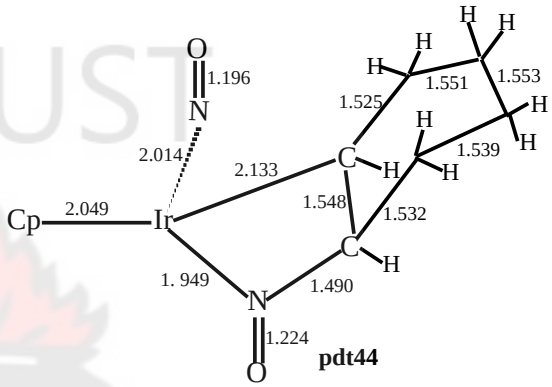

Figure 4.5c (*Continued*) Optimized geometries of the stationary points involved in the [2+2] addition reaction of $CpM(NO)_2$ (M = Co, Rh, Ir) with cyclohexene. Bond lengths in Å.

The [2+2] addition of cyclohexene across the Co-N bond of $CpCo(NO)_2$ leads to product **pdt39** (Figure 4.5c) which is 6.74 kcal mol^{-1} endothermic (Figure 4.5d). The activation barrier for this reaction through transition state **TS37** is 38.00 $kcalmol^{-1}$. The formation of product **pdt42** by [2+2] addition of cyclohexene across the Rh-N

bond of $CpRh(NO)_2$ through transition state **TS40** is 8.62 kcal mol^{-1} endothermic and has activation barrier of 37.59 kcal mol^{-1} while the formation of product **pdt44** by [2+2] addition across the Ir-N bonds of $CpIr(NO)_2$ through transition state **TS42** is 4.58 kcal mol^{-1} endothermic and has an activation barrier of 35.27 kcal mol^{-1} (4.5d).

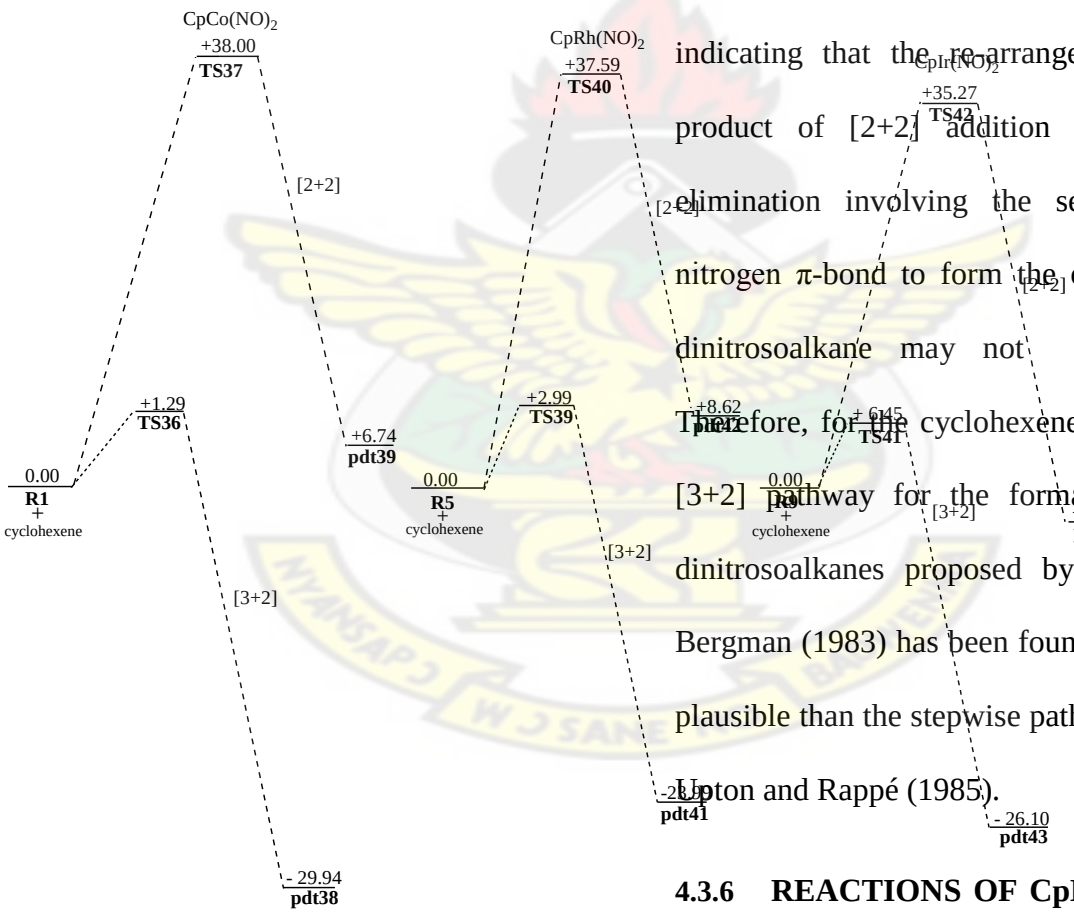

Figure 4.5d Energy profiles of the [3+2] and [2+2] addition reaction of $CpM(NO)_2$ (M = Co, Rh, Ir) with cyclohexene. Relative energies in kcal mol^{-1}.

The activation barriers for the [2+2] addition pathway are higher than the barriers for the [3+2] addition pathway (Figure 4.5d). A transition state for the re-arrangement of the products of [2+2] addition to the products corresponding to [3+2] addition could not be located, indicating that the re-arrangement of the product of [2+2] addition by reductive elimination involving the second metal-nitrogen π-bond to form the observed 1,2-dinitrosoalkane may not be possible. Therefore, for the cyclohexene the one-step [3+2] pathway for the formation of 1,2-dinitrosoalkanes proposed by Becker and Bergman (1983) has been found to be more plausible than the stepwise path proposed by Upton and Rappé (1985).

4.3.6 REACTIONS OF $CpM(NO)_2$ (M= Co, Rh, Ir) WITH 2,3-DIMETHYL-2-BUTENE

The π-complex **pi-comp16** (Figure 4.6a) optimized from the reaction of $CpCo(NO)_2$ with 2,3-dimethyl-2-butene is 14.83 kcal mol^{-1} endothermic, which is 7.81 kcal mol^{-1} less stable than the $CpCo(NO)_2$-ethylene π-complex while the π-complex **pi-comp17** optimized from the interaction of $CpRh(NO)_2$ with 2,3-dimethyl-2-butene is 4.01 kcal mol^{-1} endothermic, which is 3.36 kcal mol^{-1} less stable than the $CpRh(NO)_2$-ethylene π-complex. The π-complex **pi-comp18** optimized from the interaction of 2,3-dimethyl-2-butene with $CpIr(NO)_2$ is 10.49 kcal mol^{-1} endothermic, which is 6.70 kcal mol^{-1} less stable than the $CpIr(NO)_2$-ethylene π-complex. The **pi-comp18** is also 4.34 kcal mol^{-1} more stable than **pi-comp16** but 6.48 kcal mol^{-1} less stable than **pi-comp17**. Thus the order of stability of the π-complexes formed from the reactions of the CpM(M=Co, Rh, Ir) complexes with 2,3-dimethyl-2-butene is Rh > Ir > Co, an order that is observed in all the olefins studied.

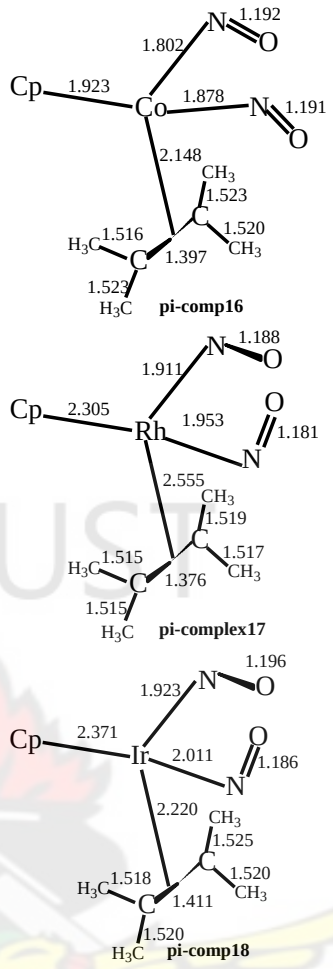

Figure 4.6a Optimized geometries of the π-complexes formed from the interaction of $CpM(NO)_2$ (M = Co, Rh, Ir) with 2,3-dimethyl-2-butene. Bond lengths in Å.

The transition state **TS44** (Figure 4.6b) for the [3+2] addition of the olefinic C-C bond of 2,3-dimethyl-2-butene across the two Co-N bonds of $CpCo(NO)_2$ (**R1**) is 1.56 kcal mol^{-1} below the reactants (Figure 4.6d). The resulting product **pdt47** is 33.24 kcal mol^{-1} exothermic. This is comparable

with the exothermicity of **pdt1** (-34.88 kcalmol^{-1}) formed from the [3+2] addition of $CpCo(NO)_2$ with ethylene. The transition state **TS46** for the [3+2] addition of the olefinic C-C bond of 2,3-dimethyl-2-butene across the Rh-N bonds of $CpRh(NO)_2$ is 0.81 kcal mol^{-1} above the reactants, leading to **pdt49** which is 26.05 kcal mol^{-1} exothermic. This barrier is comparable with the barrier of 0.59 kcal mol^{-1} found for the formation of **pdt2** from the reaction of $CpRh(NO)_2$ with ethylene. The activation barrier for the formation of **pdt51** from the [3+2] addition of 2,3-dimethyl-2-butene to the Ir-N bonds of $CpIr(NO)_2$ (**R9**) through transition state **TS48** is 4.61 kcalmol^{-1}, a barrier which is higher than the corresponding barrier in the reaction of 2,3-dimethyl-2-butene with $CpCO(NO)_2$ and $CpRh(NO)_2$ but comparable with the corresponding barrier in the reaction of $CpIr(NO)_2$ with ethylene (5.05 kcalmol^{-1}). The resulting product **pdt51** is 27.77 kcal mol^{-1} exothermic, which is comparable with the exothermicities of products **pdt47** (33.24 kcalmol^{-1}) and **pdt49** (26.05 kcalmol^{-1}) which are formed from the reaction of 2,3-dimethyl-2-butene with $CpCo(NO)_2$ and $CpRh(NO)_2$ respectively.

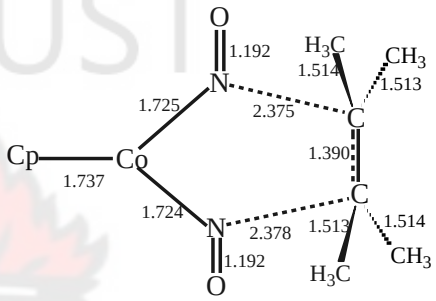

TS44

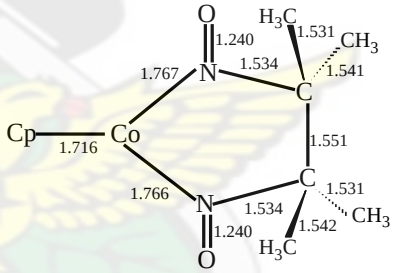

pdt47

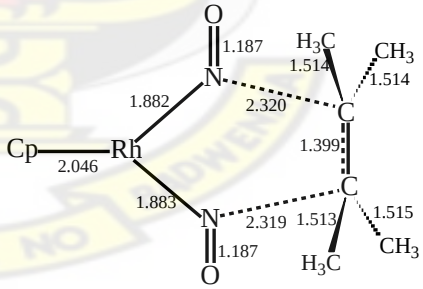

TS46

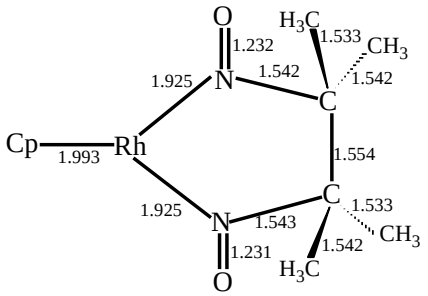

pdt49

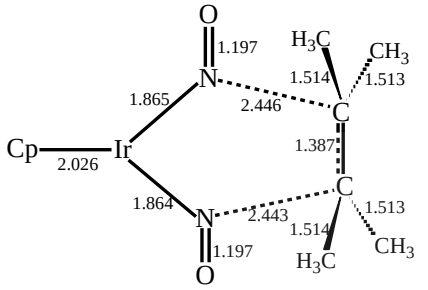

TS48

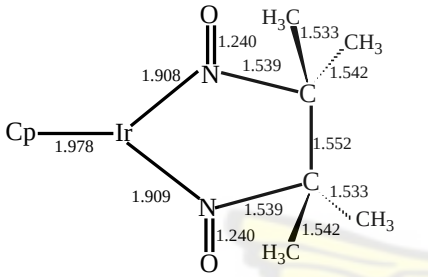

pdt51

Fig. 4.6b Optimized geometries of the stationary points involved in the [3+2] addition reaction of $CpM(NO)_2$ (M = Co, Rh, Ir) with 2,3-dimethyl-2-butene. Bond lengths in Å.

The product **pdt48** (Figure 4.6c) formed from the [2+2] addition of the olefinic C-C bond of 2,3-dimethyl-2-butene across the Co-N bond of $CpCo(NO)_2$ is 5.99 kcal mol^{-1} endothermic, making it 8.96 kcal mol^{-1} less stable than the product of [2+2] addition of ethylene to $CpCo(NO)_2$. The formation of **pdt48** through transition state **TS45** has an activation barrier of 32.21 $kcalmol^{-1}$. The product **pdt50** formed from the [2+2] addition of the olefinic C-C bond of 2,3-dimethyl-2-butene to the Rh-N bond of $CpRh(NO)_2$ is 7.08 kcal mol^{-1} endothermic , which makes it 7.62 kcal mol^{-1} less stable than the product of [2+2] addition of ethylene to $CpRh(NO)_2$. The activation barrier for the formation of **pdt50** through transition state **TS47** is 32.98 kcal mol^{-1}, which is comparable to the barrier of 32.08 kcal mol^{-1} found for the formation of the ethylene derivative of **pdt48**.

The activation barrier for the formation of **pdt52** (Figure 4.6c) by [2+2] addition of 2,3-dimthyl-2-butene to the Ir-N bond of $CpIr(NO)_2$ (**R9**) through transition state **TS49** is 34.20 kcal mol^{-1} (Figure 4.6d). This barrier is comparable with the barriers of 32.21 kcal mol^{-1} found for the corresponding reaction of 2,3-dimethyl-2-butene with $CpCo(NO)_2$ and 35.50 kcal mol^{-1} found for the reaction of 2,3-dimethyl-2-

butene with $CpRh(NO)_2$. It is also comparable with the corresponding barrier in the reaction of $CpIr(NO)_2$ with ethylene (34.36 kcalmol^{-1}). The product **pdt52** is 2.10 kcal mol^{-1} endothermic.

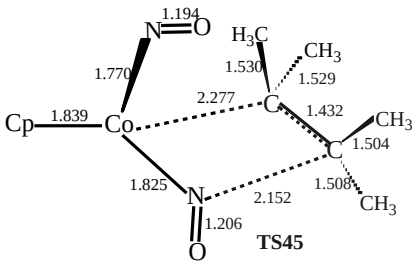

TS45

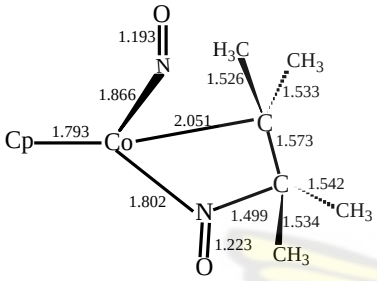

pdt48

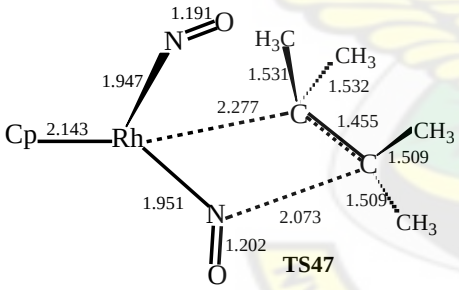

TS47

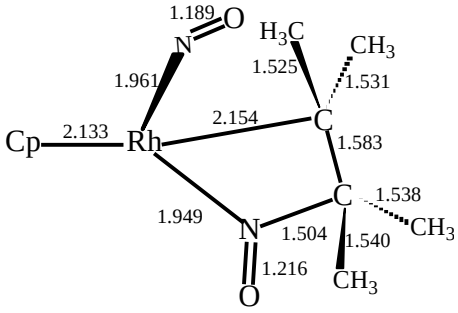

pdt50

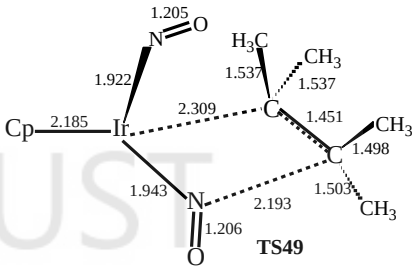

TS49

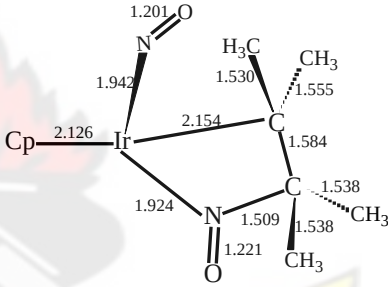

pdt52

Fig. 4.6c Optimized geometries of the stationary points involved in the [2+2] addition reaction of $CpM(NO)_2$ (M = Co, Rh, Ir) with 2,3-dimethyl-2-butene. Bond lengths in Å.

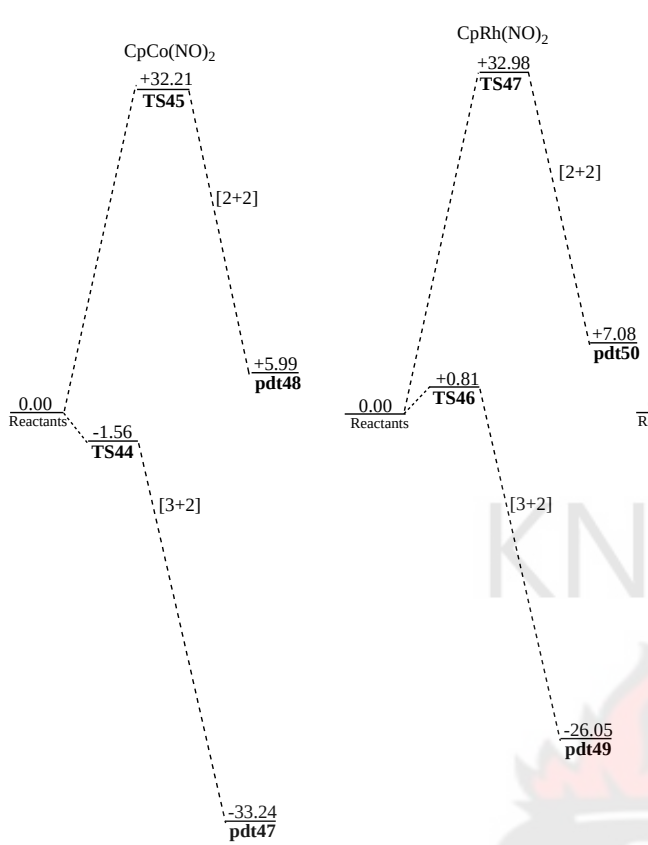

Figure 4.6d Energy profiles of the [3+2] and [2+2] addition reaction between $CpM(NO)_2$ (M=Co, Rh, Ir) and 2,3-dimethyl-2-butene. Relative energies in $kcalmol^{-1}$.

The activation barriers for the [2+2] addition pathway are higher than the barrier for the [3+2] pathway (Figure 4.6d). An attempt to locate a transition state for the re-arrangement of the products of [2+2] addition to the products corresponding to [3+2] addition was unsuccessful, indicating that the re-arrangement of the product of [2+2] addition by reductive elimination involving the second metal-nitrogen π-bond to form the observed 1,2-dinitrosoalkane may not be possible. Therefore, for the 2,3-dimethyl-2-butene the one-step [3+2] pathway for the formation of 1,2-dinitrosoalkanes proposed by Becker and Bergman (1983) may be more favorable than the stepwise path proposed by Upton and Rappé (1985).

4.4 CONCLUSIONS

From the results presented and the foregoing discussion, the following conclusions are drawn:

1. The π-complexes optimized from the reaction of the $CpM(NO)_2$ (M=Co, Rh, Ir) complexes with each of the olefins are endothermic. The order of stability of the π-complexes with respect to changing metal is Rh > Ir > Co. These energetics must be viewed in relation to the well-known difficulties for density functional

theory methods to describe weak interactions. The B3LYP functional in particular does not describe dispersion, and therefore underestimates the interaction energies of π-bonded systems. This may well result in a repulsive interaction.

2. The activation barriers for the one-step [3+2] addition pathway for the formation of 1,2-dinitrosoalkanes are generally very low. The highest barriers of this step occur in the reaction of $CpM(NO)_2$ (M = Co, Rh, Ir) with cyclohexene, which is 1.29 kcal mol^{-1} for the Co complex, 2.99 kcal mol^{-1} for the Rh complex and 6.45 kcal mol^{-1} for the Ir complex. The order in the activation barrier for [3+2] addition with respect to changing metal is Ir > Rh > Co for each of the olefins studied.

3. The dinitrosoalkanes formed have also been found to be very stable thermodynamically. The highest exothermicity is 42.09 kcal mol^{-1} obtained for the reaction of $CpCo(NO)_2$ with 2-norbonene and the lowest is 22.05 kcal mol^{-1} obtained for the reaction of $CpRh(NO)_2$ with trans-1-phenylpropene. The order in thermodynamic stability of the dinitrosoalkane complexes of Co, Rh and Ir with respect to changing olefins has been found to be: norbonene > ethylene ≈ cyclopentene > 2,3-dimethyl-2-butene > cyclohexene > trans-1-phenylpropene while the order in thermodynamic stability with respect to changing metal is Co > Ir > Rh for each of the olefins studied.

4. The activation barriers for the [2+2] addition of the olefinic bonds across the M-N bonds to form an intermediate are generally very high; the lowest barrier is 29.86 kcal mol^{-1}

found for the reaction of $CpRh(NO)_2$ with cyclopentene. The order of the activation barriers for this step with respect to changing olefins for the Co complex has been found to be: cyclohexene > trans-1-phenylpropene > 2,3-dimethyl-2-butene > ethylene ≈ cyclopentene ≈ norbonene. The corresponding order for the Rh and Ir complexes have been found to be: cyclohexene > trans-1-phenylpropene > 2,3-dimethyl-2-butene > norbonene > ethylene ≈ cyclopentene, and trans-1-phenylpropene > cyclohexene > cyclopentene ≈ 2,3-dimethyl-2-butene > norbonene > ethylene respectively. The intermediates formed are generally either slightly exothermic (highest exothermicity being 2.98 $kcalmol^{-1}$) or endothermic (highest endothermicity being 12.04 $kcalmol^{-1}$).

5. An attempt to locate a transition state for the re-arrangement of the products of [2+2] addition to the products corresponding to [3+2] addition was unsuccessful in each of the complexes with each of the olefins, indicating that the re-arrangement of the product of [2+2] addition by reductive elimination involving the second metal-nitrogen π-bond to form the observed 1,2-dinitrosoalkane may not be possible.

6. Since the activation barriers for the one-step [3+2] pathway are generally very low, and those for the [2+2] addition pathway leading to the intermediates are generally very high, coupled with the fact that no transition state has been located for the re-arrangement of the products of the latter pathway to those of the former pathway, it is very unlikely that 1,2-dinitrosoalkanes can be formed by the stepwise pathway

proposed by Upton and Rappé (1985). Therefore the direct one-step [3+2] pathway proposed by Becker and Bergman (1983) is the most plausible pathway for the formation of 1,2-dinitrosoalkanes.

REFERENCES

Becker, P. N.; White, M.A.; Bergman, R. G. (1980) A new method for 1,2-diamination of alkenes using cyclopentadienylnitrosylcobalt dimer/NO/LiAlH4. *J. Am. Chem. Soc.* 102: 5676 – 5677.

Becker, P.N.; Bergman, R. G.(1983) Reversible exchange of (η^5-cyclopentadienyl) (dinitrosoalkane)cobalt complexes with alkenes. Kinetic and spectroscopic evidence for cyclopentadienyldinitrosylcobalt as a reactive intermediate. *J. Am. Chem. Soc*. 105, 2985-2995.

Biellman, J.; Hemmer, H.; Lavisalles, J. (1970) The Chemistry of alkenes. Zabicky, J. (Ed.) Interscience; New York; Pp. 215 - 265.

Brunner, H. (1968) Über nitrosyl-metall-komplexe III. Cyclopentadienylnitrosylkobalt. *J. Organomet. Chem*. 12: 517-522.

Brunner, H.; Loskot, S. (1971) Incorporation of Olefin and Nitric Oxide into Organocobalt compounds. *Angew. Chem., Int. Ed. Engl*. 10: 515 – 516.

Brunner, H.; Loskot, S. (1973) Über nitrosyl-metall-komplexe: XV. Die reaktion von organokobalt-verbindungen mit no und olefinen - eine neue

dreikomponentensynthese. *J. Organomet. Chem*. 61: 401 – 414.

Casey, C. P. (1983) The structure of intermediates formed in the reaction of osmium tetroxide with 1,1-diphenylethylene. *J. Chem. Soc., Chem. Commun.* 126.

Clark, M.; Cramer, R. D.; Opdenbosch, N. V. (1989) Validation of the general purpose tripos 5.2 force field. *J. Comp. Chem*. 10: 982 – 1012.

Dunning, T. H., Jnr.; Hay, P. J. (1976) In: Modern Theoretical Chemistry, H. F. Schaefer, III,; Plenum, New York, Vol. 3.

Garcia, A.; Cruz, E. M.; Sarasola, C.; Ugalde, J. M. (1997) Density functional studies of the bπ. aσ charge-transfer complex formed between ethyne and chlorine monofluoride. *J. Phys. Chem. A* 101: 3021 – 3024.

Hay, P. J.; Wadt, W, R. (1985) *Ab initio* effective core potentials for molecular calculations. Potentials for the transition metal atoms Sc to Hg. *J. Chem. Phys*. 82: 270.

Hay, P. J.; Wadt, W, R. (1985) *Ab initio* effective core potentials for molecular calculations. Potentials for K to Au including the outermost core orbitals. *J. Chem. Phys*. 82: 299.

Kristyán, S.; Pulay, P. (1994) Can (semi)local density functional theory account for the London dispersion forces? *Chem. Phys. Lett*. 229: 175 – 180.

Le Gall, T.; Mioskowski, C.; Lucet, D. (1998) The Chemistry of vicinal diamines. *Angew. Chem., Int. Ed.* 37: 2580 – 2627.

Michalson, E. T.; Szuszkovicz, J. (1989) *Prog. Drug. Res.* 33, 135.

Mourik, T. V. (2008) assessment of density functionals for intramolecular dispersion-rich interactions. *J. Chem. Theory Comput*. 41610 – 1619.

Mourik, T. V.; Gdanitz, R. J. (2002) A critical note on density functional theory studies on rare-gas dimers. *J. Chem. Phys.* 116, 9620 – 9623.

Norton, J. R. (1979) Organometallic elimination mechanisms: studies on osmium alkyls and hydrides. *Acc. Chem. Res*. 12, 139 – 145.

Peréz-Jordá, J. M.; Becke, A. D. (1995) A density functional study of van der Waals forces: rare gas diatomics. *Chem. Phys. Lett.* 233, 134.

Philipp, D. M.; Muller, R. P.; Goddard, W. A., III; Storer, J.; McAdon, Mullins, M. (2002) Computational Insights on the Challenges for Polymerizing Polar Monomers. *J. Am. Chem. Soc.* 124: 10198 – 10210.

Ruiz, E.; Salahub, D. R.; Vela, A. (1996) Charge-transfer complexes: Stringent tests for widely used density functionals. *J. Phys. Chem.* 100: 12265 – 12276.

Schomaker, J. M.; Boyd, W.C.; Stewart, I. C.; Toste, F. D.; Bergman, R. G. (2008) Cobalt Dinitrosoalkane Complexes in the

C−H Functionalization of Olefins. *J. Am. Chem. Soc.* 130: 3777 - 3779.

Schomaker, J. M.; Toste, F.D.; Bergman, R. G. (2009) Cobalt-mediated [3 + 2]-annulation reaction of alkenes with α,β-unsaturated ketones and imines. *Org. Lett.* 11: 3698 – 3700.

Schroder, M. (1980) Osmium tetroxide cis hydroxylation of unsaturated substrates. *Chem. Rev*. 80: 187 – 213.

Schröder, M.; Constable, E. C. J. (1982) Direct spectroscopic evidence for the formation of an asymmetric intermediate in the oxidation of alkenes by osmium tetraoxide. *J. Chem. Soc., Chem. Commun*. 734 - 736.

Spartan, Wavefunction, Inc.; 18401 Von Karman Ave., # 370, Irvine, CA, 92715, USA.

Upton, T. H.; Rappė, A. K. (1984) Activation of single-bond cleavage processes on metal surfaces: a comparison of dissociative hydrogen adsorption with simple gas-phase exchange reactions. *J. Am. Chem. Soc.* 106: 1561 – 1571.

Upton, T. H.; Rappė, A. K. (1985) A theoretical basis for low barriers in transition-metal complex 2π + 2π reactions: the isomerization of the dicyclopentadienyltitanium complex $Cp_2TiC_3H_6$ to $Cp_2TiCH_2(C_2H_4)$. *J. Am. Chem. Soc.* 107: 1206 – 1218.

Wadt, W. R.; Hay, P. J. Hay (1985) *Ab initio* effective core potentials for molecular calculations. Potentials for main group elements Na to Bi. *J. Chem. Phys*. 82, 284.

Wright, T. C. (1996) Geometric structure of Ar·NO+: revisited. A failure of density functional theory. *J. Chem. Phys.* 105: 7579.

CHAPTER FIVE

CONCLUDING REMARKS

The mechanistic pathways of three organometallic reactions have been studied using hybrid density functional theory (DFT). The hybrid density functional theory

method was chosen for use throughout the work based on the dual criteria of efficiency and accuracy. Although DFT calculations may underestimate weak interactions such as van der Waals interactions, they generally give better and more reliable descriptions of the geometries and relative energies for transition metal systems than either Hartree-Fock or MP2 methods (Ziegler, 1991; Parr and Yang, 1989; Koch and Holthuasen, 2001; Dedieu, 1991; Torrent *et. al*., 2001; Niu and Hall, 2000; Frenking and Frölich, 2000). Hybrid and gradient-corrected DFT methods often outperform MP2 while using less computer time. There are also no difficulties for DFT with the calculation of compounds of the first transition metal row.

The studies presented here illustrate the general approach usually taken in a theoretical investigation. Using the experimental findings, possible reaction pathways are proposed and a reasonable computational method chosen for the studies. By determining the structures and energies of reactants, intermediates, transition states, and products, the reaction path is elucidated. By changing the transition metal, the ligands, and their substituents and by examining the electronic structures of the reaction system, the factors that contribute to the chemical reactivity and selectivity are explored. Through this process, an 'understanding' of the underlying chemistry can be reached, and the rules on which the rational design of new catalysts should be based are created. The work has demonstrated that not only do quantum chemical studies unveil detailed structural information on postulated intermediates, but they also provide insight otherwise unavailable into reaction mechanisms. Using the computed reaction energy and activation energy of each elementary step, different proposed mechanisms for some organometallic reactions have been verified while some new reaction pathways have been proposed.

In the study of the oxidation of ethylene by chromyl chloride, the mechanism of epoxide precursor formation which has been the subject of prolonged controversy (Criegee, 1936; Criegee *et. al*., 1942; Corey *et. al*., 1989; Corey *et. al*., 1993; Schröder, 1980; Jorgensen and Hoffmann, 1986; Wu *et. al*., 1992; Gable and Phan, 1994; Hentges and Sharpless, 1980; Nortey *et. al*., 1994; Nortey *et. al*., 1996; Wallis and Kochi, 1988a; 1988b; Göbel and Sharpless, 1993; Pidun *et. al*., 1996; Dapprich *et. al*., 1996; Torrent *et. al*., 1998; Del Monte *et. al*., 1997; Torrent *et. al*., 1999; 1999; Limberg *et. al*., 1998; Limberg and Köppe, 1999), has been rationalized in favor of the [2+2] mechanism through a chromaoxetane intermediate. In addition, a new pathway involving initial [3+2] ethylene addition across the Cr=O and Cr-Cl bonds has been explored and found to be more feasible than the pathway involving initial [3+2] ethylene addition across the two Cr=O bonds of CrO_2Cl_2 which had earlier been put up as the most plausible reaction pathway. The formation of the 1,2-dichloroethane precursor was found to take place via initial [3+2] addition of ethylene across the two Cr-Cl bonds of CrO_2Cl_2 while the 1,2-chlorohydrin precursor was found to originate from initial [3+2] ethylene addition across the Cr-O and Cr-Cl bonds of CrO_2Cl_2. Also the formation of vinyl alcohol and acetaldehyde precursors from chromyl chloride and ethylene, which had not been explored in earlier studies, were found to proceed by a direct attack of one of the carbon atoms of ethylene on an oxygen atom of CrO_2Cl_2 through a triplet intermediate.

Future determination of the activation barriers for the formation of the acetaldehyde and vinyl alcohol precursors would fill in the gap in the knowledge of the kinetics of formation of these species in the present study of the oxidation of ethylene by chromyl chloride. Also since the five-membered ring ester complex intermediate formed from [3+2] addition of ethylene

across the two Cr=O bonds of CrO_2Cl_2 (**A3**) and the epoxide precursor (**A5**) both appear to be very stable according to the present study and those of others (Torrent *et. al*, 1999), they might well be isolated experimentally if sought for.

In the reactions of Cl_4MCH_2(M=Cr, Mo, W, Ru, Re) with ethylene it was found that the formation of the metallacyclobutane through formal [2+2] cycloaddition, a key step in the olefin metathesis reaction according to the Herrison-Chauvin mechanism, is a low-barrier process in each of the complexes studied. It was also found that the active species for the formation of the metallacyclobutane is a carbene complex and not a carbenoid complex. One key factor was found to be responsible for the difference in metathesis activity in these complexes: the stability of the carbenoid complexes relative to the carbenes. In Cr and Ru, the carbenoid complexes are more stable than the carbenes and thus Cl_4CrCH_2 and Cl_4RuCH_2 are likely to exist in the lower-energy carbenoid Cl_3MCH_2Cl form as opposed to the carbene $Cl_4M{=}CH_2$ form. This is likely to deplete the reaction surface of the active species of the process, making Cl_4MCH_2(M=Cr, Ru) not suitable for olefin metathesis. This suggests that whereas Cl_4MCH_2 (M = Mo, W, Re) may catalyze olefin metathesis, Cl_4MCH_2 (M = Cr, Ru) may not. The W and Re complexes have been found to have greater metathesis activity than the Mo complex.

In the $Cl_2(O)MCH_2$ (M=Mo, W, Re) complexes the metathesis reaction has favorable energetics and is found to be more feasible than the side reactions studied, namely the [2+2] ethylene addition across the M-O bond, [3+2] ethylene addition across the M-O and M-C bonds and the [3+2] ethylene addition across the M-O and M-Cl bonds, while in the $Cl_2(O)MCH_2$(M=Cr, Ru) complexes the olefin metathesis is found to be less favorable than the side reactions. Thus the $Cl_2(O)MCH_2$(M=Mo, W, Re) complexes are

expected to undergo olefin metathesis while the $Cl_2(O)MCH_2$(M = Cr, Ru) complexes may not. However, in the $Cl_2(O)CrCH_2$ complex the metathesis reaction could be competitive with the side reactions and thus metathesis may occur to some extent. The W carbene complexes have been found to be the best complexes for olefin metathesis reactions as these complexes have the lowest barriers among the Mo, W, and Re complexes and the most unambiguous preference for the metathesis pathway over the side reactions.

Even though the Cl_4MCH_2(Cr, Mo, W, Ru, Re) complexes were found to display triplet ground state electronic structures in addition to the singlet structures, the reaction mechanisms can be satisfactorily rationalized solely on the singlet potential energy surface. The Cl_4ReCH_2 and $Cl_2(O)ReCH_2$ complexes were found to display predominantly doublet ground state electronic structures.

It is recommended that future theoretical work in this area should investigate solvent effects by incorporating a relevant solvent field model in the calculations, since the presence of elongation of the M-Cl bonds seem to indicate the importance of solvent effects on the course of the reaction. Also work with substituted alkenes could be initiated to explore the influence of steric hindrances on the energetics of the reactions of the various metals.

In the transition-metal-assisted formation of 1,2-dinitrosoalkanes, it was found that the activation barriers for the one-step [3+2] addition pathway for the formation 1,2-dinitrosoalkanes are generally very low while the activation barriers for the [2+2] addition of the C=C bond of the olefins across the M-N bonds of $CpM(NO)_2$ (M=Co, Rh, Ir) to form an intermediate are generally very high. A transition state for the re-arrangement of the products of [2+2] addition to the products of

[3+2] addition could not be located, indicating that the re-arrangement of the products of [2+2] addition by reductive elimination involving the second metal-nitrogen π-bond to form the observed 1,2-dintrosoalkanes as suggested in the work of Rappé and Upton (Upton and Rappé, 1984; 1985) may not be possible. Therefore it is concluded that the direct one-step [3+2] addition pathway proposed by Becker and Bergman (1983) for the formation of 1,2-dinitrosoalkanes is a more plausible pathway.

It is recommended that future work in this area could focus on a systematic study of the effect of the nature of the olefin (electron-withdrawing and electron-donating) on the energetics of the reaction to help explore how it might influence the overall mechanisms of the reactions involving the various metals.

REFERENCES

Becker, P. N.; White, M.A.; Bergman, R. G. (1980) A new method for 1,2-diamination of alkenes using cyclopentadienylnitrosylcobalt dimer/NO/LiAlH4. *J. Am. Chem. Soc.* 102: 5676-5677.

Becker, P.N.; Bergman, R. G.(1983) Reversible exchange of (η^5-cyclopentadienyl) (dinitrosoalkane)cobalt complexes with alkenes. Kinetic and spectroscopic evidence for cyclopentadienyldinitrosylcobalt as a reactive intermediate. *J. Am. Chem. Soc*. 105: 2985 – 2995.

Corey, E. J.; Jardine, P. D.; Virgils, S.; Yuen, P.-W.; Connell, R. D. (1989) Enantioselective vicinal hydroxylation of terminal and E-1,2-disubstituted olefins by a chiral complex of osmium tetraoxide. An effective controller system and a rational mechanistic model. *J. Am. Chem. Soc.* 111: 9243 – 9244.

Corey, E. J.; Noe, M. C.; Sarshar, S. (1993) The origin of high enantioselectivity in the dihydroxylation of olefins using osmium

tetraoxide and cinchona alkaloid catalysts. *J. Am. Chem. Soc*. 115, 3828-3829.

Criegee, R. (1936) Osmiumsäure-ester als Zwischenprodukte bei Oxydationen. *Justus Liebigs Ann. Chem.* 522: 75 – 96.

Criegee, R.; Marchaand, B.; Wannowius, H. (1942) *1942)* Zur Kenntnis der organischen Osmium-Verbindungen. II. Mitteilung. *Justus Liebigs Ann. Chem*. 550: 99 – 133.

Dapprich, S.; Ujaque, G.; Maseras, F.; Lledós, A.; Musaev, D. G.; Morokuma, K. (1996) Theory does not support an osmaoxetane intermediate in the osmium-catalyzed dihydroxylation of olefins. *J. Am. Chem. Soc.*118: 11660 – 11661.

Dedieu, A. (2000) Theoretical studies in palladium and platinum molecular chemistry. *Chem. Rev.* 100, 543-600

Del Monte, A. J.; Haller, J.; Houk, K. N.; Sharpless, K. B.; Singleton, D. A.; Strassner, T.;

Thomas, A. A. (1997) Experimental and theoretical kinetic isotope effects for asymmetric dihydroxylation. Evidence supporting a rate-limiting "(3 + 2)" cycloaddition. *J. Am. Chem. Soc.* 119: 9907 – 9908.

Frenking, G.; Frölich, N. (2000) The nature of the bonding in transition-metal compounds. *Chem. Rev.* 100: 717 – 774.

Gable, K. P.; Phan, T. N. (1994) Extrusion of alkenes from rhenium (v) diolates: Energetics and mechanism. *J. Am. Chem. Soc*. 116: 833 – 839.

Göbel, T.; Sharpless, K. B. (1993) Temperature effects in asymmetric dihydroxylation: evidence for a stepwise mechanism. *Angew. Chem.; Int. Ed. Engl*. 32: 1329 – 1331.

Hentges, S. G.; Sharpless, K. B. (1980) Asymmetric induction in the reaction of osmium tetroxide with olefins. *J. Am. Chem. Soc*. 102, 4263-4265.

Jorgensen, K. A.; Hoffmann, R. W. (1986) Binding of alkenes to the ligands in OsO_2X_2 (X = O and NR) and $CpCo(NO)_2$. A frontier orbital study of the formation of intermediates in the transition-metal-catalyzed synthesis of diols, amino alcohols, and diamines. *J. Am. Chem. Soc.* 108, 1867-1876.

Koch, W.; Holthuasen, M. C. (2001) A Chemist's Guide to Density Functional Theory, 2nd Ed., Wiley-VCH, Weinheim.

Limberg, C.; Köppe, R. (1999) Reactive intermediates in olefin oxidations with chromyl chloride. IR-Spectroscopic proof for $O{=}CrCl_2{-}$epoxide complexes. *Inorg. Chem*. 38: 2106 – 2116.

Limberg, C.; Köppe, R.; Schnöckel, H. (1998) Matrix isolation and characterization of a reactive intermediate in the olefin oxidation with chromyl chloride. *Angew. Chem. Int. Ed*. 37: 496.

Niu, S.; Hall, M. B. (2000) Theoretical studies of transition-metal complexes. *Chem. Rev*. 100: 353-405

Nortey, P. O. Becker, H.; Sharpless, K. B. (1996) Toward an understanding of the high enantioselectivity in the osmium-catalyzed asymmetric dihydroxylation. 3. New insights into isomeric forms of the putative osmaoxetane intermediate. *J. Am. Chem. Soc.* 118: 35 – 42.

Nortey, P. O.; Kolb, H. C.; Sharpless, K. B. (1994) Calculations on the reaction of ruthenium tetroxide with olefins using density functional theory (DFT). Implications for the possibility of intermediates in osmium-catalyzed asymmetric dihydroxylation. *Organometallics* 13: 344 – 347.

Par, R. G.; Yang, W. (1989) Density Functional Theory of Atoms and Molecules; Oxford University Press, Oxford.

Pidun, U.; Boeheme, C..; Frenking, G. (1996) Theory rules out a [2 + 2] addition of osmium tetroxide to olefins as initial step of the dihydroxylation reaction. *Angew. Chem.; Int. Ed. Engl*. 35: 2817 – 2820.

Schröder, M. (1980) Osmium tetraoxide cis-hydroxylation of unsaturated substrates. *Chem. Rev*. 80: 187 – 213.

Torrent, M.; Deng, L.; Duran, M.; Solá, M.; Ziegler, T. (1997) Density functional study of the [2+2]- and [2+3]-cycloaddition mechanisms for the osmium-catalyzed dihydroxylation of olefins. *Organometallics* 16: 13 – 19.

Torrent, M.; Deng, L.; Duran, M.; Solá, M.; Ziegler, T. (1999) Mechanisms for the formation of epoxide and chlorine-containing products in the oxidation of ethylene by chromyl chloride: A density functional study. *Can. J. Chem.* 77: 1476 – 1491.

Torrent, M.; Deng, L.; Ziegler, T. (1998) A Density functional study of [2+3] versus [2+2] addition of ethylene to chromium-oxygen bonds in chromyl chloride. *Inorg. Chem.* 37: 1307 -1314.

Torrent, M.; Solá, M.; Frenking, G. (2000) Theoretical studies of some transition-metal-mediated reactions of industrial and synthetic importance. *Chem. Rev*. 100: 439 – 494.

Upton, T. H.; Rappė, A. K. (1984) Activation of single-bond cleavage processes on metal surfaces: A comparison of dissociative hydrogen adsorption with simple gas-phase exchange reactions. *J. Am. Chem. Soc.* 106: 1561 – 1571.

Upton, T. H.; Rappė, A. K. (1985) A theoretical basis for low barriers in transition-metal complex 2π + 2π reactions: the isomerization of the dicyclopentadienyltitanium complex $Cp_2TiC_3H_6$ to $Cp_2TiCH_2(C_2H_4)$. *J. Am. Chem. Soc.* 107: 1206 – 1218.

Wallis, J. M.; Kochi, J. K. (1988) Direct osmylation of benzenoid hydrocarbons. Charge-transfer photochemistry of osmium tetraoxide. *J. Org. Chem.* 53: 1679 – 1686.

Wallis, J. M.; Kochi, J. K. (1988) Electron-transfer activation in the thermal and photochemical osmylations of aromatic electron donor-acceptor complexes with osmium (VIII) tetroxide. *J. Am. Chem. Soc.* 110: 8207 – 8223.

Wu, Y.-D.; Wang, Y.; Houk, K. N. (1982) A new model for the stereoselectivities of dihydroxylations of alkenes by chiral diamine complexes of osmium tetroxide. *J. Org. Chem.* 57: 1362 – 1369.

Ziegler, T. (1991) Approximate density functional theory as practical tool in molecular energetics and dynamics. *Chem. Rev*. 91, 651 – 667.

APPENDIX

The optimized geometries in Cartesian and internal coordinates(in Å), absolute energies (in hartrees) and symmetry point groups of some of the structures reported in the thesis. The structure labels correspond to those in the respective chapters.

Chapter Two

A1

Coordinates (Angstroms)

ATOM	X	Y	Z
1 Cr	0.000000	0.000000	0.351958
2 Cl	-1.745057	0.000000	-0.841337
3 Cl	1.745057	0.000000	-0.841337
4 O	0.000000	1.262265	1.259904
5 O	0.000000	-1.262265	1.259904

Distance Matrix (Angstroms)

	Cr(1)	Cl(2)	Cl(3)	O (4)
Cl(2)	2.114042			
Cl(3)	2.114042	3.490114		
O (4)	1.554889	3.008945	3.008945	
O (5)	1.554889	3.008945	3.008945	2.524529

Point Group: C_{2v} Number of degrees of freedom: 4

Energy = -1157.200739279

A1/t Coordinates (Angstroms)

ATOM	X	Y	Z
1 Cr	0.000000	0.000000	0.296071
2 Cl	-1.757457	0.000000	-0.877973
3 Cl	1.757457	0.000000	-0.877973
4 O	0.000000	1.191371	1.421585
5 O	0.000000	-1.191371	1.421585

Distance Matrix (Angstroms)

	Cr(1)	Cl(2)	Cl(3)	O (4)
Cl(2)	2.113536			
Cl(3)	2.113536	3.514915		
O (4)	1.638947	3.129854	3.129854	
O (5)	1.638947	3.129854	3.129854	2.382741

Point Group: C_{2v} Number of degrees of freedom: 4

Energy = -1157.140140978

Ethylene

Coordinates (Angstroms)

ATOM	X	Y	Z
1 H	1.240641	-0.922990	0.000000
2 C	0.665417	0.000000	0.000000
3 C	-0.665417	0.000000	0.000000
4 H	1.240641	0.922990	0.000000
5 H	-1.240641	-0.922990	0.000000
6 H	-1.240641	0.922990	0.000000

Distance Matrix (Angstroms)

	H (1)	C (2)	C (3)	H (4)	H (5)
C (2)	1.087562				
C (3)	2.117774	1.330835			
H (4)	1.845980	1.087562	2.117774		
H (5)	2.481281	2.117774	1.087562	3.092636	
H (6)	3.092636	2.117774	1.087562	2.481281	1.845980

Point Group: D_{2h} Number of degrees of freedom: 3

Energy = -78.587447729

A2

Coordinates (Angstroms)

ATOM	X	Y	Z
1 Cr	0.049360	0.103618	-0.299545
2 O	-0.041653	-0.079819	-1.831678
3 Cl	0.930600	-1.832930	0.304647
4 Cl	1.608534	1.398700	0.455691
5 O	-1.311416	1.216655	0.028853
6 C	-1.644055	-0.865348	0.533703
7 H	-1.912097	-1.664766	-0.152709
8 H	-1.338221	-1.217467	1.515181
9 C	-2.404013	0.435287	0.485408
10 H	-3.220618	0.465692	-0.246667
11 H	-2.766032	0.797298	1.455467

Distance Matrix (Angstroms)

	Cr(1)	O (2)	Cl(3)	Cl(4)	O (5)	C (6)
O (2)	1.545756					
Cl(3)	2.211753	2.929600				
Cl(4)	2.163017	3.184524	3.305426			
O (5)	1.788409	2.598983	3.795084	2.956593		
C (6)	2.121521	2.963068	2.759987	3.963753	2.168008	
H (7)	2.645006	2.971456	2.884160	4.706359	2.948961	1.087234
H (8)	2.638916	3.765208	2.644189	4.080467	2.852164	1.086656
C (9)	2.597151	3.348875	4.036970	4.126692	1.418713	1.507156
H (10)	3.290387	3.593836	4.777051	4.968352	2.070002	2.205945
H (11)	3.389350	4.358543	4.680553	4.527479	2.080143	2.207458

	H (7)	H (8)	C (9)	H (10)
H (8)	1.819689			
C (9)	2.249311	2.219896		
H (10)	2.501981	3.079050	1.097133	
H (11)	3.062220	2.470119	1.096869	1.792726

Point Group: C_1 Number of degrees of freedom: 27

Energy = -1235.771797141

A3

Coordinates (Angstroms)

ATOM	X	Y	Z
1 Cr	0.000000	0.000000	0.300818
2 Cl	0.096773	1.852576	1.347977
3 Cl	-0.096773	-1.852576	1.347977
4 O	1.220014	-0.095249	-0.946703
5 O	-1.220014	0.095249	-0.946703
6 C	0.687372	-0.337170	-2.255409
7 H	0.593404	-1.419489	-2.412168
8 H	1.383047	0.076235	-2.993126
9 C	-0.687372	0.337170	-2.255409
10 H	-0.593404	1.419489	-2.412168
11 H	-1.383047	-0.076235	-2.993126

Distance Matrix (Angstroms)

	Cr(1)	Cl(2)	Cl(3)	O (4)	O (5)	C (6)
Cl(2)	2.130245					
Cl(3)	2.130245	3.710203				
O (4)	1.747518	3.212670	3.176111			
O (5)	1.747518	3.176111	3.212670	2.447453		
C (6)	2.668420	4.257721	3.986945	1.433508	2.353257	
H (7)	3.118874	5.009165	3.847414	2.072157	2.780379	1.097642
H (8)	3.573332	4.863647	4.975474	2.060056	3.311213	1.095031
C (9)	2.668420	3.986945	4.257721	2.353257	1.433508	1.531226
H (10)	3.118874	3.847414	5.009165	2.780379	2.072157	2.179636
H (11)	3.573332	4.975474	4.863647	3.311213	2.060056	2.213356

	H (7)	H (8)	C (9)	H (10)
H (8)	1.788362			
C (9)	2.179636	2.213356		
H (10)	3.077063	2.459310	1.097642	
H (11)	2.459310	2.770293	1.095031	1.788362

Point Group: C_2 Number of degrees of freedom: 14

Energy = -1235.827133229

A3/os Coordinates (Angstroms)

ATOM	X	Y	Z
1 Cr	0.000000	0.000000	0.300506
2 Cl	0.097168	1.852555	1.347665
3 Cl	-0.097168	-1.852555	1.347665
4 O	1.219994	-0.095510	-0.947016
5 O	-1.219994	0.095510	-0.947016
6 C	0.687300	-0.337317	-2.255722
7 H	0.593102	-1.419616	-2.412480
8 H	1.383063	0.075940	-2.993438
9 C	-0.687300	0.337317	-2.255722
10 H	-0.593102	1.419616	-2.412480
11 H	-1.383063	-0.075940	-2.993438

Distance Matrix (Angstroms)

	Cr(1)	Cl(2)	Cl(3)	O (4)	O (5)	C (6)

Cl(2) 2.130245
Cl(3) 2.130245 3.710203
O (4) 1.747518 3.212670 3.176111
O (5) 1.747518 3.176111 3.212670 2.447453
C (6) 2.668420 4.257721 3.986945 1.433508 2.353257
H (7) 3.118874 5.009165 3.847414 2.072157 2.780379 1.097642
H (8) 3.573332 4.863647 4.975475 2.060056 3.311213 1.095031
C (9) 2.668420 3.986945 4.257721 2.353257 1.433508 1.531226
H (10) 3.118874 3.847414 5.009165 2.780379 2.072157 2.179636
H (11) 3.573332 4.975475 4.863647 3.311213 2.060056 2.213356
H (7) H (8) C (9) H (10)
H (8) 1.788362
C (9) 2.179636 2.213356
H (10) 3.077063 2.459310 1.097642
H (11) 2.459310 2.770293 1.095031 1.78836
Point Group: C_2 Number of degrees of freedom: 14
Energy = -1235.827132954

A3/t

Coordinates (Angstroms)

ATOM	X	Y	Z
1 Cr	0.000000	0.000000	0.268890
2 Cl	0.054141	1.819414	1.397822
3 Cl	-0.054141	-1.819414	1.397822
4 O	1.240984	0.015238	-0.975191
5 O	-1.240984	-0.015238	-0.975191
6 C	0.716532	-0.263171	-2.285278
7 H	0.747984	-1.347317	-2.453343
8 H	1.358712	0.230603	-3.023115
9 C	-0.716532	0.263171	-2.285278
10 H	-0.747984	1.347317	-2.453343
11 H	-1.358712	-0.230603	-3.023115

Distance Matrix (Angstroms)
Cr(1) Cl(2) Cl(3) O (4) O (5) C (6)
Cl(2) 2.141889
Cl(3) 2.141889 3.640440
O (4) 1.757274 3.208557 3.267184
O (5) 1.757274 3.267184 3.208557 2.482154
C (6) 2.665793 4.282656 4.071984 1.438363 2.368473
H (7) 3.128145 5.033992 3.962038 2.069912 2.813424 1.097546
H (8) 3.568833 4.875541 5.073796 2.062579 3.318561 1.095724
C (9) 2.665793 4.071984 4.282656 2.368473 1.438363 1.526665
H (10) 3.128145 3.962038 5.033992 2.813424 2.069912 2.183282
H (11) 3.568833 5.073796 4.875541 3.318561 2.062579 2.202748
H (7) H (8) C (9) H (10)
H (8) 1.785346
C (9) 2.183282 2.202748
H (10) 3.082039 2.451501 1.097546
H (11) 2.451501 2.756284 1.095724 1.785346
Point Group: C_2 Number of degrees of freedom: 14
Energy = -1235.867667657

A4

Coordinates (Angstroms)

ATOM	X	Y	Z
1 Cr	0.593993	-0.235656	0.440817
2 Cl	-1.084087	1.387972	-0.082101
3 O	-0.575415	-1.458106	-0.155153
4 C	-2.423842	0.101561	-0.152279
5 H	-3.233741	0.542912	-0.734309
6 H	-2.716065	-0.049250	0.887299
7 C	-1.797823	-1.133881	-0.778339
8 H	-2.501455	-1.969759	-0.649588
9 H	-1.650735	-0.975080	-1.856324
10 O	0.758699	-0.130227	1.975131
11 Cl	2.247236	0.196678	-0.933263

Point Group: C_1 Number of degrees of freedom: 27
Energy is -1235.816816313

Distance Matrix (Angstroms)
Cr(1) Cl(2) O (3) C (4) H (5) H (6)
Cl(2) 2.392815
O (3) 1.793622 2.892101
C (4) 3.093994 1.858688 2.418522
H (5) 4.079048 2.400107 3.377306 1.090636
H (6) 3.345232 2.380902 2.766581 1.090349 1.802291
C (7) 2.830889 2.711809 1.409881 1.519924 2.208038 2.189508
H (8) 3.711858 3.688540 2.053262 2.131597 2.618575 2.469096
H (9) 3.295816 3.008815 2.069689 2.158847 2.463559 3.085378
O (10) 1.546727 3.151665 2.842752 3.835122 4.871731 3.641967
Cl(11) 2.192765 3.638870 3.363202 4.736871 5.495505 5.292380
C (7) H (8) H (9) O (10)
H (8) 1.100167
H (9) 1.099502 1.780259
O (10) 3.889053 4.571831 4.604259
Cl(11) 4.261091 5.227235 4.173636 3.283499

A5

Coordinates (Angstroms)

ATOM	X	Y	Z
1 Cr	-0.621879	-0.399052	0.000000
2 O	1.361138	-0.575528	0.000000
3 C	2.383683	0.155060	-0.736565
4 H	2.006016	1.019447	-1.273031
5 H	3.052681	-0.504350	-1.281890
6 C	2.383683	0.155060	0.736565
7 H	3.052681	-0.504350	1.281890
8 H	2.006016	1.019447	1.273031
9 O	-1.021843	-1.882858	0.000000
10 Cl	-0.777839	0.775109	1.855263
11 Cl	-0.777839	0.775109	-1.855263

Distance Matrix (Angstroms)
Cr(1) O (2) C (3) H (4) H (5) C (6)
O (2) 1.990854
C (3) 3.143719 1.456669
H (4) 3.246318 2.140192 1.085169
H (5) 3.893164 2.123588 1.086168 1.848660
C (6) 3.143719 1.456669 1.473130 2.219971 2.226329
H (7) 3.893164 2.123588 2.226329 3.153583 2.563780 1.086168
H (8) 3.246318 2.140192 2.219971 2.546063 3.153583 1.085169
O (9) 1.536767 2.718035 4.036489 4.383140 4.488349 4.036489
Cl(10) 2.201131 3.137108 4.134882 4.194732 5.113867 3.410449
Cl(11) 2.201131 3.137108 3.410449 2.854566 4.079051 4.134882
H (7) H (8) O (9) Cl(10)
H (8) 1.848660
O (9) 4.488349 4.383140
Cl(10) 4.079051 2.854566 3.250589
Cl(11) 5.113867 4.194732 3.250589 3.710527
Point Group: Cs Number of degrees of freedom: 15
Energy = -1235.805203098

A5/t

Coordinates (Angstroms)

ATOM	X	Y	Z
1 Cr	-0.584477	-0.420107	0.000000
2 O	1.428248	-0.652212	0.000000
3 C	2.448678	0.098098	-0.734202
4 H	2.052192	0.951940	-1.274531
5 H	3.127049	-0.553446	-1.277227
6 C	2.448678	0.098098	0.734202
7 H	3.127049	-0.553446	1.277227
8 H	2.052192	0.951940	1.274531
9 O	-1.372712	-1.757748	0.000000
10 Cl	-0.769396	0.805532	1.824023
11 Cl	-0.769396	0.805532	-1.824023

Distance Matrix (Angstroms)
Cr(1) O (2) C (3) H (4) H (5) C (6)
O (2) 2.026064
C (3) 3.163482 1.464000
H (4) 3.234032 2.141737 1.085451
H (5) 3.927405 2.127672 1.086082 1.849733
C (6) 3.163482 1.464000 1.468403 2.218390 2.220482
H (7) 3.927405 2.127672 2.220482 3.151662 2.554453 1.086082
H (8) 3.234032 2.141737 2.218390 2.549062 3.151662 1.085451
O (9) 1.552610 3.011243 4.311176 4.549374 4.830062 4.311176
Cl(10) 2.205322 3.206511 4.171448 4.193308 5.162059 3.470471
Cl(11) 2.205322 3.206511 3.470471 2.878321 4.162702 4.171448
H (7) H (8) O (9) Cl(10)
H (8) 1.849733
O (9) 4.830062 4.549374
Cl(10) 4.162702 2.878321 3.203350
Cl(11) 5.162059 4.193308 3.203350 3.648046
Point Group: C_s Number of degrees of freedom: 15
Energy = -1235.836287730

C1/t

Coordinates (Angstroms)

ATOM	X	Y	Z
1 Cr	-0.207678	0.005000	-0.175577
2 O	0.113120	0.009478	-1.691669
3 Cl	-1.477549	1.697624	0.229647
4 Cl	-1.475245	-1.691808	0.219680
5 O	1.083603	0.002606	0.949924
6 C	3.054433	0.003768	-0.545666
7 H	3.174166	-0.927171	-1.089864
8 H	3.200774	0.935886	-1.081123
9 C	2.542181	0.003741	0.843223
10 H	2.853614	-0.886608	1.400547
11 H	2.853245	0.893808	1.400888

Distance Matrix (Angstroms)
Cr(1) O (2) C l(3) Cl(4) O (5) C (6)

O (2) 1.549666
Cl(3) 2.154472 3.011896
Cl(4) 2.154556 3.011732 3.389447
O (5) 1.712941 2.814231 3.154581 3.154678
C (6) 3.283038 3.156687 4.899909 4.896806 2.474058
H (7) 3.625153 3.257220 5.501736 4.890460 3.065236 1.084959
H (8) 3.647480 3.280946 4.917831 5.519240 3.078730 1.084884
C (9) 2.932521 3.510847 4.404990 4.404929 1.462476 1.480343
H (10) 3.556775 4.227893 5.177666 4.558707 2.031428 2.149615
H (11) 3.555907 4.225427 4.557818 5.178464 2.032054 2.149818
H (7) H (8) C (9) H (10)
H (8) 1.863267
C (9) 2.236701 2.237353
H (10) 2.511285 3.098498 1.095593
H (11) 3.102064 2.506576 1.095431 1.780416
Point Group: C_1 Number of degrees of freedom: 27
Energy = -1235.788056527

A6

Coordinates (Angstroms)

ATOM	X	Y	Z
1 Cr	-0.761296	0.048579	-0.395014
2 O	-1.213122	0.080732	-1.863478
3 Cl	-0.807429	1.869161	0.820324
4 Cl	-0.900786	-1.808576	0.763234
5 O	1.164862	-0.008598	-0.611722
6 C	2.030787	-0.104057	0.264919
7 H	1.727073	-0.181495	1.316971
8 C	3.479484	-0.115369	-0.068218
9 H	3.973329	0.721286	0.444342
10 H	3.935004	-1.034554	0.323246
11 H	3.636287	-0.042764	-1.145899

Distance Matrix (Angstroms)

Cr(1) O (2) Cl(3) Cl(4) O (5) C (6)
O (2) 1.536739
Cl(3) 2.189451 3.250516
Cl(4) 2.193175 3.250639 3.679364
O (5) 1.939153 2.688806 3.076794 3.065506
C (6) 2.873071 3.884220 3.501076 3.427510 1.235896
H (7) 3.029159 4.339213 3.297810 3.140010 2.016391 1.097749
C (8) 4.256511 5.028118 4.806817 4.769175 2.379974 1.486550
H (9) 4.855278 5.712759 4.930986 5.500808 3.087959 2.118219
H (10) 4.872813 5.703405 5.582949 4.917069 3.098458 2.120205
H (11) 4.462164 4.903768 5.221887 5.229523 2.528726 2.138175
H (7) C (8) H (9) H (10)
C (8) 2.234740
H (9) 2.573356 1.098450
H (10) 2.567130 1.098018 1.760428
H (11) 3.119306 1.091446 1.796172 1.797573
Point Group: C_1 Number of degrees of freedom: 27
Energy = -1235.853460980

A6/t

Coordinates (Angstroms)

ATOM	X	Y	Z
1 Cr	-0.704729	-0.040606	-0.413964
2 O	-1.457193	-0.251626	-1.756813
3 Cl	-1.251987	1.763350	0.709184
4 Cl	-0.580572	-1.812810	0.900234
5 O	1.275725	0.312660	-0.578780
6 C	2.188145	-0.012240	0.186810
7 H	1.948061	-0.620040	1.071320
8 C	3.598526	0.387535	-0.046604
9 H	3.950217	0.961264	0.822043
10 H	4.224618	-0.513713	-0.093154
11 H	3.702681	0.976652	-0.959130

Distance Matrix (Angstroms)

Cr(1) O (2) Cl(3) Cl(4) O (5) C (6)
O (2) 1.553697
Cl(3) 2.194358 3.191141
Cl(4) 2.209805 3.204006 3.643654
O (5) 2.018455 3.029030 3.186327 3.186054
C (6) 2.954734 4.138051 3.906418 3.378878 1.234584
H (7) 3.095013 4.441826 4.006494 2.801063 2.011167 1.099736
C (8) 4.340077 5.375280 5.098192 4.816937 2.384161 1.484411
H (9) 4.919348 6.112421 5.264884 5.313158 3.088025 2.110955
H (10) 4.962380 5.926165 5.985145 5.075857 3.100758 2.115911
H (11) 4.556016 5.363699 5.286861 5.439171 2.544733 2.141239
H (7) C (8) H (9) H (10)
C (8) 2.233606
H (9) 2.563453 1.098817
H (10) 2.559301 1.098365 1.757396
H (11) 3.122634 1.091152 1.798357 1.800978
Point Group: C_1 Number of degrees of freedom: 27
Energy = -1235.880934475

A7

Coordinates (Angstroms)

ATOM	X	Y	Z
1 Cr	0.674852	-0.192245	0.359643
2 Cl	1.646813	1.433824	-0.764464
3 Cl	-0.043348	-1.935051	-0.789546
4 O	1.021442	-0.359585	1.847541
5 O	-1.022386	0.782071	0.408717
6 C	-2.364875	0.229092	0.227010
7 H	-2.661655	-0.214339	1.189076
8 H	-2.282010	-0.618058	-0.491921
9 C	-3.260020	1.163154	-0.379681
10 H	-4.257205	0.688595	-0.409236
11 H	-0.996855	1.668823	-0.008998

Distance Matrix (Angstroms)

Cr(1) Cl(2) Cl(3) O (4) O (5) C (6)
Cl(2) 2.202822
Cl(3) 2.207673 3.769163
O (4) 1.536869 3.229547 3.251168
O (5) 1.957631 2.987601 3.126836 2.747877
C (6) 3.071654 4.304421 3.332626 3.799975 1.463243
H (7) 3.438129 5.009557 3.705581 3.744313 2.070989 1.100128
H (8) 3.106366 4.440737 2.614318 4.056191 2.087621 1.114178
C (9) 4.226929 4.929334 4.484846 5.060649 2.402873 1.428926
H (10) 5.068752 5.961458 4.978428 5.835739 3.337940 2.048625
H (11) 2.528651 2.759516 3.808719 3.410968 0.980545 2.000002
H (7) H (8) C (9) H (10)
H (8) 1.769992
C (9) 2.171757 2.035146
H (10) 2.432216 2.369721 1.104744
H (11) 2.784465 2.667332 2.348409 3.427962
Point Group: C_1 Number of degrees of freedom: 27
Energy = -1235.704931286

A7/t

Coordinates (Angstroms)

ATOM	X	Y	Z
1 Cr	0.658489	-0.143285	0.386930
2 Cl	1.556635	1.473647	-0.809490
3 Cl	0.058392	-1.910313	-0.794746
4 O	1.364345	-0.467231	1.732268
5 O	-1.137425	0.768599	0.492708
6 C	-2.458684	0.144800	0.336383
7 H	-2.820173	-0.088804	1.350832
8 H	-2.303888	-0.817925	-0.185968
9 C	-3.363428	0.988323	-0.402869
10 H	-4.361079	0.531079	-0.475918
11 H	-1.146673	1.613435	-0.002806

Distance Matrix (Angstroms)

Cr(1) Cl(2) Cl(3) O (4) O (5) C (6)
Cl(2) 2.202851
Cl(3) 2.208815 3.700829
O (4) 1.553418 3.203828 3.189639
O (5) 2.016936 3.074211 3.203761 3.053300
C (6) 3.130865 4.381968 3.440728 4.115656 1.469451
H (7) 3.610148 5.124909 4.025858 4.218873 2.074405 1.101976
H (8) 3.091768 4.532518 2.672880 4.154341 2.082857 1.106188
C (9) 4.252074 4.960635 4.501612 5.387883 2.409445 1.441037
H (10) 5.137640 6.001587 5.059029 6.217169 3.374403 2.104318
H (11) 2.548836 2.824562 3.807381 3.693895 0.979473 1.998327
H (7) H (8) C (9) H (10)
H (8) 1.777617
C (9) 2.128566 2.105280
H (10) 2.468940 2.477079 1.099871
H (11) 2.744186 2.698927 2.337695 3.424579
Point Group: C_1 Number of degrees of freedom: 27
Energy = -1235.734759857

A8/t

Coordinates (Angstroms)

ATOM	X	Y	Z
1 Cr	-0.705401	0.116634	-0.362755
2 O	-1.468764	0.376214	-1.689262
3 Cl	-0.305609	1.913994	0.826649
4 Cl	-1.352047	-1.666294	0.764480
5 O	1.212212	-0.615993	-0.517843
6 H	1.245280	-1.538686	-0.199819
7 C	2.428615	0.047260	-0.293176
8 H	2.340096	1.091347	-0.560696
9 C	3.509264	-0.555586	0.178753
10 H	4.419902	0.015016	0.316248
11 H	3.529635	-1.609605	0.444566

Distance Matrix (Angstroms)

Cr(1) O (2) Cl(3) Cl(4) O (5) H (6)
O (2) 1.552329
Cl(3) 2.192036 3.169780

Cl(4)	2.206272	3.194732	3.730598			
O (5)	2.058649	3.089389	3.242264	3.053343		
H (6)	2.563549	3.640235	3.921720	2.773493	0.976522	
C (7)	3.135556	4.152930	3.494952	4.283492	1.403573	1.980965
H (8)	3.203795	4.036395	3.098585	4.795059	2.046697	2.871572
C (9)	4.302152	5.398008	4.590409	5.020865	2.401113	2.497084
H (10)	5.171084	6.231285	5.118309	6.028525	3.373893	3.571910
H (11)	4.644049	5.786249	5.222148	4.892481	2.698878	2.374561

	C (7)	H (8)	C (9)	H (10)
H (8)	1.081444			
C (9)	1.324365	2.150844		
H (10)	2.082705	2.500623	1.083399	
H (11)	2.121723	3.117803	1.087210	1.856996

Point Group: C_1 Number of degrees of freedom: 27

Energy = -1235.848766515

TS[A1-A2]

Coordinates (Angstroms)

ATOM	X	Y	Z
1 Cr	0.035069	0.290967	0.100615
2 O	0.310616	0.879100	1.514208
3 Cl	-0.631052	-1.901189	-0.106069
4 Cl	-2.086915	0.734227	-0.186208
5 O	0.850976	1.136289	-1.045218
6 C	2.004866	-0.781930	0.259044
7 H	2.090357	-0.850163	1.336803
8 H	1.965227	-1.711791	-0.291616
9 C	2.409683	0.401186	-0.420022
10 H	2.749596	1.257269	0.154602
11 H	2.801822	0.309478	-1.428133

Distance Matrix (Angstroms)

	Cr(1)	O (2)	Cl(3)	Cl(4)	O (5)	C (6)
O (2)	1.555658					
Cl(3)	2.300432	3.352916				
Cl(4)	2.186679	2.942883	3.011873			
O (5)	1.641100	2.628459	3.507804	3.087193		
C (6)	2.248624	2.684202	2.886887	4.386303	2.590777	
H (7)	2.656040	2.487831	3.254628	4.720112	3.340072	1.083295
H (8)	2.808985	3.565312	2.609783	4.734340	3.149767	1.081406
C (9)	2.433516	2.894085	3.826953	4.514973	1.833252	1.422944
H (10)	2.881894	2.817829	4.633853	4.876635	2.249214	2.173445
H (11)	3.161066	3.897171	4.291798	5.061871	2.153146	2.161685

	H (7)	H (8)	C (9)	H (10)
H (8)	1.846566			
C (9)	2.180431	2.163030		
H (10)	2.504689	3.103170	1.085639	
H (11)	3.081529	2.465176	1.085574	1.845558

Point Group: C_1 Number of degrees of freedom: 27

Energy = -1235.746257451

TS[A1-A3]

Coordinates (Angstroms)

ATOM	X	Y	Z
1 Cr	0.000000	0.000000	0.294998
2 Cl	0.000125	1.817602	1.410783
3 Cl	-0.000125	-1.817602	1.410783
4 O	1.222204	-0.000140	-0.744486
5 O	-1.222204	0.000140	-0.744486
6 C	0.698046	-0.000367	-2.648452
7 H	1.242015	-0.919269	-2.838119
8 H	1.242917	0.917819	-2.838567
9 C	-0.698046	0.000367	-2.648452
10 H	-1.242015	0.919269	-2.838119
11 H	-1.242917	-0.917819	-2.838567

Distance Matrix (Angstroms)

	Cr(1)	Cl(2)	Cl(3)	O (4)	O (5)	C (6)
Cl(2)	2.132757					
Cl(3)	2.132757	3.635204				
O (4)	1.604466	3.072921	3.072856			
O (5)	1.604466	3.072856	3.072921	2.444408		
C (6)	3.025090	4.502165	4.501907	1.974798	2.704153	
H (7)	3.493433	5.204413	4.516977	2.286589	3.361693	1.084553
H (8)	3.493775	4.517866	5.204292	2.286537	3.362161	1.084478
C (9)	3.025090	4.501907	4.502165	2.704153	1.974798	1.396093
H (10)	3.493433	4.516977	5.204413	3.361693	2.286589	2.155352
H (11)	3.493775	5.204292	4.517866	3.362161	2.286537	2.155272

	H (7)	H (8)	C (9)	H (10)
H (8)	1.837088			
C (9)	2.155352	2.155272		
H (10)	3.090408	2.484932	1.084553	
H (11)	2.484932	3.090135	1.084478	1.837088

Point Group: C_2 Number of degrees of freedom: 14

Energy = -1235.774229724

TS[A1-A4]

Coordinates (Angstroms)

ATOM	X	Y	Z
1 Cr	0.554733	-0.067276	0.371407
2 Cl	-0.765580	1.524567	-0.177482
3 O	-0.517420	-1.294419	0.147457
4 C	-2.790767	0.002672	-0.482395
5 H	-2.881838	0.405997	-1.484200
6 H	-3.282972	0.551840	0.312034
7 C	-2.304990	-1.291007	-0.267956
8 H	-2.580719	-1.792489	0.653675
9 H	-2.177702	-1.938377	-1.129538
10 O	0.874999	0.045451	1.884342
11 Cl	2.251406	-0.218607	-0.936586

Distance Matrix (Angstroms)

	Cr(1)	Cl(2)	O (3)	C (4)	H (5)	H (6)
Cl(2)	2.139736					
O (3)	1.644855	2.848483				
C (4)	3.453439	2.551572	2.692075			
H (5)	3.934118	2.727134	3.338291	1.083779		
H (6)	3.887777	2.742824	3.329269	1.083959	1.846248	
C (7)	3.175582	3.210207	1.835207	1.398417	2.166062	2.165392
H (8)	3.589861	3.871487	2.182094	2.134802	3.081318	2.470983
H (9)	3.635940	3.859078	2.191332	2.135958	2.473395	3.082358
O (10)	1.550565	3.021656	2.598241	4.363613	5.058744	4.474070
Cl(11)	2.147660	3.566104	3.162107	5.067422	5.200020	5.725555

	C (7)	H (8)	H (9)	O (10)
H (8)	1.084856			
H (9)	1.085180	1.834000		
O (10)	4.065813	4.102994	4.726313	
Cl(11)	4.728409	5.324985	4.755191	3.149898

Point Group: C_1 Number of degrees of freedom: 27

Energy = -1235.773732356

TS[A4-A5]

Coordinates (Angstroms)

ATOM	X	Y	Z
1 Cr	0.199076	0.160608	-0.375209
2 Cl	0.377444	-1.885285	0.529871
3 O	-1.165771	1.241494	0.298643
4 C	-2.202428	-0.333850	-0.161664
5 H	-1.906762	-1.336083	0.131203
6 H	-2.510912	-0.146105	-1.183490
7 C	-2.383469	0.742162	0.831572
8 H	-3.208437	1.440201	0.670807
9 H	-2.293026	0.446982	1.879715
10 O	0.081105	-0.061475	-1.897776
11 Cl	2.040606	0.963411	0.466149

Distance Matrix (Angstroms)

	Cr(1)	Cl(2)	O (3)	C (4)	H (5)	H (6)
Cl(2)	2.244252					
O (3)	1.866868	3.494528				
C (4)	2.461161	3.088837	1.941198			
H (5)	2.632697	2.382889	2.687193	1.085201		
H (6)	2.844544	3.781925	2.435479	1.083761	1.873356	
C (7)	2.909307	3.823237	1.419907	1.475499	2.244297	2.205842
H (8)	3.787169	4.892572	2.085779	2.202797	3.113403	2.537976
H (9)	3.373020	3.793805	2.098033	2.187495	2.527016	3.127691
O (10)	1.543195	3.050831	2.841951	2.881458	3.113358	2.689967
Cl(11)	2.177982	3.299278	3.222769	4.481113	4.580565	4.966755

	C (7)	H (8)	H (9)	O (10)
H (8)	1.092554			
H (9)	1.092664	1.812710		
O (10)	3.764213	4.435508	4.490486	
Cl(11)	4.444651	5.274624	4.587508	3.237001

Point Group: C_1 Number of degrees of freedom: 27

Energy = -1235.750976286

TS[A2-A5] Coordinates (Angstroms)

ATOM	X	Y	Z
1 Cr	0.261919	-0.022439	-0.337763
2 Cl	1.088718	-1.874864	0.438706
3 Cl	1.316239	1.721616	0.430339
4 O	0.011338	0.100680	-1.855261
5 O	-1.282302	0.877390	0.471026
6 C	-2.614548	0.375286	0.348262
7 H	-3.128353	0.754782	-0.539507
8 H	-3.188685	0.542112	1.262206
9 C	-1.917388	-0.895984	0.208340
10 H	-1.840459	-1.396335	-0.752103
11 H	-1.653504	-1.457165	1.096212

Distance Matrix (Angstroms)

	Cr(1)	Cl(2)	Cl(3)	O (4)	O (5)	C (6)
Cl(2)	2.172091					
Cl(3)	2.177911	3.603679				

O (4) 1.542967 3.213380 3.090981
O (5) 1.961747 3.632862 2.732542 2.772796
C (6) 2.983769 4.334228 4.155770 3.438924 1.429006
H (7) 3.484066 5.065138 4.650781 3.466514 2.108107 1.093685
H (8) 3.845164 4.981576 4.730494 4.489277 2.091093 1.092135
C (9) 2.410537 3.169850 4.166227 2.995292 1.901891 1.456618
H (10) 2.545440 3.197983 4.591789 2.624341 2.641479 2.224558
H (11) 2.789905 2.850713 4.400841 3.729581 2.445157 2.200206

	H (7)	H (8)	C (9)	H (10)
H (8)	1.815224			
C (9)	2.179619	2.189737		
H (10)	2.516182	3.103664	1.085689	
H (11)	3.121452	2.526151	1.082993	1.858741

Point Group: C_1 Number of degrees of freedom: 27
Energy = -1235.750517711

TS[A3-A5]

Coordinates (Angstroms)

ATOM	X	Y	Z
1 Cr	-0.274331	-0.115072	-0.373210
2 Cl	0.382725	-2.002976	0.509959
3 Cl	-2.126891	0.651810	0.471554
4 O	-0.165193	0.069248	-1.904369
5 O	0.558640	1.342816	0.552804
6 C	2.074349	0.577956	-0.457306
7 H	2.309057	-0.476546	-0.553100
8 H	2.072643	1.188790	-1.351742
9 C	1.951585	1.244926	0.840382
10 H	2.157064	0.622334	1.715694
11 H	2.405414	2.235507	0.930729

Distance Matrix (Angstroms)

	Cr(1)	Cl(2)	Cl(3)	O (4)	O (5)	C (6)
Cl(2)	2.185381					
Cl(3)	2.175710	3.653427				
O (4)	1.546070	3.228514	3.135705			
O (5)	1.917494	3.350687	2.774197	2.860701		
C (6)	2.450236	3.233946	4.303330	2.714466	1.975527	
H (7)	2.614750	2.677843	4.690495	2.871538	2.756277	1.084546
H (8)	2.857598	4.063142	4.609646	2.562553	2.437873	1.083114
C (9)	2.876996	3.622067	4.137848	3.660140	1.425685	1.464211
H (10)	3.289220	3.390328	4.461056	4.336316	2.103893	2.175026
H (11)	3.795591	4.715194	4.822937	4.397554	2.085737	2.187171

	H (7)	H (8)	C (9)	H (10)
H (8)	1.862005			
C (9)	2.243445	2.196181		
H (10)	2.525483	3.120442	1.093624	
H (11)	3.092938	2.532987	1.093331	1.811125

Point Group: C_1 Number of degrees of freedom: 27
Energy = -1235.752161627

TS[A3-A5]/os

Coordinates (Angstroms)

ATOM	X	Y	Z
1 Cr	-0.273205	-0.118237	-0.372912
2 Cl	0.384722	-2.000503	0.521568
3 Cl	-2.129523	0.649524	0.462756
4 O	-0.160056	0.058606	-1.904661
5 O	0.554526	1.345773	0.548130
6 C	2.074460	0.578598	-0.453843
7 H	2.311326	-0.475945	-0.543684
8 H	2.074196	1.184939	-1.351332
9 C	1.946823	1.251838	0.840131
10 H	2.150933	0.634011	1.719132
11 H	2.398619	2.243677	0.926792

Distance Matrix (Angstroms)

	Cr(1)	Cl(2)	Cl(3)	O (4)	O (5)	C (6)
Cl(2)	2.185381					
Cl(3)	2.175710	3.653427				
O (4)	1.546070	3.228514	3.135705			
O (5)	1.917494	3.350687	2.774197	2.860701		
C (6)	2.450236	3.233946	4.303330	2.714466	1.975527	
H (7)	2.614750	2.677843	4.690495	2.871538	2.756277	1.084546
H (8)	2.857598	4.063142	4.609646	2.562553	2.437873	1.083114
C (9)	2.876996	3.622067	4.137848	3.660140	1.425685	1.464211
H (10)	3.289220	3.390328	4.461056	4.336316	2.103893	2.175026
H (11)	3.795591	4.715194	4.822937	4.397554	2.085737	2.187171

	H (7)	H (8)	C (9)	H (10)
H (8)	1.862005			
C (9)	2.243445	2.196181		
H (10)	2.525483	3.120442	1.093624	
H (11)	3.092938	2.532987	1.093331	1.811125

Point Group: C_1 Number of degrees of freedom: 27
Energy = -1235.752165623

TS[C1-A3]/t

Coordinates (Angstroms)

ATOM	X	Y	Z
1 Cr	-0.248106	-0.027971	-0.149716
2 O	0.405627	0.119003	-1.558569
3 Cl	-1.266490	1.828416	0.261868
4 Cl	-1.636811	-1.656172	0.062157
5 O	1.025043	-0.117209	1.028762
6 C	2.920813	0.101976	-0.514923
7 H	3.409936	-0.566316	-1.214417
8 H	2.808536	1.145067	-0.789557
9 C	2.432359	-0.372135	0.798493
10 H	2.590457	-1.448200	0.932630
11 H	2.945160	0.154669	1.616728

Distance Matrix (Angstroms)

	Cr(1)	O (2)	Cl(3)	Cl(4)	O (5)	C (6)
O (2)	1.560075					
Cl(3)	2.157008	3.005338				
Cl(4)	2.150449	3.154291	3.509897			
O (5)	1.737147	2.670909	3.102371	3.223073		
C (6)	3.192539	2.723168	4.595378	4.918947	2.454577	
H (7)	3.847684	3.100641	5.457391	5.318560	3.304734	1.084042
H (8)	3.335938	2.723630	4.263602	5.322919	2.842618	1.084467
C (9)	2.863991	3.147158	4.337266	4.330022	1.448638	1.479334
H (10)	3.353500	3.665471	5.105113	4.320969	2.057013	2.146530
H (11)	3.653852	4.066081	4.730230	5.166266	2.026443	2.132441

	H (7)	H (8)	C (9)	H (10)
H (8)	1.863067			
C (9)	2.246146	2.228299		
H (10)	2.461519	3.120661	1.095858	
H (11)	2.958246	2.605718	1.099998	1.778481

Point Group: C_1 Number of degrees of freedom: 27
Energy = -1235.784601946

TS[A5-X]

Coordinates (Angstroms)

ATOM	X	Y	Z
1 Cr	0.500799	0.111772	-0.351605
2 O	-0.827249	1.071217	0.389504
3 C	-2.227370	1.254800	0.053338
4 H	-2.382696	1.240433	-1.028672
5 H	-2.552892	2.206407	0.482517
6 C	-2.648667	0.057694	0.760657
7 H	-2.933012	-0.853526	0.254101
8 H	-2.613850	0.051449	1.844249
9 O	0.463093	0.409504	-1.863602
10 Cl	-0.519382	-1.790666	0.024942
11 Cl	2.322068	0.315116	0.788136

Distance Matrix (Angstroms)

	Cr(1)	O (2)	C (3)	H (4)	H (5)	C (6)
O (2)	1.798191					
C (3)	2.985531	1.451568				
H (4)	3.169675	2.111700	1.093197			
H (5)	3.795825	2.067644	1.093488	1.801601		
C (6)	3.340537	2.117203	1.452877	2.161321	2.168756	
H (7)	3.617974	2.856082	2.232324	2.516548	3.091901	1.080635
H (8)	3.811358	2.519554	2.191981	3.117818	2.549877	1.084169
O (9)	1.541493	2.679428	3.409952	3.079945	4.222476	4.085775
Cl(10)	2.191307	2.901390	3.491832	3.710742	4.507897	2.914030
Cl(11)	2.158096	3.263249	4.703224	5.127554	5.237902	4.977472

	H (7)	H (8)	O (9)	Cl(10)
H (8)	1.857259			
O (9)	4.196836	4.831556		
Cl(10)	2.599299	3.330174	3.061471	
Cl(11)	5.409878	5.054521	3.239817	3.618096

Point Group: C_1 Number of degrees of freedom: 27
Energy = -1235.768146124

B1

Coordinates (Angstroms)

ATOM	X	Y	Z
1 Cr	0.000000	0.000000	0.351958
2 Cl	-1.745057	0.000000	-0.841337
3 Cl	1.745057	0.000000	-0.841337
4 O	0.000000	1.262265	1.259904
5 O	0.000000	-1.262265	1.259904

Point Group: C_{2v} Number of degrees of freedom: 4
Energy is -1157.200739279

Distance Matrix (Angstroms)

	Cr(1)	Cl(2)	Cl(3)	O (4)
Cl(2)	2.114042			
Cl(3)	2.114042	3.490114		
O (4)	1.554889	3.008945	3.008945	
O (5)	1.554889	3.008945	3.008945	2.524529

B2

Coordinates (Angstroms)

ATOM	X	Y	Z
1 Cr	0.593993	-0.235656	0.440817
2 Cl	-1.084087	1.387972	-0.082101
3 O	-0.575415	-1.458106	-0.155153
4 C	-2.423842	0.101561	-0.152279
5 H	-3.233741	0.542912	-0.734309
6 H	-2.716065	-0.049250	0.887299
7 C	-1.797823	-1.133881	-0.778339
8 H	-2.501455	-1.969759	-0.649588
9 H	-1.650735	-0.975080	-1.856324
10 O	0.758699	-0.130227	1.975131
11 Cl	2.247236	0.196678	-0.933263

Distance Matrix (Angstroms)

	Cr(1)	Cl(2)	O (3)	C (4)	H (5)	H (6)
Cl(2)	2.392815					
O (3)	1.793622	2.892101				
C (4)	3.093994	1.858688	2.418522			
H (5)	4.079048	2.400107	3.377306	1.090636		
H (6)	3.345232	2.380902	2.766581	1.090349	1.802291	
C (7)	2.830889	2.711809	1.409881	1.519924	2.208038	2.189508
H (8)	3.711858	3.688540	2.053262	2.131597	2.618575	2.469096
H (9)	3.295816	3.008815	2.069689	2.158847	2.463559	3.085378
O (10)	1.546727	3.151665	2.842752	3.835122	4.871731	3.641967
Cl(11)	2.192765	3.638870	3.363202	4.736871	5.495505	5.292380

	C (7)	H (8)	H (9)	O (10)
H (8)	1.100167			
H (9)	1.099502	1.780259		
O (10)	3.889053	4.571831	4.604259	
Cl(11)	4.261091	5.227235	4.173636	3.283499

Point Group: C_1 Number of degrees of freedom: 27

Energy = -1235.816816313

B2/os

Coordinates (Angstroms)

ATOM	X	Y	Z
1 Cr	0.593357	-0.235260	0.441726
2 Cl	-1.083741	1.390689	-0.076041
3 O	-0.575393	-1.455897	-0.158059
4 C	-2.423270	0.104443	-0.151419
5 H	-3.232213	0.546892	-0.733345
6 H	-2.716928	-0.048482	0.887189
7 C	-1.798074	-1.130374	-0.779252
8 H	-2.502012	-1.965853	-0.649609
9 H	-1.652733	-0.971606	-1.857335
10 O	0.760530	-0.140482	1.976377
11 Cl	2.243169	0.198246	-0.936362

Distance Matrix (Angstroms)

	Cr(1)	Cl(2)	O (3)	C (4)	H (5)	H (6)
Cl(2)	2.392582					
O (3)	1.793230	2.892784				
C (4)	3.093099	1.858615	2.418544			
H (5)	4.077688	2.399995	3.376508	1.090315		
H (6)	3.345342	2.380405	2.767586	1.090104	1.801699	
C (7)	2.830364	2.713032	1.409537	1.519808	2.207280	2.189020
H (8)	3.710428	3.688746	2.052690	2.130849	2.618032	2.466627
H (9)	3.297394	3.012839	2.069477	2.159111	2.462508	3.084977
O (10)	1.546636	3.155668	2.840920	3.837198	4.874123	3.645204
Cl(11)	2.192928	3.637362	3.359499	4.732926	5.490226	5.290442

	C (7)	H (8)	H (9)	O (10)
H (8)	1.100164			
H (9)	1.099361	1.780001		
O (10)	3.888423	4.568585	4.605644	
Cl(11)	4.256943	5.223246	4.170707	3.285880

Point Group: C_1 Number of degrees of freedom: 27

Energy = -1235.816814237

B2/t

Coordinates (Angstroms)

ATOM	X	Y	Z
1 Cr	-0.739905	-0.436454	-0.293542
2 Cl	1.497249	1.192278	-0.719357
3 O	0.483174	-1.293085	0.684434
4 C	2.508554	-0.059144	0.164383
5 H	3.360693	0.475381	0.588266
6 H	2.837019	-0.765591	-0.599845
7 C	1.648318	-0.723908	1.230702
8 H	2.244726	-1.525401	1.691346
9 H	1.395540	0.003358	2.015795
10 O	-1.313468	-1.128185	-1.569527
11 Cl	-2.061761	0.912145	0.808046

Distance Matrix (Angstroms)

	Cr(1)	Cl(2)	O (3)	C (4)	H (5)	H (6)
Cl(2)	2.799812					
O (3)	1.784987	3.029192				
C (4)	3.302203	1.835699	2.428008			
H (5)	4.292311	2.386680	3.378881	1.091575		
H (6)	3.605072	2.375398	2.732802	1.091330	1.796066	
C (7)	2.847729	2.738124	1.407100	1.522811	2.187064	2.183037
H (8)	3.746146	3.708907	2.042280	2.133337	2.542695	2.485493
H (9)	3.175940	2.984113	2.070192	2.161118	2.474363	3.083945
O (10)	1.560642	3.742656	2.887119	4.330952	5.392150	4.277651
Cl(11)	2.186211	3.883039	3.369721	4.716512	5.444454	5.366097

	C (7)	H (8)	H (9)	O (10)
H (8)	1.100130			
H (9)	1.099628	1.778620		
O (10)	4.095961	4.842708	4.633966	
Cl(11)	4.076763	5.026697	3.773258	3.221140

Point Group: C_1 Number of degrees of freedom: 27

Energy = -1235.842536459

B3

Coordinates (Angstroms)

ATOM	X	Y	Z
1 Cr	-1.137493	-0.000031	0.000342
2 O	-1.878705	-0.171196	-1.395867
3 O	-1.878351	0.170997	1.396756
4 Cl	0.621446	1.616005	-0.134209
5 Cl	0.621646	-1.615882	0.134431
6 C	2.165053	0.687137	0.306643
7 H	2.194366	0.665644	1.396408
8 H	2.984111	1.288486	-0.091562
9 C	2.165045	-0.686864	-0.306814
10 H	2.984263	-1.288131	0.091186
11 H	2.194082	-0.665370	-1.396587

Distance Matrix (Angstroms)

	Cr(1)	O (2)	O (3)	Cl(4)	Cl(5)	C (6)
O (2)	1.589998					
O (3)	1.589998	2.813511				
Cl(4)	2.392393	3.322142	3.268163			
Cl(5)	2.392389	3.268132	3.322106	3.243033		
C (6)	3.387157	4.470711	4.219463	1.854689	2.777708	
H (7)	3.673338	5.008694	4.102645	2.391663	3.044897	1.090371
H (8)	4.319299	5.242029	5.206478	2.385638	3.750689	1.091349
C (9)	3.387159	4.219463	4.470697	2.777714	1.854684	1.504728
H (10)	4.319297	5.206471	5.242002	3.750695	2.385634	2.149234
H (11)	3.673348	4.102659	5.008691	3.044906	2.391661	2.175111

	H (7)	H (8)	C (9)	H (10)
H (8)	1.796019			
C (9)	2.175110	2.149235		
H (10)	2.478866	2.583089	1.091350	
H (11)	3.093933	2.478868	1.090371	1.796019

Point Group: C_1 Number of degrees of freedom: 27

Energy = -1235.760757919

B3/os

Coordinates (Angstroms)

ATOM	X	Y	Z
1 Cr	-1.138757	0.000017	-0.000001
2 O	-1.879797	-0.184426	-1.394610
3 O	-1.879786	0.184416	1.394619
4 Cl	0.620301	1.614588	-0.149747
5 Cl	0.620265	-1.614587	0.149741
6 C	2.163793	0.689877	0.300157
7 H	2.192962	0.678790	1.390082
8 H	2.982940	1.287347	-0.103665
9 C	2.163779	-0.689918	-0.300152
10 H	2.982908	-1.287407	0.103679
11 H	2.192960	-0.678833	-1.390077

Distance Matrix (Angstroms)

	Cr(1)	O (2)	O (3)	Cl(4)	Cl(5)	C (6)
O (2)	1.589998					
O (3)	1.589998	2.813511				
Cl(4)	2.392393	3.322142	3.268163			
Cl(5)	2.392389	3.268132	3.322106	3.243033		
C (6)	3.387157	4.470711	4.219463	1.854689	2.777708	
H (7)	3.673338	5.008694	4.102645	2.391663	3.044897	1.090371
H (8)	4.319299	5.242029	5.206478	2.385638	3.750689	1.091349
C (9)	3.387159	4.219463	4.470697	2.777714	1.854684	1.504728
H (10)	4.319297	5.206471	5.242002	3.750695	2.385634	2.149234
H (11)	3.673348	4.102659	5.008691	3.044906	2.391661	2.175111

	H (7)	H (8)	C (9)	H (10)
H (8)	1.796019			
C (9)	2.175110	2.149235		
H (10)	2.478866	2.583089	1.091350	
H (11)	3.093933	2.478868	1.090371	1.796019

Point Group: C_1 Number of degrees of freedom: 27

Energy = -1235.760761042

B3/t

Coordinates (Angstroms)

ATOM	X	Y	Z

1	Cr	0.000000	0.000000	-1.345770
2	O	1.465832	0.030603	-2.000203
3	O	-1.465832	-0.030603	-2.000203
4	Cl	0.024376	1.710816	0.807125
5	Cl	-0.024376	-1.710816	0.807125
6	C	-0.403041	0.640293	2.216454
7	H	-1.476118	0.455286	2.156472
8	H	-0.173195	1.221631	3.112394
9	C	0.403041	-0.640293	2.216454
10	H	0.173195	-1.221631	3.112394
11	H	1.476118	-0.455286	2.156472

Distance Matrix (Angstroms)

	Cr(1)	O (2)	O (3)	Cl(4)	Cl(5)	C (6)
O (2)	1.605578					
O (3)	1.605578	2.932303				
Cl(4)	2.749990	3.575192	3.624134			
Cl(5)	2.749990	3.624134	3.575192	3.421980		
C (6)	3.641684	4.652376	4.399980	1.820691	2.767185	
H (7)	3.827781	5.110124	4.184989	2.376673	2.936033	1.090559
H (8)	4.625754	5.499418	5.420114	2.364868	3.733049	1.092470
C (9)	3.641684	4.399980	4.652376	2.767185	1.820691	1.513165
H (10)	4.625754	5.420114	5.499418	3.733049	2.364868	2.145115
H (11)	3.827781	4.184989	5.110124	2.936033	2.376673	2.176035

	H (7)	H (8)	C (9)	H (10)
H (8)	1.788485			
C (9)	2.176035	2.145115		
H (10)	2.538911	2.467695	1.092470	
H (11)	3.089472	2.538911	1.090559	1.788485

Point Group: C_2 Number of degrees of freedom: 14

Energy = -1235.771285865

B4

Coordinates (Angstroms)

ATOM		X	Y	Z
1	Cr	-0.684228	0.257841	0.000000
2	O	-0.296249	1.050663	-1.283962
3	O	-0.296249	1.050663	1.283962
4	Cl	-2.707380	-0.408850	0.000000
5	Cl	2.764188	0.396742	0.000000
6	C	0.496967	-1.338017	0.000000
7	H	0.112632	-1.837907	-0.897560
8	H	0.112632	-1.837907	0.897560
9	C	2.023829	-1.263102	0.000000
10	H	2.422843	-1.755203	-0.887692
11	H	2.422843	-1.755203	0.887692

Distance Matrix (Angstroms)

	Cr(1)	O (2)	O (3)	Cl(4)	Cl(5)	C (6)
O (2)	1.558093					
O (3)	1.558093	2.567924				
Cl(4)	2.130170	3.097142	3.097142			
Cl(5)	3.451212	3.382669	3.382669	5.530555		
C (6)	1.985443	2.825516	2.825516	3.336344	2.854765	
H (7)	2.415110	2.942843	3.642809	3.286379	3.581902	1.096912
H (8)	2.415110	3.642809	2.942843	3.286379	3.581902	1.096912
C (9)	3.105936	3.519208	3.519208	4.807711	1.817475	1.528699
H (10)	3.807129	3.927260	4.470171	5.377718	2.352740	2.161259
H (11)	3.807129	4.470171	3.927260	5.377718	2.352740	2.161259

	H (7)	H (8)	C (9)	H (10)
H (8)	1.795119			
C (9)	2.188307	2.188307		
H (10)	2.311712	2.920794	1.090584	
H (11)	2.920794	2.311712	1.090584	1.775384

Point Group: C_s Number of degrees of freedom: 16

Energy = -1235.785288221

B5

Coordinates (Angstroms)

ATOM		X	Y	Z
1	Cr	-0.998744	0.343146	-0.004539
2	O	-0.929163	1.189802	-1.315057
3	O	-0.927922	1.266604	1.252882
4	Cl	-2.513062	-1.146375	0.041318
5	Cl	3.521035	-0.457777	-0.005696
6	C	0.791360	-0.521968	0.014887
7	H	0.751333	-1.160044	-0.874546
8	H	0.756553	-1.119480	0.932195
9	C	1.939838	0.455927	-0.010867
10	H	1.950182	1.098535	0.869860
11	H	1.937565	1.066331	-0.914488

Distance Matrix (Angstroms)

	Cr(1)	O (2)	O (3)	Cl(4)	Cl(5)	C (6)
O (2)	1.561769					
O (3)	1.561697	2.569087				
Cl(4)	2.124602	3.131487	3.130977			
Cl(5)	4.590193	4.922723	4.934645	6.073442		
C (6)	1.988284	2.767509	2.772644	3.363003	2.730506	
H (7)	2.465616	2.922310	3.637921	3.390467	2.986524	1.095370
H (8)	2.469375	3.636559	2.938314	3.388917	2.993301	1.095302
C (9)	2.940752	3.235839	3.237021	4.732696	1.826216	1.508623
H (10)	3.167230	3.615635	2.908339	5.064251	2.378295	2.167920
H (11)	3.157991	2.897211	3.598419	5.061394	2.378274	2.167999

	H (7)	H (8)	C (9)	H (10)
H (8)	1.807204			
C (9)	2.183998	2.184362		
H (10)	3.095379	2.519569	1.090290	
H (11)	2.522992	3.095610	1.090472	1.784683

Point Group: C_1 Number of degrees of freedom: 27

Energy = -1235.797739904

B6

Coordinates (Angstroms)

ATOM		X	Y	Z
1	Cr	1.370013	0.361657	0.064939
2	O	2.222292	1.619568	0.359127
3	Cl	2.392339	-1.484750	-0.256337
4	O	-0.341720	0.497756	0.006306
5	C	-1.519214	1.264584	0.137284
6	H	-1.365277	2.248202	-0.327445
7	H	-1.720058	1.408927	1.204942
8	C	-2.695177	0.582662	-0.543291
9	H	-3.564076	1.245322	-0.526564
10	H	-2.450662	0.328034	-1.576271
11	Cl	-3.171049	-0.949961	0.287496

Distance Matrix (Angstroms)

	Cr(1)	O (2)	Cl(3)	O (4)	C (5)	H (6)
O (2)	1.547665					
Cl(3)	2.134851	3.169306				
O (4)	1.718136	2.820833	3.387387			
C (5)	3.027894	3.764850	4.797293	1.411266		
H (6)	3.345867	3.706374	5.297137	2.055022	1.098715	
H (7)	3.456142	4.037560	5.236460	2.041268	1.095931	1.782823
C (8)	4.116376	5.105980	5.499032	2.418269	1.520227	2.142253
H (9)	5.047372	5.865710	6.557834	3.350579	2.150006	2.424898
H (10)	4.158396	5.220184	5.336953	2.642156	2.163560	2.534694
Cl(11)	4.731924	5.974590	5.615428	3.190619	2.766826	3.723870

	H (7)	C (8)	H (9)	H (10)
C (8)	2.165615			
H (9)	2.534814	1.092878		
H (10)	3.072012	1.091637	1.784094	
Cl(11)	2.917436	1.807095	2.374117	2.371888

Point Group: C_1 Number of degrees of freedom: 27

Energy = -1235.809293020

TS[B1-B2]

Coordinates (Angstroms)

ATOM		X	Y	Z
1	Cr	0.554733	-0.067276	0.371407
2	Cl	-0.765580	1.524567	-0.177482
3	O	-0.517420	-1.294419	0.147457
4	C	-2.790767	0.002672	-0.482395
5	H	-2.881838	0.405997	-1.484200
6	H	-3.282972	0.551840	0.312034
7	C	-2.304990	-1.291007	-0.267956
8	H	-2.580719	-1.792489	0.653675
9	H	-2.177702	-1.938377	-1.129538
10	O	0.874999	0.045451	1.884342
11	Cl	2.251406	-0.218607	-0.936586

Distance Matrix (Angstroms)

	Cr(1)	Cl(2)	O (3)	C (4)	H (5)	H (6)
Cl(2)	2.139736					
O (3)	1.644855	2.848483				
C (4)	3.453439	2.551572	2.692075			
H (5)	3.934118	2.727134	3.338291	1.083779		
H (6)	3.887777	2.742824	3.329269	1.083959	1.846248	
C (7)	3.175582	3.210207	1.835207	1.398417	2.166062	2.165392
H (8)	3.589861	3.871487	2.182094	2.134802	3.081318	2.470983
H (9)	3.635940	3.859078	2.191332	2.135958	2.473395	3.082358
O (10)	1.550565	3.021656	2.598241	4.363613	5.058744	4.474070
Cl(11)	2.147660	3.566104	3.162107	5.067422	5.200020	5.725555

	C (7)	H (8)	H (9)	O (10)
H (8)	1.084856			
H (9)	1.085180	1.834000		
O (10)	4.065813	4.102994	4.726313	
Cl(11)	4.728409	5.324985	4.755191	3.149898

Point Group: C_1 Number of degrees of freedom: 27

Energy = -1235.773732356

TS[B1-B3]

Coordinates (Angstroms)

ATOM		X	Y	Z
1	Cr	-1.082242	-0.000205	-0.000182

2	O	-1.893251	-0.122370	-1.346800
3	O	-1.892842	0.122402	1.346556
4	Cl	0.497090	1.575737	-0.107358
5	Cl	0.497667	-1.576075	0.107874
6	C	2.379785	0.710910	0.149365
7	H	2.568695	0.987462	1.182686
8	H	2.887338	1.340328	-0.576080
9	C	2.380138	-0.710428	-0.148906
10	H	2.888494	-1.339897	0.576084
11	H	2.568754	-0.986313	-1.182464

Distance Matrix (Angstroms)

	Cr(1)	O (2)	O (3)	Cl(4)	Cl(5)	C (6)
O (2)	1.576719					
O (3)	1.576645	2.704456				
Cl(4)	2.233689	3.183318	3.152431			
Cl(5)	2.234089	3.153700	3.183346	3.159152		
C (6)	3.537468	4.603444	4.476042	2.087672	2.962159	
H (7)	3.962827	5.247760	4.547581	2.510344	3.466424	1.086241
H (8)	4.229214	5.058411	5.294336	2.447121	3.831935	1.086301
C (9)	3.537599	4.476897	4.603083	2.962118	2.087816	1.452297
H (10)	4.230082	5.295747	5.058964	3.832339	2.447662	2.155616
H (11)	3.962319	4.547845	5.247002	3.465796	2.510417	2.165651

	H (7)	H (8)	C (9)	H (10)
H (8)	1.821896			
C (9)	2.165992	2.155303		
H (10)	2.426280	2.917377	1.086401	
H (11)	3.080539	2.425377	1.086246	1.822017

Point Group: C_1 Number of degrees of freedom: 27

Energy = -1235.755113119

TS[B1-B4]

Coordinates (Angstroms)

ATOM		X	Y	Z
1	Cr	0.267793	0.386097	-0.069051
2	O	0.359145	1.560396	0.954074
3	O	0.292370	0.913911	-1.531212
4	Cl	2.313184	-0.441175	0.182910
5	Cl	-2.140415	0.528749	0.169827
6	C	-0.216349	-1.879378	0.044254
7	H	0.259709	-2.130279	0.987600
8	H	0.349342	-2.093070	-0.858566
9	C	-1.599348	-1.856791	-0.026672
10	H	-2.212546	-1.998102	0.855824
11	H	-2.114889	-1.902051	-0.980493

Distance Matrix (Angstroms)

	Cr(1)	O (2)	O (3)	Cl(4)	Cl(5)	C (6)
O (2)	1.560163					
O (3)	1.554704	2.568861				
Cl(4)	2.220695	2.901594	2.976265			
Cl(5)	2.424227	2.815516	2.993380	4.558011		
C (6)	2.319398	3.604304	3.247052	2.913106	3.084943	
H (7)	2.729236	3.692166	3.951274	2.778013	3.674204	1.086040
H (8)	2.603124	4.078428	3.081823	2.769496	3.759045	1.086625
C (9)	2.918658	4.058907	3.676823	4.166030	2.454011	1.385001
H (10)	3.562567	4.391600	4.522429	4.833122	2.619307	2.158135
H (11)	3.426882	4.674605	3.745374	4.805777	2.689364	2.157563

	H (7)	H (8)	C (9)	H (10)
H (8)	1.848714			
C (9)	2.135331	2.131964		
H (10)	2.479291	3.084059	1.083872	
H (11)	3.092603	2.474629	1.085175	1.841418

Point Group: C_1 Number of degrees of freedom: 27

Energy = -1235.747367381

TS[B4-B2] Coordinates (Angstroms)

ATOM		X	Y	Z
1	Cr	0.893957	-0.352146	0.138102
2	Cl	1.467921	1.616281	-0.474601
3	O	0.699332	-1.482096	-1.015102
4	O	1.465698	-0.891008	1.482686
5	Cl	-2.225274	0.948113	0.500708
6	C	-1.085600	-1.473200	-0.199317
7	H	-1.104184	-1.716255	0.863905
8	H	-1.148725	-2.376625	-0.800360
9	C	-2.059574	-0.425443	-0.659731
10	H	-3.051607	-0.884370	-0.748888
11	H	-1.785330	-0.011970	-1.632865

Distance Matrix (Angstroms)

	Cr(1)	Cl(2)	O (3)	O (4)	Cl(5)	C (6)
Cl(2)	2.139987					
O (3)	1.626206	3.237716				
O (4)	1.557294	3.180798	2.678740			
Cl(5)	3.398788	3.877804	4.093521	4.239095		
C (6)	2.299839	4.017603	1.962541	3.110821	2.766161	
H (7)	2.525895	4.417365	2.614989	2.769155	2.913351	1.090808
H (8)	3.025190	4.785003	2.064367	3.775523	3.729024	1.086929
C (9)	3.060271	4.079967	2.975629	4.151415	1.805749	1.502798
H (10)	4.078908	5.172486	3.807583	5.038453	2.366920	2.124602
H (11)	3.229648	3.817907	2.952363	4.587870	2.380639	2.163301

	H (7)	H (8)	C (9)	H (10)
H (8)	1.791047			
C (9)	2.213692	2.157901		
H (10)	2.661877	2.418767	1.096673	
H (11)	3.098775	2.586489	1.092319	1.773684

Point Group: C_1 Number of degrees of freedom: 27

Energy = -1235.748377535

TS[B4-B3]

Coordinates (Angstroms)

ATOM		X	Y	Z
1	Cr	0.452229	0.727296	-0.081998
2	O	0.724045	1.580620	1.223122
3	O	0.757419	1.278948	-1.535562
4	Cl	1.636802	-1.312092	0.355428
5	Cl	-1.994751	0.399938	0.220198
6	C	-0.390754	-1.538699	-0.706915
7	H	-0.078152	-2.572547	-0.805444
8	H	-0.370119	-1.016800	-1.661952
9	C	-1.638104	-1.394016	0.099500
10	H	-1.529933	-1.747973	1.125613
11	H	-2.499593	-1.881844	-0.374537

Distance Matrix (Angstroms)

	Cr(1)	O (2)	O (3)	Cl(4)	Cl(5)	C (6)
O (2)	1.582840					
O (3)	1.584396	2.775330				
Cl(4)	2.398678	3.154965	3.326056			
Cl(5)	2.487207	3.129172	3.380797	4.017152		
C (6)	2.497174	3.833793	3.153426	2.300197	2.681540	
H (7)	3.419597	4.691204	4.008150	2.424343	3.682521	1.084560
H (8)	2.492867	4.033291	2.560816	2.860900	2.861654	1.088531
C (9)	2.983689	3.961153	3.944198	3.285913	1.833040	1.492354
H (10)	3.393265	4.021126	4.634229	3.288068	2.376837	2.167875
H (11)	3.950500	4.993297	4.684732	4.238777	2.411453	2.162274

	H (7)	H (8)	C (9)	H (10)
H (8)	1.799777			
C (9)	2.154370	2.202905		
H (10)	2.552758	3.106493	1.090823	
H (11)	2.554629	2.634463	1.097657	1.791260

Point Group: C_1 Number of degrees of freedom: 27

Energy = -1235.706456674

TS[B5-B6]

Coordinates (Angstroms)

ATOM		X	Y	Z
1	Cr	1.126986	0.362131	-0.106811
2	O	2.003359	1.633008	0.114771
3	Cl	1.997794	-1.567154	0.159678
4	O	-0.176525	0.594193	-1.042552
5	C	-0.938290	0.884417	0.771339
6	H	-0.637632	1.894923	1.045395
7	H	-0.770091	0.150283	1.560070
8	C	-2.330194	0.821623	0.209251
9	H	-3.009243	1.250104	0.955554
10	H	-2.425978	1.375278	-0.724107
11	Cl	-2.890666	-0.867284	-0.084887

Distance Matrix (Angstroms)

	Cr(1)	O (2)	Cl(3)	O (4)	C (5)	H (6)
O (2)	1.559570					
Cl(3)	2.133416	3.200482				
O (4)	1.621297	2.677765	3.293090			
C (5)	2.304191	3.105603	3.873618	1.988647		
H (6)	2.605936	2.812382	4.440263	2.502807	1.089323	
H (7)	2.534220	3.461125	3.545683	2.706108	1.090569	1.823789
C (8)	3.501874	4.409870	4.943702	2.501405	1.502425	2.171606
H (9)	4.361824	5.097030	5.800067	3.528022	2.111044	2.459350
H (10)	3.745807	4.515437	5.385976	2.402403	2.165761	2.568920
Cl(11)	4.201603	5.499346	4.944357	3.227941	2.759230	3.739450

	H (7)	C (8)	H (9)	H (10)
C (8)	2.170100			
H (9)	2.566876	1.096208		
H (10)	3.075718	1.089434	1.782450	
Cl(11)	2.870221	1.803623	2.362183	2.377735

Point Group: C_1 Number of degrees of freedom: 27

Energy = -1235.746900011

Chapter Three

R1

Coordinates (Angstroms)

ATOM	X	Y	Z
1 Cr	0.000000	0.000000	0.148813
2 Cl	2.302956	0.000000	0.353783
3 Cl	0.000000	-1.886461	-0.814677
4 Cl	0.000000	1.886461	-0.814677
5 Cl	-2.302956	0.000000	0.353783
6 C	0.000000	0.000000	1.904818
7 H	0.000000	-0.935480	2.469384
8 H	0.000000	0.935480	2.469384

Distance Matrix (Angstroms)

	Cr(1)	Cl(2)	Cl(3)	Cl(4)	Cl(5)	C (6)
Cl(2)	2.312059					
Cl(3)	2.118266	3.198068				
Cl(4)	2.118266	3.198068	3.772922			
Cl(5)	2.312059	4.605912	3.198068	3.198068		
C (6)	1.756005	2.776565	3.309742	3.309742	2.776565	
H (7)	2.502033	3.264122	3.418980	4.329944	3.264122	1.092638
H (8)	2.502033	3.264122	4.329944	3.418980	3.264122	1.092638
	H (7)					
H (8)	1.870961					

Point Group: C_{2v} Number of degrees of freedom: 7

Energy = -1966.378887383

R2

Coordinates (Angstroms)

ATOM	X	Y	Z
1 Cr	-0.402782	-0.019828	0.000000
2 Cl	2.707349	-0.203836	0.000000
3 Cl	-1.289703	-0.613850	-1.821759
4 Cl	-0.132923	2.088829	0.000000
5 Cl	-1.289703	-0.613850	1.821759
6 C	1.227891	-1.183983	0.000000
7 H	1.192046	-1.797115	0.901233
8 H	1.192046	-1.797115	-0.901233

Distance Matrix (Angstroms)

	Cr(1)	Cl(2)	Cl(3)	Cl(4)	Cl(5)	C (6)
Cl(2)	3.115570					
Cl(3)	2.111468	4.411728				
Cl(4)	2.125855	3.650131	3.458529			
Cl(5)	2.111468	4.411728	3.643518	3.458529		
C (6)	2.003585	1.774679	3.159452	3.544448	3.159452	
H (7)	2.552342	2.376321	3.869610	4.203371	2.899408	1.090613
H (8)	2.552342	2.376321	2.899408	4.203371	3.869610	1.090613
	H (7)					
H (8)	1.802465					

Point Group: C_s Number of degrees of freedom: 11

Energy = -1966.434393933

R3

Coordinates (Angstroms)

ATOM	X	Y	Z
1 Cr	0.000000	0.000000	0.566060
2 Cl	1.893166	0.000000	1.695274
3 Cl	-1.893166	0.000000	1.695274
4 Cl	0.000000	1.464207	-1.462672
5 Cl	0.000000	-1.464207	-1.462672
6 C	0.000000	0.000000	-2.537648
7 H	-0.910101	0.000000	-3.134009
8 H	0.910101	0.000000	-3.134009

Distance Matrix (Angstroms)

	Cr(1)	Cl(2)	Cl(3)	Cl(4)	Cl(5)	C (6)
Cl(2)	2.204359					
Cl(3)	2.204359	3.786332				
Cl(4)	2.501931	3.962399	3.962399			
Cl(5)	2.501931	3.962399	3.962399	2.928414		
C (6)	3.103708	4.636993	4.636993	1.816446	1.816446	
H (7)	3.810354	5.583930	4.928325	2.401157	2.401157	1.088086
H (8)	3.810354	4.928325	5.583930	2.401157	2.401157	1.088086
	H (7)					
H (8)	1.820202					

Point Group: C_{2v} Number of degrees of freedom: 7

Energy = -1966.404774410

Ethylene

Coordinates (Angstroms)

ATOM	X	Y	Z
1 H	1.240641	-0.922990	0.000000
2 C	0.665417	0.000000	0.000000
3 C	-0.665417	0.000000	0.000000
4 H	1.240641	0.922990	0.000000
5 H	-1.240641	-0.922990	0.000000
6 H	-1.240641	0.922990	0.000000

Distance Matrix (Angstroms)

	H (1)	C (2)	C (3)	H (4)	H (5)
C (2)	1.087562				
C (3)	2.117774	1.330835			
H (4)	1.845980	1.087562	2.117774		
H (5)	2.481281	2.117774	1.087562	3.092636	
H (6)	3.092636	2.117774	1.087562	2.481281	1.845980

Point Group: D_{2h} Number of degrees of freedom: 3

Energy = -78.587447729

p1 Coordinates (Angstroms)

ATOM	X	Y	Z
1 Cr	-0.295118	0.000336	-0.077082
2 C	1.365239	0.000524	-1.324347
3 H	1.421109	0.922501	-1.891751
4 H	1.421670	-0.921266	-1.892034
5 Cl	2.510679	0.000356	0.018981
6 Cl	-2.345301	0.000176	-0.623082
7 Cl	-0.053191	2.266403	-0.310740
8 Cl	-0.052787	-2.266198	-0.312265
9 C	-0.308282	-0.683017	2.134758
10 H	0.606025	-1.255280	2.244785
11 H	-1.234092	-1.248992	2.164541
12 C	-0.308847	0.679973	2.135165
13 H	0.605123	1.252885	2.245826
14 H	-1.235473	1.244656	2.165950

Distance Matrix (Angstroms)

	Cr(1)	C (2)	H (3)	H (4)	Cl(5)	Cl(6)
C (2)	2.076645					
H (3)	2.662489	1.084024				
H (4)	2.662848	1.084043	1.843766			
Cl(5)	2.807441	1.765379	2.385038	2.384807		
Cl(6)	2.121642	3.776225	4.079957	4.080363	4.898243	
Cl(7)	2.290891	2.858942	2.545433	3.851874	3.437603	3.238381
Cl(8)	2.291552	2.858870	3.851616	2.545297	3.437783	3.238622
C (9)	2.315033	3.902987	4.667039	4.389140	3.590272	3.495980
H (10)	2.789211	3.859036	4.745316	4.229671	3.187246	4.302459
H (11)	2.732649	4.526605	5.312154	4.859658	4.493063	3.250546
C (12)	2.314331	3.902875	4.389489	4.666581	3.590242	3.495310
H (13)	2.788407	3.859057	4.230192	4.745057	3.187289	4.301733
H (14)	2.731994	4.527001	4.860673	5.312142	4.493485	3.249483
	Cl(7)	Cl(8)	C (9)	H (10)	H (11)	C (12)
Cl(8)	4.532601					
C (9)	3.839871	2.925689				
H (10)	4.400855	2.827453	1.084227			
H (11)	4.458649	2.926560	1.085513	1.841876		
C (12)	2.926528	3.838671	1.362990	2.143411	2.139591	
H (13)	2.827830	4.400070	2.143447	2.508166	3.106237	1.084350
H (14)	2.928438	4.457172	2.139294	3.105963	2.493648	1.085564
	H (13)					
H (14)	1.842347					

Point Group: C_1 Number of degrees of freedom: 36

Energy = -2045.018131456

TS1 Coordinates (Angstroms)

ATOM	X	Y	Z
1 Cr	0.148630	0.046957	0.184932
2 Cl	2.086776	-0.955537	-0.229401
3 Cl	1.029415	1.939211	0.718756
4 Cl	-2.169727	0.485889	0.535502
5 Cl	-0.426995	0.865871	-1.895889
6 C	-0.185691	-0.706972	1.807046
7 H	0.768495	-0.895714	2.315671
8 H	-1.081106	-0.869375	2.396735
9 C	-0.714614	-1.934135	-0.965707
10 H	0.105301	-2.081482	-1.656783
11 H	-1.652055	-1.575011	-1.371542
12 C	-0.646044	-2.377675	0.339615
13 H	-1.567484	-2.456056	0.908551
14 H	0.224217	-2.929402	0.683392

Distance Matrix (Angstroms)

	Cr(1)	Cl(2)	Cl(3)	Cl(4)	Cl(5)	C (6)
Cl(2)	2.221053					
Cl(3)	2.154385	3.224373				
Cl(4)	2.385444	4.558575	3.518556			
Cl(5)	2.309065	3.523316	3.179553	3.015488		
C (6)	1.819735	3.061537	3.108560	2.641238	4.030359	
H (7)	2.410998	2.866851	3.264202	3.702834	4.719070	1.097632
H (8)	2.691466	4.115761	3.893337	2.546767	4.676063	1.084378
C (9)	2.448242	3.057382	4.569668	3.198046	2.964456	3.077962
H (10)	2.814968	2.689129	4.760583	4.071027	3.004564	3.737923
H (11)	2.880253	3.958168	4.889722	2.855190	2.780939	3.606540
C (12)	2.556223	3.132820	4.646118	3.249612	3.945384	2.270799
H (13)	3.119895	4.110974	5.108647	3.026037	4.494530	2.403318
H (14)	3.018756	2.863295	4.934874	4.173374	4.634746	2.523849

	H (7)	H (8)	C (9)	H (10)	H (11)	C (12)
H (8)	1.851565					
C (9)	3.747716	3.545990				
H (10)	4.198365	4.394061	1.082385			
H (11)	4.462740	3.876056	1.082805	1.850993		
C (12)	2.846389	2.587661	1.380324	2.153567	2.141117	
H (13)	3.141887	2.229083	2.124295	3.085361	2.445856	1.085764
H (14)	2.663918	2.980456	2.142776	2.491893	3.094758	1.086250

	H (13)
H (14)	1.866801

Point Group: C_1 Number of degrees of freedom: 36

Energy = -2044.954388231

Pdt1 Coordinates (Angstroms)

ATOM	X	Y	Z
1 Cr	0.282480	0.073847	0.000000
2 Cl	0.433170	-2.139825	0.000000
3 Cl	1.105910	0.221197	2.039102
4 Cl	-0.384484	2.182519	0.000000
5 Cl	1.105910	0.221197	-2.039102
6 C	-1.559153	-0.282310	1.194356
7 H	-1.326461	-1.154965	1.794201
8 H	-1.682019	0.623525	1.777880
9 C	-1.559153	-0.282310	-1.194356
10 H	-1.326461	-1.154965	-1.794201
11 H	-1.682019	0.623525	-1.777880
12 C	-2.464029	-0.475182	0.000000
13 H	-3.270255	0.267405	0.000000
14 H	-2.893732	-1.483042	0.000000

Distance Matrix (Angstroms)

	Cr(1)	Cl(2)	Cl(3)	Cl(4)	Cl(5)	C (6)
Cl(2)	2.218796					
Cl(3)	2.204016	3.191386				
Cl(4)	2.211637	4.399002	3.197811			
Cl(5)	2.204016	3.191386	4.078205	3.197811		
C (6)	2.223724	2.974257	2.840718	2.980220	4.220348	
H (7)	2.705148	2.699150	2.805392	3.904519	4.743887	1.084199
H (8)	2.705967	3.907811	2.828896	2.697205	4.743814	1.084497
C (9)	2.223724	2.974257	4.220348	2.980220	2.840718	2.388711
H (10)	2.705148	2.699150	4.743887	3.904519	2.805392	3.122041
H (11)	2.705967	3.907811	4.743814	2.697205	2.828896	3.109633
C (12)	2.800848	3.341378	4.169814	3.374593	4.169814	1.510790
H (13)	3.558005	4.417027	4.828136	3.463428	4.828136	2.157902
H (14)	3.537263	3.391113	4.802032	4.442146	4.802032	2.156234

	H (7)	H (8)	C (9)	H (10)	H (11)	C (12)
H (8)	1.813757					
C (9)	3.122041	3.109633				
H (10)	3.588402	4.006146	1.084199			
H (11)	4.006146	3.555759	1.084497	1.813757		
C (12)	2.230543	2.231491	1.510790	2.230543	2.231491	
H (13)	3.003437	2.410430	2.157902	3.003437	2.410430	1.096101
H (14)	2.404814	3.011101	2.156234	2.404814	3.011101	1.095640

	H (13)
H (14)	1.790485

Point Group: C_s Number of degrees of freedom: 21

Energy = -2044.984558072

TS Coordinates (Angstroms)

ATOM	X	Y	Z
1 Cl	-1.374037	-1.598068	-0.135754
2 C	-3.222890	0.550796	0.176061
3 H	-3.392639	0.042790	1.119607
4 H	-3.490505	0.006794	-0.721529
5 C	-2.738502	1.823805	0.122863
6 H	-2.747743	2.362202	-0.820278
7 H	-2.702912	2.430471	1.022593
8 C	-0.603836	1.458369	0.192642
9 H	-0.525317	2.184243	-0.611901
10 H	-0.563057	1.868842	1.199270
11 Cr	0.350939	-0.150478	-0.025261
12 Cl	0.926971	-0.534302	-2.034352
13 Cl	1.033826	-1.042484	1.791646
14 Cl	2.024475	1.511226	0.170760

Distance Matrix (Angstroms)

	Cl(1)	C (2)	H (3)	H (4)	C (5)	H (6)
C (2)	2.851859					
H (3)	2.888442	1.084972				
H (4)	2.719954	1.083154	1.844086			
C (5)	3.692947	1.363090	2.143223	2.140101		
H (6)	4.247279	2.121238	3.091718	2.471719	1.086036	
H (7)	4.397363	2.126070	2.487198	3.088118	1.085737	1.844680
C (8)	3.169047	2.771897	3.261986	3.357921	2.166844	2.537570
H (9)	3.905498	3.250528	3.975610	3.680440	2.359657	2.239256
H (10)	3.802557	3.139891	3.368582	3.965683	2.427600	3.015764
Cr(11)	2.254610	3.647543	3.919497	3.907201	3.669384	4.067855
Cl(12)	3.167162	4.825424	5.379547	4.640085	4.863121	4.833967
Cl(13)	3.133903	4.823722	4.606848	5.280777	5.023038	5.719642
Cl(14)	4.616443	5.334538	5.692252	5.785715	4.773463	4.947765

	H (7)	C (8)	H (9)	H (10)	Cr(11)	Cl(12)
C (8)	2.457625					
H (9)	2.733883	1.086437				
H (10)	2.219374	1.087865	1.838815			
Cr(11)	4.133437	1.883472	2.561814	2.532295		
Cl(12)	5.595609	3.357619	3.394554	4.295532	2.124989	
Cl(13)	5.159076	3.390135	4.315058	3.372946	2.136155	3.861078
Cl(14)	4.890687	2.628933	2.750809	2.807320	2.366518	3.201752

	Cl(13)
Cl(14)	3.182780

Point Group: C_1 Number of degrees of freedom: 36

Energy = -2044.971282245

pdt2 Coordinates (Angstroms)

ATOM	X	Y	Z
1 Cl	-2.743254	-0.445581	0.639108
2 C	-2.672509	0.150576	-1.075170
3 H	-3.682551	0.486159	-1.315604
4 H	-2.429556	-0.715390	-1.695730
5 C	-1.672911	1.287154	-1.261681
6 H	-1.923944	1.767042	-2.222763
7 H	-1.829612	2.050576	-0.491156
8 C	-0.199285	0.920061	-1.331432
9 H	0.013726	0.107672	-2.056132
10 H	0.422414	1.785875	-1.586048
11 Cr	0.808887	-0.028756	0.042193
12 Cl	0.432209	-2.120878	0.117239
13 Cl	2.830651	0.174555	-0.651698
14 Cl	0.477463	1.283908	1.658286

Distance Matrix (Angstroms)

	Cl(1)	C (2)	H (3)	H (4)	C (5)	H (6)
C (2)	1.816359					
H (3)	2.360364	1.091151				
H (4)	2.371218	1.092711	1.777136			
C (5)	2.785858	1.525055	2.164060	2.184283		
H (6)	3.709080	2.119029	2.357180	2.587639	1.103172	
H (7)	2.888432	2.159063	2.561347	3.075956	1.095937	1.757200
C (8)	3.495681	2.602809	3.510223	2.789538	1.520262	2.118088
H (9)	3.895042	2.860068	3.788681	2.603257	2.206144	2.556529
H (10)	4.466786	3.537478	4.314295	3.795009	2.178147	2.431287
Cr(11)	3.625984	3.660708	4.720357	3.738898	3.096938	3.977849
Cl(12)	3.628021	4.027482	5.077492	3.667690	4.236464	5.113021
Cl(13)	5.754926	5.519482	6.554363	5.436155	4.678892	5.254564
Cl(14)	3.795111	4.321869	5.175533	4.867995	3.626338	4.589413

	H (7)	C (8)	H (9)	H (10)	Cr(11)	Cl(12)
C (8)	2.154552					
H (9)	3.101923	1.109297				
H (10)	2.518031	1.095889	1.790075			
Cr(11)	3.401435	1.950259	2.248080	2.468484		
Cl(12)	4.784037	3.427060	3.140876	4.261925	2.127086	
Cl(13)	5.026260	3.193483	3.148329	3.044498	2.147172	3.407756
Cl(14)	3.245069	3.086873	3.923708	3.283399	2.108242	3.737572

	Cl(13)
Cl(14)	3.479107

Point Group: C_1 Number of degrees of freedom: 36

Energy = -2045.069618158

TS3

Coordinates (Angstroms)

ATOM	X	Y	Z
1 Cr	0.585199	0.003313	-0.222090
2 Cl	1.487610	1.834062	0.368931
3 Cl	1.491166	-1.835187	0.338659
4 Cl	-0.868477	0.014201	-1.899458
5 Cl	-1.515113	-0.009670	1.333890
6 C	-2.919336	-0.005837	0.450555
7 H	-3.305814	-0.956225	0.109900
8 H	-3.308727	0.947810	0.122669

Distance Matrix (Angstroms)

	Cr(1)	Cl(2)	Cl(3)	Cl(4)	Cl(5)	C (6)
Cl(2)	2.124922					
Cl(3)	2.124922	3.669375				
Cl(4)	2.219652	3.742810	3.741299			
Cl(5)	2.613915	3.653332	3.655230	3.297460		
C (6)	3.568515	4.776302	4.776146	3.119132	1.658957	
H (7)	4.021307	5.552451	4.882204	3.304521	2.366585	1.081040
H (8)	4.021640	4.883742	5.552539	3.303852	2.366616	1.081007

	H (7)
H (8)	1.904080

Point Group: C_1 Number of degrees of freedom: 18

Energy = -1966.362913047

R4eq Coordinates (Angstroms)

ATOM	X	Y	Z
1 Mo	0.000000	0.000000	0.169456
2 Cl	2.380303	0.000000	-0.054973
3 Cl	0.000000	-2.112168	-0.664127
4 Cl	0.000000	2.112168	-0.664127
5 Cl	-2.380303	0.000000	-0.054973
6 C	0.000000	0.000000	2.025767
7 H	0.000000	-0.937257	2.588838
8 H	0.000000	0.937257	2.588838

Distance Matrix (Angstroms)

	Mo(1)	Cl(2)	Cl(3)	Cl(4)	Cl(5)	C (6)
Cl(2)	2.390860					
Cl(3)	2.270708	3.240088				
Cl(4)	2.270708	3.240088	4.224337			
Cl(5)	2.390860	4.760607	3.240088	3.240088		
C (6)	1.856312	3.161539	3.420057	3.420057	3.161539	
H (7)	2.594583	3.678863	3.458642	4.458787	3.678863	1.093389
H (8)	2.594583	3.678863	4.458787	3.458642	3.678863	1.093389

	H (7)
H (8)	1.874515

Point Group: C_{2v} Number of degrees of freedom: 7

Energy = -1947.702885268

R4ax Coordinates (Angstroms)

ATOM	X	Y	Z
1 Mo	0.052746	0.205328	0.000000
2 Cl	-2.234299	-0.010639	0.000000
3 Cl	0.926900	0.314083	-2.094351
4 Cl	0.271240	-2.209161	0.000000
5 Cl	0.926900	0.314083	2.094351
6 C	-0.022762	2.152716	0.000000
7 H	-0.055669	2.758734	0.909874
8 H	-0.055669	2.758734	-0.909874

Distance Matrix (Angstroms)

	Mo(1)	Cl(2)	Cl(3)	Cl(4)	Cl(5)	C (6)
Cl(2)	2.297219					
Cl(3)	2.272065	3.805907				
Cl(4)	2.424354	3.333350	3.344093			
Cl(5)	2.272065	3.805907	4.188702	3.344093		
C (6)	1.948852	3.093703	2.944271	4.371774	2.944271	
H (7)	2.712842	3.639193	3.995889	5.061099	2.888727	1.093715
H (8)	2.712842	3.639193	2.888727	5.061099	3.995889	1.093715

	H (7)
H (8)	1.819749

Point Group: C_s Number of degrees of freedom: 11

Energy = -1947.682401258

R5 Coordinates (Angstroms)

ATOM	X	Y	Z
1 Mo	-0.466268	-0.053487	0.000000
2 Cl	2.887555	-0.354043	0.000000
3 Cl	-1.286302	-0.496932	-2.047443
4 Cl	0.234652	2.117551	0.000000
5 Cl	-1.286302	-0.496932	2.047443
6 C	1.286220	-1.194079	0.000000
7 H	1.261350	-1.836521	0.888122
8 H	1.261350	-1.836521	-0.888122

Distance Matrix (Angstroms)

	Mo(1)	Cl(2)	Cl(3)	Cl(4)	Cl(5)	C (6)
Cl(2)	3.367264					
Cl(3)	2.249693	4.651185				
Cl(4)	2.281380	3.625834	3.652512			
Cl(5)	2.249693	4.651185	4.094885	3.652512		
C (6)	2.090972	1.808296	3.360939	3.474577	3.360939	
H (7)	2.636785	2.372982	4.111274	4.180616	3.103072	1.096408
H (8)	2.636785	2.372982	3.103072	4.180616	4.111274	1.096408

	H (7)
H (8)	1.776244

Point Group: C_s Number of degrees of freedom: 11

Energy = -1947.690641634

p2

Coordinates (Angstroms)

ATOM	X	Y	Z
1 Mo	-0.258101	-0.000148	-0.025783
2 C	1.446856	0.000328	-1.365347
3 H	1.569013	0.917503	-1.934464
4 H	1.569911	-0.917030	-1.933956
5 Cl	2.564460	0.001210	0.040996
6 Cl	-2.455698	-0.001297	-0.505533
7 Cl	-0.010113	2.369053	-0.372149
8 Cl	-0.007559	-2.369133	-0.371608
9 C	-0.156724	-0.706211	2.059441
10 H	0.754399	-1.270401	2.233634
11 H	-1.072666	-1.261517	2.252400
12 C	-0.157880	0.707020	2.059299
13 H	0.752254	1.272835	2.233498
14 H	-1.074684	1.260862	2.252429

Distance Matrix (Angstroms)

	Mo(1)	C (2)	H (3)	H (4)	Cl(5)	Cl(6)
C (2)	2.168250					
H (3)	2.797050	1.086290				
H (4)	2.797038	1.086280	1.834533			
Cl(5)	2.823352	1.796341	2.394358	2.394312		
Cl(6)	2.249354	3.996150	4.368562	4.368580	5.049821	
Cl(7)	2.407193	2.952974	2.653575	3.966618	3.522187	3.408407
Cl(8)	2.407168	2.952488	3.966116	2.652913	3.521939	3.408515
C (9)	2.203852	3.847056	4.643909	4.355793	3.461128	3.515861
H (10)	2.782745	3.879035	4.777401	4.261307	3.114639	4.406630
H (11)	2.728495	4.585666	5.408920	4.962606	4.439985	3.332736
C (12)	2.204019	3.847439	4.356214	4.644231	3.461625	3.515686
H (13)	2.783102	3.879875	4.262072	4.778257	3.115796	4.406434
H (14)	2.728957	4.586438	4.963577	5.409520	4.440780	3.332657

	Cl(7)	Cl(8)	C (9)	H (10)	H (11)	C (12)
Cl(8)	4.738187					
C (9)	3.923184	2.949163				
H (10)	4.540948	2.928323	1.085726			
H (11)	4.604162	3.040836	1.088369	1.827183		
C (12)	2.948920	3.923598	1.413231	2.184683	2.179279	
H (13)	2.927848	4.541786	2.184756	2.543237	3.123080	1.085742
H (14)	3.041350	4.604475	2.179282	3.123010	2.522380	1.088379

	H (13)
H (14)	1.827075

Point Group: C_1 Number of degrees of freedom: 36

Energy = -2026.314240052

TS4 Coordinates (Angstroms)

ATOM		X	Y	Z
1	Mo	0.087131	0.015259	0.116380
2	Cl	2.276674	-0.645336	-0.472636
3	Cl	0.984888	1.971515	0.947232
4	Cl	-2.277279	-0.086245	0.719370
5	Cl	-0.899634	1.334141	-1.631789
6	C	0.035254	-1.237652	1.635824
7	H	1.032541	-1.516508	1.991886
8	H	-0.789774	-1.577219	2.252394
9	C	-0.382071	-1.710564	-1.316903
10	H	0.413033	-1.755226	-2.050360
11	H	-1.377118	-1.504931	-1.695118
12	C	-0.254681	-2.431078	-0.095865
13	H	-1.165892	-2.800635	0.364345
14	H	0.658743	-2.992002	0.077366

Distance Matrix (Angstroms)

	Mo(1)	Cl(2)	Cl(3)	Cl(4)	Cl(5)	C (6)
Cl(2)	2.361657					
Cl(3)	2.307211	3.245404				
Cl(4)	2.442198	4.740458	3.863681			
Cl(5)	2.401926	3.918022	3.257149	3.073003		
C (6)	1.970072	3.133753	3.416828	2.741064	4.262091	
H (7)	2.599544	2.894940	3.641412	3.823592	4.999052	1.095045
H (8)	2.804907	4.206816	4.176887	2.604963	4.855405	1.084498
C (9)	2.291924	2.986038	4.533497	3.221278	3.104392	3.019337
H (10)	2.817018	2.682206	4.816761	4.206504	3.382674	3.741463
H (11)	2.781462	3.947603	4.964551	2.941549	2.879641	3.627865
C (12)	2.479203	3.120672	4.691206	3.202147	4.117268	2.122987
H (13)	3.092056	4.146940	5.266785	2.954511	4.599110	2.345703
H (14)	3.061352	2.902937	5.049707	4.180408	4.905635	2.428018

	H (7)	H (8)	C (9)	H (10)	H (11)	C (12)
H (8)	1.841843					
C (9)	3.603729	3.594980				
H (10)	4.096404	4.471255	1.082656			
H (11)	4.404610	3.991622	1.084182	1.842141		
C (12)	2.617648	2.555331	1.423482	2.173170	2.162226	
H (13)	3.021751	2.280995	2.151563	3.068661	2.442305	1.085666
H (14)	2.445852	2.971625	2.160870	2.473298	3.081852	1.085813

	H (13)
H (14)	1.856952

Point Group: C_1 Number of degrees of freedom:36

Energy = -2026.281920802

pdt3 Coordinates (Angstroms)

ATOM		X	Y	Z
1	Mo	0.178978	0.092463	0.000000
2	Cl	0.886199	-2.099659	0.000000
3	Cl	0.925873	0.312974	2.222527
4	Cl	-0.420076	2.318505	0.000000
5	Cl	0.925873	0.312974	-2.222527
6	C	-1.659595	-0.533557	1.144978
7	H	-1.356254	-1.153536	1.987068
8	H	-2.076580	0.413707	1.490654
9	C	-1.659595	-0.533557	-1.144978
10	H	-1.356254	-1.153536	-1.987068
11	H	-2.076580	0.413707	-1.490654
12	C	-2.401338	-1.184799	0.000000
13	H	-3.482094	-0.985144	0.000000
14	H	-2.249928	-2.268658	0.000000

Distance Matrix (Angstroms)

	Mo(1)	Cl(2)	Cl(3)	Cl(4)	Cl(5)	C (6)
Cl(2)	2.303381					
Cl(3)	2.355017	3.280549				
Cl(4)	2.305239	4.607226	3.282280			
Cl(5)	2.355017	3.280549	4.445054	3.282280		
C (6)	2.254601	3.200737	2.926153	3.313855	4.329128	
H (7)	2.803193	3.142004	2.722903	4.108520	5.007939	1.088809
H (8)	2.722643	4.161384	3.092008	2.931605	4.776252	1.091181
C (9)	2.254601	3.200737	4.329128	3.313855	2.926153	2.289956
H (10)	2.803193	3.142004	5.007939	4.108520	2.722903	3.207196
H (11)	2.722643	4.161384	4.776252	2.931605	3.092008	2.831562
C (12)	2.879137	3.412458	4.272386	4.024741	4.272386	1.511712
H (13)	3.816371	4.508230	5.104402	4.504448	5.104402	2.199184
H (14)	3.387399	3.140677	4.657270	4.938665	4.657270	2.161028

	H (7)	H (8)	C (9)	H (10)	H (11)	C (12)
H (8)	1.794867					
C (9)	3.207196	2.831562				
H (10)	3.974137	3.881967	1.088809			
H (11)	3.881967	2.981308	1.091181	1.794867		
C (12)	2.245355	2.209692	1.511712	2.245355	2.209692	
H (13)	2.914789	2.480787	2.199184	2.914789	2.480787	1.099044
H (14)	2.447568	3.073626	2.161028	2.447568	3.073626	1.094383

	H (13)
H (14)	1.779225

Point Group: C_s Number of degrees of freedom: 21

Energy = -2026.309727837

TS5 Coordinates (Angstroms)

ATOM		X	Y	Z
1	Cl	-1.601945	1.408828	0.000000
2	C	-3.445015	-0.556521	0.000000
3	H	-3.759533	-0.079446	-0.921432
4	H	-3.759533	-0.079446	0.921432
5	C	-2.805006	-1.771850	0.000000
6	H	-2.796596	-2.349804	0.919568
7	H	-2.796596	-2.349804	-0.919568
8	C	-0.673541	-1.592274	0.000000
9	H	-0.565165	-2.176876	0.916110
10	H	-0.565165	-2.176876	-0.916110
11	Mo	0.348012	0.054657	0.000000
12	Cl	0.799235	0.766345	2.113420
13	Cl	0.799235	0.766345	-2.113420
14	Cl	2.421821	-1.150256	0.000000

Distance Matrix (Angstroms)

	Cl(1)	C (2)	H (3)	H (4)	C (5)	H (6)
C (2)	2.694347					
H (3)	2.778342	1.084232				
H (4)	2.778342	1.084232	1.842864			
C (5)	3.400599	1.373549	2.150439	2.150439		
H (6)	4.049705	2.117054	3.077507	2.466126	1.086143	
H (7)	4.049705	2.117054	2.466126	3.077507	1.086143	1.839135

C (8) 3.141424 2.958691 3.558235 3.558235 2.139017 2.434506
H (9) 3.843364 3.429044 4.240255 3.821417 2.453608 2.238124
H (10) 3.843364 3.429044 3.821417 4.240255 2.453608 2.894633
Mo(11) 2.374049 3.841952 4.211763 4.211763 3.643852 4.063939
Cl(12) 3.262667 4.922416 5.541485 4.787334 4.888715 4.905678
Cl(13) 3.262667 4.922416 4.787334 5.541485 4.888715 5.642641
Cl(14) 4.768606 5.896803 6.340726 6.340726 5.263659 5.432899
H (7) C (8) H (9) H (10) Mo(11) Cl(12)
C (8) 2.434506
H (9) 2.894633 1.092136
H (10) 2.238124 1.092136 1.832219
Mo(11) 4.063939 1.938028 2.579320 2.579320
Cl(12) 5.642641 3.492663 3.457990 4.438715 2.275224
Cl(13) 4.905678 3.492663 4.438715 3.457990 2.275224 4.226840
Cl(14) 5.432899 3.126762 3.288660 3.288660 2.398437 3.282177
Cl(13)
Cl(14) 3.282177
Point Group: C_s Number of degrees of freedom: 21
Energy = -2026.279298220

pdt4 Coordinates (Angstroms)

ATOM	X	Y	Z
1 Cl	-2.146163	0.315611	0.908031
2 C	-2.860920	0.187431	-0.786846
3 H	-2.827875	1.202358	-1.188065
4 H	-3.895760	-0.124059	-0.640772
5 C	-2.044261	-0.797324	-1.602448
6 H	-2.171601	-1.806384	-1.191953
7 H	-2.476352	-0.811962	-2.615613
8 C	-0.553862	-0.449959	-1.670622
9 H	0.006041	-1.183138	-2.262952
10 H	-0.388334	0.542974	-2.139760
11 Mo	0.474500	0.031454	0.084164
12 Cl	0.397483	-1.923519	1.247300
13 Cl	2.589998	-0.240744	-0.822625
14 Cl	0.615512	2.277892	0.478261

Distance Matrix (Angstroms)
Cl(1) C (2) H (3) H (4) C (5) H (6)
C (2) 1.843887
H (3) 2.375852 1.091854
H (4) 2.377644 1.090531 1.788656
C (5) 2.748002 1.517195 2.187348 2.192294
H (6) 2.985539 2.148156 3.079488 2.471183 1.096779
H (7) 3.714366 2.119214 2.493782 2.527435 1.101553 1.763110
C (8) 3.125855 2.551439 2.852043 3.512134 1.531861 2.164738
H (9) 4.115017 3.503829 3.857079 4.356279 2.188346 2.505514
H (10) 3.525718 2.840857 2.700347 3.872200 2.197088 3.098042
Mo(11)2.761770 3.450799 3.727635 4.432706 3.142561 3.465252
Cl(12) 3.405722 4.383041 5.109310 5.023426 3.918098 3.544554
Cl(13) 5.073058 5.467826 5.618669 6.489356 4.732257 5.025978
Cl(14) 3.414981 4.249247 3.973705 5.231938 4.567351 5.219092
H (7) C (8) H (9) H (10) Mo(11) Cl(12)
C (8) 2.172561
H (9) 2.534643 1.096311
H (10) 2.534187 1.110588 1.774872
Mo(11) 4.087502 2.090110 2.683960 2.439667
Cl(12) 4.941313 3.404512 3.608775 4.263011 2.276122
Cl(13) 5.404534 3.262932 3.104751 3.349555 2.317691 3.453033
Cl(14) 5.355266 3.664192 4.456954 3.297223 2.285100 4.276776
Cl(13)
Cl(14) 3.454625
Point Group: C_1 Number of degrees of freedom: 36
Energy = -2026.332828092

R6eq Coordinates (Angstroms)

ATOM	X	Y	Z
1 W	0.000000	0.000000	0.127888
2 Cl	2.349686	0.000000	-0.221974
3 Cl	0.000000	-2.171449	-0.558750
4 Cl	0.000000	2.171449	-0.558750
5 Cl	-2.349686	0.000000	-0.221974
6 C	0.000000	0.000000	1.991042
7 H	0.000000	-0.929034	2.567355
8 H	0.000000	0.929034	2.567355

Distance Matrix (Angstroms)
W (1) Cl(2) Cl(3) Cl(4) Cl(5) C (6)
Cl(2) 2.375589
Cl(3) 2.277425 3.217084
Cl(4) 2.277425 3.217084 4.342898
Cl(5) 2.375589 4.699371 3.217084 3.217084
C (6) 1.863154 3.227764 3.349124 3.349124 3.227764
H (7) 2.610384 3.763574 3.363946 4.402900 3.763574 1.093271
H (8) 2.610384 3.763574 4.402900 3.363946 3.763574 1.093271
H (7)
H (8) 1.858069
Point Group: C_{2v} Number of degrees of freedom: 7
Energy = -1948.028406028

R6ax Coordinates (Angstroms)

ATOM	X	Y	Z
1 W	0.056565	0.169389	0.000000
2 Cl	-2.232867	0.181143	0.000000
3 Cl	0.896406	0.138882	-2.112134
4 Cl	0.067442	-2.256282	0.000000
5 Cl	0.896406	0.138882	2.112134
6 C	0.247104	2.095078	0.000000
7 H	0.308793	2.708199	0.904011
8 H	0.308793	2.708199	-0.904011

Distance Matrix (Angstroms)
W (1) Cl(2) Cl(3) Cl(4) Cl(5) C (6)
Cl(2) 2.289462
Cl(3) 2.273185 3.775612
Cl(4) 2.425696 3.351487 3.299258
Cl(5) 2.273185 3.775612 4.224267 3.299258
C (6) 1.935092 3.132635 2.951170 4.355068 2.951170
H (7) 2.706734 3.696387 4.005472 5.051887 2.899352 1.094056
H (8) 2.706734 3.696387 2.899352 5.051887 4.005472 1.094056
H (7)
H (8) 1.808021
Point Group: C_s Number of degrees of freedom: 11
Energy = -1948.007162653

R7 Coordinates (Angstroms)

ATOM	X	Y	Z
1 W	-0.378347	-0.048741	0.000000
2 Cl	3.001797	-0.325780	0.000000
3 Cl	-1.154040	-0.480690	-2.065579
4 Cl	0.306796	2.128348	0.000000
5 Cl	-1.154040	-0.480690	2.065579
6 C	1.370367	-1.173811	0.000000
7 H	1.383374	-1.825275	0.882129
8 H	1.383374	-1.825275	-0.882129

Distance Matrix (Angstroms)
W (1) Cl(2) Cl(3) Cl(4) Cl(5) C (6)
Cl(2) 3.391478
Cl(3) 2.248310 4.643446
Cl(4) 2.282354 3.644965 3.634245
Cl(5) 2.248310 4.643446 4.131158 3.634245
C (6) 2.079371 1.838674 3.334616 3.469213 3.334616
H (7) 2.652902 2.376116 4.115260 4.191457 3.105951 1.096689
H (8) 2.652902 2.376116 3.105951 4.191457 4.115260 1.096689
H (7)
H (8) 1.764259
Point Group: C_s Number of degrees of freedom: 11
Energy = -1947.978633867

p3 Coordinates (Angstroms)

ATOM	X	Y	Z
1 W	-0.191379	-0.000011	-0.005935
2 C	1.477261	0.000112	-1.379308
3 H	1.637567	0.911070	-1.950042
4 H	1.637466	-0.910776	-1.950149
5 Cl	2.604520	-0.000081	0.047324
6 Cl	-2.408464	0.000130	-0.405544
7 Cl	-0.031543	2.354995	-0.431000
8 Cl	-0.031754	-2.355025	-0.431063
9 C	-0.015450	-0.717378	2.027673
10 H	0.896747	-1.277269	2.215159
11 H	-0.919849	-1.262359	2.298464
12 C	-0.015652	0.717327	2.027759
13 H	0.896441	1.277406	2.215202
14 H	-0.920179	1.262031	2.298658

Distance Matrix (Angstroms)
W (1) C (2) H (3) H (4) Cl(5) Cl(6)
C (2) 2.161137
H (3) 2.820401 1.086867
H (4) 2.820307 1.086849 1.821846
Cl(5) 2.796406 1.818238 2.398888 2.398845
Cl(6) 2.252810 4.005880 4.425568 4.425505 5.033398
Cl(7) 2.398391 2.953177 2.679242 3.969718 3.567072 3.346010
Cl(8) 2.398397 2.953467 3.970052 2.679510 3.567150 3.346066
C (9) 2.163592 3.788205 4.605054 4.311913 3.361627 3.487389
H (10) 2.783643 3.858612 4.763039 4.246500 3.040922 4.407296
H (11) 2.726619 4.567930 5.414238 4.971336 4.368313 3.334894
C (12) 2.163647 3.788310 4.312026 4.605135 3.361859 3.487246
H (13) 2.783630 3.858670 4.246495 4.763129 3.041249 4.407056

H (14)	2.726728	4.568106	4.971588	5.414332	4.368630	3.334681
	Cl(7)	Cl(8)	C (9)	H (10)	H (11)	C (12)
Cl(8)	4.710020					
C (9)	3.935074	2.954241				
H (10)	4.588814	3.004357	1.086615			
H (11)	4.617825	3.071311	1.090078	1.818567		
C (12)	2.954268	3.935151	1.434705	2.201364	2.193174	
H (13)	3.004120	4.588989	2.201335	2.554675	3.123500	1.086617
H (14)	3.071689	4.617767	2.193177	3.123497	2.524389	1.090072
	H (13)					
H (14)	1.818601					

Point Group: C_1 Number of degrees of freedom: 36

Energy = -2026.621537896

TS6

Coordinates (Angstroms)

ATOM	X	Y	Z
1 W	0.047743	-0.018181	0.099651
2 Cl	2.191519	-0.757147	-0.456354
3 Cl	0.985120	1.905695	1.009482
4 Cl	-2.257535	0.070857	0.676609
5 Cl	-0.660022	1.422927	-1.716980
6 C	0.015859	-1.247470	1.652497
7 H	0.964771	-1.680871	1.983029
8 H	-0.826563	-1.535570	2.276064
9 C	-0.534479	-1.656536	-1.376314
10 H	0.242890	-1.731953	-2.127937
11 H	-1.520345	-1.394696	-1.745162
12 C	-0.440767	-2.440542	-0.198316
13 H	-1.353464	-2.747797	0.301292
14 H	0.441330	-3.049962	-0.032467

Distance Matrix (Angstroms)

	W (1)	Cl(2)	Cl(3)	Cl(4)	Cl(5)	C (6)
Cl(2)	2.334735					
Cl(3)	2.325461	3.270291				
Cl(4)	2.378049	4.665113	3.740621			
Cl(5)	2.424432	3.804364	3.220738	3.179530		
C (6)	1.980783	3.069392	3.360861	2.803331	4.352151	
H (7)	2.674433	2.882493	3.716405	3.893397	5.095448	1.094314
H (8)	2.793502	4.144981	4.090077	2.680772	4.972408	1.086974
C (9)	2.280715	3.014348	4.548702	3.188620	3.100791	3.105463
H (10)	2.817311	2.746196	4.860739	4.167460	3.307174	3.818108
H (11)	2.785145	3.980632	4.975742	2.925110	2.946176	3.731714
C (12)	2.489028	3.135176	4.730931	3.220756	4.157019	2.248875
H (13)	3.074874	4.135653	5.255997	2.983793	4.685000	2.439628
H (14)	3.060075	2.915449	5.093123	4.186427	4.904824	2.503819
	H (7)	H (8)	C (9)	H (10)	H (11)	C (12)
H (8)	1.820951					
C (9)	3.678795	3.666034				
H (10)	4.174178	4.536245	1.083941			
H (11)	4.489667	4.083067	1.084685	1.835553		
C (12)	2.703868	2.662775	1.418142	2.166315	2.156854	
H (13)	3.056270	2.376308	2.162394	3.079194	2.459005	1.084911
H (14)	2.492113	3.038133	2.167894	2.483449	3.085677	1.084893
	H (13)					
H (14)	1.850402					

Point Group: C_1 Number of degrees of freedom: 36

Energy = -2026.611182571

pdt5 Coordinates (Angstroms)

ATOM	X	Y	Z
1 W	0.113559	0.068559	0.000000
2 Cl	0.980042	-2.054939	0.000000
3 Cl	0.901967	0.348811	2.198532
4 Cl	-0.509913	2.282504	0.000000
5 Cl	0.901967	0.348811	-2.198532
6 C	-1.664427	-0.624302	1.139482
7 H	-1.368183	-1.229257	1.998082
8 H	-2.146407	0.291536	1.494548
9 C	-1.664427	-0.624302	-1.139482
10 H	-1.368183	-1.229257	-1.998082
11 H	-2.146407	0.291536	-1.494548
12 C	-2.398574	-1.308252	0.000000
13 H	-3.485867	-1.156136	0.000000
14 H	-2.205831	-2.386187	0.000000

Distance Matrix (Angstroms)

	W (1)	Cl(2)	Cl(3)	Cl(4)	Cl(5)	C (6)
Cl(2)	2.293477					
Cl(3)	2.352376	3.258474				
Cl(4)	2.300058	4.586216	3.250557			
Cl(5)	2.352376	3.258474	4.397065	3.250557		
C (6)	2.222546	3.215332	2.941924	3.328790	4.321535	
H (7)	2.805748	3.191903	2.772014	4.130548	5.025481	1.091295
H (8)	2.718609	4.185009	3.129131	2.979218	4.789019	1.094136
C (9)	2.222546	3.215332	4.321535	3.328790	2.941924	2.278964
H (10)	2.805748	3.191903	5.025481	4.130548	2.772014	3.209056
H (11)	2.718609	4.185009	4.789019	2.979218	3.129131	2.830049
C (12)	2.864685	3.460142	4.298020	4.057163	4.298020	1.518282
H (13)	3.802071	4.555458	5.133372	4.547587	5.133372	2.213349
H (14)	3.377180	3.203047	4.687448	4.967173	4.687448	2.166974
	H (7)	H (8)	C (9)	H (10)	H (11)	C (12)
H (8)	1.781008					
C (9)	3.209056	2.830049				
H (10)	3.996165	3.888047	1.091295			
H (11)	3.888047	2.989095	1.094136	1.781008		
C (12)	2.249506	2.203766	1.518282	2.249506	2.203766	
H (13)	2.912433	2.474587	2.213349	2.912433	2.474587	1.097883
H (14)	2.456109	3.067149	2.166974	2.456109	3.067149	1.095031
	H (13)					
H (14)	1.775252					

Point Group: C_s Number of degrees of freedom: 21

Energy = -2026.636744262

TS7 Coordinates (Angstroms)

ATOM	X	Y	Z
1 Cl	-1.672662	1.348864	0.000000
2 C	-3.469879	-0.539792	0.000000
3 H	-3.822436	-0.089869	-0.921212
4 H	-3.822436	-0.089869	0.921212
5 C	-2.773949	-1.740434	0.000000
6 H	-2.815639	-2.328079	0.913645
7 H	-2.815639	-2.328079	-0.913645
8 C	-0.760703	-1.598413	0.000000
9 H	-0.595976	-2.193006	0.903669
10 H	-0.595976	-2.193006	-0.903669
11 W	0.289096	0.049200	0.000000
12 Cl	0.664159	0.688969	2.158283
13 Cl	0.664159	0.688969	-2.158283
14 Cl	2.409176	-1.029570	0.000000

Distance Matrix (Angstroms)

	Cl(1)	C (2)	H (3)	H (4)	C (5)	H (6)
C (2)	2.607109					
H (3)	2.745927	1.084139				
H (4)	2.745927	1.084139	1.842424			
C (5)	3.279725	1.387753	2.161555	2.161555		
H (6)	3.957405	2.112048	3.064298	2.454237	1.087112	
H (7)	3.957405	2.112048	2.454237	3.064298	1.087112	1.827290
C (8)	3.085144	2.908662	3.535328	3.535328	2.018250	2.364301
H (9)	3.810606	3.436430	4.261856	3.851432	2.401043	2.223791
H (10)	3.810606	3.436430	3.851432	4.261856	2.401043	2.871894
W (11)	2.353215	3.804840	4.215764	4.215764	3.547540	4.015667
Cl(12)	3.248750	4.822687	5.497219	4.718736	4.730832	4.770817
Cl(13)	3.248750	4.822687	4.718736	5.497219	4.730832	5.536092
Cl(14)	4.724230	5.899421	6.369038	6.369038	5.231646	5.460729
	H (7)	C (8)	H (9)	H (10)	W (11)	Cl(12)
C (8)	2.364301					
H (9)	2.871894	1.094209				
H (10)	2.223791	1.094209	1.807339			
W (11)	4.015667	1.953639	2.574385	2.574385		
Cl(12)	5.536092	3.452612	3.386410	4.389678	2.282140	
Cl(13)	4.770817	3.452612	4.389678	3.386410	2.282140	4.316565
Cl(14)	5.460729	3.220514	3.346811	3.346811	2.378756	3.264451
	Cl(13)					
Cl(14)	3.264451					

Point Group: C_s Number of degrees of freedom: 21

Energy = -2026.593764066

pdt6 Coordinates (Angstroms)

ATOM	X	Y	Z
1 Cl	-2.073109	0.244772	0.970731
2 C	-2.991642	0.211673	-0.655264
3 H	-3.030324	1.256366	-0.969984
4 H	-3.988653	-0.151549	-0.405634
5 C	-2.220879	-0.676586	-1.608476
6 H	-2.338778	-1.724799	-1.307913
7 H	-2.689956	-0.574755	-2.598623
8 C	-0.721832	-0.324105	-1.686536
9 H	-0.197051	-1.014615	-2.359448
10 H	-0.582987	0.688297	-2.121460
11 W	0.353740	0.020365	0.073910
12 Cl	0.376663	-2.043964	1.037444
13 Cl	2.489064	-0.181409	-0.832574
14 Cl	0.532270	2.270107	0.466830

Distance Matrix (Angstroms)

	Cl(1)	C (2)	H (3)	H (4)	C (5)	H (6)
C (2)	1.867795					
H (3)	2.388714	1.091755				
H (4)	2.391811	1.090080	1.794188			
C (5)	2.742817	1.513834	2.190702	2.201708		
H (6)	3.023576	2.145252	3.078924	2.451797	1.096808	
H (7)	3.713813	2.118047	2.474129	2.583586	1.100360	1.764046
C (8)	3.034903	2.550023	2.887987	3.513204	1.541907	2.172512

H (9)	4.024393	3.495392	3.887853	4.351841	2.184972	2.489394
H (10)	3.461043	2.859811	2.763703	3.904863	2.192886	3.093168
W (11)	2.596968	3.429268	3.750907	4.372172	3.153543	3.493520
Cl(12)	3.353230	4.393022	5.150680	4.971890	3.951942	3.602247
Cl(13)	4.924120	5.497644	5.705236	6.491840	4.799041	5.090781
Cl(14)	3.338247	4.232517	3.972931	5.202341	4.535386	5.229904

	H (7)	C (8)	H (9)	H (10)	W (11)	Cl(12)
C (8)	2.183630					
H (9)	2.542687	1.097729				
H (10)	2.502459	1.110583	1.762240			
W (11)	4.093982	2.091575	2.701071	2.478556		
Cl(12)	4.978324	3.403626	3.595495	4.285423	2.278240	
Cl(13)	5.485973	3.325578	3.200123	3.443126	2.328526	3.380579
Cl(14)	5.279486	3.597178	4.394217	3.231898	2.290763	4.354425

	Cl(13)
Cl(14)	3.395206

Point Group: C_1 Number of degrees of freedom: 36

Energy = -2026.624358131

R8eq Coordinates (Angstroms)

ATOM	X	Y	Z
1 Ru	0.000000	0.000000	-0.001091
2 Cl	0.000000	-2.270669	0.461498
3 Cl	2.339333	0.000000	0.003936
4 Cl	-2.339333	0.000000	0.003936
5 Cl	0.000000	2.270669	0.461498
6 C	0.000000	0.000000	-1.834501
7 H	0.942864	0.000000	-2.384882
8 H	-0.942864	0.000000	-2.384882

Distance Matrix (Angstroms)

	Ru(1)	Cl(2)	Cl(3)	Cl(4)	Cl(5)	C (6)
Cl(2)	2.317310					
Cl(3)	2.339338	3.292078				
Cl(4)	2.339338	3.292078	4.678666			
Cl(5)	2.317310	4.541337	3.292078	3.292078		
C (6)	1.833410	3.229172	2.975287	2.975287	3.229172	
H (7)	2.563484	3.761225	2.767052	4.059467	3.761225	1.091747
H (8)	2.563484	3.761225	4.059467	2.767052	3.761225	1.091747

	H (7)
H (8)	1.885728

Point Group: C_{2v} Number of degrees of freedom: 7

Energy = -1973.972019323

R9 Coordinates (Angstroms)

ATOM	X	Y	Z
1 Ru	-0.338012	0.032841	0.000000
2 Cl	2.840218	-0.492841	0.000000
3 Cl	-1.432883	-0.539656	-1.855176
4 Cl	0.324570	2.161206	0.000000
5 Cl	-1.432883	-0.539656	1.855176
6 C	1.248672	-1.281915	0.000000
7 H	1.148558	-1.883713	0.905983
8 H	1.148558	-1.883713	-0.905983

Distance Matrix (Angstroms)

	Ru(1)	Cl(2)	Cl(3)	Cl(4)	Cl(5)	C (6)
Cl(2)	3.221411					
Cl(3)	2.228940	4.658676				
Cl(4)	2.229115	3.656836	3.718196			
Cl(5)	2.228940	4.658676	3.710351	3.718196		
C (6)	2.060618	1.776417	3.344153	3.564975	3.344153	
H (7)	2.589184	2.370030	4.011773	4.226243	3.061257	1.092240
H (8)	2.589184	2.370030	3.061257	4.226243	4.011773	1.092240

	H (7)
H (8)	1.811966

Point Group: C_s Number of degrees of freedom: 11

Energy = -1974.025450210

p4

Coordinates (Angstroms)

ATOM	X	Y	Z
1 Ru	-0.168064	-0.000317	-0.027422
2 C	1.399323	0.003809	-1.378341
3 H	1.439139	0.937200	-1.933442
4 H	1.444251	-0.929306	-1.933525
5 Cl	2.519059	0.006790	-0.017350
6 Cl	-2.360384	-0.006674	-0.474303
7 Cl	-0.157431	2.399657	-0.336425
8 Cl	-0.143319	-2.400338	-0.336521
9 C	-0.089005	-0.706550	2.033127
10 H	0.826431	-1.269604	2.180119
11 H	-1.007409	-1.263794	2.191039
12 C	-0.093094	0.705666	2.033351
13 H	0.819067	1.273974	2.180445
14 H	-1.014742	1.257512	2.191309

Distance Matrix (Angstroms)

	Ru(1)	C (2)	H (3)	H (4)	Cl(5)	Cl(6)
C (2)	2.069227					
H (3)	2.663634	1.086711				
H (4)	2.663796	1.086716	1.866513			
Cl(5)	2.687150	1.762417	2.388157	2.388140		
Cl(6)	2.237412	3.866884	4.178081	4.178018	4.900811	
Cl(7)	2.419808	3.041243	2.690405	4.024688	3.604333	3.265340
Cl(8)	2.419970	3.040569	4.024114	2.689747	3.603386	3.265577
C (9)	2.179651	3.789175	4.557500	4.258500	3.393421	3.454880
H (10)	2.733742	3.822620	4.708161	4.173676	3.053366	4.335521
H (11)	2.687460	4.487722	5.276487	4.809839	4.350557	3.242675
C (12)	2.179637	3.789400	4.258731	4.557704	3.393692	3.454904
H (13)	2.733665	3.822954	4.173964	4.708509	3.053855	4.335512
H (14)	2.687334	4.487970	4.810166	5.276654	4.350888	3.242592

	Cl(7)	Cl(8)	C (9)	H (10)	H (11)	C (12)
Cl(8)	4.800016					
C (9)	3.907426	2.913263				
H (10)	4.556803	2.924457	1.084739			
H (11)	4.531160	2.902920	1.085782	1.833882		
C (12)	2.913689	3.907182	1.412221	2.183748	2.177064	
H (13)	2.924952	4.556521	2.183752	2.543589	3.126723	1.084735
H (14)	2.903259	4.530913	2.177051	3.126717	2.521317	1.085781

	H (13)
H (14)	1.833915

Point Group: C_1 Number of degrees of freedom: 36

Energy = -2052.623463781

TS8

Coordinates (Angstroms)

ATOM	X	Y	Z
1 Ru	-0.145433	0.035712	0.061115
2 Cl	-2.387140	0.490328	-0.296734
3 Cl	-0.719011	-2.220780	0.483057
4 Cl	2.271135	0.017843	0.865835
5 Cl	1.084767	-0.829306	-1.730454
6 C	-0.256726	0.500850	1.879811
7 H	-1.264826	0.631023	2.280166
8 H	0.579091	0.592350	2.568484
9 C	0.381060	2.087716	-1.075251
10 H	-0.409113	2.090069	-1.819972
11 H	1.393579	1.899090	-1.412318
12 C	0.147841	2.551757	0.191990
13 H	0.976040	2.716591	0.874923
14 H	-0.837795	2.899260	0.485690

Distance Matrix (Angstroms)

	Ru(1)	Cl(2)	Cl(3)	Cl(4)	Cl(5)	C (6)
Cl(2)	2.315164					
Cl(3)	2.366175	3.277321				
Cl(4)	2.547094	4.824348	3.754853			
Cl(5)	2.339096	3.981347	3.176389	2.977558		
C (6)	1.880530	3.045672	3.093847	2.766139	4.074670	
H (7)	2.555705	2.814214	3.414717	3.857375	4.872189	1.092472
H (8)	2.668648	4.125338	3.734672	2.468215	4.556061	1.086846
C (9)	2.404005	3.289478	4.711859	3.409482	3.071403	3.414279
H (10)	2.797927	2.965133	4.897285	4.323356	3.280616	4.029545
H (11)	2.830501	4.186044	5.002880	3.082073	2.764185	3.939123
C (12)	2.536458	3.303705	4.859348	3.373894	4.000651	2.686752
H (13)	3.017797	4.200000	5.234920	2.993425	4.401500	2.727457
H (14)	2.976497	2.969109	5.121418	4.255880	4.744444	2.834358

	H (7)	H (8)	C (9)	H (10)	H (11)	C (12)
H (8)	1.866723					
C (9)	4.011199	3.943620				
H (10)	4.435335	4.741124	1.085812			
H (11)	4.723299	4.268225	1.083692	1.858050		
C (12)	3.169437	3.110141	1.369534	2.138070	2.133458	
H (13)	3.368350	2.745563	2.133697	3.094130	2.464573	1.086040
H (14)	2.923594	3.415762	2.140268	2.480854	3.095449	1.085586

	H (13)

H (14) 1.864099
Point Group: C_1 Number of degrees of freedom: 36
Energy = -2052.558692808

pdt7 Coordinates (Angstroms)

ATOM		X	Y	Z
1	Ru	-0.252247	0.136795	0.000000
2	Cl	-2.490603	-0.348827	0.000000
3	Cl	-0.036824	1.107679	-2.031749
4	Cl	2.236006	0.599234	0.000000
5	Cl	-0.036824	1.107679	2.031749
6	C	0.534867	-1.653881	-1.099696
7	H	-0.430185	-1.944543	-1.515992
8	H	1.236348	-1.226549	-1.807055
9	C	0.534867	-1.653881	1.099696
10	H	-0.430185	-1.944543	1.515992
11	H	1.236348	-1.226549	1.807055
12	C	1.076578	-2.518710	0.000000
13	H	2.166446	-2.548701	0.000000
14	H	0.662756	-3.533025	0.000000

Distance Matrix (Angstroms)

	Ru(1)	Cl(2)	Cl(3)	Cl(4)	Cl(5)	C (6)
Cl(2)	2.290429					
Cl(3)	2.262085	3.502919				
Cl(4)	2.530860	4.820751	3.090675			
Cl(5)	2.262085	3.502919	4.063498	3.090675		
C (6)	2.243970	3.473610	2.970146	3.029806	4.214142	
H (7)	2.581058	3.014939	3.120384	3.984671	4.696515	1.090465
H (8)	2.709256	4.233911	2.668346	2.756491	4.669689	1.083995
C (9)	2.243970	3.473610	4.214142	3.029806	2.970146	2.199391
H (10)	2.581058	3.014939	4.696515	3.984671	3.120384	2.803147
H (11)	2.709256	4.233911	4.669689	2.756491	2.668346	3.020577
C (12)	2.969424	4.175305	4.303297	3.326536	4.303297	1.500236
H (13)	3.614134	5.150490	4.727739	3.148703	4.727739	2.161500
H (14)	3.782170	4.481382	5.114054	4.421615	5.114054	2.181025

	H (7)	H (8)	C (9)	H (10)	H (11)	C (12)
H (8)	1.837816					
C (9)	2.803147	3.020577				
H (10)	3.031983	3.786223	1.090465			
H (11)	3.786223	3.614109	1.083995	1.837816		
C (12)	2.213196	2.227252	1.500236	2.213196	2.227252	
H (13)	3.066877	2.424586	2.161500	3.066877	2.424586	1.090280
H (14)	2.452759	2.985681	2.181025	2.452759	2.985681	1.095484

	H (13)
H (14)	1.797214

Point Group: C_s Number of degrees of freedom: 21
Energy = -2052.586035507

TS9 Coordinates (Angstroms)

ATOM		X	Y	Z
1	Cl	1.668141	-1.544022	0.100509
2	C	3.275931	0.748322	-0.148169
3	H	3.524394	0.326190	-1.116667
4	H	3.634576	0.209208	0.720262
5	C	2.605591	1.940879	-0.030078
6	H	2.583768	2.423968	0.942725
7	H	2.565634	2.600619	-0.892523
8	C	0.530260	1.610962	-0.181146
9	H	0.375015	2.309235	0.635411
10	H	0.469104	2.003648	-1.193199
11	Ru	-0.219215	-0.178418	0.021341
12	Cl	-1.022593	-0.611813	2.062938
13	Cl	-1.060889	-1.003170	-1.884502
14	Cl	-2.058947	1.520339	-0.137806

Distance Matrix (Angstroms)

	Cl(1)	C (2)	H (3)	H (4)	C (5)	H (6)
C (2)	2.810991					
H (3)	2.902565	1.085319				
H (4)	2.706433	1.083255	1.843945			
C (5)	3.611150	1.373133	2.152230	2.149536		
H (6)	4.158442	2.115875	3.086510	2.461473	1.086369	
H (7)	4.355417	2.118865	2.478404	3.076127	1.086584	1.843820
C (8)	3.365713	2.878184	3.389790	3.523383	2.106813	2.478095
H (9)	4.099498	3.386112	4.113494	3.878408	2.356699	2.232979
H (10)	3.961986	3.247493	3.486333	4.111151	2.433385	3.034904
Ru(11)	2.330934	3.619893	3.945161	3.935791	3.531797	3.934218
Cl(12)	3.458351	5.021581	5.627152	4.915901	4.905169	4.845274
Cl(13)	3.417658	4.989046	4.835451	5.504730	5.054640	5.746477
Cl(14)	4.830971	5.390458	5.792914	5.905214	4.684695	4.851689

	H (7)	C (8)	H (9)	H (10)	Ru(11)	Cl(12)
C (8)	2.372388					
H (9)	2.686689	1.085564				
H (10)	2.200504	1.087288	1.856354			
Ru(11)	4.039007	1.950537	2.630325	2.590425		
Cl(12)	5.650651	3.519659	3.538880	4.434888	2.236374	
Cl(13)	5.207973	3.502408	4.402704	3.443796	2.240729	3.966978
Cl(14)	4.808675	2.591155	2.672899	2.781813	2.509126	3.234714

	Cl(13)
Cl(14)	3.227253

Point Group: C_1 Number of degrees of freedom: 36
Energy = -2052.565871521

pdt8 Coordinates (Angstroms)

ATOM		X	Y	Z
1	Cl	-2.125068	0.110859	0.947689
2	C	-2.872866	0.164224	-0.719993
3	H	-2.853667	1.212551	-1.024957
4	H	-3.904084	-0.170139	-0.599413
5	C	-2.060879	-0.735052	-1.632793
6	H	-2.140892	-1.772257	-1.289323
7	H	-2.513801	-0.695842	-2.636838
8	C	-0.597425	-0.332011	-1.742230
9	H	0.002644	-1.077082	-2.276974
10	H	-0.449850	0.645427	-2.229517
11	Ru	0.443780	0.002817	-0.009497
12	Cl	0.641522	-1.735495	1.410065
13	Cl	2.509666	-0.111368	-0.959930
14	Cl	0.481374	2.158650	0.662150

Distance Matrix (Angstroms)

	Cl(1)	C (2)	H (3)	H (4)	C (5)	H (6)
C (2)	1.828445					
H (3)	2.374008	1.091953				
H (4)	2.374316	1.090756	1.787819			
C (5)	2.716353	1.516978	2.188866	2.187328		
H (6)	2.924140	2.147063	3.080100	2.480242	1.095522	
H (7)	3.694687	2.131416	2.521039	2.521974	1.102172	1.764519
C (8)	3.124978	2.543393	2.826796	3.502317	1.521879	2.159103
H (9)	4.041883	3.497655	3.868912	4.347330	2.188626	2.460381
H (10)	3.631357	2.895034	2.747896	3.905652	2.203909	3.096576
Ru(11)	2.743512	3.395732	3.656196	4.391108	3.074550	3.386646
Cl(12)	3.358100	4.527361	5.180411	5.210650	4.190805	3.876838
Cl(13)	5.016888	5.394921	5.524702	6.424143	4.661718	4.949217
Cl(14)	3.326939	4.139925	3.855377	5.123187	4.483673	5.112392

	H (7)	C (8)	H (9)	H (10)	Ru(11)	Cl(12)
C (8)	2.145972					
H (9)	2.570475	1.095977				
H (10)	2.494957	1.102094	1.781583			
Ru(11)	4.017255	2.049044	2.549949	2.477904		
Cl(12)	5.235873	3.666295	3.799465	4.484020	2.252995	
Cl(13)	5.328120	3.211650	2.992051	3.308069	2.276894	3.427044
Cl(14)	5.291741	3.626050	4.397453	3.393930	2.258348	3.968550

	Cl(13)
Cl(14)	3.449361

Point Group: C_1 Number of degrees of freedom: 36
Energy = -2052.663958050

R10eq/d Coordinates (Angstroms)

ATOM		X	Y	Z
1	Re	0.000000	0.000000	-0.061182
2	Cl	0.000000	-2.258026	0.496843
3	Cl	2.310442	0.000000	0.051352
4	Cl	-2.310442	0.000000	0.051352
5	Cl	0.000000	2.258026	0.496843
6	C	0.000000	0.000000	-1.923290
7	H	0.930316	0.000000	-2.493857
8	H	-0.930316	0.000000	-2.493857

Distance Matrix (Angstroms)

	Re(1)	Cl(2)	Cl(3)	Cl(4)	Cl(5)	C (6)
Cl(2)	2.325956					
Cl(3)	2.313181	3.261179				
Cl(4)	2.313181	3.261179	4.620884			
Cl(5)	2.325956	4.516052	3.261179	3.261179		
C (6)	1.862108	3.309943	3.039301	3.039301	3.309943	
H (7)	2.604495	3.861146	2.895313	4.120752	3.861146	1.091345
H (8)	2.604495	3.861146	4.120752	2.895313	3.861146	1.091345

	H (7)
H (8)	1.860631

Point Group: C_{2v} Number of degrees of freedom: 7

Energy = -1959.257911679

R11/d

Coordinates (Angstroms)

ATOM	X	Y	Z
1 Re	0.216207	-0.001244	-0.007826
2 Cl	-0.034607	1.900636	1.199406
3 Cl	2.236638	0.002424	-0.997137
4 Cl	-2.588511	0.001225	-0.555757
5 Cl	-0.033453	-1.910521	1.188533
6 C	-1.091038	0.005040	-1.580740
7 H	-1.088018	-0.895709	-2.203211
8 H	-1.088047	0.910771	-2.195790

Distance Matrix (Angstroms)

	Re(1)	Cl(2)	Cl(3)	Cl(4)	Cl(5)	C (6)
Cl(2)	2.266598					
Cl(3)	2.249643	3.685996				
Cl(4)	2.857739	3.634664	4.845295			
Cl(5)	2.266924	3.811173	3.686438	3.636707		
C (6)	2.045235	3.526832	3.378466	1.814670	3.529410	
H (7)	2.705695	4.528468	3.648917	2.402098	3.694033	1.094910
H (8)	2.705556	3.690112	3.649027	2.401743	4.530508	1.094826

	H (7)
H (8)	1.806495

Point Group: C_1 Number of degrees of freedom: 18

Energy = -1959.249696116

p5/d

Coordinates (Angstroms)

ATOM	X	Y	Z
1 Re	-0.161368	0.000789	0.057225
2 C	1.369564	-0.013087	-1.385089
3 H	1.470605	0.905288	-1.957842
4 H	1.455759	-0.934737	-1.955192
5 Cl	2.563667	-0.020691	-0.035368
6 Cl	-2.383825	0.025874	-0.283750
7 Cl	-0.099269	2.380902	-0.344958
8 Cl	-0.149898	-2.379518	-0.347025
9 C	0.074938	-0.717765	2.071777
10 H	0.989026	-1.289374	2.200472
11 H	-0.827410	-1.256680	2.355075
12 C	0.089432	0.712460	2.071253
13 H	1.014931	1.265315	2.199557
14 H	-0.801749	1.269878	2.352982

Distance Matrix (Angstroms)

	Re(1)	C (2)	H (3)	H (4)	Cl(5)	Cl(6)
C (2)	2.103382					
H (3)	2.746260	1.087045				
H (4)	2.745930	1.087146	1.840087			
Cl(5)	2.726692	1.802134	2.397525	2.397637		
Cl(6)	2.248602	3.911828	4.293318	4.296383	4.953943	
Cl(7)	2.414652	2.995083	2.691344	4.000554	3.599267	3.281631
Cl(8)	2.414417	2.997722	4.001338	2.692903	3.608965	3.283344
C (9)	2.151878	3.757999	4.562895	4.262655	3.334629	3.485257
H (10)	2.753441	3.824914	4.726524	4.196803	3.014636	4.390599
H (11)	2.702769	4.512433	5.343803	4.888243	4.329122	3.321260
C (12)	2.150741	3.756522	4.263617	4.559865	3.331247	3.483452
H (13)	2.751780	3.822272	4.197764	4.721917	3.007870	4.388003
H (14)	2.700218	4.509299	4.886688	5.340135	4.323866	3.317057

	Cl(7)	Cl(8)	C (9)	H (10)	H (11)	C (12)
Cl(8)	4.760689					
C (9)	3.933534	2.943225				
H (10)	4.597229	2.995881	1.085752			
H (11)	4.588286	3.003520	1.088540	1.823297		
C (12)	2.942343	3.932642	1.430298	2.198478	2.190585	
H (13)	2.993414	4.596380	2.198300	2.554820	3.127118	1.085661
H (14)	3.001122	4.586179	2.190521	3.127284	2.526689	1.088251

	H (13)
H (14)	1.823153

Point Group: C_1 Number of degrees of freedom: 36

Energy = -2037.871496373

TS10/d

Coordinates (Angstroms)

ATOM	X	Y	Z
1 Re	-0.053195	-0.021147	0.063425
2 Cl	1.318299	0.460896	-1.845238
3 Cl	2.078903	-0.861159	0.900286
4 Cl	0.272924	2.230510	0.583297
5 Cl	-2.271865	0.449873	-0.439153
6 C	-0.556697	-0.834743	1.750379
7 H	0.068392	-1.385067	2.445562
8 H	-1.581389	-0.658862	2.089330
9 C	-0.346429	-1.922083	-1.120859
10 H	0.638401	-2.216385	-1.466218
11 H	-1.080870	-1.694533	-1.886607
12 C	-0.782828	-2.372789	0.141545
13 H	-1.846472	-2.435503	0.350065
14 H	-0.111665	-2.984692	0.735757

Distance Matrix (Angstroms)

	Re(1)	Cl(2)	Cl(3)	Cl(4)	Cl(5)	C (6)
Cl(2)	2.399240					
Cl(3)	2.439631	3.140740				
Cl(4)	2.333791	3.181528	3.594504			
Cl(5)	2.323132	3.855707	4.737308	3.269866		
C (6)	1.939398	4.257082	2.769430	3.383212	3.063672	
H (7)	2.747661	4.835371	2.589307	4.072133	4.143114	1.084838
H (8)	2.616553	5.014267	3.853893	3.749011	2.845922	1.093534
C (9)	2.258776	2.995770	3.330590	4.531200	3.130208	3.077422
H (10)	2.763545	2.788145	3.084157	4.910087	4.078412	3.699147
H (11)	2.767482	3.225461	4.294817	4.831060	2.848170	3.773812
C (12)	2.463470	4.048681	3.324187	4.743429	3.243742	2.237201
H (13)	3.021112	4.819155	4.264959	5.130099	3.021460	2.487335
H (14)	3.039416	4.536344	3.055332	5.231585	4.224111	2.418635

	H (7)	H (8)	C (9)	H (10)	H (11)	C (12)
H (8)	1.837404					
C (9)	3.630402	3.664174				
H (10)	4.039557	4.471607	1.084333			
H (11)	4.492689	4.138986	1.085150	1.845250		
C (12)	2.647388	2.714611	1.409697	2.151571	2.159227	
H (13)	3.026752	2.500354	2.162717	3.085691	2.477475	1.085704
H (14)	2.348330	3.066225	2.152040	2.449814	3.079068	1.085345

	H (13)
H (14)	1.860087

Point Group: C_1 Number of degrees of freedom: 36

Energy = -2037.841240801

pdt9/d

Coordinates (Angstroms)

ATOM	X	Y	Z
1 Re	-0.165975	-0.118197	0.000000
2 Cl	-0.508249	-0.818881	-2.189850
3 Cl	-2.259478	0.863206	0.000000
4 Cl	-0.508249	-0.818881	2.189850
5 Cl	1.910840	-1.140394	0.000000
6 C	0.715023	1.576127	1.142566
7 H	-0.141732	2.095373	1.573533
8 H	1.350802	1.163428	1.924515
9 C	0.715023	1.576127	-1.142566
10 H	-0.141732	2.095373	-1.573533
11 H	1.350802	1.163428	-1.924515
12 C	1.402604	2.292627	0.000000
13 H	2.479929	2.103829	0.000000
14 H	1.239261	3.377564	0.000000

Distance Matrix (Angstroms)

	Re(1)	Cl(2)	Cl(3)	Cl(4)	Cl(5)	C (6)
Cl(2)	2.324555					
Cl(3)	2.312122	3.269811				
Cl(4)	2.324555	4.379700	3.269811			
Cl(5)	2.314746	3.278842	4.626658	3.278842		
C (6)	2.225387	4.282226	3.265175	2.886047	3.180397	
H (7)	2.715968	4.773915	2.911888	3.001176	4.142371	1.090585
H (8)	2.765308	4.930884	4.102196	2.730572	3.053685	1.089027
C (9)	2.225387	2.886047	3.265175	4.282226	3.180397	2.285132
H (10)	2.715968	3.001176	2.911888	4.773915	4.142371	2.894968
H (11)	2.765308	2.730572	4.102196	4.930884	3.053685	3.159354
C (12)	2.876197	4.257733	3.931169	4.257733	3.470437	1.513802
H (13)	3.455171	4.718781	4.899095	4.718781	3.293758	2.167677
H (14)	3.767629	5.045729	4.308500	5.045729	4.567598	2.196692

	H (7)	H (8)	C (9)	H (10)	H (11)	C (12)
H (8)	1.794259					
C (9)	2.894968	3.159354				
H (10)	3.147066	3.915675	1.090585			
H (11)	3.915675	3.849029	1.089027	1.794259		
C (12)	2.213569	2.231934	1.513802	2.213569	2.231934	
H (13)	3.057643	2.421372	2.167677	3.057643	2.421372	1.093743
H (14)	2.455027	2.935744	2.196692	2.455027	2.935744	1.097164

	H (13)

H (14) 1.778105

Point Group: C_s Number of degrees of freedom: 21

Energy = -2037.867250341

TS11/d

Coordinates (Angstroms)

ATOM	X	Y	Z
1 Cl	-1.528037	-1.408847	0.344724
2 C	-3.514158	0.309474	-0.189116
3 H	-3.834278	0.149631	0.834989
4 H	-3.758579	-0.472052	-0.899031
5 C	-2.966762	1.501584	-0.594364
6 H	-2.917053	1.713359	-1.658858
7 H	-3.057375	2.366776	0.056489
8 C	-0.818551	1.551490	-0.359018
9 H	-0.699641	2.073152	-1.310221
10 H	-0.856962	2.210555	0.513935
11 Re	0.311201	0.044647	-0.065766
12 Cl	2.331586	1.248880	-0.418409
13 Cl	0.707903	-1.121084	-1.964190
14 Cl	0.868441	-0.228731	2.115804

Distance Matrix (Angstroms)

	Cl(1)	C (2)	H (3)	H (4)	C (5)	H (6)
C (2)	2.679979					
H (3)	2.826299	1.084812				
H (4)	2.720263	1.083745	1.843650			
C (5)	3.379708	1.372952	2.150213	2.148263		
H (6)	3.961298	2.118389	3.083151	2.462016	1.086493	
H (7)	4.083783	2.121666	2.474949	3.076304	1.086451	1.840939
C (8)	3.124454	2.972838	3.533479	3.609722	2.161640	2.473761
H (9)	3.943272	3.505559	4.257677	4.000530	2.445195	2.273305
H (10)	3.684975	3.342017	3.635230	4.196693	2.486408	3.035162
Re(11)	2.379903	3.836498	4.243511	4.186217	3.625896	3.967892
Cl(12)	4.747902	5.925182	6.387272	6.346866	5.307288	5.413193
Cl(13)	3.226968	4.798248	5.484664	4.637377	4.717836	4.611681
Cl(14)	3.205075	4.980913	4.888683	5.527906	5.004776	5.687684

	H (7)	C (8)	H (9)	H (10)	Re(11)	Cl(12)
C (8)	2.418609					
H (9)	2.740989	1.091356				
H (10)	2.252883	1.094481	1.836076			
Re(11)	4.093231	1.906020	2.585595	2.528204		
Cl(12)	5.524140	3.165196	3.265438	3.458456	2.378338	
Cl(13)	5.515943	3.471209	3.551337	4.437311	2.262811	3.262287
Cl(14)	5.137068	3.484232	4.415336	3.390150	2.268149	3.278165

	Cl(13)
Cl(14)	4.179524

Point Group: C_1 Number of degrees of freedom: 36

Energy = -2037.834780161

pdt10/d Coordinates (Angstroms)

ATOM	X	Y	Z
1 Cl	-1.891273	0.225139	0.848566
2 C	-2.615466	0.252653	-0.852927
3 H	-2.611815	1.304398	-1.145027
4 H	-3.638399	-0.104921	-0.731273
5 C	-1.760918	-0.622786	-1.746415
6 H	-1.855968	-1.667523	-1.430443
7 H	-2.173940	-0.553668	-2.764396
8 C	-0.282703	-0.210340	-1.756875
9 H	0.314764	-0.930293	-2.329940
10 H	-0.143964	0.771087	-2.238968
11 Re	0.644585	0.021838	0.094531
12 Cl	2.813258	-0.144153	-0.648516
13 Cl	0.543800	-2.103777	0.951041
14 Cl	0.729785	2.265953	0.562791

Distance Matrix (Angstroms)

	Cl(1)	C (2)	H (3)	H (4)	C (5)	H (6)
C (2)	1.849402					
H (3)	2.378737	1.091560				
H (4)	2.378504	1.090437	1.791995			
C (5)	2.733111	1.514914	2.190829	2.196277		
H (6)	2.962651	2.144163	3.079786	2.471361	1.095604	
H (7)	3.706742	2.121040	2.503298	2.545506	1.100749	1.766694
C (8)	3.092809	2.544261	2.844917	3.510508	1.534712	2.169124
H (9)	4.037886	3.488147	3.868168	4.343325	2.177961	2.462656
H (10)	3.589431	2.880660	2.751621	3.905331	2.190897	3.087310
Re(11)	2.653390	3.402776	3.712897	4.363712	3.096945	3.381162
Cl(12)	4.950782	5.447043	5.637041	6.452307	4.728378	4.973302
Cl(13)	3.371043	4.334515	5.095788	4.931166	3.844649	3.408911
Cl(14)	3.334147	4.153112	3.873954	5.135823	4.458794	5.111882

	H (7)	C (8)	H (9)	H (10)	Re(11)	Cl(12)
C (8)	2.170196					
H (9)	2.554260	1.097134				
H (10)	2.480293	1.102207	1.764483			
Re(11)	4.055707	2.083621	2.625528	2.574569		
Cl(12)	5.432936	3.289045	3.112503	3.480282	2.298437	
Cl(13)	4.857306	3.406027	3.492042	4.349025	2.293906	3.398404
Cl(14)	5.239471	3.540905	4.330834	3.293618	2.294031	3.408333

	Cl(13)
Cl(14)	4.390885

Point Group: C_1 Number of degrees of freedom: 36

Energy = -2037.889616910

R12

Coordinates (Angstroms)

ATOM	X	Y	Z
1 Cr	-0.118785	-0.303724	0.000000
2 Cl	0.039289	0.860367	-1.799244
3 Cl	0.039289	0.860367	1.799244
4 O	-1.250319	-1.341854	0.000000
5 C	1.316172	-1.325314	0.000000
6 H	2.282113	-0.813122	0.000000
7 H	1.320686	-2.413580	0.000000

Distance Matrix (Angstroms)

	Cr(1)	Cl(2)	Cl(3)	O (4)	C (5)	H (6)
Cl(2)	2.148808					
Cl(3)	2.148808	3.598489				
O (4)	1.535605	3.122523	3.122523			
C (5)	1.761461	3.105626	3.105626	2.566544		
H (6)	2.454342	3.326876	3.326876	3.571783	1.093336	
H (7)	2.554127	3.949429	3.949429	2.785438	1.088275	1.867032

Point Group: Cs Number of degrees of freedom: 10

Energy is -1121.252754486

R13 Coordinates (Angstroms)

ATOM	X	Y	Z
1 Cr	-0.242881	-0.398549	0.080264
2 Cl	-2.031370	0.786038	0.032873
3 C	1.096012	0.188665	-1.194167
4 O	-0.256505	-1.934850	0.103055
5 Cl	1.951318	0.586477	0.430260
6 H	1.702547	-0.544887	-1.721992
7 H	0.963447	1.124110	-1.737035

Distance Matrix (Angstroms)

	Cr(1)	Cl(2)	C (3)	O (4)	Cl(5)	H (6)
Cl(2)	2.145736					
C (3)	1.939492	3.412183				
O (4)	1.536531	3.249354	2.832208			
Cl(5)	2.430491	4.007436	1.878448	3.367290		
H (6)	2.655981	4.335095	1.088386	3.016733	2.444189	
H (7)	2.660130	3.495110	1.089649	3.772459	2.441743	1.825389

Point Group: C_1 Number of degrees of freedom: 15

Energy = -1121.247001456

TS12 Coordinates (Angstroms)

ATOM	X	Y	Z
1 Cr	-0.043461	0.334608	0.096387
2 Cl	-0.013787	-1.979871	-0.044734
3 Cl	-2.267507	0.229393	0.026613
4 O	0.092494	1.663590	0.890123
5 C	2.050727	-0.056084	0.910840
6 H	1.978624	-1.078748	1.256127
7 H	2.189389	0.720244	1.655020
8 C	2.297686	0.213798	-0.433623
9 H	2.720046	1.174741	-0.713969
10 H	2.437741	-0.615616	-1.119101
11 C	0.464499	0.872687	-1.537314
12 H	0.718717	1.893371	-1.813483
13 H	0.411706	0.137905	-2.342085

Distance Matrix (Angstroms)

	Cr(1)	Cl(2)	Cl(3)	O (4)	C (5)	H (6)
Cl(2)	2.318967					
Cl(3)	2.227626	3.156769				
O (4)	1.553929	3.762986	2.893471			
C (5)	2.280701	2.979312	4.417069	2.606220		
H (6)	2.726059	2.544398	4.610050	3.348412	1.081787	
H (7)	2.750213	3.877341	4.770384	2.423209	1.084304	1.854699

C (8)	2.403430	3.210346	4.588360	2.952469	1.393343	2.151215
H (9)	2.999912	4.227683	5.130091	3.117068	2.145442	3.083698
H (10)	2.921763	3.004238	4.915899	3.838222	2.140915	2.463125
C (11)	1.793469	3.254787	3.213029	2.579993	3.061403	3.728804
H (12)	2.580361	4.320538	3.882307	2.784679	3.605075	4.454589
H (13)	2.488375	3.153386	3.577329	3.588422	3.647676	4.108844

	H (7)	C (8)	H (9)	H (10)	C (11)	H (12)
C (8)	2.151894					
H (9)	2.469873	1.086460				
H (10)	3.089005	1.085091	1.857204			
C (11)	3.631732	2.238938	2.420046	2.506717		
H (12)	3.945836	2.686657	2.393884	3.119652	1.087517	
H (13)	4.413176	2.684195	3.009024	2.483606	1.091030	1.858854

Point Group: C_1 Number of degrees of freedom: 33
Energy = -1199.820933520

pdt11 Coordinates (Angstroms)

ATOM	X	Y	Z
1 Cr	0.162995	-0.000070	-0.302688
2 Cl	1.294286	-1.745189	0.338335
3 Cl	1.295513	1.744376	0.338132
4 O	-0.269145	0.000314	-1.779987
5 C	-1.526539	-1.065864	0.430282
6 H	-1.541942	-1.919456	-0.246144
7 H	-1.244511	-1.335846	1.446783
8 C	-2.582035	0.000979	0.327231
9 H	-3.342563	0.001064	1.117316
10 H	-3.069917	0.001685	-0.650891
11 C	-1.525322	1.066528	0.431279
12 H	-1.540230	1.921126	-0.243610
13 H	-1.242781	1.334546	1.448249

Distance Matrix (Angstroms)

	Cr(1)	Cl(2)	Cl(3)	O (4)	C (5)	H (6)
Cl(2)	2.176274					
Cl(3)	2.176313	3.489565				
O (4)	1.539207	3.158858	3.158534			
C (5)	2.127837	2.902928	3.983707	2.757365		
H (6)	2.567889	2.901064	4.670781	2.767346	1.089224	
H (7)	2.612665	2.800305	4.143501	3.626114	1.088900	1.815232
C (8)	2.816379	4.251481	4.251462	3.128870	1.504276	2.258013
H (9)	3.782241	5.015633	5.015776	4.223773	2.215467	2.964736
H (10)	3.251611	4.803791	4.803344	3.019798	2.165782	2.487833
C (11)	2.127617	3.983037	2.902630	2.757624	2.132393	3.061908
H (12)	2.568163	4.670654	2.900191	2.768687	3.062095	3.840583
H (13)	2.612123	4.141665	2.800582	3.626244	2.622736	3.680896

	H (7)	C (8)	H (9)	H (10)	C (11)	H (12)
C (8)	2.197605					
H (9)	2.509522	1.096648				
H (10)	3.085666	1.093047	1.789104			
C (11)	2.623262	1.504282	2.215451	2.165815		
H (12)	3.681405	2.257915	2.964314	2.487985	1.089052	
H (13)	2.670393	2.197426	2.509337	3.085665	1.088986	1.815197

Point Group: C_1 Number of degrees of freedom: 33
Energy = -1199.862983334

TS13 Coordinates (Angstroms)

ATOM	X	Y	Z
1 Cr	0.540110	-0.134102	0.281056
2 Cl	-0.879928	1.500441	0.008844
3 Cl	2.307549	-0.023553	-0.976764
4 C	0.938001	-0.211863	1.985623
5 H	1.727737	0.480381	2.299557
6 H	0.476815	-0.834365	2.750057
7 C	-2.743344	0.087255	-0.450400
8 H	-3.317240	0.426556	0.404475
9 H	-2.903734	0.624009	-1.377157
10 C	-2.207671	-1.231357	-0.469921
11 H	-2.080289	-1.681419	-1.451326
12 H	-2.602090	-1.918060	0.274486
13 O	-0.583279	-1.321463	0.062265

Distance Matrix (Angstroms)

	Cr(1)	Cl(2)	Cl(3)	C (4)	H (5)	H (6)
Cl(2)	2.182279					
Cl(3)	2.172136	3.667969				
C (4)	1.752117	3.185045	3.269077			
H (5)	2.421238	3.617708	3.365176	1.096102		
H (6)	2.567166	3.847899	4.230627	1.088375	1.869843	
C (7)	3.371216	2.383342	5.079455	4.424475	5.263780	4.632681
H (8)	3.899836	2.692627	5.809361	4.584178	5.389436	4.635357
H (9)	3.896725	2.604788	5.266605	5.173577	5.915182	5.530720
C (10)	3.052579	3.074872	4.701371	4.118776	5.107591	4.210977
H (11)	3.501689	3.700972	4.714536	4.804403	5.765723	4.990782
H (12)	3.613305	3.836999	5.409191	4.286181	5.347975	4.096646
O (13)	1.649151	2.837956	3.334823	2.691619	3.686857	2.930067

	C (7)	H (8)	H (9)	C (10)	H (11)	H (12)
H (8)	1.084109					
H (9)	1.082916	1.839615				
C (10)	1.423399	2.178162	2.179441			
H (11)	2.137686	3.068811	2.449195	1.087170		
H (12)	2.136984	2.454702	3.046478	1.086862	1.818434	
O (13)	2.629295	3.263007	3.352805	1.711721	2.159065	2.115789

Point Group: C_1 Number of degrees of freedom: 33
Energy = -1199.796449245

pdt12

Coordinates (Angstroms)

ATOM	X	Y	Z
1 Cr	0.013389	0.074557	0.277070
2 Cl	1.843413	-1.081960	-0.412799
3 Cl	0.247205	1.993017	-0.605428
4 O	-1.740079	-0.006645	0.685184
5 C	-0.958139	-1.323624	-0.882967
6 H	-0.606251	-1.142931	-1.898340
7 H	-0.707812	-2.317750	-0.516248
8 C	-2.266998	-0.741904	-0.419369
9 H	-3.008454	-1.471886	-0.067449
10 H	-2.742593	-0.070193	-1.145160
11 C	0.509221	0.015034	1.947271
12 H	1.101081	0.860145	2.309052
13 H	0.306487	-0.806626	2.637241

Distance Matrix (Angstroms)

	Cr(1)	Cl(2)	Cl(3)	O (4)	C (5)	H (6)
Cl(2)	2.272100					
Cl(3)	2.124609	3.469939				
O (4)	1.802165	3.899139	3.100584			
C (5)	2.060209	2.850992	3.539773	2.192023		
H (6)	2.568781	2.865555	3.497740	3.041596	1.089705	
H (7)	2.621567	2.836658	4.416189	2.801824	1.088776	1.816780
C (8)	2.520277	4.124459	3.719627	1.427686	1.505468	2.259703
H (9)	3.411995	4.879747	4.784798	2.078981	2.211525	3.038248
H (10)	3.104694	4.753049	3.672470	2.087877	2.196386	2.506392
C (11)	1.743263	2.924619	3.239960	2.579280	3.457658	4.168200
H (12)	2.434990	3.425099	3.241403	3.385330	4.381578	4.962806
H (13)	2.536296	3.426470	4.284439	2.939206	3.776034	4.638716

	H (7)	C (8)	H (9)	H (10)	C (11)	H (12)
C (8)	2.218949					
H (9)	2.491959	1.098398				
H (10)	3.096349	1.097342	1.787984			
C (11)	3.604439	3.725766	4.317878	4.488283		
H (12)	4.620977	4.621125	5.289084	5.250803	1.093342	
H (13)	3.640988	3.996233	4.329753	4.913836	1.091918	1.875423

Point Group: C_1 Number of degrees of freedom: 33
Energy = -1199.802011237

TS14

Coordinates (Angstroms)

ATOM	X	Y	Z
1 Cr	0.398356	0.011761	-0.292667
2 Cl	0.346737	2.146357	0.078984
3 Cl	2.184801	-1.119786	0.278649
4 O	-0.457078	-0.574350	-1.456561
5 C	-2.881116	-0.806935	-0.379612
6 H	-3.121696	-1.866993	-0.345733
7 H	-3.027490	-0.303146	-1.329021
8 C	-2.364585	-0.143705	0.767978
9 H	-2.366033	0.944376	0.694536
10 H	-2.873429	-0.487926	1.680249
11 C	-0.822435	-0.631048	1.074189
12 H	-0.532387	-0.203178	2.040974
13 H	-0.828442	-1.720474	1.134779

Distance Matrix (Angstroms)

	Cr(1)	Cl(2)	Cl(3)	O (4)	C (5)	H (6)
Cl(2)	2.167322					
Cl(3)	2.190477	3.753137				
O (4)	1.558827	3.225874	3.207488			
C (5)	3.381236	4.399008	5.118076	2.662682		
H (6)	3.990401	5.321409	5.395098	3.163077	1.087543	
H (7)	3.592996	4.400904	5.515386	2.587825	1.084715	1.849688
C (8)	2.963609	3.615296	4.678578	2.961859	1.422547	2.187074
H (9)	3.079965	3.030311	5.014361	3.252361	2.118063	3.091437

H (10) 3.853136 4.457910 5.286721 3.960529 2.084431 2.463345
C (11) 1.942120 3.173542 3.148844 2.557615 2.526389 2.971589
H (12) 2.521579 3.184741 3.365869 3.517981 3.426410 3.894762
H (13) 2.557982 4.177095 3.189579 2.857718 2.709503 2.733569

	H (7)	C (8)	H (9)	H (10)	C (11)	H (12)
C (8)	2.205056					
H (9)	2.467513	1.090558				
H (10)	3.018871	1.099840	1.811234			
C (11)	3.277988	1.646054	2.238033	2.143447		
H (12)	4.194329	2.231816	2.547946	2.385724	1.096300	
H (13)	3.593737	2.231698	3.107961	2.449221	1.091126	1.791933

Point Group: C_1 Number of degrees of freedom: 33
Energy = -1199.824595089

pdt13

Coordinates (Angstroms)

ATOM	X	Y	Z
1 Cr	0.296813	-0.000268	0.264035
2 Cl	1.266717	1.892655	-0.037005
3 Cl	1.662849	-1.642678	-0.127664
4 O	-1.147081	-0.174104	1.149173
5 C	-2.349008	0.243764	-0.801295
6 H	-3.172348	-0.088595	-1.449596
7 H	-2.380601	1.337961	-0.752861
8 C	-2.473870	-0.331182	0.610465
9 H	-3.174331	0.196115	1.265918
10 H	-2.713216	-1.401368	0.610195
11 C	-0.983206	-0.234421	-1.277341
12 H	-0.958062	-1.303068	-1.516995
13 H	-0.537168	0.348748	-2.090770

Distance Matrix (Angstroms)

	Cr(1)	Cl(2)	Cl(3)	O (4)	C (5)	H (6)
Cl(2)	2.148138					
Cl(3)	2.171864	3.558613				
O (4)	1.702503	3.391892	3.418001			
C (5)	2.862664	4.046782	4.484132	2.328855		
H (6)	3.870324	5.062220	5.248029	3.295849	1.099385	
H (7)	3.161247	3.758067	5.062072	2.725004	1.095724	1.774082
C (8)	2.811797	4.399620	4.401966	1.440573	1.529451	2.188738
H (9)	3.618173	4.929377	5.359248	2.064082	2.226386	2.730399
H (10)	3.338140	5.206661	4.444391	2.061421	2.198047	2.485340
C (11)	2.017205	3.335422	3.210382	2.432790	1.523383	2.200745
H (12)	2.538516	4.165652	2.985758	2.901507	2.199920	2.526371
H (13)	2.522388	3.139363	3.558038	3.338053	2.226327	2.747098

	H (7)	C (8)	H (9)	H (10)	C (11)	H (12)
C (8)	2.157173					
H (9)	2.451385	1.094672				
H (10)	3.077739	1.096624	1.787331			
C (11)	2.167989	2.407333	3.384458	2.813804		
H (12)	3.095570	2.787171	3.860570	2.759558	1.095479	
H (13)	2.483302	3.392608	4.271449	3.885010	1.095765	1.798573

Point Group: C_1 Number of degrees of freedom: 33
Energy = -1199.888848343

TS15

Coordinates (Angstroms)

ATOM	X	Y	Z
1 Cr	-0.544740	0.134404	0.280022
2 Cl	-2.310615	0.049304	-0.981543
3 O	0.581893	1.322549	0.083287
4 Cl	0.871220	-1.499073	-0.018690
5 C	2.205112	1.237846	-0.452631
6 H	2.602434	1.910717	0.302744
7 H	2.077507	1.704924	-1.426021
8 C	2.737722	-0.082156	-0.456620
9 H	2.894802	-0.603441	-1.392707
10 H	3.312253	-0.437458	0.391267
11 C	-0.944476	0.183130	1.985266
12 H	-0.481592	0.790423	2.760880
13 H	-1.736428	-0.512151	2.286581

Distance Matrix (Angstroms)

	Cr(1)	Cl(2)	O (3)	Cl(4)	C (5)	H (6)
Cl(2)	2.171889					
O (3)	1.649150	3.334909				
Cl(4)	2.182296	3.667237	2.838249			
C (5)	3.052220	4.699379	1.711497	3.075434		
H (6)	3.613933	5.408539	2.115819	3.837588	1.086836	
H (7)	3.500471	4.711078	2.158955	3.701528	1.087168	1.818386
C (8)	3.371067	5.077256	2.629125	2.383959	1.423410	2.136932
H (9)	3.895239	5.262271	3.352245	2.604796	2.179393	3.046477
H (10)	3.900743	5.808459	3.263027	2.693275	2.178204	2.454711
C (11)	1.752147	3.268976	2.691765	3.184714	4.120154	4.289057
H (12)	2.566905	4.230876	2.929788	3.846804	4.212507	4.099842
H (13)	2.421658	3.365346	3.687172	3.617750	5.108963	5.350852

	H (7)	C (8)	H (9)	H (10)	C (11)	H (12)
C (8)	2.137588					
H (9)	2.449006	1.082899				
H (10)	3.068703	1.084084	1.839669			
C (11)	4.804698	4.426259	5.173920	4.587560		
H (12)	4.991537	4.634402	5.531291	4.638536	1.088413	
H (13)	5.765842	5.265744	5.915554	5.393234	1.096081	1.869832

Point Group: C_1 Number of degrees of freedom: 33
Energy = -1199.796480000

pdt14

Coordinates (Angstroms)

ATOM	X	Y	Z
1 Cr	0.594466	-0.414219	-0.118116
2 Cl	2.237453	1.050942	-0.061178
3 O	-0.595192	-0.281880	-1.433276
4 Cl	-1.184527	0.357487	1.355818
5 C	-1.797913	0.451500	-1.294933
6 H	-2.486636	0.151054	-2.097816
7 H	-1.606244	1.528836	-1.400621
8 C	-2.472495	0.166914	0.037597
9 H	-3.269287	0.867323	0.291084
10 H	-2.814765	-0.865238	0.122524
11 C	0.973162	-2.063665	0.348168
12 H	0.525054	-2.988939	-0.017462
13 H	1.766860	-2.157992	1.099839

Distance Matrix (Angstroms)

	Cr(1)	Cl(2)	O (3)	Cl(4)	C (5)	H (6)
Cl(2)	2.202123					
O (3)	1.778327	3.418032				
Cl(4)	2.435740	3.768116	2.921498			
C (5)	2.803185	4.262119	1.415458	2.722419		
H (6)	3.705664	5.222520	2.051002	3.696714	1.099649	
H (7)	3.203656	4.098353	2.074123	3.024543	1.099345	1.777485
C (8)	3.125414	4.793211	2.426757	1.852805	1.520424	2.135519
H (9)	4.091257	5.521050	3.383027	2.395792	2.203021	2.613891
H (10)	3.447345	5.406515	2.772602	2.381964	2.185629	2.463824
C (11)	1.755421	3.386262	2.967833	3.396021	4.087137	4.781007
H (12)	2.577621	4.388036	3.253866	4.000892	4.343354	4.822625
H (13)	2.428716	3.444804	3.939004	3.886367	5.025135	5.800769

	H (7)	C (8)	H (9)	H (10)	C (11)	H (12)
C (8)	2.161873					
H (9)	2.462758	1.090737				
H (10)	3.084167	1.090734	1.799103			
C (11)	4.755803	4.116369	5.156775	3.979389		
H (12)	5.183228	4.352900	5.418762	3.960315	1.091154	
H (13)	5.587740	4.950321	5.930379	4.859799	1.097207	1.865721

Point Group: C_1 Number of degrees of freedom: 33
Energy = -1199.824272517

R14

Coordinates (Angstroms)

ATOM	X	Y	Z
1 Mo	-0.092085	-0.269820	0.000000
2 Cl	0.035904	0.998994	-1.918272
3 Cl	0.035904	0.998994	1.918272
4 O	-1.275713	-1.462881	0.000000
5 C	1.482007	-1.303615	0.000000
6 H	2.432087	-0.759273	0.000000
7 H	1.539536	-2.390775	0.000000

Distance Matrix (Angstroms)

	Mo(1)	Cl(2)	Cl(3)	O (4)	C (5)	H (6)
Cl(2)	2.303484					
Cl(3)	2.303484	3.836545				
O (4)	1.680586	3.385401	3.385401			
C (5)	1.883215	3.327611	3.327611	2.762315		
H (6)	2.571188	3.537367	3.537367	3.773969	1.094970	
H (7)	2.675937	4.175071	4.175071	2.964222	1.088681	1.859690

Point Group: C_s Number of degrees of freedom: 10
Energy = -1102.546991928

TS16

Coordinates (Angstroms)

ATOM	X	Y	Z
1 Mo	-0.058273	-0.310611	-0.039918
2 Cl	-0.007899	2.135914	-0.031418
3 Cl	-2.384910	-0.170797	0.003249
4 O	0.086111	-1.887241	-0.666840
5 C	1.947002	0.059928	-1.085494
6 H	1.922575	1.062835	-1.493157
7 H	2.073700	-0.757968	-1.787619
8 C	2.390482	-0.121512	0.252569
9 H	2.878703	-1.054830	0.514746
10 H	2.676868	0.755927	0.823611
11 C	0.812339	-0.596520	1.670710
12 H	1.141408	-1.562970	2.045999
13 H	0.861828	0.233495	2.376383

Distance Matrix (Angstroms)

	Mo(1)	Cl(2)	Cl(3)	O (4)	C (5)	H (6)
Cl(2)	2.447058					
Cl(3)	2.331234	3.312446				
O (4)	1.702833	4.074110	3.082392			
C (5)	2.291649	3.040138	4.472590	2.725739		
H (6)	2.814608	2.648568	4.723930	3.571883	1.082871	
H (7)	2.792829	3.973896	4.840577	2.545960	1.085350	1.850641
C (8)	2.473400	3.305882	4.782150	3.045199	1.421270	2.160827
H (9)	3.080152	4.337235	5.361787	3.144459	2.161370	3.070890
H (10)	3.060094	3.137422	5.210893	3.989962	2.159121	2.455721
C (11)	1.940607	3.322081	3.630987	2.767220	3.052056	3.741142
H (12)	2.712690	4.395260	4.306494	2.928873	3.617877	4.475568
H (13)	2.642186	3.189535	4.041847	3.789520	3.632124	4.097113

	H (7)	C (8)	H (9)	H (10)	C (11)	H (12)
C (8)	2.160507					
H (9)	2.457039	1.085439				
H (10)	3.078020	1.085359	1.847965			
C (11)	3.684717	2.174234	2.411672	2.454212		
H (12)	4.026639	2.618087	2.370893	3.037952	1.087729	
H (13)	4.448657	2.640720	3.032038	2.445078	1.090572	1.847865

Point Group: C_1 Number of degrees of freedom: 33

Energy = -1181.125831491

pdt15

Coordinates (Angstroms)

ATOM	X	Y	Z
1 Mo	0.168928	0.002623	-0.328981
2 Cl	1.237527	-1.834719	0.572365
3 Cl	1.182036	1.872552	0.568812
4 O	0.062026	-0.002969	-2.007317
5 C	-1.694221	-1.152764	0.159669
6 H	-2.074597	-1.433618	-0.825752
7 H	-1.453258	-2.037716	0.747723
8 C	-2.472291	-0.036081	0.824544
9 H	-2.302998	-0.027887	1.906924
10 H	-3.558957	-0.055783	0.659006
11 C	-1.732566	1.099618	0.147651
12 H	-2.122590	1.356168	-0.840610
13 H	-1.522688	1.998860	0.726087

Point Group: C_1 Number of degrees of freedom: 33

Energy is -1181.152855073

Distance Matrix (Angstroms)

	Mo(1)	Cl(2)	Cl(3)	O (4)	C (5)	H (6)
Cl(2)	2.308713					
Cl(3)	2.308474	3.707688				
O (4)	1.681746	3.375185	3.377638			
C (5)	2.246113	3.038178	4.194375	3.016995		
H (6)	2.709793	3.617427	4.845743	2.829843	1.092987	
H (7)	2.820242	2.704123	4.718789	3.745200	1.089500	1.796336
C (8)	2.882387	4.130549	4.130663	3.800433	1.514738	2.198805
H (9)	3.333260	4.192971	4.188994	4.573318	2.165377	3.081520
H (10)	3.857027	5.116481	5.118947	4.497063	2.220348	2.511226
C (11)	2.246387	4.196685	3.044619	3.013327	2.252740	2.735284
H (12)	2.710148	4.844445	3.629556	2.825067	2.734739	2.790238
H (13)	2.821293	4.726388	2.712235	3.740339	3.206710	3.807193

	H (7)	C (8)	H (9)	H (10)	C (11)	H (12)
C (8)	2.247414					
H (9)	2.470874	1.095571				
H (10)	2.893078	1.099379	1.770738			
C (11)	3.206394	1.514988	2.166034	2.220842		
H (12)	3.806475	2.198496	3.081737	2.511096	1.092976	
H (13)	4.037231	2.247760	2.472037	2.893519	1.089622	1.796518

TS17

Coordinates (Angstroms)

ATOM	X	Y	Z
1 Mo	-0.050241	0.190373	0.111483
2 Cl	0.832848	-2.002900	-0.166809
3 Cl	2.110596	0.960966	-0.452563
4 C	-0.146713	0.465569	1.966028
5 H	0.451512	-0.179856	2.614820
6 H	-0.711803	1.260378	2.454745
7 C	-2.016394	-0.948002	-0.167912
8 H	-1.879388	-1.710360	-0.929631
9 H	-2.346743	-1.326855	0.793870
10 C	-2.541365	0.320639	-0.608100
11 H	-3.173162	0.898042	0.061992
12 H	-2.773561	0.454594	-1.661018
13 O	-1.159206	1.412664	-0.586061

Distance Matrix (Angstroms)

	Mo(1)	Cl(2)	Cl(3)	C (4)	H (5)	H (6)
Cl(2)	2.380702					
Cl(3)	2.362452	3.240185				
C (4)	1.877332	3.406152	3.345212			
H (5)	2.579829	3.347592	3.669179	1.093334		
H (6)	2.659595	4.461779	4.063007	1.090822	1.858278	
C (7)	2.289043	3.038255	4.556011	3.169793	3.797921	3.668409
H (8)	2.835928	2.832614	4.825304	4.015180	4.509842	4.652154
H (9)	2.835764	3.389652	5.162905	3.070321	3.530113	3.482142
C (10)	2.596242	4.120545	4.698399	3.518735	4.426627	3.689367
H (11)	3.202481	4.951357	5.309127	3.601636	4.562571	3.451788
H (12)	3.260069	4.612822	5.056853	4.478383	5.393182	4.673290
O (13)	1.791749	3.976195	3.303552	2.904356	3.921246	3.077314

	C (7)	H (8)	H (9)	C (10)	H (11)	H (12)
H (8)	1.086360					
H (9)	1.085211	1.826459				
C (10)	1.441808	2.160221	2.172011			
H (11)	2.190626	3.075862	2.483702	1.087007		
H (12)	2.184020	2.453874	3.063039	1.086506	1.823483	
O (13)	2.546048	3.223349	3.289288	1.761638	2.177344	2.163232

Point Group: C_1 Number of degrees of freedom: 33

Energy = -1181.085460127

pdt16

Coordinates (Angstroms)

ATOM	X	Y	Z
1 Mo	0.040326	0.070033	0.230074
2 Cl	1.679632	-1.503601	-0.418603
3 Cl	0.731374	2.025646	-0.701706
4 O	-1.867679	0.293788	0.558202
5 C	-1.238394	-1.216402	-0.954818
6 H	-0.915822	-1.172204	-1.997968
7 H	-1.183583	-2.238643	-0.573164
8 C	-2.459934	-0.429207	-0.528498
9 H	-3.302200	-1.028917	-0.159274
10 H	-2.835151	0.267112	-1.289063
11 C	0.354764	0.002449	2.072550
12 H	1.115962	0.694531	2.447331
13 H	-0.122961	-0.659472	2.797563

Distance Matrix (Angstroms)

	Mo(1)	Cl(2)	Cl(3)	O (4)	C (5)	H (6)
Cl(2)	2.363140					
Cl(3)	2.273803	3.665368				
O (4)	1.948902	4.094896	3.367755			
C (5)	2.166567	2.980752	3.801964	2.228431		
H (6)	2.724251	3.056239	3.823583	3.096639	1.092780	
H (7)	2.733703	2.960096	4.676295	2.856779	1.092538	1.799737
C (8)	2.660071	4.278131	4.029982	1.433320	1.514459	2.257358
H (9)	3.540023	5.011110	5.088644	2.078983	2.219760	3.015978
H (10)	3.258065	4.927107	4.019642	2.085450	2.205032	2.501599
C (11)	1.870336	3.198329	3.454223	2.705066	3.631626	4.423044
H (12)	2.542286	3.655555	3.440379	3.554084	4.557332	5.231971
H (13)	2.674106	3.782277	4.492731	2.994576	3.954077	4.887600

	H (7)	C (8)	H (9)	H (10)	C (11)	H (12)
C (8)	2.214752					
H (9)	2.474527	1.097902				
H (10)	3.085287	1.097318	1.781642			
C (11)	3.793258	3.856722	4.406602	4.641772		
H (12)	4.797375	4.785956	5.411544	5.454779	1.094925	
H (13)	3.870465	4.071505	4.357400	4.991497	1.091789	1.868399

Point Group: C_1 Number of degrees of freedom: 33

Energy = -1181.104321832

TS18

Coordinates (Angstroms)

ATOM	X	Y	Z
1 Mo	0.498580	-0.244425	-0.126420
2 Cl	2.388706	1.064554	0.177888

3	O	-0.799031	0.210367	-1.371270
4	Cl	-1.157131	-0.066391	1.473149
5	C	-2.249476	0.738730	-1.145309
6	H	-2.754097	0.273674	-1.994086
7	H	-2.167509	1.816811	-1.294163
8	C	-2.855323	0.380902	0.137296
9	H	-3.257158	1.172826	0.759208
10	H	-3.386809	-0.563643	0.203947
11	C	0.826552	-2.074060	-0.365207
12	H	0.275236	-2.791350	-0.972803
13	H	1.684527	-2.465042	0.198391

Distance Matrix (Angstroms)

	Mo(1)	Cl(2)	O (3)	Cl(4)	C (5)	H (6)
Cl(2)	2.319182					
O (3)	1.854800	3.645710				
Cl(4)	2.309047	3.940774	2.880200			
C (5)	3.091366	4.834227	1.560133	2.949196		
H (6)	3.786359	5.638385	2.052849	3.832448	1.091486	
H (7)	3.566561	4.846847	2.111715	3.496474	1.091391	1.793111
C (8)	3.421878	5.288561	2.556010	2.206452	1.462931	2.136476
H (9)	4.110779	5.676745	3.392292	2.540764	2.197964	2.939756
H (10)	3.912454	6.000690	3.126818	2.613349	2.193216	2.435728
C (11)	1.874072	3.547700	2.978807	3.368276	4.240554	4.581064
H (12)	2.693153	4.545200	3.212963	3.931889	4.343431	4.428798
H (13)	2.538328	3.599214	3.973627	3.931101	5.248435	5.657641

	H (7)	C (8)	H (9)	H (10)	C (11)	H (12)
C (8)	2.141028					
H (9)	2.412132	1.084154				
H (10)	3.065549	1.085857	1.827690			
C (11)	4.996623	4.453712	5.336971	4.511951		
H (12)	5.225459	4.593027	5.585012	4.444996	1.089783	
H (13)	5.949804	5.358485	6.161887	5.416068	1.098467	1.861256

Point Group: C_1 Number of degrees of freedom: 33

Energy = -1181.063602710

pdt17

Coordinates (Angstroms)

ATOM		X	Y	Z
1	Mo	0.515450	-0.256136	-0.158215
2	Cl	2.372536	1.036127	0.374263
3	O	-0.783290	0.521500	-1.358821
4	Cl	-1.389653	-0.284184	1.364713
5	C	-2.021222	1.090816	-0.906030
6	H	-2.665695	1.206854	-1.787226
7	H	-1.844257	2.088464	-0.480241
8	C	-2.720347	0.209550	0.102147
9	H	-3.492193	0.706724	0.689056
10	H	-3.072782	-0.734881	-0.314104
11	C	0.843947	-2.044267	-0.605370
12	H	0.347347	-2.686032	-1.334711
13	H	1.668623	-2.498919	-0.037158

Distance Matrix (Angstroms)

	Mo(1)	Cl(2)	O (3)	Cl(4)	C (5)	H (6)
Cl(2)	2.324273					
O (3)	1.932070	3.636984				
Cl(4)	2.439163	4.108318	2.904212			
C (5)	2.967863	4.576816	1.435834	2.728696		
H (6)	3.861826	5.484975	2.048583	3.712977	1.097869	
H (7)	3.342015	4.429326	2.086368	3.039733	1.099051	1.777697
C (8)	3.279487	5.166694	2.446208	1.899630	1.510572	2.137132
H (9)	4.207869	5.882401	3.400921	2.420555	2.203538	2.658044
H (10)	3.623383	5.767304	2.812775	2.419603	2.188452	2.471061
C (11)	1.872237	3.575625	3.130295	3.459493	4.257739	4.927896
H (12)	2.704957	4.569075	3.401056	4.009106	4.478668	4.943455
H (13)	2.524785	3.627852	4.108723	4.027822	5.220737	5.965049

	H (7)	C (8)	H (9)	H (10)	C (11)	H (12)
C (8)	2.153376					
H (9)	2.447887	1.089674				
H (10)	3.083529	1.090608	1.805675			
C (11)	4.931689	4.276033	5.295809	4.140059		
H (12)	5.322504	4.456422	5.508946	4.067666	1.091060	
H (13)	5.794888	5.159290	6.118623	5.066503	1.099847	1.861297

Point Group: C_1 Number of degrees of freedom: 33

Energy is -1181.067782602

TS19

Coordinates (Angstroms)

ATOM		X	Y	Z
1	Mo	0.339277	0.007294	-0.244236
2	Cl	1.151715	2.126703	0.168115
3	Cl	1.607473	-1.862614	0.332792
4	O	-0.758640	-0.274218	-1.505361
5	C	-3.109439	-0.518473	-0.282044
6	H	-3.241216	-1.567061	-0.027980
7	H	-3.458631	-0.197916	-1.256103
8	C	-2.512920	0.387849	0.673217
9	H	-2.414475	1.403840	0.279674
10	H	-3.142613	0.443221	1.580322
11	C	-1.129449	-0.170075	1.222177
12	H	-0.778464	0.411073	2.087412
13	H	-1.291313	-1.203653	1.542025

Distance Matrix (Angstroms)

	Mo(1)	Cl(2)	Cl(3)	O (4)	C (5)	H (6)
Cl(2)	2.306942					
Cl(3)	2.331918	4.018641				
O (4)	1.695613	3.494910	3.391208			
C (5)	3.488767	5.035576	4.943076	2.661281		
H (6)	3.917307	5.742838	4.871067	3.165009	1.086946	
H (7)	3.935745	5.356075	5.564281	2.712546	1.083274	1.852057
C (8)	3.020193	4.087577	4.707240	2.874375	1.445606	2.200856
H (9)	3.131768	3.640424	5.181564	2.957029	2.119856	3.099097
H (10)	3.955073	4.823867	5.425544	3.964781	2.096274	2.576353
C (11)	2.083023	3.404401	3.338628	2.754598	2.510861	2.823831
H (12)	2.617053	3.217558	3.733771	3.657600	3.451351	3.801717
H (13)	2.704801	4.352848	3.209274	3.230194	2.665011	2.529645

	H (7)	C (8)	H (9)	H (10)	C (11)	H (12)
C (8)	2.227053					
H (9)	2.452447	1.093985				
H (10)	2.925104	1.105631	1.773318			
C (11)	3.401137	1.589537	2.239823	2.134767		
H (12)	4.328194	2.238041	2.632495	2.418134	1.099798	
H (13)	3.679443	2.186328	3.107095	2.478099	1.093977	1.779832

Point Group: C_1 Number of degrees of freedom: 33

Energy = -1181.091799069

pdt18

Coordinates (Angstroms)

ATOM		X	Y	Z
1	Mo	0.244802	-0.055681	-0.285639
2	Cl	1.535825	-1.853246	0.326300
3	Cl	1.492255	1.877569	0.049006
4	O	-1.381818	-0.132410	-1.144454
5	C	-2.459624	-0.225397	0.946691
6	H	-3.286908	0.165473	1.556367
7	H	-2.446941	-1.315395	1.064895
8	C	-2.670850	0.113842	-0.531583
9	H	-3.409107	-0.511856	-1.042139
10	H	-2.920661	1.169888	-0.687056
11	C	-1.101835	0.375289	1.318730
12	H	-1.155713	1.466893	1.433824
13	H	-0.663988	-0.053467	2.229741

Distance Matrix (Angstroms)

	Mo(1)	Cl(2)	Cl(3)	O (4)	C (5)	H (6)
Cl(2)	2.296181					
Cl(3)	2.324991	3.741359				
O (4)	1.841017	3.692835	3.704681			
C (5)	2.976804	4.358714	4.565704	2.354400		
H (6)	3.989345	5.370945	5.295641	3.318515	1.099492	
H (7)	3.264399	4.086225	5.171491	2.723080	1.096462	1.772022
C (8)	2.930913	4.722447	4.558427	1.448397	1.531337	2.177551
H (9)	3.759180	5.303235	5.560872	2.065030	2.222390	2.688111
H (10)	3.418085	5.479643	4.529506	2.067179	2.197385	2.485142
C (11)	2.138496	3.592845	3.255510	2.530499	1.530630	2.207950
H (12)	2.690024	4.415236	3.016308	3.042435	2.191193	2.500140
H (13)	2.674517	3.420741	3.624071	3.450609	2.213614	2.716814

	H (7)	C (8)	H (9)	H (10)	C (11)	H (12)
C (8)	2.154437					
H (9)	2.451740	1.094161				
H (10)	3.077397	1.096271	1.786876			
C (11)	2.175352	2.440045	3.418221	2.821824		
H (12)	3.089418	2.826519	3.888910	2.775136	1.098977	
H (13)	2.475530	3.417659	4.295462	3.885469	1.097944	1.785153

Point Group: C_1 Number of degrees of freedom: 33

Energy = -1181.135196731

R15

Coordinates (Angstroms)

ATOM		X	Y	Z
1	W	0.000007	-0.199011	0.059185
2	Cl	-1.914426	1.066577	-0.060503
3	Cl	1.914298	1.066523	-0.060967
4	O	-0.000371	-1.334055	1.309765

5	C	0.000111	-1.296589	-1.473614
6	H	0.000670	-0.775509	-2.438600
7	H	-0.001161	-2.383303	-1.525973

Distance Matrix (Angstroms)

	W (1)	Cl(2)	Cl(3)	O (4)	C (5)	H (6)
Cl(2)	2.298063					
Cl(3)	2.297940	3.828724				
O (4)	1.688867	3.362183	3.362683			
C (5)	1.885246	3.353638	3.353206	2.783632		
H (6)	2.563451	3.565980	3.564855	3.789751	1.096686	
H (7)	2.698862	4.208308	4.209100	3.023629	1.087975	1.848754

Point Group: C_1 Number of degrees of freedom: 15

Energy = -1102.870985829

TS20

Coordinates (Angstroms)

ATOM	X	Y	Z
1 W	-0.045900	-0.235794	-0.023162
2 Cl	0.054960	2.196158	-0.005675
3 Cl	-2.368607	-0.047459	-0.058704
4 O	0.069619	-1.808617	-0.676198
5 C	2.020457	0.097829	-1.078361
6 H	1.983158	1.097530	-1.494969
7 H	2.106028	-0.729588	-1.775643
8 C	2.466416	-0.076448	0.236895
9 H	2.875931	-1.029564	0.554063
10 H	2.703798	0.787178	0.848989
11 C	0.648199	-0.589679	1.740823
12 H	0.955249	-1.564213	2.115584
13 H	0.681790	0.224158	2.468842

Distance Matrix (Angstroms)

	W (1)	Cl(2)	Cl(3)	O (4)	C (5)	H (6)
Cl(2)	2.434105					
Cl(3)	2.330601	3.303075				
O (4)	1.706919	4.060546	3.070492			
C (5)	2.344052	3.068684	4.508292	2.757179		
H (6)	2.839197	2.672625	4.723528	3.574591	1.083677	
H (7)	2.818832	3.987437	4.841026	2.553437	1.085423	1.852629
C (8)	2.530762	3.322454	4.844138	3.094961	1.399696	2.147351
H (9)	3.082265	4.321628	5.370773	3.161622	2.160476	3.085467
H (10)	3.060713	3.119619	5.220136	4.000405	2.157970	2.471797
C (11)	1.928381	3.341119	3.554353	2.768131	3.209915	3.885761
H (12)	2.709471	4.410289	4.251599	2.939068	3.754775	4.601908
H (13)	2.636508	3.225668	3.970792	3.794496	3.793499	4.262409

	H (7)	C (8)	H (9)	H (10)	C (11)	H (12)
C (8)	2.146342					
H (9)	2.471896	1.084772				
H (10)	3.089758	1.084831	1.848557			
C (11)	3.809248	2.414771	2.562164	2.629941		
H (12)	4.142769	2.833115	2.532433	3.192292	1.088320	
H (13)	4.577525	2.873472	3.170560	2.651308	1.092461	1.843323

Point Group: C_1 Number of degrees of freedom: 33

Energy = -1181.457892269

pdt19

Coordinates (Angstroms)

ATOM	X	Y	Z
1 W	0.085544	-0.000788	-0.201393
2 Cl	1.322970	-1.825440	0.494249
3 Cl	1.307820	1.845662	0.462722
4 O	-0.332770	-0.016445	-1.839399
5 C	-1.622262	-1.125744	0.576593
6 H	-1.769157	-2.052567	0.012526
7 H	-1.396930	-1.370042	1.620917
8 C	-2.649108	-0.006217	0.446566
9 H	-3.448459	-0.003733	1.200009
10 H	-3.114381	-0.015193	-0.544155
11 C	-1.630873	1.123012	0.559733
12 H	-1.785157	2.040159	-0.017991
13 H	-1.407142	1.384442	1.600278

Distance Matrix (Angstroms)

	W (1)	Cl(2)	Cl(3)	O (4)	C (5)	H (6)
Cl(2)	2.311817					
Cl(3)	2.311792	3.671269				
O (4)	1.690649	3.385240	3.385075			
C (5)	2.188011	3.028325	4.174638	2.954717		
H (6)	2.774071	3.137657	4.986647	3.104614	1.094874	
H (7)	2.719081	2.979031	4.358651	3.865029	1.095933	1.786425
C (8)	2.810374	4.369125	4.368866	3.254407	1.524684	2.269417
H (9)	3.801725	5.155895	5.156165	4.352663	2.232163	2.903083
H (10)	3.218262	4.903607	4.902289	3.068390	2.171593	2.504079
C (11)	2.188225	4.174069	3.027796	2.956226	2.248836	3.225346
H (12)	2.774639	4.986552	3.136147	3.107503	3.225370	4.092871
H (13)	2.719006	4.356622	2.979559	3.866282	2.719419	3.803293

	H (7)	C (8)	H (9)	H (10)	C (11)	H (12)
C (8)	2.192503					
H (9)	2.500546	1.098473				
H (10)	3.077789	1.094571	1.775907			
C (11)	2.719588	1.524719	2.232291	2.171376		
H (12)	3.803447	2.269335	2.903032	2.503629	1.094864	
H (13)	2.754579	2.192592	2.500844	3.077699	1.095962	1.786520

Point Group: C_1 Number of degrees of freedom: 33

Energy = -1181.484882060

TS21

Coordinates (Angstroms)

ATOM	X	Y	Z
1 W	-0.044743	0.132089	0.094251
2 Cl	0.914922	-2.022409	-0.182585
3 Cl	2.056021	1.023743	-0.499773
4 C	-0.187693	0.326869	1.961542
5 H	0.392698	-0.352835	2.591810
6 H	-0.745289	1.100981	2.488261
7 C	-1.967244	-1.004401	-0.328692
8 H	-1.812668	-1.680546	-1.167316
9 H	-2.312753	-1.495057	0.576133
10 C	-2.538660	0.278883	-0.642169
11 H	-3.172352	0.781230	0.082837
12 H	-2.752413	0.531904	-1.676493
13 O	-1.142829	1.408497	-0.502112

Distance Matrix (Angstroms)

	W (1)	Cl(2)	Cl(3)	C (4)	H (5)	H (6)
Cl(2)	2.374754					
Cl(3)	2.358203	3.268295				
C (4)	1.882857	3.366325	3.402640			
H (5)	2.581532	3.279857	3.770875	1.093659		
H (6)	2.675967	4.432300	4.096542	1.089769	1.849140	
C (7)	2.272994	3.060158	4.508802	3.191277	3.810931	3.723041
H (8)	2.828914	2.919985	4.767132	4.057094	4.556038	4.715871
H (9)	2.832610	3.357326	5.156366	3.123243	3.561893	3.585050
C (10)	2.604512	4.175450	4.656843	3.508369	4.410277	3.700218
H (11)	3.194284	4.963531	5.266320	3.555863	4.504512	3.432046
H (12)	3.259887	4.712284	4.974698	4.455909	5.375211	4.658065
O (13)	1.786241	4.013421	3.221907	2.855134	3.877175	3.032315

	C (7)	H (8)	H (9)	C (10)	H (11)	H (12)
H (8)	1.088282					
H (9)	1.085739	1.823214				
C (10)	1.439306	2.154578	2.163829			
H (11)	2.193198	3.077655	2.482686	1.086071		
H (12)	2.189358	2.457096	3.062058	1.086065	1.825857	
O (13)	2.555740	3.230072	3.310885	1.801107	2.203313	2.176775

Point Group: C_1 Number of degrees of freedom: 33

Energy = -1181.416676186

R16

Coordinates (Angstroms)

ATOM	X	Y	Z
1 Ru	-0.055736	-0.379264	0.000000
2 Cl	-0.027297	1.097344	-1.752337
3 Cl	-0.027297	1.097344	1.752337
4 O	-1.360142	-1.446621	0.000000
5 C	1.652900	-1.072334	0.000000
6 H	2.556756	-0.456643	0.000000
7 H	1.781779	-2.158339	0.000000

Distance Matrix (Angstroms)

	Ru(1)	Cl(2)	Cl(3)	O (4)	C (5)	H (6)
Cl(2)	2.291695					
Cl(3)	2.291695	3.504674				
O (4)	1.685444	3.364359	3.364359			
C (5)	1.843850	3.255956	3.255956	3.036200		
H (6)	2.613638	3.487534	3.487534	4.040067	1.093632	
H (7)	2.557649	4.116177	4.116177	3.221522	1.093626	1.869855

Point Group: C_s Number of degrees of freedom: 10

Energy is -1128.786525093

R17

Coordinates (Angstroms)

ATOM	X	Y	Z
1 Ru	0.454917	-0.402418	0.004086
2 Cl	1.645422	1.487461	-0.152977
3 C	-1.363014	-0.020204	0.866757

4	O	0.834291	-2.002249	-0.172988
5	Cl	-2.564346	0.625082	-0.305873
6	H	-1.711497	-0.987692	1.241508
7	H	-1.260018	0.696428	1.683638

Distance Matrix (Angstroms)

	Ru(1)	Cl(2)	C (3)	O (4)	Cl(5)	H (6)
Cl(2)	2.239110					
C (3)	2.048210	3.516191				
O (4)	1.653705	3.582794	3.136515			
Cl(5)	3.204338	4.299909	1.798514	4.297821		
H (6)	2.562637	4.397712	1.094492	3.084017	2.392233	
H (7)	2.639954	3.527105	1.091541	3.887936	2.380024	1.798769

Point Group: C_1 Number of degrees of freedom: 15

Energy = -1128.780003421

TS23

Coordinates (Angstroms)

ATOM		X	Y	Z
1	Ru	-0.100827	-0.319594	-0.022773
2	Cl	0.139052	2.119360	-0.184284
3	Cl	-2.368762	-0.111694	-0.034620
4	O	0.232069	-1.955794	-0.542172
5	C	1.996668	-0.104607	-1.024814
6	H	1.996633	0.876794	-1.482476
7	H	1.999855	-0.973893	-1.673831
8	C	2.351667	-0.248058	0.322632
9	H	2.639295	-1.227378	0.692821
10	H	2.692170	0.629440	0.863164
11	C	0.587371	-0.174304	1.720165
12	H	0.649842	-1.082089	2.326352
13	H	0.865478	0.767819	2.192852

Distance Matrix (Angstroms)

	Ru(1)	Cl(2)	Cl(3)	O (4)	C (5)	H (6)
Cl(2)	2.456039					
Cl(3)	2.277475	3.359930				
O (4)	1.748641	4.091897	3.228411			
C (5)	2.334479	3.017160	4.476328	2.602624		
H (6)	2.821598	2.584546	4.704260	3.467191	1.082867	
H (7)	2.750811	3.905067	4.745020	2.317294	1.084846	1.860556
C (8)	2.477730	3.279831	4.735892	2.856036	1.400790	2.156329
H (9)	2.973956	4.268628	5.182138	2.801881	2.150316	3.093942
H (10)	3.079996	3.136147	5.193103	3.835427	2.141730	2.459061
C (11)	1.879510	3.014765	3.438301	2.901399	3.086404	3.653456
H (12)	2.581334	4.100423	3.953204	3.027594	3.741622	4.489793
H (13)	2.650510	2.829335	4.024361	3.911475	3.520525	3.847002

	H (7)	C (8)	H (9)	H (10)	C (11)	H (12)
C (8)	2.153246					
H (9)	2.464585	1.085744				
H (10)	3.079986	1.085412	1.865365			
C (11)	3.762135	2.251950	2.524836	2.410525		
H (12)	4.223234	2.758027	2.578267	3.039959	1.093361	
H (13)	4.389944	2.595860	3.062243	2.263630	1.090125	1.867211

Point Group: C_1 Number of degrees of freedom: 33

Energy = -1207.352050078

pdt22

Coordinates (Angstroms)

ATOM		X	Y	Z
1	Ru	-0.003606	-0.000502	-0.347087
2	Cl	1.417102	-1.631341	0.496489
3	Cl	1.415161	1.633565	0.495022
4	O	-0.201921	-0.001970	-2.005610
5	C	-1.557422	-1.126390	0.564350
6	H	-1.699609	-1.955692	-0.133146
7	H	-1.194787	-1.478608	1.529810
8	C	-2.577457	-0.000129	0.612498
9	H	-3.209901	0.001371	1.509009
10	H	-3.219772	-0.001058	-0.272712
11	C	-1.557533	1.126397	0.562431
12	H	-1.700648	1.955434	-0.135368
13	H	-1.195236	1.479315	1.527765

Distance Matrix (Angstroms)

	Ru(1)	Cl(2)	Cl(3)	O (4)	C (5)	H (6)
Cl(2)	2.321567					
Cl(3)	2.322116	3.264908				
O (4)	1.670337	3.396555	3.397512			
C (5)	2.124308	3.017843	4.056896	3.115509		
H (6)	2.597107	3.196174	4.793658	3.092931	1.092913	
H (7)	2.669541	2.813013	4.191448	3.957958	1.089805	1.802186
C (8)	2.746909	4.316343	4.315525	3.535204	1.520281	2.269544
H (9)	3.704783	5.010001	5.008335	4.626067	2.212445	2.967786
H (10)	3.217026	4.974947	4.974336	3.479994	2.174960	2.480115
C (11)	2.124102	4.056836	3.016400	3.115401	2.252787	3.162797
H (12)	2.598165	4.794222	3.195192	3.094417	3.163504	3.911127
H (13)	2.669253	4.190946	2.811498	3.957981	2.801615	3.848674

	H (7)	C (8)	H (9)	H (10)	C (11)	H (12)
C (8)	2.222417					
H (9)	2.500291	1.097141				
H (10)	3.087524	1.093695	1.781751			
C (11)	2.802402	1.520464	2.211790	2.175237		
H (12)	3.849851	2.269873	2.966510	2.480819	1.093027	
H (13)	2.957924	2.221936	2.498708	3.087389	1.089808	1.802260

Point Group: C_1 Number of degrees of freedom: 33

Energy = -1207.424069617

TS24 Coordinates (Angstroms)

ATOM		X	Y	Z
1	Ru	0.059139	0.215390	0.066989
2	Cl	-0.785642	-2.039520	0.121850
3	Cl	-2.160292	0.835290	0.162071
4	C	0.089579	0.745049	-1.699176
5	H	-0.705425	1.372095	-2.103797
6	H	0.885837	0.442791	-2.383607
7	C	1.994716	-0.921929	-0.304596
8	H	1.932156	-1.806645	0.318613
9	H	1.987225	-1.096893	-1.374378
10	C	2.589026	0.250708	0.213449
11	H	2.936280	1.027185	-0.460736
12	H	3.039595	0.226392	1.200307
13	O	1.170395	1.298356	0.971421

Distance Matrix (Angstroms)

	Ru(1)	Cl(2)	Cl(3)	C (4)	H (5)	H (6)
Cl(2)	2.408586					
Cl(3)	2.306337	3.186819				
C (4)	1.844126	3.440345	2.921353			
H (5)	2.575817	4.074194	2.745715	1.090383		
H (6)	2.596258	3.902951	3.989164	1.092626	1.863871	
C (7)	2.275528	3.026757	4.535381	2.890192	3.973717	2.722931
H (8)	2.767695	2.734844	4.873649	3.738677	4.788454	3.668342
H (9)	2.741740	3.288774	4.826582	2.664451	3.725361	2.145279
C (10)	2.534369	4.079451	4.785436	3.185866	4.180974	3.111663
H (11)	3.035695	4.857653	5.138070	3.117217	4.010066	2.871109
H (12)	3.188675	4.574917	5.337370	4.168765	5.123955	4.186877
O (13)	1.796024	3.960968	3.458750	2.933666	3.602929	3.474072

	C (7)	H (8)	H (9)	C (10)	H (11)	H (12)
H (8)	1.083987					
H (9)	1.084021	1.836573				
C (10)	1.413029	2.162230	2.167807			
H (11)	2.170246	3.105840	2.499431	1.085370		
H (12)	2.162209	2.477306	3.080190	1.085123	1.846892	
O (13)	2.690239	3.263046	3.450681	1.919532	2.289751	2.166889

Point Group: C_1 Number of degrees of freedom: 33

Energy = -1207.346864253

pdt23

Coordinates (Angstroms)

ATOM		X	Y	Z
1	Ru	-0.079056	0.163812	-0.104464
2	Cl	-1.329576	-1.558866	0.733930
3	Cl	-1.346769	2.110080	0.349947
4	O	1.501509	1.036022	0.501893
5	C	1.609962	-1.190205	0.203980
6	H	1.414037	-1.736572	1.125631
7	H	1.809197	-1.865516	-0.624645
8	C	2.503197	0.030518	0.368295
9	H	3.117757	0.232747	-0.520425
10	H	3.148665	0.026611	1.256017
11	C	-0.021225	-0.119912	-1.905672
12	H	-0.909859	-0.480273	-2.435711
13	H	0.846328	0.163767	-2.508144

Distance Matrix (Angstroms)

	Ru(1)	Cl(2)	Cl(3)	O (4)	C (5)	H (6)
Cl(2)	2.287865					
Cl(3)	2.366758	3.689024				
O (4)	1.904365	3.847380	3.047848			
C (5)	2.186614	3.009592	4.433446	2.248689		
H (6)	2.711811	2.777126	4.797965	2.843234	1.089194	
H (7)	2.820330	3.433898	5.168686	3.127728	1.087363	1.798956
C (8)	2.628554	4.165331	4.375745	1.425575	1.521523	2.209623
H (9)	3.224498	4.956012	4.920764	2.074281	2.196134	3.080646
H (10)	3.505412	4.779221	5.036936	2.073821	2.225989	2.476842
C (11)	1.824333	3.278699	3.437695	3.074292	2.873487	3.723219
H (12)	2.557302	3.374336	3.828930	4.091866	3.717724	4.434178

H (13)	2.575658	4.267677	4.094690	3.201627	3.126020	4.139795
	H (7)	C (8)	H (9)	H (10)	C (11)	H (12)
C (8)	2.250002					
H (9)	2.475055	1.099275				
H (10)	2.985164	1.097586	1.788629			
C (11)	2.835244	3.400920	3.449128	4.479502		
H (12)	3.548538	4.446606	4.516460	5.509755	1.095660	
H (13)	2.931327	3.322179	3.019135	4.414575	1.093661	1.871958

Point Group: C_1 Number of degrees of freedom: 33
Energy = -1207.381903199

TS25

Coordinates (Angstroms)

ATOM	X	Y	Z
1 Ru	-0.445306	0.185669	0.145234
2 Cl	-2.561909	0.068365	-0.805372
3 O	0.861625	1.381402	-0.074643
4 Cl	0.884441	-1.604639	-0.169631
5 C	2.727296	1.158404	-0.283363
6 H	2.950685	1.656467	0.653728
7 H	2.720413	1.789758	-1.164883
8 C	3.082860	-0.176514	-0.426933
9 H	3.176015	-0.630501	-1.406841
10 H	3.445365	-0.754108	0.415416
11 C	-0.728574	-0.118337	1.927651
12 H	-1.011987	0.731085	2.559419
13 H	-0.552564	-1.078020	2.420931

Distance Matrix (Angstroms)

	Ru(1)	Cl(2)	O (3)	Cl(4)	C (5)	H (6)
Cl(2)	2.323234					
O (3)	1.784991	3.738799				
Cl(4)	2.252237	3.883354	2.987638			
C (5)	3.345940	5.425529	1.890508	3.323169		
H (6)	3.735582	5.919436	2.229429	3.947416	1.084486	
H (7)	3.783026	5.567348	2.193278	3.985379	1.084312	1.837971
C (8)	3.592563	5.662738	2.735891	2.634159	1.388900	2.131929
H (9)	4.023560	5.811536	3.343487	2.780457	2.159568	3.086575
H (10)	4.011670	6.184991	3.387664	2.761161	2.159077	2.472321
C (11)	1.830211	3.296269	2.964310	3.034716	4.296707	4.278990
H (12)	2.539074	3.763412	3.297213	4.061989	4.716593	4.493413
H (13)	2.605228	3.969974	3.778436	3.008874	4.803362	4.782592
	H (7)	C (8)	H (9)	H (10)	C (11)	H (12)
C (8)	2.131236					
H (9)	2.474626	1.083975				
H (10)	3.081258	1.083778	1.846198			
C (11)	5.010001	4.480456	5.160133	4.484732		
H (12)	5.377920	5.148768	5.926592	5.164352	1.095888	
H (13)	5.638670	4.705248	5.362315	4.484468	1.093296	1.871660

Point Group: C_1 Number of degrees of freedom: 33
Energy = -1207.357724376

pdt24

Coordinates (Angstroms)

ATOM	X	Y	Z
1 Ru	0.492228	-0.207743	0.144261
2 Cl	2.692003	0.456054	0.240461
3 O	-0.407454	1.356987	-0.601550
4 Cl	-1.968560	-0.978175	0.503563
5 C	-1.678555	1.653544	-0.080573
6 H	-2.051130	2.541433	-0.615098
7 H	-1.650047	1.904745	0.993157
8 C	-2.675526	0.528453	-0.297345
9 H	-3.642093	0.696842	0.179527
10 H	-2.793590	0.270211	-1.349998
11 C	0.679338	-1.334151	-1.273770
12 H	-0.179468	-1.683283	-1.859288
13 H	1.667844	-1.656157	-1.621665

Distance Matrix (Angstroms)

	Ru(1)	Cl(2)	O (3)	Cl(4)	C (5)	H (6)
Cl(2)	2.299758					
O (3)	1.952957	3.335760				
Cl(4)	2.603487	4.883347	3.018495			
C (5)	2.868316	4.542997	1.405368	2.711322		
H (6)	3.821422	5.251485	2.026023	3.694031	1.101306	
H (7)	3.126112	4.638820	2.094557	2.941493	1.103092	1.775591
C (8)	3.282022	5.394890	2.433754	1.846938	1.518806	2.131414
H (9)	4.232272	6.338963	3.392457	2.389852	2.199639	2.562247
H (10)	3.641134	5.714528	2.726702	2.382191	2.183656	2.499955
C (11)	1.820610	3.090073	2.979131	3.208893	3.988697	4.786383
H (12)	2.577325	4.151030	3.298049	3.046488	4.067616	4.785327
H (13)	2.568749	2.996306	3.798228	4.266109	4.952522	5.697694
	H (7)	C (8)	H (9)	H (10)	C (11)	H (12)
C (8)	2.147366					
H (9)	2.467644	1.090877				
H (10)	3.077299	1.090278	1.800394			
C (11)	4.588621	3.959522	4.991170	3.826359		
H (12)	4.813833	3.682628	4.670282	3.302901	1.096482	
H (13)	5.525009	5.038968	6.080816	4.867144	1.096294	1.862729

Point Group: C_1 Number of degrees of freedom: 33
Energy = -1207.399966177

R18

Coordinates (Angstroms)

ATOM	X	Y	Z
1 Re	-0.049948	-0.258199	0.000000
2 Cl	0.032794	1.180724	-1.790205
3 Cl	0.032794	1.180724	1.790205
4 O	-1.358120	-1.327785	0.000000
5 C	1.558483	-1.202936	0.000000
6 H	2.531134	-0.700098	0.000000
7 H	1.593541	-2.294170	0.000000

Distance Matrix (Angstroms)

	Re(1)	Cl(2)	Cl(3)	O (4)	C (5)	H (6)
Cl(2)	2.298299					
Cl(3)	2.298299	3.580410				
O (4)	1.689771	3.381138	3.381138			
C (5)	1.865362	3.348790	3.348790	2.919273		
H (6)	2.618636	3.603336	3.603336	3.939579	1.094941	
H (7)	2.616530	4.208997	4.208997	3.105833	1.091797	1.849363

Point Group: C_s Number of degrees of freedom: 10
Energy = -1114.089300173

R19

Coordinates (Angstroms)

ATOM	X	Y	Z
1 Re	-0.359643	-0.339445	-0.134692
2 Cl	-2.050622	1.117043	0.208817
3 C	1.309665	0.361585	-1.090275
4 O	-0.343988	-2.006928	-0.100021
5 Cl	2.368421	0.998197	0.291118
6 H	1.872168	-0.412810	-1.614728
7 H	1.127909	1.208776	-1.756270

Distance Matrix (Angstroms)

	Re(1)	Cl(2)	C (3)	O (4)	Cl(5)	H (6)
Cl(2)	2.258045					
C (3)	2.047235	3.681018				
O (4)	1.667917	3.573119	3.053691			
Cl(5)	3.068051	4.421407	1.853236	4.067054		
H (6)	2.678968	4.588469	1.091397	3.122002	2.422696	
H (7)	2.690597	3.738053	1.092848	3.905175	2.403125	1.789831

Point Group: C_1 Number of degrees of freedom: 15
Energy = -1114.042564502

TS26

Coordinates (Angstroms)

ATOM	X	Y	Z
1 Re	-0.086184	-0.232517	-0.013859
2 Cl	0.299438	2.179299	-0.109531
3 Cl	-2.362812	0.093003	-0.197907
4 O	0.052669	-1.882470	-0.506603
5 C	2.102424	-0.151542	-1.068288
6 H	2.092144	0.813791	-1.560929
7 H	2.077381	-1.039621	-1.691197
8 C	2.466364	-0.250528	0.258615
9 H	2.701046	-1.214884	0.697492
10 H	2.705574	0.637682	0.833152
11 C	0.346784	-0.298693	1.823906
12 H	0.479909	-1.262288	2.322765
13 H	0.447529	0.583034	2.462843

Distance Matrix (Angstroms)

	Re(1)	Cl(2)	Cl(3)	O (4)	C (5)	H (6)
Cl(2)	2.444323					
Cl(3)	2.307136	3.383493				
O (4)	1.727548	4.088586	3.135655			
C (5)	2.430716	3.098837	4.555842	2.741003		
H (6)	2.869372	2.680478	4.714234	3.541312	1.083821	
H (7)	2.854101	4.003024	4.819550	2.492612	1.085048	1.858044
C (8)	2.567113	3.276455	4.862856	3.012428	1.379464	2.140924
H (9)	3.039690	4.235503	5.306126	2.984865	2.146398	3.096247
H (10)	3.044434	3.009106	5.200797	3.896667	2.145260	2.477687
C (11)	1.889238	3.143385	3.403391	2.833042	3.386549	3.967494

H (12) 2.615473 4.218194 4.033816 2.927880 3.919892 4.689615
H (13) 2.661583 3.031024 3.900992 3.879721 3.968270 4.353016

	H (7)	C (8)	H (9)	H (10)	C (11)	H (12)
C (8)	2.139099					
H (9)	2.474977	1.085205				
H (10)	3.095208	1.084543	1.857532			
C (11)	3.987467	2.635352	2.766002	2.724386		
H (12)	4.325897	3.038154	2.752673	3.283659	1.093205	
H (13)	4.748208	3.103087	3.380431	2.785255	1.093541	1.850914

Point Group: C_1 Number of degrees of freedom: 33
Energy = -1192.664314803

pdt25

Coordinates (Angstroms)

ATOM	X	Y	Z
1 Re	0.015656	-0.000532	-0.239325
2 Cl	1.441020	-1.676233	0.524022
3 Cl	1.428972	1.689956	0.514104
4 O	-0.327944	-0.007322	-1.881940
5 C	-1.574018	-1.136286	0.630448
6 H	-1.756941	-2.026088	0.019670
7 H	-1.262088	-1.442891	1.633297
8 C	-2.606105	-0.006864	0.628655
9 H	-3.297975	-0.006566	1.480232
10 H	-3.196340	-0.012276	-0.293092
11 C	-1.582360	1.130135	0.622838
12 H	-1.771622	2.014111	0.005609
13 H	-1.273000	1.446110	1.623533

Distance Matrix (Angstroms)

	Re(1)	Cl(2)	Cl(3)	O (4)	C (5)	H (6)
Cl(2)	2.328591					
Cl(3)	2.328705	3.366225				
O (4)	1.678180	3.420986	3.421773			
C (5)	2.138575	3.064853	4.125424	3.023136		
H (6)	2.704081	3.256337	4.919704	3.119867	1.094650	
H (7)	2.686958	2.931166	4.278916	3.910291	1.094081	1.785719
C (8)	2.761713	4.379151	4.378831	3.390148	1.529968	2.273589
H (9)	3.733238	5.114705	5.114256	4.486122	2.229446	2.930272
H (10)	3.212467	4.994151	4.994263	3.279048	2.179049	2.495021
C (11)	2.139016	4.126293	3.064855	3.023455	2.266449	3.218079
H (12)	2.704281	4.920209	3.256907	3.119813	3.217836	4.040250
H (13)	2.687685	4.280638	2.931031	3.910746	2.783092	3.855222

	H (7)	C (8)	H (9)	H (10)	C (11)	H (12)
C (8)	2.208588					
H (9)	2.496256	1.097209				
H (10)	3.082039	1.094543	1.776244			
C (11)	2.782816	1.529985	2.229473	2.179211		
H (12)	3.854848	2.273519	2.930428	2.495052	1.094625	
H (13)	2.889038	2.208638	2.496263	3.082138	1.094045	1.785757

Point Group: C_1 Number of degrees of freedom: 33
Energy = -1192.717684721

TS27

Coordinates (Angstroms)

ATOM	X	Y	Z
1 Re	0.073697	-0.076889	-0.143353
2 Cl	-1.089343	1.818078	0.595364
3 Cl	2.068830	0.958161	0.674331
4 C	0.470659	-0.151827	-1.956407
5 H	0.330973	0.761801	-2.544472
6 H	0.898686	-1.004208	-2.483885
7 C	-2.047710	-1.050221	-0.281258
8 H	-2.682008	-0.471974	0.383981
9 H	-2.313223	-1.012808	-1.333318
10 C	-1.471791	-2.230669	0.220910
11 H	-1.149480	-3.028323	-0.440833
12 H	-1.586211	-2.507631	1.263942
13 O	0.413304	-1.666116	0.579432

Distance Matrix (Angstroms)

	Re(1)	Cl(2)	Cl(3)	C (4)	H (5)	H (6)
Cl(2)	2.342918					
Cl(3)	2.391755	3.274104				
C (4)	1.857514	3.581295	3.272156			
H (5)	2.556358	3.604385	3.663250	1.095468		
H (6)	2.649268	4.625942	3.898008	1.089951	1.856006	
C (7)	2.338111	3.148662	4.678959	3.155221	3.750159	3.678985
H (8)	2.833388	2.797428	4.969915	3.939444	4.379052	4.618366
H (9)	2.826544	3.637529	5.207473	2.979854	3.407037	3.411780
C (10)	2.675816	4.083973	4.786464	3.582653	4.455578	3.799906
H (11)	3.208679	4.956302	5.243393	3.632636	4.580620	3.530735
H (12)	3.262558	4.405183	5.071360	4.489006	5.372969	4.741435
O (13)	1.778593	3.794445	3.104288	2.954122	3.957314	3.171377

	C (7)	H (8)	H (9)	C (10)	H (11)	H (12)
H (8)	1.085931					
H (9)	1.085693	1.837831				
C (10)	1.406169	2.141080	2.146350			
H (11)	2.178341	3.092552	2.492615	1.085375		
H (12)	2.173630	2.473662	3.083635	1.085226	1.835242	
O (13)	2.678937	3.323422	3.394021	2.000210	2.310593	2.274810

Point Group: C_1 Number of degrees of freedom: 33
Energy = -1192.634257432

pdt26

Coordinates (Angstroms)

ATOM	X	Y	Z
1 Re	0.012652	0.015464	-0.155817
2 Cl	-1.053546	-1.907575	0.486651
3 Cl	-1.807313	1.440340	0.430828
4 O	1.213577	1.292148	0.508335
5 C	1.902094	-0.867304	0.424444
6 H	1.779024	-1.445851	1.344422
7 H	2.411905	-1.469788	-0.325988
8 C	2.450022	0.533659	0.665258
9 H	3.162165	0.882501	-0.090555
10 H	2.852569	0.735847	1.663097
11 C	0.207124	-0.035429	-1.994589
12 H	-0.467314	-0.659514	-2.589365
13 H	0.883308	0.617290	-2.549862

Distance Matrix (Angstroms)

	Re(1)	Cl(2)	Cl(3)	O (4)	C (5)	H (6)
Cl(2)	2.290768					
Cl(3)	2.384679	3.432173				
O (4)	1.874364	3.921549	3.025515			
C (5)	2.164711	3.133982	4.368634	2.268111		
H (6)	2.739750	2.995399	4.693247	2.918118	1.093720	
H (7)	2.826897	3.586279	5.181063	3.124160	1.089056	1.786444
C (8)	2.623636	4.273934	4.359120	1.459016	1.523454	2.197718
H (9)	3.267331	5.088213	5.027796	2.079297	2.216939	3.064876
H (10)	3.448555	4.861013	4.871272	2.080683	2.237802	2.452318
C (11)	1.849728	3.354217	3.481164	3.006665	3.068658	3.950842
H (12)	2.570626	3.370934	3.914914	4.028663	3.839312	4.597721
H (13)	2.617574	4.398495	4.098947	3.149140	3.476843	4.497145

	H (7)	C (8)	H (9)	H (10)	C (11)	H (12)
C (8)	2.235581					
H (9)	2.480238	1.095487				
H (10)	3.002577	1.094809	1.786799			
C (11)	3.114911	3.525512	3.633210	4.579510		
H (12)	3.750909	4.530682	4.668510	5.572440	1.094581	
H (13)	3.411468	3.577511	3.363290	4.651996	1.091603	1.859024

Point Group: C_1 Number of degrees of freedom: 33
Energy = -1192.664309911

TS28 Coordinates (Angstroms)

ATOM	X	Y	Z
1 Re	0.287921	0.073748	-0.191992
2 Cl	1.195028	1.935463	0.809269
3 Cl	1.424119	-1.902513	0.018485
4 O	-0.974998	0.243877	-1.322356
5 C	-2.966541	-0.051616	-0.411721
6 H	-3.192747	1.002130	-0.272885
7 H	-3.369231	-0.523682	-1.300227
8 C	-2.428859	-0.842057	0.719084
9 H	-3.177348	-0.880783	1.529591
10 H	-2.243969	-1.875969	0.407478
11 C	-1.138064	-0.208857	1.306847
12 H	-1.365606	0.750680	1.788909
13 H	-0.704593	-0.880888	2.057565

Distance Matrix (Angstroms)

	Re(1)	Cl(2)	Cl(3)	O (4)	C (5)	H (6)
Cl(2)	2.300293					
Cl(3)	2.289291	3.925287				
O (4)	1.703417	3.480560	3.487206			
C (5)	3.264279	4.770530	4.784223	2.209710		
H (6)	3.603260	4.614622	5.462353	2.568024	1.086657	
H (7)	3.867799	5.597306	5.159107	2.514357	1.083720	1.847885
C (8)	3.008263	4.566761	4.057197	2.731380	1.480749	2.229025
H (9)	3.985356	5.250502	4.949836	3.774759	2.121473	2.606629
H (10)	3.251343	5.149287	3.688752	3.016018	2.126373	3.105886

C (11) 2.088017 3.207649 3.330635 2.672876 2.514265 2.860728
H (12) 2.667650 2.986679 4.237500 3.176381 2.837154 2.766345
H (13) 2.637598 3.619204 3.119772 3.572405 3.449851 3.894569

	H (7)	C (8)	H (9)	H (10)	C (11)	H (12)
C (8)	2.250173					
H (9)	2.858708	1.103928				
H (10)	2.451765	1.095562	1.766559			
C (11)	3.445875	1.553241	2.158652	2.193434		
H (12)	3.896316	2.193592	2.451801	3.095022	1.097667	
H (13)	4.301472	2.183148	2.528492	2.466303	1.096859	1.780767

Point Group: C_1 Number of degrees of freedom: 33
Energy = -1192.658668609

pdt27

Coordinates (Angstroms)

ATOM	X	Y	Z
1 Re	0.223565	0.074944	0.220853
2 Cl	1.012625	2.141476	-0.282035
3 Cl	1.564104	-1.711156	-0.276755
4 O	-1.283094	-0.282369	1.215451
5 C	-2.518904	0.051777	-0.815587
6 H	-3.309669	-0.359423	-1.457496
7 H	-2.696400	1.130315	-0.724267
8 C	-2.560604	-0.583493	0.567177
9 H	-3.340007	-0.191923	1.226766
10 H	-2.644340	-1.675694	0.522495
11 C	-1.111893	-0.213649	-1.377156
12 H	-1.012624	-1.244114	-1.745989
13 H	-0.853807	0.470427	-2.193182

Distance Matrix (Angstroms)

	Re(1)	Cl(2)	Cl(3)	O (4)	C (5)	H (6)
Cl(2)	2.268494					
Cl(3)	2.287971	3.891905				
O (4)	1.840358	3.658936	3.517761			
C (5)	2.931873	4.138021	4.479868	2.400833		
H (6)	3.935641	5.130149	5.193745	3.355233	1.098381	
H (7)	3.245497	3.869739	5.140633	2.784891	1.096854	1.770040
C (8)	2.881853	4.573246	4.358562	1.463888	1.522282	2.170393
H (9)	3.712428	5.163975	5.349668	2.058933	2.214680	2.689654
H (10)	3.373515	5.347097	4.283813	2.067495	2.188688	2.468927
C (11)	2.102467	3.355514	3.257970	2.599162	1.538015	2.204070
H (12)	2.671431	4.207970	3.002716	3.125417	2.194050	2.478371
H (13)	2.672958	3.150946	3.778662	3.517068	2.201268	2.694650

	H (7)	C (8)	H (9)	H (10)	C (11)	H (12)
C (8)	2.150210					
H (9)	2.443168	1.093551				
H (10)	3.070963	1.096318	1.783684			
C (11)	2.177881	2.452749	3.427153	2.845109		
H (12)	3.084952	2.860664	3.919322	2.827504	1.098977	
H (13)	2.447103	3.412255	4.279713	3.897018	1.095658	1.779004

Point Group: C_1 Number of degrees of freedom: 33
Energy = -1192.691538396

TS29

Coordinates (Angstroms)

ATOM	X	Y	Z
1 Re	-0.389982	-0.047567	0.145933
2 Cl	-2.396772	0.294008	-0.960837
3 O	0.902241	1.234988	-0.135809
4 Cl	1.004971	-1.840295	-0.232822
5 C	2.451148	1.337746	0.101863
6 H	2.567142	1.270613	1.184826
7 H	2.603856	2.362982	-0.240128
8 C	3.211089	0.355408	-0.636908
9 H	3.334613	0.455069	-1.710911
10 H	3.587565	-0.543440	-0.165806
11 C	-0.758898	-0.074703	1.966181
12 H	-1.228403	-0.928137	2.468172
13 H	-0.500966	0.770988	2.610860

Distance Matrix (Angstroms)

	Re(1)	Cl(2)	O (3)	Cl(4)	C (5)	H (6)
Cl(2)	2.317071					
O (3)	1.842326	3.528399				
Cl(4)	2.302873	4.081312	3.078527			
C (5)	3.161179	5.071593	1.570402	3.507618		
H (6)	3.400217	5.495277	2.125380	3.758703	1.091223	
H (7)	3.863011	5.459519	2.044198	4.497112	1.091506	1.795859
C (8)	3.707147	5.617544	2.521020	3.138686	1.445089	2.137985
H (9)	4.192030	5.782501	3.000941	3.588965	2.201313	3.104740
H (10)	4.020442	6.094726	3.220974	2.890695	2.214035	2.481181
C (11)	1.857455	3.374316	2.982119	3.326284	3.971786	3.671911
H (12)	2.621287	3.823196	3.999934	3.621513	4.926737	4.570300
H (13)	2.599657	4.071684	3.119051	4.144053	3.915515	3.420012

	H (7)	C (8)	H (9)	H (10)	C (11)	H (12)
C (8)	2.134601					
H (9)	2.517407	1.085667				
H (10)	3.069283	1.082405	1.856975			
C (11)	4.703001	4.766745	5.527973	4.863828		
H (12)	5.731715	5.567593	6.340276	5.502670	1.095801	
H (13)	4.505829	4.949753	5.786983	5.114067	1.094228	1.853794

Point Group: C_1 Number of degrees of freedom: 33
Energy = -1192.615056665

pdt28

Coordinates (Angstroms)

ATOM	X	Y	Z
1 Re	0.346842	-0.132234	0.486794
2 Cl	1.822123	1.611019	0.662347
3 O	-1.052309	-1.188622	-0.190006
4 Cl	-1.893615	1.745410	0.020604
5 C	-2.284803	-0.845984	-0.788294
6 H	-2.937164	-1.729180	-0.754712
7 H	-2.109574	-0.589189	-1.840651
8 C	-2.994443	0.292955	-0.071524
9 H	-3.893902	0.607348	-0.603991
10 H	-3.234245	0.033005	0.960541
11 C	1.501023	-1.539428	0.845991
12 H	1.216971	-2.574608	0.622954
13 H	2.487188	-1.425823	1.308027

Distance Matrix (Angstroms)

	Re(1)	Cl(2)	O (3)	Cl(4)	C (5)	H (6)
Cl(2)	2.290460					
O (3)	1.879265	4.102055				
Cl(4)	2.960157	3.773143	3.059526			
C (5)	3.010124	5.000807	1.412229	2.742749		
H (6)	3.856977	5.984631	2.040533	3.709837	1.098516	
H (7)	3.414643	5.154043	2.049819	2.993537	1.097317	1.778694
C (8)	3.414190	5.047293	2.445607	1.824811	1.521358	2.135195
H (9)	4.440800	5.940027	3.386967	2.384628	2.176084	2.529314
H (10)	3.616065	5.305272	2.752631	2.369199	2.175428	2.477023
C (11)	1.855088	3.172089	2.777743	4.795310	4.181415	4.721839
H (12)	2.596316	4.229331	2.780556	5.357344	4.152371	4.457527
H (13)	2.632276	3.175157	3.850767	5.559282	5.244299	5.811240

	H (7)	C (8)	H (9)	H (10)	C (11)	H (12)
C (8)	2.165868					
H (9)	2.478882	1.091509				
H (10)	3.081994	1.090980	1.792423			
C (11)	4.599718	4.940514	5.984673	4.990835		
H (12)	4.590985	5.142103	6.144206	5.169810	1.096371	
H (13)	5.634212	5.908099	6.964762	5.914704	1.094945	1.844582

Point Group: C_1 Number of degrees of freedom: 33
Energy = -1192.623456790